CONTROL OF HAPTIC INTERACTION

An Energy-Based Approach

能源

Michel Franken

CONTROL OF HAPTIC INTERACTION

AN ENERGY-BASED APPROACH

Michel Franken

The research described in this thesis has been conducted at the Control Engineering Group, which is part of the Faculty of Electrical Engineering, Math, and Computer Science at the University of Twente, and has been financially supported by MIRA - Institute of Biomedical Technology and Technical Medicine of the University of Twente.

UNIVERSITY OF TWENTE.

MIRA
BIOMEDICAL TECHNOLOGY
AND TECHNICAL MEDICINE

The research described in this thesis is part of the project TeleFLEX, which is a joint research project of the Control Engineering Group, Laboratory of Mechanical Automation and Mechatronics, Department of Design Production & Management, and Technical Medicine of the University of Twente and Demcon.

TeleFLEX

This dissertation has been completed in partial fulfillment of the requirements of the Dutch Institute of Systems and Control (DISC) for graduate study. The author has also successfully completed the educational program of the Graduate School DISC.

disc

The cover picture of this thesis is the Chinese symbol (Kanji) for *Energy Source* which is a central theme in this thesis.

ISBN: 978-90-365-3189-4
DOI: 10.3990/1.9789036531894

DEMCON
advanced mechatronics

The printing of this thesis has been financially supported by Demcon, Oldenzaal

Printed by Wöhrmann Print Service, Zutphen, The Netherlands.

CONTROL OF HAPTIC INTERACTION
AN ENERGY-BASED APPROACH

PROEFSCHRIFT

ter verkrijging van

de graad van doctor aan de Universiteit Twente,

op gezag van de rector magnificus

prof. dr. H. Brinksma,

volgens besluit van het College van Promoties,

in het openbaar te verdedigen

op vrijdag 9 September 2011 om 12:45 uur

door

Michaël Christianus Johannes Franken

geboren op 6 Oktober 1982

te Anna Paulowna, Nederland

Dit proefschrift is goedgekeurd door:
Prof.dr.ir. S. Stramigioli, promotor
Dr. S. Misra, assistent-promotor

ISBN: 978-90-365-3189-4

PhD dissertation committee:

Chairman and Secretary:
Prof. dr. ir. A.J. Mouthaan
University of Twente, Enschede, the Netherlands

Acting chairman
Prof. dr. ir. C.H. Slump
University of Twente, Enschede, the Netherlands

Promotor:
Prof. dr. ir. S. Stramigioli
Control Engineering
University of Twente, Enschede, the Netherlands

Assistant-promotor:
Dr. S. Misra
Control Engineering
University of Twente, Enschede, the Netherlands

Opponents:
Prof. dr. B. Hannaford
Biorobotics Laboratory
University of Washington, Seattle, United States of America
Prof. dr. H. Bruyninckx
Division of Production Engineering, Machine Design and Automation
Catholic University of Leuven, Leuven, Belgium
Prof. dr. A.J. van der Schaft
Systems, Control and Applied Analysis
University of Groningen, Groningen, the Netherlands
Prof. dr. I.A.M.J. Broeders
Minimal Invasive Surgery and Robotics
University of Twente, Enschede, the Netherlands
Prof. dr. ir. J. van Amerongen
Control Engineering
University of Twente, Enschede, the Netherlands

Paranymphs:
Dr. W.P.J. Ferket-Franken
Ir. J. de Vries

To my parents

Samenvatting

Haptic feedback systemen zijn systemen die een gewenste kracht uitsturen, en door de gebruiker ervaren wordt, om een fysieke interactie na te bootsen. Dit soort systemen kunnen het realisme verhogen van de interactie met objecten die zich niet in het directe invloedsgebied van de gebruiker bevinden. Hetzelfde geldt voor de interactie met virtuele objecten. Het basis probleem in de aansturing van deze systemen is hoe de transparantie van het systeem, en daarmee samenhangend het realisme van de interactie zoals ervaren door de gebruiker, te maximaliseren terwijl de stabiliteit van de interactie altijd gegarandeerd blijft.

De analyse van de stabiliteit wordt bemoeilijkt door de aanwezigheid van een gesloten lus waarin meerdere onbekende, niet-lineaire en tijd-variërende elementen kunnen voorkomen, te weten de gebruiker, een fysieke omgeving, en mogelijke tijdsvertragingen in een communicatiekanaal. Tevens wordt het regel algoritme uitgevoerd op een discreet medium wat afhankelijk van het algoritme, de instellingen en de overige elementen een significante invloed kan hebben op de stabiliteit van de interactie.

In dit proefschrift wordt voor al deze factoren een oplossing gezocht door middel van een energie- en poort-gebaseerde aanpak. Voor beide toepassingen wordt een algoritme afgeleid dat gebaseerd is op de energie uitwisseling tussen de fysieke wereld met het systeem. Door energie neutraliteit van deze uitwisseling, oftewel passiviteit, te handhaven wordt stabiliteit van de interactie gegarandeerd.

Het algoritme voor de interactie met virtuele objecten voorziet in een passieve koppeling tussen de fysieke wereld en het discrete systeem. Het dynamisch gedrag van het virtuele object wordt berekend met behulp van een energie gebaseerde integratiemethode. Iedere integratie-stap wordt de aanwezige energie in het systeem geëvalueerd. Een nieuwe distributie van die energie over de energie opslag elementen wordt berekend op basis van het model dat het dynamisch gedrag van het fysieke object beschrijft. Dit algoritme garandeert stabiliteit onafhankelijk van de executie-frequentie van het algoritme, maar past het realisme van de interactie dusdanig aan zodat de passiviteit gehandhaafd blijft.

Het tweede algoritme splitst de doelstellingen van een regel algoritme voor de passieve interactie met fysieke objecten door middel van een telemanipulatie systeem op in twee lagen die hierarchisch geordend zijn. De bovenste laag, de *Transparantie*-laag, bevat een willekeurig regel algoritme dat de gewenste mate van transparantie kan bereiken. De *Passiviteits*-laag bevat een algoritme dat passiviteit van de interactie garandeert en waar nodig de gewenste krachten door de *Transparantie*-laag aanpast om passiviteit te behouden. De implementatie van dit algoritme werk ook in de aanwezigheid van communicatie vertragingen, door bijvoorbeeld afstand, tussen de beide locaties die het systeem verbindt, respectievelijk de gebruiker en de fysieke omgeving.

Summary

Haptic feedback systems are systems that exert a desired force, to be experienced by the user, to recreate a physical interaction. This type of systems can increase the realism of the interaction with objects that are not in the direct area of influence of the user. The same applies to the interaction with virtual objects. The fundamental problem in the control of these systems is how to maximize the transparency of the system, and related to that the realism of the interaction as perceived by the user, while guaranteeing stability of the interaction under all possible operating conditions.

The stability analysis is complicated due to the presence of a closed loop, which can contain multiple unknown, non-linear, and time-varying elements, e.g. the user, a physical environment, and time delays in a possible communication channel. Furthermore, the control algorithm is executed on a discrete medium which, depending on the algorithm, parameter settings, and remaining elements, can have a significant influence on the stability of the interaction.

In this thesis a solution is sought to all these factors by means of energy- and port-based reasoning. For both applications an algorithm is derived that is based on the energy exchange between the physical world and the system. By enforcing energy neutrality, in other words passivity, of this exchange a stable interaction is guaranteed.

The algorithm for the interaction with virtual environments provides a passive coupling between the physical system and the discrete system. The dynamic behavior of the virtual object is computed with an energy-based integration method. Each iteration the algorithm evaluates the energy that is present in the system. A redistribution of that energy over the energy storing elements is computed based on the model that describes the dynamic behavior of the physical object. This algorithm ensures stability independent of the sample frequency of the algorithm, but adapts the realism of the interaction in such a way that passivity is maintained.

The second algorithm divides the control objectives for the passive interaction with physical objects in remote environments by means of a telemanipulation system into two layers that are placed in a hierarchical order. The top layer, the *Transparency*-layer, contains an arbitrary control algorithm that provides the desired measure of transparency. The *Passivity*-layer contains an algorithm that guarantees passivity of the interaction and when necessary adapts the desired forces computed by the *Transparency*-layer to maintain passivity. The implementation of this algorithm also works in the presence of communication delays, by e.g. physical distance, between both locations that are connected by the system, the user and remote environment, respectively.

List of Abbreviations

DOF	Degree of Freedom
EBA	Energy Bounding Algorithm
IP	Internet Protocol
IR	Impedance Reflection
LST	Laparoscopic Skills Training
LTI	Linear Time Invariant
MDI	Minimal Damping Injection
MIS	Minimal Invasive Surgery
NOTES	Natural Orifice Transluminal Endoscopic Surgery
PC	Passivity Controller
PD	Proportional-Differential
PF	Position-Force
PO	Passivity Observer
P-P	Position-Position
PSPH	Passive Sampled Port-Hamiltonian
PSPM	Passive Set-Position Modulation
RAS	Robot Assisted Surgery
RTT	Round-Trip Time
SETP	Simple Energy Transfer Protocol
SCS	Shared Control System
TCP	Transmission Communication Protocol
TDP	Time Domain Passivity
TDPC	Time Domain Passivity Control
TLC	Tank Level Controller
UDP	User Datagram Protocol

Contents

CHAPTER 1

Introduction

Human ingenuity has always been directed to improving our own capabilities in shaping our environment. For centuries people have developed and applied tools to perform tasks that would otherwise have been hard to accomplish at best, or even impossible. A simple example is the introduction of the hammer which allows a blacksmith to shape red-hot metal. Here the tool used, the hammer, is a simple extension of the blacksmith's arm, but it allows him to interact with materials that would have been dangerous to interact with directly. Also the hammer can be shaped in such a way that the ability of the blacksmith to shape the metal is beneficially influenced.

With modern technology an interesting extension to the above concept became possible. A new generation of 'tools' can be developed that allows the user to interact with objects that are not in his/her direct area of influence. This is called *Telemanipulation* where the greek *Tele* means *at a distance*. *Distance* does not necessarily have to relate to a physical distance, but to a general 'barrier' preventing the user from directly manipulating the object (Niemeyer et al., 2008). Telemanipulation systems can prove useful in application area's such as space, underwater, and surgical robotics.

A telemanipulation system is composed of a master system which is operated by the user and a slave system that interacts with the remote environment. The coupling between these two systems is established by means of a control algorithm and depending on the application the communication between the master and slave system can occur through a communication channel with time delays. As the coupling between the user and the remote environment is no longer mechanical, a telemanipulation system can be designed to improve the manipulation capabilities of a user even further.

When directly manipulating objects the human sensory system provides us with feedback on our interaction with the object. This sensory system is multi-modal in nature and comprises the 5 senses:

- vision
- somatosensory - touch and proprioception
- auditory
- gustatory - taste
- olfactory - smell.

Not every sensory subsystem provides information which is relevant for the completion of a certain task, e.g. the olfactory sense during the stacking of blocks. Even if a sensory subsystem does provide information relevant to a task, it is not necessarily required for the completion of the task, e.g. the sense of touch during the stacking of blocks. However, the performance of the task might very well decrease when the information of that sensory

subsystem is not present, e.g. the loss of proprioceptive feedback in humans imposes a severe limitation on the manipulation capabilities of humans and only with intense training and concentration simple tasks can be executed on visual feedback alone (Abbott, 2006). Of course, this decrease in performance is dependent on the metric that is applied to express performance of the task execution.

This thesis is related to restoring the sense of touch to users in applications were this information is not directly present to be experienced by the user. The two situations that are considered are the interaction with simulated and remote objects. In both situations there is not a physical object for the human to touch directly. However, using sensors, control algorithms, and haptic interfaces it is possible to mimic the direct interaction with the physical object. Haptic interfaces are bidirectional devices that measure a position and reflect a force based on the recorded motion, *impedance-displays*, or measure force and impose a velocity based on the recorded force, *admittance-displays*.

Haptic is derived from the greek *Haptikos*, which means *pertaining to the sense of touch*. Haptic feedback in this thesis is used to indicate direct haptic feedback by means of impedance-displays (the application of a desired force to the user) and disregards methods for sensory substitution, e.g. the visual display of force levels (Okamura, 2004) or mechanical tissue properties (Yamamoto et al., 2009). When a telemanipulation system reflects haptic information about the remote interaction to the user it is called a *bilateral telemanipulation system*.

Haptic feedback can be divided into kinesthetic and tactile feedback. Humans sense kinesthetic feedback in e.g. ligaments, tendons, and muscles. When combined with the information about the related joint movements, kinesthetic feedback can be used to discriminate object properties such as shape, weight, and stiffness. Tactile feedback is provided by mechanoreceptive nerve endings. This information is used to detect object properties such as surface roughness. Although tactile feedback can be a rich source of information, it is not considered in this thesis. The word haptic from this point on refers only to kinesthetic feedback.

There are two requirements for a haptic feedback system to be useful:

1. *Guaranteed stability of the interaction under all possible operating conditions*
2. *The display of the desired behavior to the user.*

For the first requirement well-defined analysis methods are available, e.g. Lyapunov asymptotic stability, whereas the desired behavior has a more subjective nature. A haptic feedback system reflects the interaction perfectly when the user perceives it as real. As such the human perception, and the influence of multi-model feedback, play a crucial role. If the system is capable of perfectly reflecting the impedance of the object, the user will experience exactly the same feedback with respect to his motions whether the object is touched directly, or through the system. Therefore, the cognitive perception process of the human will have to perceive the interaction with the object through the system as real.

Lawrence (1993) defined the *Transparency* of a system as the difference between the true impedance of the object and the impedance experienced by the user. He investigated the obtainable transparency of a single bilateral control algorithm with respect to the control parameters based on the perceived impedance by the user. His analysis indicated

that for regular bilateral controllers the two requirements, *Transparency* and *Stability*, are conflicting objectives.

This statement by Lawrence (1993) is based on an analysis using linear systems theory. The application of non-linear control systems can significantly reduce the conflictive nature of stability and transparency. Transparency will still be subjected to the required need for stability, but far less when compared to the application of linear control systems. Transparency analyses and metrics based on port behavior of general non-linear systems have been proposed by Stramigioli, Fasse and Willems (2002) and Secchi et al. (2008*b*).

The focus of this thesis lies on developing non-linear control methods that allow to optimize the *Transparency* of a haptic feedback system given the boundary condition of stability using energy-based concepts in the design of the control algorithm.

1.1 Problem Statement

This research is inspired from a practical application problem in medicine. We will first elaborate on the problem statement in the application domain after which the technical challenges will be treated.

1.1.1 Medical application

Medicine can be defined as *The science relating to the prevention, cure, or alleviation of disease*. New developments in medicine are ultimately meant to increase the quality of care for the patients. An indispensable treatment method for many diseases is surgery. For surgical procedures it is generally accepted that an increased quality of care translates into reducing the invasiveness of the procedure and the required procedure time while maintaining the same (or an improved) outcome for the patient.

This reduction in invasiveness and completion time of the surgical procedure can be established in three ways:

1. research into successful treatment methods other than surgery,
2. introduction of tools that allow the surgeon to perform the surgery less invasive and more efficient,
3. training that allows the surgeon to improve his skills outside the operating room.

The engineering sciences can contribute to the last two factors by designing the required surgical tools and training systems.

A major step in the reduction of the invasiveness of surgery was made in 1987 when the first laparoscopic cholecystectomy was performed (Polychronidis et al., 2008). Cholecystectomy is the removal of the gallbladder and laparoscopic means that the procedure is performed on the basis of a video stream recorded by a slender endoscope (camera system) inserted through a small incision in the abdominal wall. The surgery is performed with slender surgical instruments inserted through similar small incisions. Instead of a single large incision (approximately $15\,\mathrm{cm}$ long), a number (usually 3 to 5) of smaller incisions (approximately $1.3\,\mathrm{cm}$ long) are made. A sufficiently large working area is created by inflating the abdomen with carbon dioxide gas.

The general description for this type of surgery is Minimal Invasive Surgery (MIS), and is these days a common method of performing various procedures in general, thoracic, urologic, and gynecologic surgery. For procedures such as cholecystectomy it is even established as the 'Golden Standard', although surgical outcomes still appear to be linked to the expertise of the surgeon (Csikesz et al., 2010). There are several benefits that are generally associated with the smaller incisions in MIS for the patient:

- the smaller wounds result in less post-operative pain,
- faster recovery due to faster healing of the smaller wounds,
- less exposure area to bacteria in the air due to the smaller incisions and positive pressure difference resulting in a smaller chance of post-operative complications,
- improved cosmetic results due to the smaller scars.

However, these benefits for the patient come at a price of increased complexity for the surgeon due to:

- misalignment of the optical surgeon-to-monitor and camera-to-target axis with respect to the manipulation axis, e.g. (Hanna and Cuschieri, 1999) and (Patil et al., 2004),
- reversed and scaled motions,
- loss of dexterity,
- reduced ergonomics.

The ergonomics for the surgeon are most notably reduced due to the limited space for positioning of the instruments in combination with the length of the instruments, and the positioning of the monitor used to present the surgeon with a view on the surgical site, e.g. (Uhrich et al., 2002) and (van Det et al., 2009).

Laparoscopic Skills Training (LST) was introduced so that prospective MIS surgeons could adjust their working style to this more complicated form of surgery outside the operating room, see e.g. (Villegas et al., 2003). The devices used in LST range from (simple) mechanical constructions to train basic MIS skills to complete surgical simulators using virtual anatomical models, or even a combination from physical objects and overlaid animations (Botden et al., 2007). A recent development is an increased focus on objective skill assessment during and following the LST, e.g. (Rosen et al., 2001a), (Rosen et al., 2001b), and (Luursema, 2010).

A new development in MIS is Natural Orifice Transluminal Endoscopic Surgery (NOTES). In NOTES procedures the entire surgical procedure takes place without any external incisions. This type of surgery most often requires the use of steerable/flexible systems, i.e. surgical endoscopes, as the operation site has to be reached through one of the natural openings of the human body. This further complicates the execution of this type of procedures with respect to MIS. In 2007 Marescaux et al. (2007) performed the first NOTES human cholecystectomy, Operation Anubis. Specialized tools for NOTES are being developed by e.g. (Karl Storz, 2011), (Olympus, 2011), and (USGI Medical, 2011).

Telemanipulation was recognized as a viable option to lessen the mental burden of MIS for the surgeon and is thought to be essential for the viability of NOTES (Canes

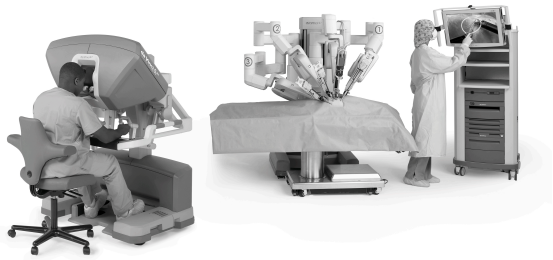

Figure 1.1: **Da Vinci Surgical System by Intuitive Surgical, Inc. (2011):** Depicted are the user console, the surgical robot, and the vision system tower.

et al., 2009). In 1998 the Zeus system was introduced for use in MIS by Computer Motion, shortly followed by the introduction of the da Vinci Surgical System by Intuitive Surgical, Inc. (2011) in 1999. At the moment the da Vinci system, Fig. 1.1, is the only commercially available system for Robot Assisted Surgery (RAS) in MIS. Several features make the da Vinci system a valuable asset for complex MIS procedures, e.g. motion scaling and filtering, 3D imagery, improved dexterity inside the patients body, and improved ergonomics. Since its introduction the da Vinci system has been successfully used in various surgical procedures, see e.g. (Melfi et al., 2002), (Hashizume et al., 2002), and (Ruurda et al., 2005), and more than 1600 systems have been installed in over 1500 hospitals worldwide as of 2011 (Intuitive Surgical, Inc., 2011).

With both the Zeus and the da Vinci system the surgeon is completely disconnected from the patient. The only source of information about his interaction with the patient's organs is the visual feedback provided by the imagery system. The forces associated with that interaction can only be estimated by the surgeon based on the visual deformation of the object being manipulated in combination with a mental model of the biomechanical tissue properties of the object. This lack of haptic feedback can negatively influence the performance of the surgeon during surgery. Studies have shown that the lack of haptic feedback during standard surgical tasks such as blunt dissection and tissue manipulation lead to the application of increased forces. Experiments with *in vivo* tissue damage assessment have shown that the application of increased forces attributes to collateral tissue damage, e.g. (Wagner et al., 2002), (Tholey et al., 2005), (Wagner and Howe, 2007), (De et al., 2007), (Famaey et al., 2010). This led Macefield et al. (1996) and King et al. (2009) to conclude that tactile feedback of the grasping forces is more important than kinesthetic feedback in surgery, although they only considered collateral tissue damage and not task performance as a whole.

Most comparative studies (telemanipulation with/without haptic feedback) so far have shown only a decrease in applied forces when haptic feedback was present and not a decrease in procedure time. Wagner and Howe (2007) state that this last effect might be dependent on the experience the surgeons has with working with a telemanipulation system. The 'expert' group in their experiments showed also to benefit from haptic feedback with respect to required procedure time, whereas the required completion time actually increased in the 'novice' group.

The forces exerted by a surgeon on tissue during standard MIS can be used as an objective skill assessment criteria. As increased forces attribute to tissue necrosis, a skilled MIS surgeon will minimize the applied forces applied to the tissue. When haptic feedback is added to current surgical simulators, the applied forces can be registered and used in the objective skill assessment. Haptic simulators have been developed for e.g. suturing tasks by Webster et al. (2001), burring surgery by Tsai and Hsieh (2010), and bone surgery by Morris et al. (2006). A collection of automatic skill assessment metrics are also proposed in Morris et al. (2006). A multi-modal feedback (visual, haptic, and auditory) simulator for dental treatment has been developed and commercialized by MOOG FCS (2009).

The problem statement from the application domain can be formulated as:

How should haptic feedback be incorporated in Robot Assisted Surgery and Laparoscopic Skills Training to result in reduced invasiveness and completion time of surgical procedures?

TeleFLEX project

The TeleFLEX project is a research project at the University of Twente in which several research groups from different disciplines are working together with an industrial partner and several medical partners. The main project partners involved are:

- Control Engineering,
  Faculty of Electrical Engineering, Mathematics, and Computer Science
- Mechanical Automation and Mechatronics,
  Faculty of Engineering Technology
- Design, Production, and Management,
  Faculty of Engineering Technology
- Minimal Invasive Surgery and Robotics,
  Faculty of Science and Technology
- Demcon

The project aims to increase the quality of surgical operations and the comfort of the patient during and after surgeries. The research is directed towards a new generation of surgical telemanipulation systems. One of the desired deliverables is a functional experimental test setup centered around an Anubiscope (Karl Storz, 2011) suitable for NOTES and Single Port Surgery (Canes et al., 2008), which can be regarded as a form of surgery in between MIS and NOTES. The various fields that are being investigated are:

- Software architectures and real-time networks
- Haptic feedback, application driven and control design
- User interfaces
- Mechanism design

1.1.2 Technical implementation

In order to fully address the problem statement from the application domain, haptic feedback systems are required with which application oriented research can be conducted in the surgical community. However, some open technological challenges exist with respect to the general introduction of haptic feedback systems. Some of these requirements are domain specific, e.g. cost-effective design and manufacturing of components with respect to sterilizability versus disposability. Other challenges persist with respect to the general concept of haptic feedback systems.

The addition of haptic feedback to telemanipulation systems and the interaction with virtual environments establishes a closed loop including all model components, Fig. 1.2. These loops are prone to stability issues due to factors as the possible presence of (non-neglible) time delays in the communication channel and the implemented control algorithm in combination with the uncertain and time-varying impedance of the user and/or remote environment. Furthermore, stability issues may arise due to system dynamics that have not been taken into account in the controller design phase and even the discrete implementation of the control algorithm can already result in stability problems. Classical design approaches impose severe restrictions on the implementation of regular control algorithms due to the large uncertainty and variation in the impedance of the user and/or remote environment. These restrictions limit the achievable transparency of systems designed with such approaches.

As stated in the introduction the stability of the interaction with a haptic feedback system is a fundamental requirement. Initial research is undertaken to address the problem statement in the application domain, but concessions are necessarily made due to the stability requirement. With respect to the problem statement in the application domain it is assumed that the obtainable transparency should be as high as possible. Therefore, the technical problem statement that is treated in this thesis is formulated as:

How should control algorithms for haptic feedback in telemanipulation and the haptic interaction with virtual environments be implemented such that the highest possible transparency is obtained while guaranteeing stability of the interaction?

1.2 Related work

In this section we will review some of the advances that have been made in the field of telemanipulation systems, with a focus on surgical telemanipulation systems, the influence of time delays in telemanipulation, and in the design of control algorithms for haptic feedback systems. Thorough overviews of the development in these area's have been written by Sheridan (1989), Sheridan (1993), Hokayem and Spong (2006), and Niemeyer et al. (2008). An overview of related work with respect to haptic interaction with virtual environments is contained within Chapter 2.

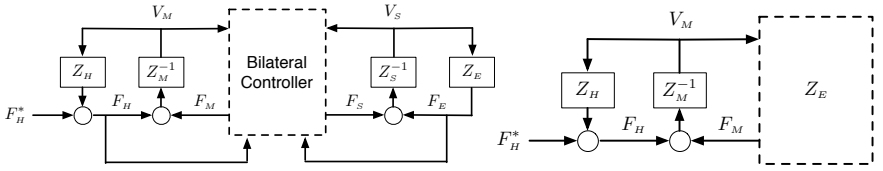

(a) Bilateral telemanipulation

(b) Haptic interaction with virtual environments

Figure 1.2: **Generalized haptic feedback systems:** F, V, and Z represent forces, velocities, and impedances, respectively. The subscripts H, M, S, and E represent the human, the master system, the slave system, and the environment, respectively. F_H^* represents the exogeneous input by the user. The dashed elements are executed in discrete time. Depending on the implemented bilateral control algorithm a specific closed loop is established comprising all components. The closed loop established by haptic interaction with virtual environments is fixed.

1.2.1 Telemanipulation systems

The initiation of the field of modern telemanipulation systems is accredited to R.C. Goertz. In the 1940s and 1950 he build several telemanipulation systems at Argonne National Lab for the handling of radioactive material. Up to then remote manipulators had been controlled solely by means of arrays of switches (Goertz, 1952). The first setup consisted of a system of mechanical linkages that allowed people to handle radioactive materials from behind a shielded wall (Goertz, 1954*b*). This device established a mechanical connection between the user and the materials to be handled. As such it was tiresome to operate due to its weight and the mechanical friction. Furthermore, the distance between the operator and the 'remote' environment was necessarily limited. A major breakthrough came when Goertz (1954*a*) broke the mechanical linkage between the user and the environment by the use of electromotors and an electrical linkage between the master and slave system. This early system was also capable of providing haptic feedback from the position servomechanism. In recent years, telemanipulation systems have been succesfully applied in amongst others:

- handling of radioactive materials, e.g. (David et al., 2005) and (Kim and Kim, 2010),
- control of unmanned underwater vehicles, e.g. (Sayers and Paul, 1994) and (Jun et al., 2009),
- control of robotic systems in space, e.g. (Hirzinger et al., 1989), (Bejczy, 1994), (Wright et al., 2005), and (Preusche et al., 2006),
- micro manipulation, e.g. (Tanikawa and Arai, 1999) and (Szemes et al., 2001),
- excavator control, e.g. (Salcudean et al., 1999) and (Kim et al., 2008),
- teleoperation of mobile robots, e.g. (Lim et al., 2003), and (Rentschler et al., 2008),
- teleoperation of aerial robots, e.g. (Guenard et al., 2006), and (Stramigioli et al., 2010),

- telesurgery, e.g. (Intuitive Surgical, Inc., 2011), (Hansen Medical, 2011), (Abbott, Becke, Rothstein and Peine, 2007), and (van den Bedem et al., 2008).

Surgical telemanipulation

In the 1980s the Stanford Research Institute (SRI) began developing a telemanipulation system suitable for hand surgery (Gourin and Terris, 2007). The results of this project led to increased awareness of the possibilities of telemanipulation in surgery and increased funding opportunities. One of the first robotic telemanipulation systems that has been designed for use during MIS was the AESOP system by Sackier and Wang (1994). This was a voice-controlled robotic endoscope holder introduced in 1994 by Computer Motion. The AESOP system was intended to restore control of the imagery system to the surgeon and removing the reliance on a surgical assistant. Prior to 1994 robotic systems were already (experimentally) applied in neurosurgery, e.g. (Kwoh et al., 1988) and (Drake et al., 1991), and orthopedic surgery, e.g. (Paul et al., 1992). In these applications a fixed sequence of operations had to be carried out by the system in a highly controlled environment, e.g. rigidly fixed and precisely known position of the patient's head/knee.

In 1998 Computer Motion introduced the Zeus system, which was a surgical telemanipulation system for MIS based on the AESOP system. This was the introduction of RAS and intended to lessen the mental and physical burden of MIS on the surgeon. The da Vinci Surgical System was introduced by Intuitive Surgical, Inc. (2011) of which the mechanical design was based on a research project carried out in collaboration with MIT (Madhani, 1998) and several features of the earlier SRI system were incorporated in early da Vinci prototypes (Intuitive Surgical, Inc., 2011).

The da Vinci system is currently the only commercially available surgical telemanipulation system. Several other companies and institutions are developing prototypes and commercial systems for MIS and other medical applications. Telemanipulation systems for MIS are being developed by e.g. Titan Medical Inc. (2011) and van den Bedem (2010), and for catheter-based electrophysiology procedures by e.g. Hansen Medical (2011) and Stereotaxis (2011). The system by Hansen Medical (2011) also provides haptic feedback based on their proprietary Intellisense Fine Force technology. A prototype telemanipulation system for NOTES has been developed by Abbott, Becke, Rothstein and Peine (2007).

Surgical telemanipulation has also already been applied over true physical distance. Marescaux et al. (2001) performed the world's first transatlantic cholecystectomies from New York, United States on both pigs and a human patient in Strasbourg, France, named *Operation Lindbergh*. The procedure was carried out using a modified Zeus system and the maximum delay that was recorded was around $150\,\mathrm{ms}$ (Butner and Ghodoussi, 2003). Arata et al. (2006) performed a laparoscopic cholecystectomy between Japan-Korea on a pig using a custom developed surgical system.

To further study the application of telemanipulation in surgery, the BioRobotics laboratory of the University of Washington, Seattle, United States developed the Raven system. The Raven system (Lum et al., 2006) is a fully functional surgical telemanipulation system for non-sterile tasks, e.g. LST. It has been used in a variety of experiments to inves-

tigate the applicability of telemanipulation in difficult circumstances. Lum et al. (2008) performed experiments with the entire system in the desert, where the communication between the master and slave system occurred through an unmanned aerial vehicle flying over the desert. Lum et al. (2009a) also performed experiments with the slave system in an underwater facility. Similar experiments have been carried out with the M7-system by (Stanford Research Institute, 2011). King et al. (2010) discuss a telemanipulation experiment where various different master and slave systems were connected over the internet using a single communication protocol designed for interoperability.

1.2.2 Telemanipulation with Time Delays

With the advent of increased computing power and fast communication methods telemanipulation over large physical distance became a real possibility. Already in the early 1960's research was conducted to come to a better understanding of how time delays effected the performance of users. Sheridan and Ferrell (1963) and Ferrell (1965) discuss that increased time delays in telemanipulation, without haptic feedback, forces users to adopt stop-and-wait policies in their manipulations and as such result in increased task completion times. Ferrell (1966) demonstrated that time delays in the communication channel connecting the master and slave system can have a destabilizing influence on bilateral telemanipulation systems.

Thompson et al. (1999) investigated the influence of time delays on surgical procedures. In their study time delay was also found to degrade task performance, but asynchronous feedback of visual and haptic information, with haptic feedback leading, improved task completion time. Similar results were obtained by Onda et al. (2010). This result can be of significant importance for time-delayed bilateral teleoperation. The time to transmit visual feedback through a communication channel is usually significantly higher compared to the control signals for the systems due to the required (de)coding processes. The asymmetric time delays reported by Arata et al. (2006) were $6.5\,\mathrm{ms}$ and $435.5\,\mathrm{ms}$ for the control signals and video stream, respectively.

Several studies have focussed on the maximum latency with which surgeons could still adequately perform tasks. Latency is defined as the total time delay between the action of the user and the resulting (visual) feedback, which includes besides the round-trip time delay, delays induced by (de)coding processes. The following studies only included visual feedback and not haptic feedback. Fabrizio et al. (2000) state that with a latency of $700\,\mathrm{ms}$ surgeons are still capable of adequate task performance. Butner and Ghodoussi (2003) performed several latency-performance test prior to *Operation Lindbergh*. Based on that study a maximum latency of $330\,\mathrm{ms}$ is recommended for surgical procedures. The latency during *Operation Lindbergh* of approximately $150\,\mathrm{ms}$ was found to be unproblematic. Anvari et al. (2005) recommends a maximum latency of $500\,\mathrm{ms}$ for surgical procedures. Lum et al. (2009b) evaluated the time delay dependency of the performance during a SAGES block transfer task, which is a basic task in LST. In their study latencies of $0\,\mathrm{ms}$, $250\,\mathrm{ms}$, and $500\,\mathrm{ms}$ were implemented and a significant difference in mean block transfer time and mean tool tip path length were shown, but a recommended maximum latency is not indicated.

If the latency further increases, direct control of the slave system eventually becomes impossible. For these applications *Supervisory*-control has been developed (Ferrell and Sheridan, 1967). With this control scheme the user only provides high-level commands to be executed autonomously by the slave system, e.g. as applied by Wright et al. (2005) in the interplanetary control of mobile robots.

1.2.3 Bilateral Control

The bilateral coupling between the user and the remote environment is established by means of the implemented control algorithm. Various control algorithms have been proposed with differing stability and transparency properties. Some common bilateral control architectures are :

- *Position-Position control:*
  The feedback force to the user is based on the position difference between the master and slave system. Mahvash and Okamura (2007) improve the transparency properties of a Position-Position controller by means of friction compensation.
- *Position-Force control:*
  The interaction force between the slave system and the environment is measured and reflected to the user, e.g. (Fite et al., 2004). Sometimes the required force sensing is avoided and instead the force exerted by the control algorithm at the slave side is reflected to the user, e.g. (Artigas et al., 2010*a*).
- *Four Channel control:*
  Lawrence (1993) showed that perfect transparency could be obtained when both the velocities and forces were exchanged between the two systems. As two forces and two velocities are exchanged through the communication channel this controller is called the four channel controller. A similar scheme was derived by Yokokohji and Yoshikawa (1994), which also explicitly required the accelerations of both devices. Salcudean et al. (2000) applied the four channel control algorithm to systems under rate control. Tavakoli et al. (2007) analyzes the stability properties of a discrete implementation of the four channel controller and Naerum and Hannaford (2009) analyzes the global transparency properties of all possible forms of this control architecture. Hashtrudi-Zaad and Salcudean (1999) showed that perfect transparency could also be obtained with three instead of four channels. Kim et al. (2005) showed that even with only two channels (Position-Force or Force-Position architecture) perfect transparency could be obtained using local feedback loops for the measured forces. Christiansson (2007) proposed to include an additional channel in the control architecture, dubbed five channel controller, where a structural compliance in the end-effector of the slave system was used to improve the stability properties of the telemanipulation system.
- *Adaptive Controllers*
  The impedances of the user and environment are usually time-varying and as such the performance of bilateral controllers with fixed parameter settings will be time-varying. A position controller that has been tuned for a certain performance during

free-space motion will show reduced position tracking performance when in contact with a physical object. Subsequently the transparency properties of the system are affected. Adaptive controllers have been proposed that adapt the parameter settings of the position controller of the slave device based on the identified parameters of the environment to improve the position tracking performance during contact phases. Examples include the work of Ibeas and de la Sen (2006), Misra and Okamura (2006), and Cortesao et al. (2006).

- *Coupled Impedance Controllers*
  The telemanipulation system itself can be thought of to have an impedance. Using the bilateral control algorithm this impedance can be shaped in such a way to beneficially influence the stability properties of the coupled system. The telemanipulation system is not necessarily designed to be perfectly transparent, but rather to mimic a tool with certain dynamic characteristics with which interaction with the remote environment can take place. Examples of this approach include the work of Lee and Li (2003), Lee and Li (2005), and Galambos et al. (2010). Also the Shared Compliance Control as applied by Kim et al. (1992) can be categorized in this category as the slave system is designed to have a certain internal compliance.

Classical control approaches have been used to analyze the parameter spaces of the above controllers for which the coupled system is stable. Loop-shaping has been applied to e.g. the Position-Force architecture by Speich et al. (2000), Fite et al. (2001), and Fite et al. (2004). Feedback linearization was applied by Speich and Goldfarb (2005) to enable the use of loop-shaping compensators, which increases the transparency bandwidth while maintaining stability robustness, on a three degrees of freedom telemanipulation system. H_∞-methods have been applied by e.g. Kazerooni et al. (1993), Yan and Salcudean (1996), and Shahdi and Sirouspour (2009*b*). Mu-analysis and synthesis have been applied by Leung et al. (1995) to obtain a pre-specified stability margin with respect to time delays and by Sirouspour (2005) in a multi-user/multi-slave scenario.

In order to apply these approaches a sufficiently accurate linear approximation, and/or maximum deviation with respect to the approximation, of the impedances of the user and environment is required. Given the large variation in these impedances, other approaches that are independent of the impedance of the user and environment have been proposed. Lyapunov-theory has been applied to design asymptotically stable bilateral telemanipulation systems by e.g. Miyazaki et al. (1986), Lee and Li (2005), Nuno et al. (2008, 2009), and Hua and Liu (2010).

Hannaford and Anderson (1988) analyzed the influence of the user grasp on the stability of a Position-Force controlled bilateral telemanipulation system during hard contact phases. It was found that the user could stabilize the system by increasing his/her impedance, i.e. applying a firmer grasp on the master device. Hasser and Cutkosky (2002) show that with a firmer grasp applied by the user the damping added by the user to the system predominantly increases. Based on this phenomena Kuchenbecker and Niemeyer (2006) proposed a different view on the stability problem. The 'problematic' closed loop is established as the force feedback to the user influences the motion of the master device, which in turn influences the motion of the slave device. They named this effect *Induced*

master motion and proposed the application of filtering techniques on the recorded master position. Such filters should remove the *Induced master motion* from the motion signal so that only the motion intended by the user is transmitted to the slave side. This should effectively break the 'problematic' feedback loop.

An approach related to the *Induced master motion*-phenomena was proposed by Polushin et al. (2007, 2008). They proposed a projection-based control of the feedback force to the user. The projection of the feedback force is limited to the force actually applied by the user. This scheme prevents the feedback force from inducing motions of the master device. However, the transparency properties of this scheme have not yet been assessed in practical applications.

The phenomena of *Induced master motion* is related to non-passive behavior of the telemanipulation system. A passive system is a system from which the energy that can be extracted is bounded by the energy that was previously injected and/or initially stored (van der Schaft, 1999). With each motion of the master and slave device a certain cost of energy is associated. An *Induced master motion* is not initiated by the user, but is rather the result of the established closed loop in the system itself. This means that the energy required to sustain that motion is not supplied by the user, but is generated within the system itself and is therefore called "virtual" energy. This additional energy can potentially destabilize the system. Using the concept of passivity it is possible to design and implement bilateral controllers that guarantee passivity of the telemanipulation system. The interaction between passive systems is guaranteed to be stable and both the user and the environment can be assumed to be passive, or at least to interact with passive systems in a stable manner (Hogan, 1989).

A well-known design approach based on the concept of passivity is Llewellyn's criterion for Absolute Stability (Llewellyn, 1952) as applied by Hashtrudi-Zaad and Salcudean (2001). A passive system can never produce energy and the interaction between passive systems is guaranteed to be stable (van der Schaft, 1999). As long as the impedances of the user and environment are guaranteed to be passive, stability of the coupled system is guaranteed. Willaert et al. (2010a) and Haddadi and Hashtrudi-Zaad (2010) both proposed methods inspired by the Absolute Stability method that reduce its conservatism by incorporating bounds on the impedances of the user and/or environment in the analysis.

A non-linear control scheme, Time Domain Passivity Control (TDPC), to guarantee stability of a bilateral telemanipulation was proposed by Ryu et al. (2002, 2004*b*). In this scheme a Passivity Observer (PO) and Passivity Controller (PC) are defined. The PO monitors the physical energy exchange between the user/environment and the telemanipulation system online. The PC consists of modulated dampers that are employed to maintain a positive value of the exchanged energy. This scheme enforces passivity and thus stability of the system. Ryu et al. (2004*a*) show that the TDPC scheme can also be generalized to other control applications.

The original implementation of the PC in the TDPC algorithm was found to excite a high-frequent mode in the devices. Therefore, Ryu et al. (2005b) extended the TDPC approach to include an energy reference following algorithm that smoothens the control action of the PC. Ye et al. (2008, 2009, 2010) propose a power-based instead of an energy-based TDPC approach. This simplified implementation of the TDPC does not contain an

integral action and is therefore not susceptible to a possible and undesirable build up effect as reported in the energy-based TDPC approach by Kim and Hannaford (2001), Hannaford et al. (2002), and Artigas et al. (2006). However, the amount of energy 'dissipated' in the control algorithm due to the power-based formulation will increase with respect to the energy-based formulation. This in turn implies increased damping added by the PC. Monfaredi et al. (2006) report that the energy-based TDPC approach is already conservative as more damping is added by the TDPC approach than necessary to guarantee stability. This conservatism increases when slave devices are used with higher internal friction.

The TDPC was originally proposed by Hannaford and Ryu (2002) for haptic interaction with virtual environments. The following extensions can also be applied to the TDPC algorithm for bilateral telemanipulation. Preusche et al. (2003) discusses the distortion of the force experienced by the user compared to the force computed by the virtual environment that occurs with the TDPC algorithm for multiple degree of freedom devices. It is proposed to project the force due to the PC along the direction of the force computed by the virtual environment instead of simply directed against the movement on the axis where energy was produced. Ryu et al. (2005a) discusses the noisy behavior of the PC when the velocity of the device is near zero and proposes methods to improve the performance. Hertkorn et al. (2010) generalizes the PC for devices with multiple degrees of freedom so that weighting by the mass matrix of the device is possible. Related to the work of Preusche et al. (2003), Hertkorn et al. (2010) indicates that is beneficial to implement a single multi degree of freedom TDPC structure in Cartesian coordinates instead of multiple single degree of freedom TDPC structures for each joint.

Two other non-linear control schemes that are based on enforcing passivity of the telemanipulation system are the Energy Bounding Algorithm (EBA) proposed by Kim and Ryu (2010) and the Passive Set-Position Modulation (PSPM) framework proposed by Lee and Huang (2008*b*, 2010). Like the TDPC, the EBA was originally developed to implement passive interaction with virtual environments and applied to bilateral telemanipulation by e.g. Seo et al. (2008) and Park et al. (2010). The EBA limits the "virtual" energy generated due to the sampling and zero-order-hold operation to the energy that is dissipated due to the mechanical friction in the device, possibly extended with an estimate of the damping added by the human arm touching the device. The non-linear operation in the PSPM framework consist of bounds on the update of the set-position signal of the PD-type controller based on the amount of energy that is available in a tank. That tank is replenished by the energy that is dissipated due to the damping in the PD-type controller. The PSPM framework was introduced as a previously proposed approach by Lee and Spong (2006), employing fixed viscous dampers, was deemed too conservative. The PSPM has also been applied to haptic interaction with virtual environments Lee and Huang (2008*a*, 2009). A likely predecessor of the PSPM framework is the work reported in Lee and Li (2002) where energy is stored in a fictitious flywheel by means of a damper. The energy in the flywheel is used to power feedforward cancellation of disturbance forces that limit position coordination of the master and slave system.

A breakthrough in the design of stable bilateral controllers in the presence of time delays was the introduction of scattering variables by Anderson and Spong (1989). A thor-

ough geometric interpretation of the scattering transformation was presented by Stramigioli et al. (2000). A conceptually simpler reformulation of scattering variables was proposed by Niemeyer (1996) and Niemeyer and Slotine (1998, 2004) in the form of wave variables. The coding scheme for the exchanged power variables (velocities and forces) in the scattering/wave variables transformation implements a passive communication channel for any arbitrary constant time delay. However, if the delays are time-varying, passivity of the coding scheme is no longer guaranteed. Yokokohji et al. (1999) proposed a compensation method to decrease the distortion of the wave variables due to time-varying delays, but this approach was also not guaranteed to be passive. Yokokohji et al. (2000) elaborated on this approach and extended it with a monitored energy balance to maintain passivity of the communication channel. Chopra et al. (2003) proposes to use time-varying gains and position feedforward to increase the stability and transparency of the teleoperation system in the presence of time-varying delays. The negative influence of packet loss on wave variable based communication was considered by e.g. Niemeyer and Slotine (1998), Hirche and Buss (2004), and Berestesky et al. (2004). Smith predictors have been introduced to decrease the negative influence of time delays on the transparency in wave variables based telemanipulation by e.g. Ganjefar et al. (2002), Munir and Book (2002), Arioui et al. (2002), and Ching and Book (2006). A different method to improve transparency was proposed by Tanner and Niemeyer (2006), where a secondary acceleration feedback path was included to restore high-frequent information of the interaction in the feedback force to the user. Passive position error correction algorithms have been proposed by Secchi et al. (2006*b*, 2008*a*) and Villegas et al. (2003). A modified wave variable scheme was proposed by Kawashima et al. (2008*a*, 2009), where an additional occurrence of the wave impedance was included to reduce tracking errors in both the position and force signals. However, this method is not guaranteed to be fully passive. Christiansson (2008) compares the standard wave variable scheme, including some of the discussed extensions, to the four channel controller proposed by Lawrence (1993). Some practical limitations associated with wave variables are discussed by Tanner and Niemeyer (2004).

Various implementations of the TDPC algorithm have been proposed for time-delayed bilateral telemanipulation. Hou and Luecke (2005) treat the combination of communication channel, slave system, and environment as a single one-port system. The TDPC algorithm is applied to this one-port system, similar to the original application of the TDPC algorithm to the haptic interaction with virtual environments. Iqbal and Roth (2006*a*,*b*) implement Kalman Filters to predict the energy at the slave side in order to deal with time delays. Artigas et al. (2006, 2007) introduce Forward and Backward PO's and PC's to enforce passivity of the communication channel. Artigas et al. (2008, 2009) extend this approach with a passive coupling between the control algorithm and the physical world. The Forward and Backward PO's estimate the energy in the communication channel based on the power variables and the time delays. A conceptually simpler formulation was proposed by Ryu and Preusche (2007) and elaborated on by Ryu (2007). Here the incoming and outgoing energy flows to the communication channel were separated. The PO's and PC's limit the outgoing energy flow at each side to the time-delayed incoming energy flow at the other side. As the energy flows are made explicit the formulation of

Ryu and Preusche (2007) is perfectly robust with respect to time-varying delays. It was recognized that the approach by Artigas et al. (2006) and Ryu and Preusche (2007) conceptually serve the same purpose and merged into a single unified approach detailed in Ryu et al. (2010). This approach has been applied in Artigas et al. (2010*a*,*b*).

The PSPM framework by Lee and Huang (2010) is also designed to handle time delays and the EBA has also reportedly been demonstrated to function in the presence of time delays Seo et al. (2008). The Lyapunov-based damping injection methods proposed by e.g. Lee and Li (2005), Nuno et al. (2008, 2009), and Hua and Liu (2010) derive parameter relations that sufficient damping to be present in the system to guarantee asymptotic stability of the system up to a certain time delay.

Time delays in the communication channel will affect the transparency of the system. In the control algorithms discussed so far, action (motion initiated by the user) and reaction (the resulting interaction force between the slave system and the environment) are separated at best by the round-trip time delay. Depending on the amount of time delay and the motion of the user, this can severely limit the achievable transparency. For schemes based on wave variables the use of Smith predictors has been proposed to reduce this loss of transparency. Two types of control algorithms that aim to reduce this loss of transparency are:

- *Predictive control:*
  Algorithms have been proposed that predict the state of the other side and use this prediction in the control of the telemanipulation system by e.g. Hirzinger et al. (1989), Prokopiou et al. (1999), and Pan et al. (2006). A scheme that tries to achieves delay free position and force tracking is proposed by Shahdi and Sirouspour (2009*a*,*b*,*c*), where the overall predictive bilateral controller is designed using H_∞-theory.
- *Impedance Reflection:*
  This group of algorithms fits a model to the environment, of which the parameters are estimated, and use this model to predict the future interaction force at the master side. This means that not the interaction force is reflected to the user, but rather the estimated impedance of the environment. Hannaford (1989) proposed such a scheme for both sides, where also the impedance of the user was estimated and reflected at the slave side. Control schemes based on this idea are discussed by Love (1995) and Hashtrudi-Zaad and Salcudean (1996). Colgate (1993) proposed to adapt the apparent impedance to the user to fit better to the user and the task to be accomplished. Love and Book (2004) and Willaert et al. (2010b) discuss algorithms were the stiffness of the environment is estimated and reflected to the user. Mitra and Niemeyer (2008) discusses a scheme were adaptive local models for haptic interaction are used. Kawashima et al. (2009) introduced a combination of an *Impedance Reflection* algorithm with a TDPC algorithm. This algorithm requires precise knowledge on the time delay that is present in the communication channel.

The performance of several of the above mentioned control algorithms with respect to transparency and stability under different operating conditions have been compared in studies such as performed by Lawn and Hannaford (1993), Arcara and Melchiorri (2002), Aliaga et al. (2004), Aziminejad et al. (2008), and Rodriguez-Seda et al. (2009).

1.3 Contributions of this thesis

Within the objectives of the TeleFLEX project, the research described in this thesis has focussed on the analysis of the control problems associated with bilateral telemanipulation systems and haptic interaction with virtual environments in general. New control algorithms that ensure stability of the interaction under all possible operating conditions are proposed as partial fulfillment to the successful introduction of haptic feedback technology in the desired applications in the medical domain. As the study focussed on the generic control algorithm the results are suitable to apply to haptic feedback systems in domains other than surgery.

The specific contributions can be formulated as follows:

- A revised implementation has been derived of a previously proposed framework that now ensures stable haptic interaction with arbitrary virtual environments
- A novel two-layer algorithm has been proposed that allows any type of bilateral control algorithm to be extended with a guaranteed stability property. The algorithm has been designed such that it works with arbitrary (varying) time delays.
- Measures are proposed that reduce the conservatism of the proposed two-layer framework and significantly increases the obtainable transparency. The proposed measures are also applicable to other algorithms proposed in literature.
- Extensions with respect to the understanding of the use and application of energy-based concepts in control algorithms for haptic interaction.
- Experimental validation of the proposed methods.

These contributions are solely coupled to the technical problem statement of Section 1.1.2. Although these contributions do not provide a direct answer to the problem statement in the application domain, this thesis is considered as a technical foundation on the basis of which research in the application domain can be improved.

1.3.1 Scientific output

The following publications have been delivered during the conduction of this research of which several form the basis of this thesis.

Journal papers

- Franken, M., Misra, S. and Stramigioli, S. (2011), 'Passive implementation of sampled virtual environments for haptic interaction', *IEEE Transactions on Haptics*, Under review.
- Franken, M., Misra, S. and Stramigioli, S. (2011), 'Improved transparency in energy-based bilateral telemanipulation', *Mechatronics*, Under review.
- Franken, M., Stramigioli, S., Misra, S., Secchi, C. and Macchelli, A. (2011), 'Bilateral telemanipulation with time delays: a two-layer approach combining passivity and transparency', *IEEE Transactions on Robotics*, 2011, In press.

Conference papers

- Franken, M., Misra, S. and Stramigioli, S. (2012), 'Internet-based two-layered bilateral telemanipulation: an experimental study', *IEEE International Conference on Robotics and Automation*, 2012, In preparation.
- Franken, M., Misra, S. and Stramigioli, S. (2011), 'Stability of position-based bilateral control systems by damping injection', *IEEE/RSJ International Conference on Intelligent Robots and Systems*, 2011, Under review.
- Franken, M., Willaert, B., Misra, S. and Stramigioli S. (2011), 'Bilateral telemanipulation: improving the complimentarity of the frequency- and time-domain passivity approaches', *Proceedings of the IEEE International Conference on Robotics and Automation*, 2011, In Press.
- Willaert, B., Franken, M., Van Brussel, H. and Vander Poorten, E.B. (2011), 'On the use of shunt impedances versus Bounded Environment Passivity for teleoperation systems', *Proceedings of the IEEE International Conference on Robotics and Automation*, 2011, In Press.
- Franken, M., Misra, S. and Stramigioli, S. (2010), 'Friction compensation in energy-based bilateral telemanipulation', *Proceedings of the IEEE/RSJ International Conference on Intelligent Robots and Systems*, 2010, pages 5264-5269.
- Reilink, R., de Bruin, G.H., Franken, M., Mariani, M.A., Misra, S. and Stramigioli, S. (2010), 'Endoscopic camera control by head movements for thoracic surgery', *Proceedings of the Third IEEE RAS and EMBS International Conference on Biomedical Robotics and Biomechatronics*, 2010, pages 510-515.
- Franken, M., Reilink, R., Misra, S. and Stramigioli, S. (2010), 'Multi-dimensional passive sampled port-Hamiltonian systems', *Proceedings of the IEEE International Conference on Robotics and Automation*, 2010, pages 1320-1326.
- Franken, M. and Stramigioli, S. (2009), 'Internal dissipation in passive sampled haptic feedback systems', *Proceedings of the IEEE/RSJ International Conference on Intelligent Robots and Systems*, 2009, pages 1755-1760.
- Franken, M., Stramigioli, S., Reilink, R., Secchi, C. and Macchelli, A. (2009), 'Bridging the gap between passivity and transparency', *Proceedings of Robotics: Science and Systems*, 2009, pages 1755-1760

1.4 Thesis outline

The chapters in this thesis are adaptations of individual papers that have been submitted to international, peer-reviewed journals and/or conferences. The specific contribution of each chapter is described below together with its relation to the other chapters and the goals of the thesis as described above.

Chapter 2 contains a revised version of the Passive Sampled Port-Hamiltonian systems framework. This framework allows any virtual environment modeled as a port-Hamiltonian system to be computed in a energy-consistent manner irrespective of the implemented model properties and/or deterministic properties of the sampling operation.

Chapter 3 introduces a novel two-layer framework for bilateral control algorithms. This framework will enforce passivity of the system for any time delay that might exist in the communication channel. A control algorithm is defined in each layer to specifically address one of the stated requirements for a useful haptic feedback system.

Chapter 4 proposes an extension to the previously discussed two-layer framework that reduces its conservatism. A model-based feedback loop is implemented to compensate for physical friction in the slave device. This extension expands the boundaries between which passivity is enforced to include part of the device dynamics.

Chapter 5 further analyzes the bounds between which passivity is enforced. Similar model-based extensions are used to increase the complimentarity between passivity-based analysis/design methods in the frequency-domain and the enforcing of passivity in the time-domain. The result is a combined approach that ensures a certain measure of transparency for a considered set of operating conditions and stability for all operating conditions.

Chapter 6 analyzes the influence a non-deterministic communication channel has on the performance of the proposed two-layer framework and its extension. Experimental data with real internet communication show that the two-layer framework is capable of handling non-deterministic communication and the beneficial effects of the proposed extensions with respect to the performance of the system.

Chapter 7 compares the efficacy of two methods to implement stable position-based bilateral controllers based on damping injection. It is shown that the proposed in Chapter 3 is less conservative with respect to the implemented damping for larger time-delays when compared to fixed-damping approaches.

CHAPTER 2

Passive Implementation of Sampled Virtual Environments for Haptic Interaction

Franken, M., Misra, S. and Stramigioli, S.
Under review with IEEE Transactions on Haptics

Haptic feedback from virtual environments establishes a closed loop comprising the user, the haptic interface, and the virtual environment. Due to the discrete nature of the virtual environment this loop is prone to stability issues. The discrete execution of a continuous-time environment model can generate "virtual" energy and this additional amount of energy can lead to instability of the haptic interaction. In this paper the framework to implement passive sampled port-Hamiltonian models proposed by Stramigioli et al. (2005) is revisited. It is shown that the original formulation of the framework handled dissipative elements in the virtual environment incorrectly. A reformulation is proposed that correctly computes the dissipated energy. Furthermore this reformulation simplifies the computation of multi-dimensional models within the framework. Experimental results for different environment models are provided to verify the validity of the proposed reformulation.

2.1 Introduction

The addition of haptic feedback to the interaction with virtual environments can increase the perceived realism of the virtual environment by the user. Intended applications are in training, e.g. surgical simulators (Basdogan et al., 2001), virtual fixtures in telemanipulation (Abbott, Marayong and Okamura, 2007), and various fabrication processes (Radi et al., 2010). In this paper we will focus on kinesthetic (force feedback) and in the remainder of the paper the term 'haptic' refers only to kinesthetic information.

The virtual environment computes an appropriate force to be fed back to the user. This force is fed back to the user through the same device by which he/she manipulates the environment through the recorded motions. A closed loop is created encompassing the virtual environment, the haptic interface and the user, Fig. 2.1. This closed loop is prone to stability issues due to the discrete implementation of the virtual environment.

Colgate et al. (1993) recognized that due to the discrete implementation of the continuous-time environment model "virtual" energy can be generated in the interconnection of the continuous and discrete domain. This additional energy can destabilize the system. Gillespie and Cutkosky (1996) introduced the term "energy-leaks" to indicate various sources that generate "virtual" energy. Abbott and Okamura (2005) and Diolaiti et al. (2006) further extended the number of factors that are taken into account in the analysis of the control problem.

A solution to this problem can be found in passivity theory. An inherent property of passive systems is that they cannot produce energy and are thus guaranteed to be stable (van der Schaft, 1999). The combination of any number of passive systems will again be passive and thus stable. As humans can be considered to be passive, or at the very least to interact with passive systems in a stable manner (Hogan, 1989), guaranteeing passivity of the haptic feedback system (virtual environment combined with the haptic interface) guarantees stability of the interaction between the user and the virtual environment.

Colgate and Schenkel (1994) applied the concept of passivity in their analysis of the model of Fig. 2.2a, a spring and damper in parallel. The derived condition ensures that any generated "virtual" energy is dissipated by the physical friction in the haptic device. Colgate et al. (1995) recognized that the apparent stiffness of the virtual environment at the interaction point played a crucial role. They proposed the virtual coupling approach where an additional spring-damper system is placed between the user and an arbitrary virtual environment. This limits the apparent stiffness of the virtual environment at the interaction point. Adams and Hannaford (1999) extended this approach to admittance-type haptic interfaces using Llewellyn's criterion for Absolute Stability (Llewellyn, 1952).

Passivity is however a sufficient condition for stable interaction and not a necessary condition. Gil et al. (2004) applied the Routh-Hurwitz stability criterion to the model of Fig. 2.2a and derived a less conservative parameter relation than Colgate and Schenkel (1994). The resulting conditions of both Colgate and Schenkel (1994) and Gil et al. (2004) can be further relaxed when the stabilizing influence of the user is included, e.g. (Hulin et al., 2008).

These approaches all focus on the analysis of Linear Time Invariant (LTI) models in the frequency-domain. As such they have to consider the worst case situation with respect

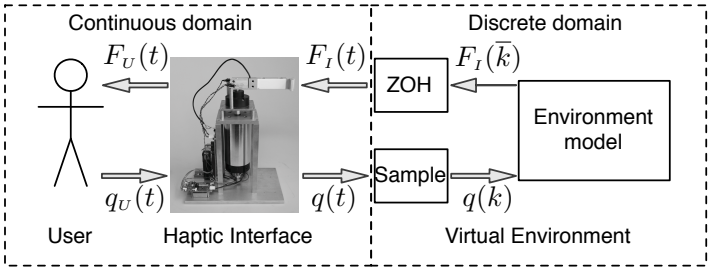

Figure 2.1: **Haptic Interaction:** The user interacts with a virtual environment through an interface of which the position is sampled. Based on the environment model and the recorded motion $q(k)$ a feedback force, $F_I(k)$ is computed in the discrete domain that is fed back to the user through the same interface.

to the possible interaction of the user with the system leading to possible conservative results. Furthermore, the reported conservatism of passive implementations is mostly valid for the analysis of LTI-models. Most physical environments are actually passive in continuous-time and thus a perfect realistic virtual implementation of the environment would retain this passivity property.

To reduce the conservatism of the application of the concept of passivity, several non-linear algorithms have been proposed in literature. The first non-linear algorithm that was proposed to implement passive haptic interaction with virtual environments, was the Time Domain Passivity Control (TDPC) algorithm proposed by Hannaford and Ryu (2002), which was extended by Ryu et al. (2005b) with a reference energy algorithm. Kim and Ryu (2010) proposed an Energy-Bounding Algorithm (EBA), where the energy generated due to the ZOH operation was limited to the energy that was dissipated by the physical viscous friction.

Lee and Huang (2008*a*) have proposed to employ a non-linear virtual coupling element, Passive Set Position Modulation (PSPM), to ensure passivity of the interaction between the user and the virtual environment. They combine the PSPM element with a non-iterative and variable-step numerical integration algorithm. This integration method takes into account the discrete supply-rate (power) of the virtual environment and as such provides an energy consistent integration of the entire virtual environment. However, a limitation of this approach is that an extended form of the passivity condition proposed by Colgate and Schenkel (1994) is required to guarantee passivity of the PSPM element (Lee, 2009).

In this paper, the framework of passive sampled port-Hamiltonian (PSPH) systems proposed by Stramigioli et al. (2005) is revisited. The benefit of this approach is that the coupled system (virtual environment, haptic interface, and the user) is considered as composed of elements exchanging energy. With the same algorithm a passive interaction of the user with the environment is implemented as well as an energy-based computation of the entire virtual environment. This framework was further elaborated on by Secchi et al. (2006*a*) and Borghesan et al. (2010). However, it was demonstrated by Franken and Stramigioli (2009) that the original formulation of the algorithm handled dissipative

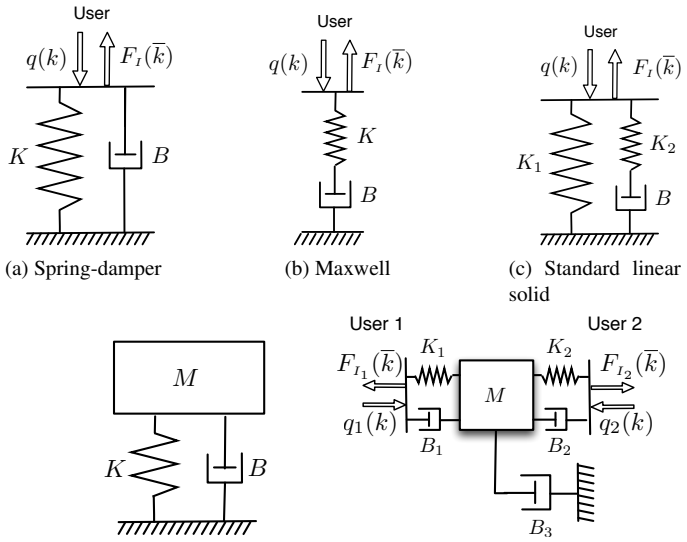

(a) Spring-damper (b) Maxwell (c) Standard linear solid

(d) Mass-spring-damper (e) Floating mass

Figure 2.2: **Environment models:** These five models are used for the analysis of the PSPH framework. $F_I(\overline{k})$ and $q(k)$ indicate the sampled interaction port.

elements incorrectly. In this paper we will treat a revised implementation of the theory of PSPH systems retaining the core concept of the approach. The extensions will be discussed based on the models depicted in Fig. 2.2.

The paper is organized as follows: in Section 2.2 the control issues related to haptic interaction with virtual environments will be briefly treated. Section 2.3 contains a summary of the theory of port-Hamiltonian systems. Section 2.4 discusses the original formulation of the framework for PSPH systems. The revised implementation of this framework will be introduced in Section 2.5. Experimental data with different virtual environments is presented in Section 2.6. Section 2.7 discusses several issues related to the applicability of the algorithm. The paper concludes in Section 2.8.

2.2 Control Issues in Haptics

Several control issues are related to the implementation of haptic interaction. In this section we will briefly summarize the desired control goals of a haptic feedback system.

- **Stability**
  The interaction with the system needs to be stable in the presence of possible time-varying factors as e.g. the grasp and motion of the user, haptic interfaces with different mechanical properties, varying virtual environment models, and adjustable parameters within those models and of the virtual environment in general.
- **Explicit integration**

The feedback force to the user needs to be computed in realtime based on the motions of the user. In order to meet this timing constraint an explicit integration method is desirable as a guaranteed cost of computation is associated with such methods. Explicit integration methods are non-iterative and as such the new state only depends on the previous state and the value of the sensor signals.

- **Realism**
  The user ideally cannot distinguish between interaction with the virtual environment and with the physical environment. However, this goal is subjected to the required need of guaranteed stability, but the virtual model should be competent to reflect the interaction with the physical environment as best as possible. Kuchenbecker et al. (2006) remark on the limited realism of haptic interaction with regular virtual environments due to the lack of higher-order dynamics. Therefore, a competent virtual environment should include at least a notion of these higher order dynamics.

2.3 Port-Hamiltonian Systems

Port-Hamiltonian modeling is centered around the conservation of energy and shares many characteristics with bond graph theory (Paynter, 1961). Every physical system can be described as a combination of energy converting, energy storing, and/or energy dissipating elements which are connected by means of a power preserving structure. Each element is connected to this structure by means of a power port through which energy exchange can take place. This port is described by two variables, efforts e and flows f, whose product is power, e.g. forces and velocities in the mechanical domain, respectively. The behavior of each element is described by a constitutive relation which relates the value of the input power port variable to the value of the output power variable. The causality of an element (which of the power port variables is an input to the element and which acts as an output) is defined by the collection of elements present in the system and the manner in which they are connected. A port-Hamiltonian system is composed of a state manifold χ, an energy function $H : \chi \rightarrow \mathbb{R}$ which expresses the total energy present in the system as function of the state x, and a state dependant network structure $D(x)$ which is lossless with respect to the energy exchange, called a Dirac structure. The Dirac structure describes how the elements are connected, see Fig. 2.3. Energy converting elements, e.g. transformers, are incorporated into the Dirac structure.

The dynamic behavior of a port-Hamiltonian system with internal dissipation and an interaction port can be expressed as (Borghesan et al., 2010):

$$\begin{aligned} \dot{x} &= [J(x) - R(x)]\frac{\partial H}{\partial x} + G(x)u \\ y &= G^T(x)\frac{\partial H}{\partial x}, \end{aligned} \tag{2.1}$$

where $J(x)$ is an interconnection matrix and skew-symmetric, so $J(x) = -J(x)^T$, $R(x)$

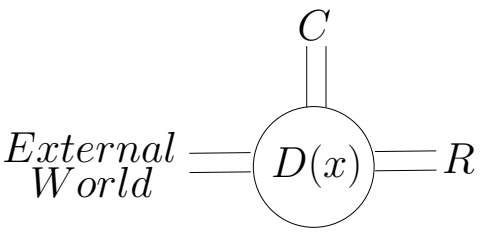

Figure 2.3: **Generic port-Hamiltonian system:** The system is composed of energy storing, C, and dissipative, R, elements connected through the Dirac structure, D(x). Connection ports allow this system to be connected to other systems.

is the dissipation matrix, and $G(x)$ is the input-state matrix, respectively. Naturally the structure of these three matrices is determined by the Dirac structure $D(x)$. The interaction power port is formed by the pair (u,y). The change of stored energy in the system can be expressed as (using the skew symmetry of $J(x)$)

$$\dot{H}(t) = \frac{\partial H^T}{\partial x}\dot{x} = y^T u - \frac{\partial H^T}{\partial x} R(x) \frac{\partial H}{\partial x}, \tag{2.2}$$

where $\frac{\partial H^T}{\partial x} R(x) \frac{\partial H}{\partial x}$ is the energy removed from the system by the dissipative elements and $y^T u$ is the energy exchanged through the interaction power port, respectively. An in-depth and thorough explanation of port-Hamiltonian modeling can be found in (Secchi et al., 2006*a*).

2.4 Passive Sampled Port-Hamiltonian Systems

It is well known that a direct discrete implementation of the continuous domain description of models can lead to the generation of "virtual" energy (Colgate et al., 1993). This is no different for port-Hamiltonian systems (Stramigioli et al., 2005) as it only a different representation of the model compared to other modeling techniques. However, the port-Hamiltonian framework is centered around energy exchange between model elements through a passive network structure and thus makes the energy exchange in the model explicit. In continuous time this energy exchange is regulated by computing the energy flow (power) through the system. In a discrete model this continuous energy flow can be replaced by a discrete energy flow that when properly implemented produces an energy consistent redistribution of energy over the various elements in the model and establishes a passive interaction with the physical world.

The energy exchange, $\Delta H_I(k)$, during sample period $\overline{k}$ between the continuous and discrete domain can be determined exactly *a posteriori* as (Stramigioli, Secchi, van der

Schaft and Fantuzzi, 2002)[1]:

$$\begin{aligned} \Delta H_I(k) &= \int_{(k-1)\Delta T}^{k\Delta T} -F_I^T(t)\dot{q}(t)dt \\ &= -F_I^T(\overline{k}) \int_{(k-1)\Delta T}^{k\Delta T} \dot{q}(t)dt \\ &= -F_I^T(\overline{k})\Delta q(k), \end{aligned} \tag{2.3}$$

where $F_I(\overline{k})$ is the feedback force to the user computed by the virtual environment, $\dot{q}(t)$ the velocity at which the haptic interface moves, and $\Delta q(k)$ the measured position difference of the haptic interface between sample instances $k-1$ and k.

The approach is that at each sample instant the energy exchange between the continuous and discrete domain is determined according to (2.3). This exchanged energy and the previous state of the model combined with the Dirac structure can then be used to determine the new energy distribution. From the redistributed energy a new state of the virtual environment can be computed and this new state in combination with the model structure finally determines the force balance for the next sample period. This entire procedure is executed at each sample instant. An interesting property is that this procedure does not place any requirements on the sample frequency and/or deterministic properties of the sampling procedure.

The key aspect to this approach is to regard a discrete domain port-Hamiltonian system as a continuous domain port-Hamiltonian system in which the efforts, e.g. forces for mechanical systems, are kept constant during the sample periods and a new energy distribution is computed *a posteriori*. This corresponds to the causality of the impedance type haptic interface. This PSPH framework was introduced by Stramigioli et al. (2005).

The continuous (the physical world) and the discrete (the virtual environment) domain are connected by means of an energy-based connection. Therefore the state of the system on either side of this connection can differ. In fact this difference is mandatory as otherwise the connection could not be implemented in a passive manner. The magnitude of this difference will depend on the motions of the user, the sample frequency, and the dynamic behavior of the virtual environment. At first glance it might be assumed that contact between the user and the virtual environment can be lost if the discrete state jump is not equal to the physical displacement of the user. However, in the PSPH framework the state of the virtual environment relates not to a physical position, but to its energy content. As long as energy is present in the virtual environment in the example above, the connection is maintained.

The difference between the state at either side of the passive connection between the continuous and discrete domain also holds important consequences for the realism of the interaction. The dynamic behavior of the environment is adapted in such a way to guarantee passivity of the entire system. As such the dynamic behavior of the virtual environment experienced by the user is not guaranteed to conform to the dynamic behavior

[1]Notation used in this paper: The index k is used to indicate instantaneous values at the sampling instant k and the index $\overline{k}$ is used to indicate variables related to an interval between sampling instants $k-1$ and k.

that would be displayed by the physical environment. A very stiff spring simulated at a low sample frequency will not be experienced as a stiff spring. However, the interaction will be stable whereas the regular implementation would very likely result in an unstable interaction. An example of this effect will be treated in Section 2.6.

2.4.1 Initial Implementation

A passive discrete implementation of the port-Hamiltonian system of (2.2) would be

$$\Delta H(k) = \Delta H_I(k) - \Delta H_R(k), \tag{2.4}$$

where $\Delta H(k)$ is the change of energy stored in the system at sample instant k, $\Delta H_I(k)$ is computed according to (2.3), and $\Delta H_R(k)$ is the energy removed from the system by the dissipative elements during sample period $\overline{k}$ evaluated at sample instant k. In the original formulation of the framework by Stramigioli et al. (2005) the dissipated energy is defined as:

$$\Delta H_R(k) = B f_R(\overline{k-1})^2 \Delta T, \tag{2.5}$$

where $f_R(\overline{k-1})$ is the flow (velocity) associated with the dissipative element, with viscous damping coefficient B, for which the dissipated energy is computed.

The distribution of energy over the storage elements, $H(\overline{k+1})$, in the model is then compensated for this change of energy as:

$$H(\overline{k+1}) = H(\overline{k}) + \Delta H(k). \tag{2.6}$$

From $H(\overline{k+1})$ the new state of the virtual environment $x(\overline{k+1})$ is derived. Finally, based on $x(\overline{k+1})$ the efforts (forces) that are exerted by the various elements in the virtual environment are computed and the new force to be fed back to the user, $F_I(\overline{k+1})$, is computed by the virtual environment.

When the virtual environment is a multi-dimensional model, containing multiple energy storing elements, the computation of the new state $x(\overline{k+1})$ is not necessarily straightforward as more than one state can correspond to the same energy level $H_S(\overline{k+1})$. Stramigioli et al. (2005) stated that the new state $x(\overline{k})$ should be 'close' in some sense to the previous state $x(\overline{k})$. In their work they assumed that when Euclidean coordinates and connections are used to describe the model this process was relatively straightforward as the new state could be chosen as the one with the minimum Euclidean distance to the previous one. However, a detailed implementation and analysis of this process was outside the scope of that paper. Borghesan et al. (2010) continued on the work of Stramigioli et al. (2005) and investigated amongst others the application of three update strategies for the state of multi-dimensional models.

2.4.2 Issues

Franken and Stramigioli (2009) found that there was a problem with the way the energy dissipated in the virtual environment is computed. (2.5) represents the energy $\Delta H_R(k)$

which is dissipated during sample period $\overline{k}$ and computed at sample instant k. However, $\Delta H_R(k)$ is computed based on the state of the virtual environment that was computed at sample instant $k-1$. Therefore, the value of $\Delta H_R(k)$ can already be computed *a priori* of sample period $\overline{k}$ at sample instant $k-1$, in fact as soon as $f_R(\overline{k-1})$ has been computed. Therefore, (2.5) implies that the energy dissipated during sample period $\overline{k}$ is independent of any interaction that might occur during that sample period.

This formulation can have severe consequences for the interaction with the virtual environment. Consider the simple spring-damper model of Fig. 2.2a. Assume that the user makes contact with this model and starts to compress the virtual spring. The resulting opposing force from the virtual environment is computed as

$$F_I(\overline{k}) = -Kx_S(\overline{k}) - B\frac{\Delta x_S(k-1)}{\Delta T}, \tag{2.7}$$

where x_S and Δx_S are the state of the spring and the change of that state, respectively. This opposing force is likely to slow down the motion of the user, but the user would still be injecting a positive amount of energy into the virtual environment. Combining (2.3) and (2.5) gives

$$\Delta H(k) = -F_I(\overline{k})\Delta q(k) - B\frac{\Delta x(k-1)^2}{\Delta T}, \tag{2.8}$$

where it was used that $f_R(\overline{k-1}) = \frac{\Delta x(k-1)}{\Delta T}$. We were considering that the user was compressing the virtual spring, so $F_I < 0$ and $\Delta q(k) > 0$ for this model. Substituting (2.7) into (2.8) indicates that if

$$\Delta q(k) < \frac{B\Delta x(k-1)^2}{Kx(\overline{k})\Delta T + B\Delta x(k-1)}, \tag{2.9}$$

the change of energy stored in the spring can actually be negative, even though $F_I < 0$, and $\Delta q(k) > 0$.

A non-empty set of 'problematic' motions by the user is represented by (2.9), for a non-trivial set of model parameters. Even though the user would actually be compressing the spring, due to (2.5) the virtual spring decompresses. The system itself will remain stable as no "virtual" energy is generated, but this problem will result in instabilities of the virtual environment (switching effects in the feedback force experienced by the user) as demonstrated by Franken and Stramigioli (2009).

This problem with the original implementation is visible in Fig. 2.4. A virtual wall, using the unilateral spring-damper model of Fig. 2.2a, was implemented according to the original formulation of Stramigioli et al. (2005). A radial stiffness of $K = 3.75\,{}^{\mathrm{Nm}}/_{\mathrm{rad}}$ at position $q_w = -0.2\,\mathrm{rad}$ was implemented, three different damping parameters were used $B = 0.00375\,{}^{\mathrm{Nm\cdot s}}/_{\mathrm{rad}}$, $B = 0.0375\,{}^{\mathrm{Nm\cdot s}}/_{\mathrm{rad}}$, and $B = 0.375\,{}^{\mathrm{Nm\cdot s}}/_{\mathrm{rad}}$. The sampling frequency of the virtual environment was $1\,\mathrm{kHz}$. Fig. 2.4 shows that for a high ratio between the implemented stiffness and damping, the contact with the virtual environment is stable. For a reduced ratio with $B = 0.0375\,{}^{\mathrm{Nm\cdot s}}/_{\mathrm{rad}}$ vibrations in the feedback force to the user occur at the beginning and end of each contact phase. Finally, for a damping

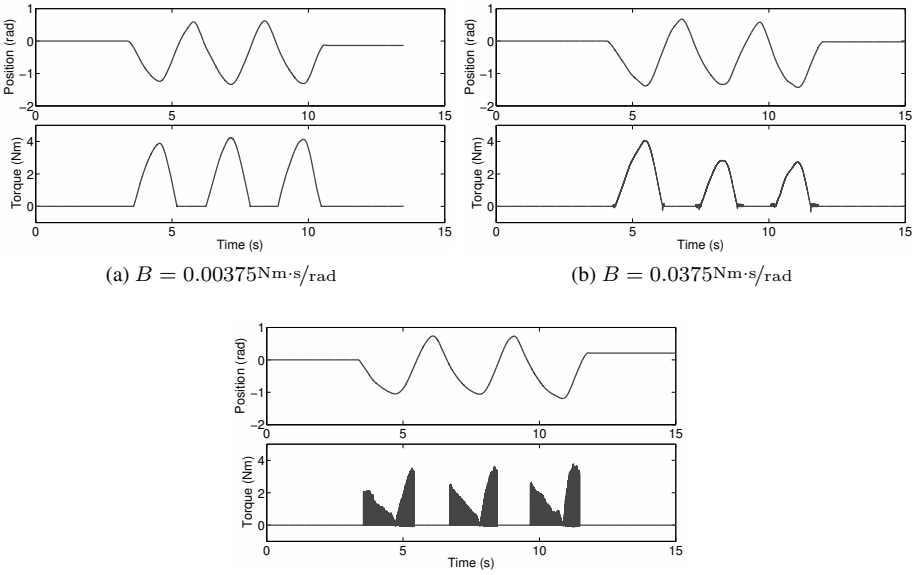

(a) $B = 0.00375^{\mathrm{Nm\cdot s}}/_{\mathrm{rad}}$ (b) $B = 0.0375^{\mathrm{Nm\cdot s}}/_{\mathrm{rad}}$

(c) $B = 0.375^{\mathrm{Nm\cdot s}}/_{\mathrm{rad}}$

Figure 2.4: **PSPH framework - original formulation Stramigioli et al. (2005):** For all experiments $K = 3.75\,^{\mathrm{Nm}}/_{\mathrm{rad}}$ and $\Delta T = 0.001\,\mathrm{s}$. These plots show that the original formulation of the framework cannot properly handle arbitrary parameter settings of at least the spring-damper model.

parameter of $B = 0.375\,^{\mathrm{Nm\cdot s}}/_{\mathrm{rad}}$ the interaction with the virtual environment is unstable in the sense that it provides a high-frequent switching feedback force. Similar results with the same ratios between the stiffness and damping parameter can be obtained when the stiffness parameter is changed.

This problem was not encountered by Stramigioli et al. (2005), Secchi et al. (2006*a*), and Borghesan et al. (2010) likely due to the implemented models, chosen parameter settings, and/or used sample frequencies. The intended strength of the approach was that the effectiveness of the PSPH framework had to be independent of such factors.

2.5 Passive Implementation Framework

In the previous section it was demonstrated that the way in which the dissipated energy was computed in the original formulation of the PSPH framework could result in instabilities of the virtual environment. The problem was due to the *a priori* fixation of the dissipated energy during the coming sample period. In this section we will present an adaptation of the approach that removes this problem. This reformulation also simplifies the implementation of multi-dimensional models as will also be discussed.

2.5.1 Energy Balance

The main idea behind the theory of the PSPH framework is that it regards sampled port-Hamiltonian systems as continuous-time port-Hamiltonian systems in which the efforts (forces) are kept constant during each sample period. At the end of the sample period the exchanged energy with the physical world is computed and a discrete state-jump is to be computed for each energy storage element to come to a consistent energy distribution.

In the 'problem' situation of the previous section the correct way to compute the new energy distribution would be to compute the injected energy by the user and then compute how this energy is divided over the spring (increase in energy stored in the spring) and the damper (the amount of energy dissipated). The port-Hamiltonian description of the spring-damper model, Fig. 2.2a, is

$$\begin{pmatrix} \dot{x}_S \\ f_R \\ F_I \end{pmatrix} = \begin{pmatrix} 0 & 0 & 1 \\ 0 & 0 & 1 \\ -1 & -1 & 0 \end{pmatrix} \begin{pmatrix} \frac{\delta H}{\delta x_S} \\ e_R \\ \dot{q} \end{pmatrix}. \tag{2.10}$$

where e_R and f_R are again the effort and flow associated with the damper. The Hamiltonian H of this model is simply the storage function of the spring, $H = \frac{1}{2}Kx_S$. The spring and damper move at the same velocity and thus the discrete state jump of the spring, $\Delta x_S(k)$ will be equal to the 'distance' that is traversed by the damper during the sample period $\overline{k}$. The force exerted by the damper during sample period $\overline{k}$ was computed based on the state jump of the spring that occured at sample instant $k-1$,

$$e_R(\overline{k}) = B\frac{\Delta x_S(k-1)}{\Delta T}, \tag{2.11}$$

so that the energy that is dissipated by the damper during the motion in sample period $\overline{k}$ is

$$\begin{aligned} \Delta H_R(k) &= e_R(\overline{k})\Delta x_S(k) \\ &= B\frac{\Delta x_S(k-1)}{\Delta T}\Delta x_S(k), \end{aligned} \tag{2.12}$$

which is in accordance with the stated general concept behind PSPH systems, a force is computed at sample instant $k-1$, held constant during sample period $\overline{k}$, and the change of energy is dependent on the computed state jump at sample instant k.

The change of energy stored in the spring, $\Delta H_S(k)$, with stiffness K due to a state jump $\Delta x_S(k)$ is

$$\begin{aligned} \Delta H_S(k) &= H_S(\overline{k+1}) - H_S(\overline{k}) \\ &= \frac{1}{2}K(x_S(\overline{k}) + \Delta x_S(k))^2 - \frac{1}{2}Kx_S(\overline{k})^2 \\ &= \frac{1}{2}K\Delta x_S(k)^2 + Kx_S(\overline{k})\Delta x_S(k). \end{aligned} \tag{2.13}$$

Both (2.12) and (2.13) are combined with $\Delta H_I(k)$ computed according to (2.3) in the energy balance (2.4). A quadratic energy balance is now obtained that can be solved for the discrete state jump $\Delta x(k)$

$$\frac{1}{2}K\Delta x_S(k)^2 + A\Delta x_S(k) - \Delta H_I(k) = 0, \tag{2.14}$$

where

$$A = Kx_S(\overline{k}) + B\frac{\Delta x_S(k-1)}{\Delta T}. \tag{2.15}$$

From the two resulting possibilities for $\Delta x_S(k)$ the one that is smallest in magnitude will be the correct state jump. If the magnitude of both possibilities is equal but opposite in sign the correct state jump can be chosen based on the state and the force balance. If storage elements of a different magnitude other than order two are used additional measures need to be implemented to compute the correct state jump.

The obtained quadratic energy balance, (2.14), is always solvable when the user is injecting energy into the system. However, when the user extracts energy from the system it can happen, depending on the motion by the user, that the energy balance is not solvable. Solving the roots of (2.14) shows that when

$$\Delta H_I < \frac{Kx_S(\overline{k}) + B\frac{\Delta x_S(k-1)}{\Delta T}}{2K}, \tag{2.16}$$

there exists no real solution to the quadratic energy balance. Due to the discrete nature of the virtual environment the feedback force to the user is kept constant during the sample period and as a result the user will have extracted a higher amount of energy from the discrete system than he would have from the continuous-time system for the same displacement (where the force exerted by the environment decreases immediately upon energy extraction).

If the quadratic energy balance is not solvable, there can still be energy stored in the spring. Dissipating this amount of energy and breaking the contact with the environment will result in a noticeable switching-off effect of the haptic interaction as suddenly the feedback force is set to zero. This will negatively influence the realism of the haptic interaction. Therefore, in these situations we need to refer to the original formulation of the algorithm where we compute the dissipated energy based on the previous state information, (2.5), until the energy in the spring is depleted or that the quadratic energy balance is again solvable (Franken and Stramigioli, 2009).

2.5.2 Components

In the previous section the energy balance of the spring-damper model of Fig. 2.2a was introduced. This energy balance consisted of the energy exchange with the physical world and the energy functions of a spring and a damper. Other models can be composed that combine these components in a different manner or include other components, e.g. mass-elements. In order to include other components in the model an appropriate energy func-

tion needs to be derived that is associated with the dynamic behavior of that component. In this section we will look into several components that are usually encountered in models.

The change in stored energy in a spring-element is given by (2.13). A change of kinetic co-energy of a mass-element, $\Delta H_{M}(k)$, with mass M can be similarly expressed as

$$\begin{aligned}\Delta H_{M}(k) = &\ H_{M}(\overline{k}) - H_{M}(\overline{k-1}) \\ = &\ \frac{1}{2}M(x_{M}(\overline{k-1}) + \Delta x_{M}(k))^2 - \frac{1}{2}Mx_{M}(\overline{k-1})^2 \\ = &\ \frac{1}{2}M\Delta x_{M}(k)^2 + Mx_{M}(\overline{k-1})\Delta x_{M}(k),\end{aligned} \tag{2.17}$$

where $x_{M}(\overline{k})$ indicates the state of the mass-element, which is its velocity in this representation. This means that the kinetic co-energy is expressed as function of the average velocity during a sample period. As the average velocity during sample period $\overline{k}$ can only be computed *a posteriori*, the same necessarily holds for the change of kinetic co-energy. $\Delta x_{M}(k)$ is the state jump computed at sample instant k and is therefore an instantaneous change of velocity. This poses an issue for the simulation of infinitely stiff mass-elements with impedance-type haptic interfaces, which will be discussed in Section 2.7.

In the previous section it was shown that for the spring-damper model of Fig. 2.2a the dissipated energy had to be expressed as (2.12) instead of (2.5). However, as detailed by Franken et al. (2010*b*), the energy function describing the correct dissipative behavior is model dependent. Consider the Maxwell-model of Fig. 2.2b consisting of a spring and damper in series

$$\begin{pmatrix}\dot{x}_{S}\\ e_{R}\\ F_{I}\end{pmatrix} = \begin{pmatrix}0 & -1 & 1\\ 1 & 0 & 0\\ -1 & 0 & 0\end{pmatrix}\begin{pmatrix}\frac{\delta H}{\delta x_{S}}\\ f_{R}\\ \dot{q}\end{pmatrix}, \tag{2.18}$$

and the application of (2.12). The 'distance', $\Delta x_{R}(k)$, that is transversed by the damper during sample period $\overline{k}$ would be

$$\Delta x_{R}(k) = \Delta q(k) - \Delta x_{S}(k). \tag{2.19}$$

Using (2.12) the energy that is dissipated by the damper is

$$\Delta H_{R}(k) = e_{R}(\overline{k})\Delta x_{R}(k). \tag{2.20}$$

The energy balance that needs to be solved is thus

$$\Delta H_{S}(k) = \Delta H_{I}(k) - \Delta H_{R}(k) \tag{2.21}$$

$$= -F_{I}(k)\Delta q(k) - e_{R}(\overline{k})\Delta x_{R}(k). \tag{2.22}$$

As the model-elements are in series (2.18) the following holds

$$F_{I}(\overline{k}) = -e_{R}(\overline{k}) = -\frac{\delta H}{\delta x_{S}} = -Kx_{S}(\overline{k}). \tag{2.23}$$

Combining (2.19) and (2.23) with (2.21) results in

$$\begin{aligned} \Delta H_{S}(k) &= Kx_{S}(\overline{k})\Delta q(k) - Kx_{S}(\overline{k})(\Delta q(k) - \Delta x_{S}(k)) \\ &= Kx_{S}(\overline{k})\Delta x_{S}(k). \end{aligned} \tag{2.24}$$

Substituting (2.13) into (2.24) it follows that the energy balance of (2.24) has the trivial solution

$$\Delta x_{S}(k) = 0. \tag{2.25}$$

By applying (2.12) the entire Maxwell-model is effectively removed as demonstrated by (2.25). The source of this problem is that (2.12) does not adhere to the causality of the damper in the model. (2.18) shows that the damper in the Maxwell model has an admittance causality and not an impedance causality as in (2.10). This was basically already known from (2.23) which stated that the spring was exerting a force on the damper. The damper thus computes a displacement due to the applied force. As the applied force is constant during the sample period $\overline{k}$, the damper moves at a constant velocity of

$$f_{R}(\overline{k}) = \frac{1}{B}\frac{\delta H}{\delta x_{S}}(\overline{k}) = \frac{Kx_{S}(\overline{k})}{B}, \tag{2.26}$$

and the dissipated energy is thus actually described by

$$\Delta H_{R}(k) = e_{R}(\overline{k})f_{R}(\overline{k})\Delta T = \frac{K^{2}x_{S}(\overline{k})^{2}\Delta T}{B} \tag{2.27}$$

instead of (2.12). It is interesting to note that (2.27) like the original formulation of (2.5) can be computed prior to sample period $\overline{k}$. This can be generalized to all elements present in the port-Hamiltonian system. The response of model-elements, with an admittance causality as seen from the Dirac-structure (except for the user interaction port), during sample period $\overline{k}$ is fixed after the force balance in the system for sample period $\overline{k}$ is computed at sample instant $k-1$.

So far the energy functions for masses, springs, and viscous dampers have been treated. However, the number of elements that can be implemented is not limited to these elements. Any (non-)linear element for which a constitutive relation and associated energy function can be derived are implementable in this framework. Transformers (and gyrators) have been left out of consideration in this section as these are energy-neutral elements and as such do not influence the energy balances of the system. Their influence needs to be taken into account in connecting the various flows and efforts in the model after all the energy balances have been evaluated.

From the treated collection of elements it is already possible to construct a model of arbitrary complexity. How such complex models are handled in the framework is treated

in the next section. A note with respect to 'suitable' models that can be implemented in this approach is given in Section 2.7

2.5.3 Multi-Dimensional Systems

Models of arbitrary size should be implementable in the framework. In Section 2.5.1 it was shown that for the simple spring-damper model an energy balance has to solved for the discrete state-jump. A port-Hamiltonian system of arbitrary size can be decomposed into a number of smaller submodels which are interacting by means of an energy connection. Each submodel will have an energy balance composed of the elements inside that submodel. Thus, implementing models of arbitrary size comes down to deriving a number of energy balances and the correct order in which to evaluate them. This greatly simplifies the computation of the correct state jump. In the original algorithm, for a system containing n energy storing elements, an n-dimensional state jump had to be computed directly, (Stramigioli et al., 2005) and (Borghesan et al., 2010). In the revised algorithm proposed in this paper, the problem is reduced to solving at most n separate energy balances (the state jump of elements can be linked when the elements are part of the same energy balance).

Components that share a common force or velocity belong to the same energy balance. Energies exchanged through connection ports, $\Delta H_{Ic}(k)$, between two submodels is calculated as

$$\Delta H_{Ic}(k) = -F_{Ic}(\overline{k})\Delta x_{Ic}(k), \tag{2.28}$$

where $F_{Ic}(\overline{k})$ is the force exerted by one of the submodel, e.g. submodel A, and $\Delta x(k)$ is the discrete displacement that occurs in the other submodel, e.g. submodel B. $\Delta H_{Ic}(k)$ represent the energy that flows from submodel A into submodel B. With respect to the mentioned order of evaluating the energy balances this shows that submodel B needs to be evaluated prior to the evaluation of submodel A.

It could be thought that this hierarchy of evaluation poses a problem as it means that certain models would not be solvable. The generic submodel structure of Fig. 2.5 for instance is not solvable as the energy balance associated with each of the submodels is at least dependent on the energy balance of one other submodel. This is a known problem in bond graph theory and is referred to as the existence of causal/algebraic loops in the model. In Fig. 2.5 the forces associated with the interconnection of the submodels, $F_{Ic1} - F_{Ic4}$, form a causal loop encompassing all submodels and is not solvable. It should be noted that such problems exist due to the implemented model and not so much due to the chosen modeling technique. Reposing the same model in any other modeling technique will result in computational problems. Furthermore such loops are usually due to an incorrect causality assignment to the components in the model and/or excessive model simplifications. For bond graphs, algorithms have been proposed to detect and fix such causal loops, e.g. (Buisson et al., 2000), and implemented in simulation packages, e.g. the program 20-sim (Controllab Products B.V., 2010). Here we will assume that a proper causality analysis has been performed on the model and that it is free of such causal loops.

When multi-dimensional models are implemented care should be taken in the inter-

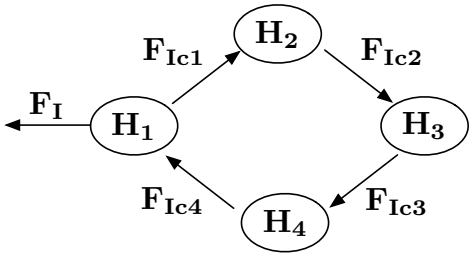

Figure 2.5: **Virtual environment model with causal loop:** F_I is the force fed back to the user and F_{Ic1}-F_{Ic4} are the forces associated with the interconnection of the various submodels. Due to the causal loop in the model, encompassing all 4 submodels, the energy balances cannot be evaluated.

connection of the states of the various model elements. Consider the mass-spring-damper model of Fig. 2.2d with only internal dynamic behavior (no interaction with a user). There are now two model elements that store energy, the spring and the mass. The energy balance to evaluate each sample instant is

$$\Delta H_S(k) + \Delta H_M(k) = -\Delta H_R. \tag{2.29}$$

Applying (2.13) and (2.17) to (2.29) indicates that the state jumps of the spring and the mass need to be related to each other. The displacement made by both the spring and the mass has to be equal and thus $\Delta x_S(k)$. This means that the discrete velocity during sample period k was $\frac{\Delta x_S(k)}{\Delta T}$. The state jump of the mass element indicates the change of kinetic co-energy, which was expressed as function of the average velocity, during sample period $\overline{k}$ with respect to $\overline{k-1}$. Therefore:

$$x_M(\overline{k-1}) + \Delta x_M(k) = \frac{\Delta x_S(k)}{\Delta T} \tag{2.30}$$

The complete energy-balance of the system (2.29) can thus be expressed as function of $\Delta x_S(k)$, using (2.12), (2.13), (2.17), and (2.30), as

$$\frac{1}{2}(K + \frac{M}{\Delta T^2})\Delta x_S(k)^2 + A\Delta x_S(k) - H_M(\overline{k-1}) = 0, \tag{2.31}$$

where

$$A = Kx_S(\overline{k}) + B\frac{\Delta x_S(k-1)}{\Delta T}, \tag{2.32}$$

and the correct solution is the one that minimizes $\sqrt{\Delta x_S(k)^2 + \Delta x_M(k)^2}$.

Multi-dimensional models can also be composed with elements that are not directly connected to each other. Such models will be composed of multiple energy-balances that need to be solved in a certain order as discussed by Franken et al. (2010*b*). There might also be more than one interaction port through which users can interact with the model.

The subdivision into multiple energy balances greatly influences the implementation of how models are handled with multiple interaction points. Both these factors will be illustrated with the floating mass model of Fig. 2.2e. The energy balances for this model can be derived to be:

$$\Delta H_{S_1}(k) = \Delta H_{I_1}(k) - \Delta H_{Ic_1}(k) - \Delta H_{B1}(k) \quad (2.33)$$

$$\Delta H_{M}(k) = \Delta H_{Ic_1}(k) + \Delta H_{Ic_2}(k) - \Delta H_{B3}(k) \quad (2.34)$$

$$\Delta H_{S_2}(k) = \Delta H_{I_2}(k) - \Delta H_{Ic_2}(k) - \Delta H_{B2}(k). \quad (2.35)$$

This model contains three states, one in each energy balance. The hierarchy of these balances is that first (2.34), which describes the motion of the mass within the global virtual environment, needs to be evaluated after which (2.33) and (2.35) can be computed in parallel, which describe the dynamic behavior of the contact model of the mass. In the original algorithm the energy exchanged through all interaction ports with the physical world was summed and added to the total energy stored in the system (2.3). (2.33)-(2.35) show that multi-point interaction models are handled differently in the reformulated algorithm. The exchanged energies with User 1 and User 2, $\Delta H_{I_1}(k)$ and $\Delta H_{I_2}(k)$, only locally affect the energy distribution within (2.33) and (2.35) and are as such handled separately from each other.

2.5.4 Deadlock Situations

The described framework for PSPH systems is centered around the measured energy exchange according to (2.3). The feedback force resulting from the virtual environment is derived from the state of the system and is thus related to the energy stored in the system. When no initial energy is present in the virtual environment and the system is at rest, the feedback force resulting from the virtual environment will be zero. This means that the user will not be able to inject energy into the virtual environment whatever motion he may execute.

The method for resolving such deadlock situation has not changed since the original formulation. The only way to start the energy exchange with the virtual environment is to initially revert to a regular Euler-discretized description of the virtual environment and generate an amount of "virtual" energy. When the system is in a deadlock situation the displacement that occurred at the interaction point, $\Delta x_I(k)$ is taken to be a fraction γ of the physical displacement, $\Delta q(k)$. For virtual environments with which switching contact is possible (e.g. a virtual wall), this is only performed when the user is in contact with the virtual environment. Depending on the motion of the user and the sampling frequency a value for γ is to be selected. As a rule, the lower the sampling frequency is the lower γ has to be selected in order to prevent excessive jumps in the feedback force to the user. Usually, for a sampling frequency of 1 kHz, γ can be selected as unity.

For the unilateral model of Fig. 2.2a this means that the amount of "virtual" energy that is generated, $\Delta H^+_{BK}(k)$, when contact with the unilateral spring-damper is estab-

lished is

$$\Delta H^{+}_{BK}(k) = \frac{1}{2} K_S (q(k) - q_w)^2, \tag{2.36}$$

where q_w is the position where the spring-damper is located. How this generated "virtual" energy is handled is treated in the next section.

Another deadlock problem can arise in models with internal dynamic behavior. Consider again the mass-spring-damper model of Fig. 2.2d which is pre-stretched, unrestricted, but initially at rest so that $x_S(0) = x_{S0}$ and $x_M(0) = 0$. For these conditions the energy balance describing the system initially reduces to

$$\frac{1}{2}(K + \frac{M}{\Delta T^2})\Delta x_S(k)^2 + K x_{S0} \Delta x_S(k) = 0, \tag{2.37}$$

of which one of the solutions is $\Delta x_S(k) = 0$, meaning that the system will remain in its initial configuration indefinitely. The solution is to initially select the other solution $\Delta x_S(k) = -\frac{K x_{S0}}{\frac{1}{2}(K + \frac{M}{\Delta T^2})}$ to move the system out of this deadlock configuration, or to apply a different integration procedure for the initial integration step. No "virtual" energy is generated in this process, but adequate measures need to be implemented to detect and handle such internal deadlock configurations in the model.

A final situation that needs to be handled is the case in which the state of the virtual environment moves through a local minimum of the Hamiltonian. Consider a linear spring and sssume that the user first compresses the spring after which the user switches to pulling on the spring. More energy will be extracted from the virtual environment in the transition between compressing and pulling than was stored due to the discretized nature. How should the new state of the virtual environment be chosen in this situation? The amount of energy stored in the virtual environment is clearly zero and therefore the only logical choice for the new state is a dynamic deadlock situation corresponding to this empty energy storage. The generated "virtual" is to be handled by the algorithm explained in the next section. The system is pulled out of such a dynamic deadlock situation depending on the interaction of the user with the model as described above. In the original formulation, Stramigioli et al. (2005) considered the dynamic deadlock situation undesirable and introduced the concept of 'Energy Leap' to handle these situations. However, the effectiveness of this approach was criticized by Babakhani (2008).

2.5.5 Passivity Control

The PSPH framework provides an energy-consistent computation of the virtual environment. However, it is unavoidable that small amounts of "virtual" energy are generated and in order to come to a fully passive implementation these amounts of "virtual" energy need to be dissipated. We differentiate between two types of "virtual" energy generation. Energy generation due to internal dynamic behavior and energy generation in the interconnection between the continuous and discrete domain.

First we will treat the energy generation due to internal dynamic behavior. Consider the model of Fig. 2.2b without interaction with a user. Assume that there is an initial

amount of energy stored in the spring, $H_S(0)$. In Section 2.5.2 it was derived that for this model the dissipated energy is given by (2.27). It is easily shown that when

$$B < 2K\Delta T, \tag{2.38}$$

the energy dissipated due to (2.27) exceeds $H_S(0)$. When such a situation is detected the corresponding storage element will be placed in a deadlock situation, e.g. $H_S(k=1)=0$ and the computation can be adjusted for the amount of energy that was available in the model, e.g. $\Delta x_S(k=1) = -x_{S0}$. These situations are always detectable and can be handled appropriately although it might involve backward adjustment of the computed state jumps.

The second location where "virtual" energy is generated is more problematic. In this situation the "virtual" energy has been injected into the continuous domain and it is not possible to adjust the state of the physical world to compensate for this excess energy. As stated before the amount of generated "virtual" energy is precisely known and can therefore be tracked by means of "bookkeeping". The bookkeeping algorithm not only needs to record the amount of "virtual" energy generated, but also needs to compensate for it by physical energy injection by the user. Possible solutions proposed by Stramigioli et al. (2005) are to deduct small amounts of energy from subsequent positive energy injections by the user and/or from the energy stored in the system. When these amounts are kept small their influence on the dynamic behavior of the virtual environment will be limited.

With respect to the more general formulation of the generation of "virtual" energy consider the breaking of contact phases. Both of the approaches mentioned above cannot be applied in this situation. No energy is stored in the system after the contact has been broken and there might be no immediate subsequent energy injections by the user. A more functional solution can be found in the concept of the TDPC algorithm proposed by Hannaford and Ryu (2002). In the TDPC approach additional energy is extracted from the user to compensate for the generated "virtual" energy independent of the virtual environment. This is accomplished by activating a modulated damper, the Passivity Controller (PC), to dissipate the generated "virtual" energy recorded by the Passivity Observer (PO). In the PSPH framework these PO and PC elements can immediately be applied to the value of the 'bookkeeping' algorithm $H_{BK}(\overline{k})$ as in fact the bookkeeping algorithm is a PO. The additional force exerted by the modulated damper, the PC, is implemented as

$$\begin{aligned} F_{BK}(\overline{k}) &= -B_{BK}(k-1)\dot{q}(k-1) \\ B_{BK}(k-1) &= \begin{cases} \alpha_{BK} H_{BK}(\overline{k}) & \text{if } H_{BK}(\overline{k}) > 0 \\ 0 & \text{otherwise} \end{cases}, \end{aligned}$$

where α_{BK} is a tuning parameter for the rate of dissipation of H_{BK}. Please note that after the completion of the energy-based algorithm for the virtual environment at sample instant $k-1$ the value of $H_{BK}(\overline{k})$ is known and can therefore be used to compute $B_{BK}(k-1)$.

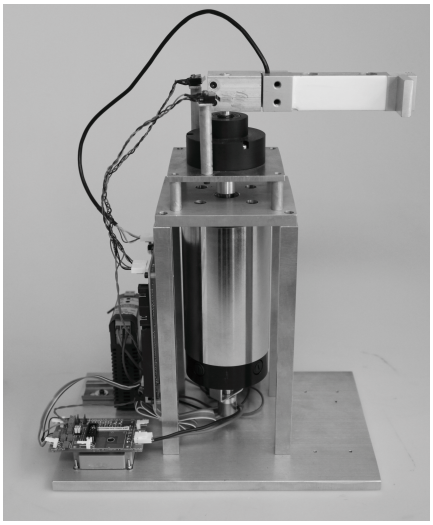

Figure 2.6: **Experimental setup:** The setup is a custom made 1 d.o.f. lightweight device with low mechanical friction. For the multi-point interaction experiments a second identical device is used

The force applied to the haptic interface, $F_H(\overline{k})$ is now

$$F_H(\overline{k}) = F_I(\overline{k}) + F_{BK}(\overline{k}), \tag{2.39}$$

and the bookkeeping algorithm is finalized as

$$H_{BK}(\overline{k+1}) = H_{BK}(\overline{k}) + \Delta H^+_{BK}(k) - \Delta H^-_{BK}(k), \tag{2.40}$$

where $\Delta H^+_{BK}(k)$ is the amount of generated "virtual" energy in the virtual environment during sample period $\overline{k}$, which is zero most of the time as explained before. $\Delta H^-_{BK}(k)$ is the amount of energy extracted from the user to compensate for $H_{BK}(\overline{k})$

$$\Delta H^-_{BK}(k) = -F_{BK}(\overline{k})\Delta q(k). \tag{2.41}$$

It should be noted that passivity of the virtual environment is mostly guaranteed in the PSPH framework by the energy-based computation of the virtual environment. Therefore the generated amounts of "virtual" energy will usually be extremely small. In most circumstances the generated "virtual" energy will not be sufficient to destabilize the system as all energy dissipated by friction in the haptic interface is neglected.

It should be noted that passivity of the virtual environment is mostly guaranteed in the PSPH framework by the energy-based computation of the virtual environment. Therefore the generated amounts of "virtual" energy will usually be extremely small. In most circumstances the generated "virtual" energy will not be sufficient to destabilize the system as all energy dissipated by friction in the haptic interface is neglected.

2.6 Experiments

In this section we will treat several examples to indicate the validity of the reformulated framework for PSPH systems. The experiments are performed with the custom lightweight haptic interface with low mechanical friction depicted in Fig. 2.6. The haptic interface is a one degree of freedom device powered by a DC motor without gearbox. The maximum continuous torque that this motor can exert is $1.38\,\mathrm{Nm}$. A high-precision encoder with $65\,\mathrm{k}$ pulses per rotation is used to record the position of the device. For the floating mass experiment with dual interaction point a second similar device is used.

Both devices are controlled from the same embedded target running a real-time Linux distribution. The virtual environment is implemented in the program 20-sim (Controllab Products B.V., 2010) and real-time executable code specific for this setup is generated directly from 20-sim and uploaded to the embedded target by means of the program 4C (Controllab Products B.V., 2010). The sampling frequency at which the virtual environment is executed is $1\,\mathrm{kHz}$ unless otherwise specified. The devices are simple rotational devices. Therefore, the models of Fig. 2.2 that are used in the experiments are also implemented in the rotational domain, meaning that torques instead of forces are computed.

The parameters for the deadlock resolving and passivity control parts of the algorithm, Section 2.5.4 and (2.39), were implemented as $\gamma = 1$ and $\alpha_{BK} = 100$ for all experiments.

2.6.1 Mass-Spring-Damper

Simulations have been performed with the model of Fig. 2.2d. For all simulations the parameters were set as $M = 1\,\mathrm{kg}$, $K = 10\,{}^{\mathrm{N}}/_{\mathrm{m}}$, $B = 1\,{}^{\mathrm{Ns}}/_{\mathrm{m}}$, and as initial condition $x_S(0) = 1\,\mathrm{m}$. A continuous-time description of the model has been implemented and simulated in continuous time and at sample frequencies of 1kHz and 500Hz. For a sample frequency of 1kHz the system is already only marginally stable and at 500Hz the system is unstable. The same model has been implemented using the PSPH framework. The dynamic behavior is governed by (2.30). The system is stable at all sample frequencies (25Hz does not pose a lower bound). Fig. 2.7d-f show that the dynamic behavior of the model is adjusted with respect to the dynamic response of Fig. 2.7a. For this model, the settling time of the system is much higher at a sample frequency of 25Hz. This adjustment is required to guarantee the energy consistency of the model and the difference in dynamic response increases with reduced sample frequencies.

2.6.2 Spring-Damper

The Spring-Damper model of Fig. 2.2a is implemented as described in Section 2.5 with the energy balances as described in Section 2.5.1. The feedback force experienced by the user is computed according to (2.7).

The same experiment as carried out in Section 2.4 is performed. The virtual wall is located at position $q_w = 0\,\mathrm{rad}$ in the virtual environment. Fig. 2.8 shows the haptic interaction for the various values of the dissipative element ($B = 0.00375\,{}^{\mathrm{Nm\cdot s}}/_{\mathrm{rad}}$, $B = 0.0375\,{}^{\mathrm{Nm\cdot s}}/_{\mathrm{rad}}$, and $B = 0.375\,{}^{\mathrm{Nm\cdot s}}/_{\mathrm{rad}}$ with $K = 3.75\,{}^{\mathrm{Nm}}/_{\mathrm{rad}}$). Each figure

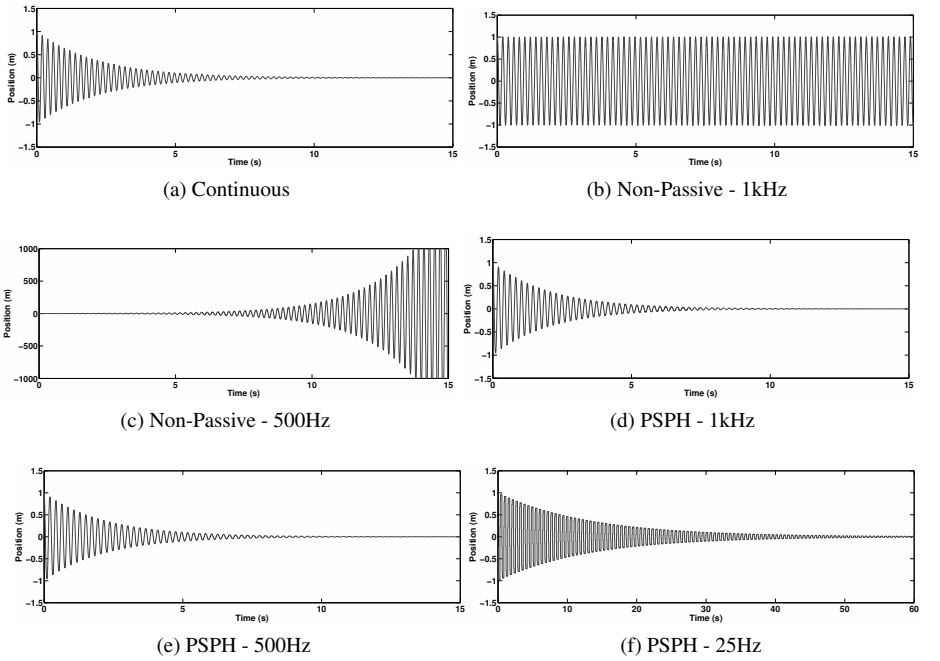

(a) Continuous (b) Non-Passive - 1kHz

(c) Non-Passive - 500Hz (d) PSPH - 1kHz

(e) PSPH - 500Hz (f) PSPH - 25Hz

Figure 2.7: **Simulation of Mass-spring-damper model:** With a discrete implementation of the continuous-time model the system is marginally stable at a sample frequency of 1kHz. With the PSPH framework the system is stable and convergent for all sample frequencies. The PSPH framework increasingly alters the dynamic behavior of the system for lower sample frequencies, e.g. comparing (d) and (f) shows that the settling time of the system is increased.

shows the position of the haptic interface, the feedback force to the user, and the energy exchanged between the continuous and discrete domain for each combination of parameters. Fig. 2.8 shows that with the reformulated PSPH framework the dissipative element is handled correctly, more energy is dissipated for higher damping values. The instability of the virtual environment at higher damping coefficients, visible in Fig. 2.4, is no longer present. Fig. 2.8c also shows that for higher values of the viscous damper the so-called 'sticky-effect' occurs when the contact with the virtual wall is broken, which is due to the use of a regular viscous damper.

Another experiment is carried out with $K = 3.75\,{}^{\mathrm{Nm}}/_{\mathrm{rad}}$ and $B = 0.375\,{}^{\mathrm{Nm\cdot s}}/_{\mathrm{rad}}$ at different sample frequencies. Fig. 2.9 shows the interaction with this virtual environment for sample frequencies of $1\mathrm{kHz}$, $100\mathrm{Hz}$, and $25\mathrm{Hz}$. The interaction at all three sample frequencies is passive and indeed stable. However, comparing Fig. 2.9a and Fig. 2.9c shows that the apparent stiffness of the virtual environment is reduced automatically by the PSPH framework at lower sample frequencies to guarantee this passive interaction.

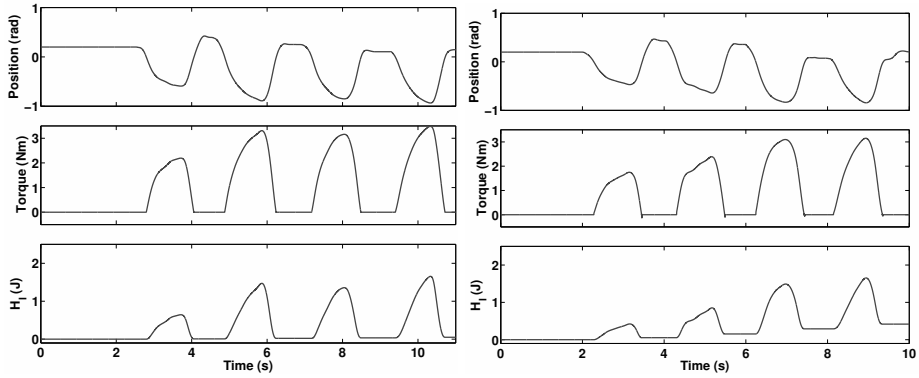

(a) $B = 0.00375^{\mathrm{Nm \cdot s}}/_{\mathrm{rad}}$ (b) $B = 0.0375^{\mathrm{Nm \cdot s}}/_{\mathrm{rad}}$

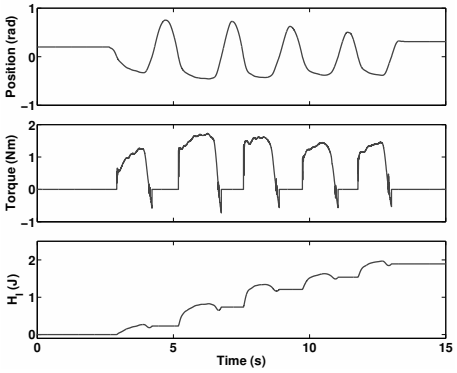

(c) $B = 0.375^{\mathrm{Nm \cdot s}}/_{\mathrm{rad}}$

Figure 2.8: **Spring-damper model with revised PSPH framework:** For all experiments $K = 3.75\,^{\mathrm{Nm}}/_{\mathrm{rad}}$ and $\Delta T = 0.001\,\mathrm{s}$. These plots show that the revised formulation of the framework correctly handles the dissipated energy inside the virtual environment.

2.6.3 Moveable Mass

The floating mass model of Fig. 2.2e is also implemented. The parameters of the model were chosen as $K_1 = K_2 = 4\,^{\mathrm{Nm}}/_{\mathrm{rad}}$, $B_1 = B_2 = 0.2\,^{\mathrm{Nm \cdot s}}/_{\mathrm{rad}}$, $B_3 = 0.1\,^{\mathrm{Nm \cdot s}}/_{\mathrm{rad}}$, and $M = 0.1\,\mathrm{kg} \cdot \mathrm{m}^2$.

Fig. 2.10 shows that the stability of the virtual environment is not guaranteed when implemented with a regular Euler-discretized integration method. The user establishes contact and pushes the virtual mass away. However, due to the discrete nature of the viscous damper the virtual mass first slows down, but then becomes unstable. This occurs when pure viscous friction is implemented and the user is not in contact with the virtual mass as otherwise its position would be dependent on the position of the haptic interface where the user has a stabilizing influence.

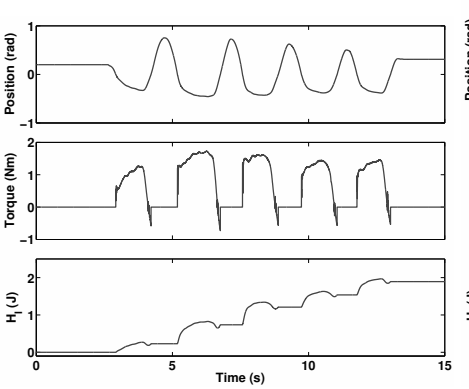

(a) $\Delta T = 0.001$s

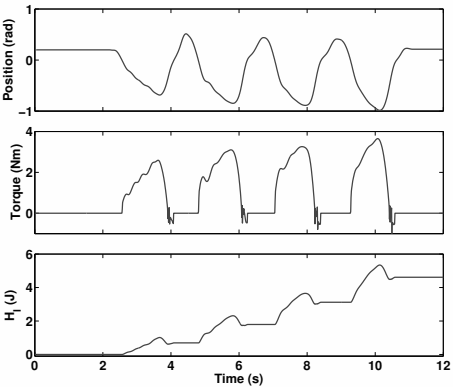

(b) $\Delta T = 0.01$s

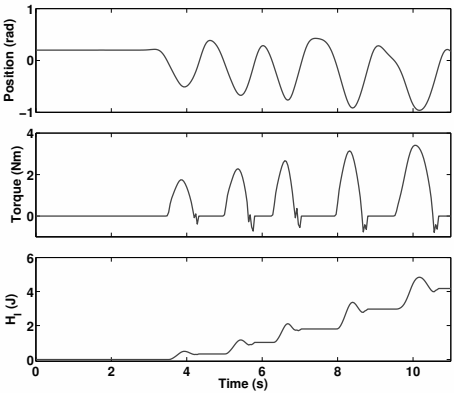

(c) $\Delta T = 0.04$s

Figure 2.9: **Spring-Damper model with revised PSPH framework for different sampling frequencies:** For all experiments $K = 3.75\,{}^{\mathrm{Nm}}/_{\mathrm{rad}}$ and $B = 0.375\,{}^{\mathrm{Nm\cdot s}}/_{\mathrm{rad}}$. The interaction with the virtual environment is stable for all sample frequencies, but at the lower frequencies the displayed dynamic behavior is altered to ensure passivity and thus stability.

The implementation of this model in the PSPH framework will be briefly described. The energy-balances of the system are listed in (2.33)-(2.35). The torques of the contact models, τ_{I_1} and τ_{I_2}, respectively, are computed as:

$$\begin{aligned} \tau_{I_1}(\overline{k}) &= -K_1 x_{S_1}(\overline{k}) - B_1 \frac{\Delta x_{S_1}(k-1)}{\Delta T} \\ \tau_{I_2}(\overline{k}) &= -K_2 x_{S_2}(\overline{k}) - B_2 \frac{\Delta x_{S_2}(k-1)}{\Delta T}. \end{aligned} \tag{2.42}$$

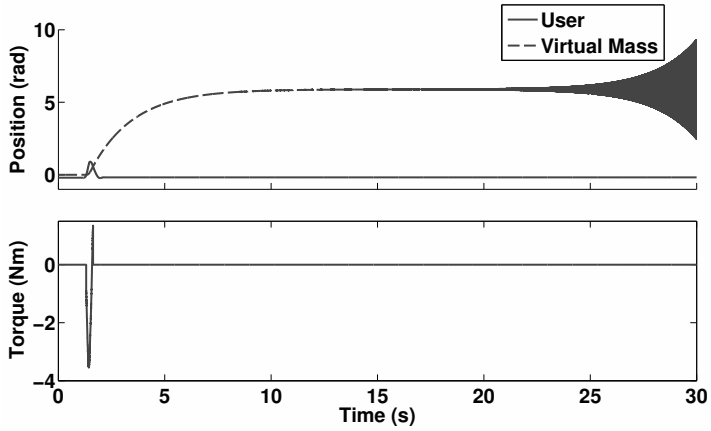

Figure 2.10: **Haptic interaction with moveable mass - Euler discretized model:** Due to the discrete nature of the viscous friction the virtual mass starts to display unstable behavior.

The motion of the mass is governed by the forces exerted on it by the contact models as described above and the viscous damper B_3:

$$\tau_{M}(\overline{k}) = -\tau_{I_1}(\overline{k}) - \tau_{I_2}(\overline{k}) - B\frac{\Delta x_{M}(k-1)}{\Delta T}. \tag{2.43}$$

This force results in a change of kinetic co-energy, $\Delta H_{M}(k)$, according to (2.17) so that the energy balance (2.34) becomes:

$$\Delta H_{M}(k) = \tau_{M}(\overline{k})\Delta x_{M}(k), \tag{2.44}$$

which can be solved for $\Delta x_{M}(k)$. The energies exchanged between the contact models and the mass-element are:

$$\begin{aligned} \Delta H_{Ic_1}(k) &= -\tau_{I_1}(\overline{k})\Delta x_{M}(k) \\ \Delta H_{Ic_2}(k) &= -\tau_{I_2}(\overline{k})\Delta x_{M}(k). \end{aligned} \tag{2.45}$$

Fig. 2.11 shows the same experiment as Fig. 2.10. With the PSPH framework implementation the interaction with the virtual mass and the dynamic behavior of the virtual mass in the global virtual environment is passive and thus guaranteed to be stable. Fig. 2.11 also shows the energy injected by the user H_{I_1}, the energy stored in the spring of the contact model H_{CM}, and the kinetic co-energy in the mass, H_{M}. The user injects energy into the contact model, from which energy flows into the mass-element which starts to accelerate. The contact between the user and the virtual mass is broken when there is no energy stored anymore in the contact model. Due to the viscous friction the kinetic co-energy is dissipated and the virtual mass slows down. As the movement of the

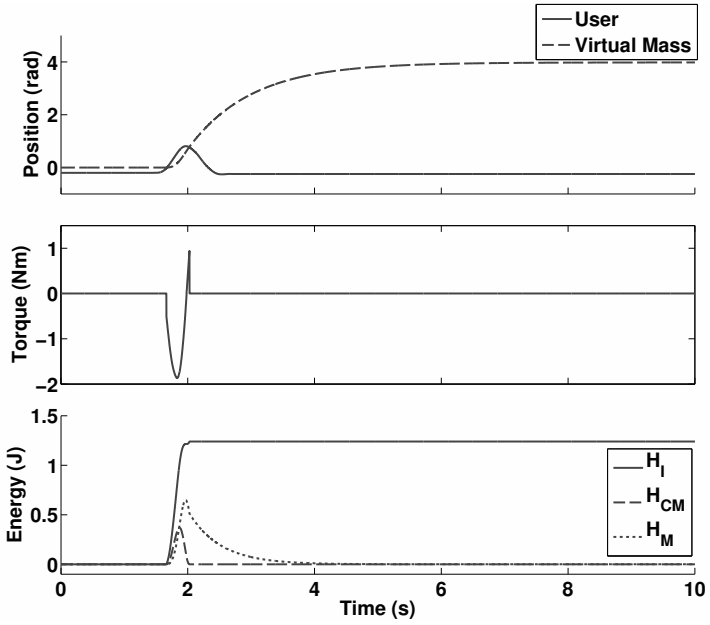

Figure 2.11: **Haptic interaction with moveable mass - PSPH framework:** The motion of the mass is determined by the stored kinetic co-energy, which is gradually dissipated.

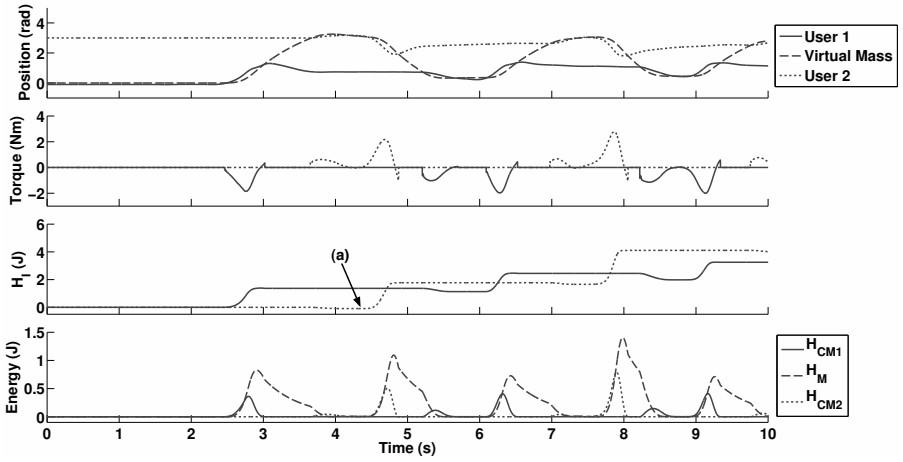

Figure 2.12: **Multi-point haptic interaction with moveable mass - PSPH framework:** Two users interact with the same virtual environment. The mass-element establishes an energy connection between the interaction ports. In the first contact phase the energy exchanged between User 2 and the virtual environment is negative, (a), as the user extracts part of the energy injected by User 1.

mass is governed by the stored energy, the mass remains perfectly stationary when no kinetic energy is present anymore.

A multi-point interaction experiment with this virtual environment is depicted in Fig. 2.12. User 1 pushes the virtual mass towards User 2. As soon as the virtual mass establishes contact with User 2 any kinetic co-energy left in the mass is stored in the second contact model, H_{CM2} upon which it is extracted by User 2. Fig. 2.12 shows that this causes the interaction energy between the virtual environment and User 2 to become negative in the first contact phase as User 2 is extracting part of the energy that was injected by User 1. User 2 finally injects energy into the virtual mass through the contact model to push it back to User 1, where the dip in H_I of User 1 during the second contact phase indicates that User 1 extracts part of the energy injected by User 2. Due to the energy-based description of the PSPH framework, passive and energy-consistent transportation of energy between different interaction ports is established.

2.7 Discussion

In this section we will briefly treat the applicability of the presented framework to admittance-type haptic interfaces and an issue related to the type of models that are implemented.

2.7.1 Admittance Causality Haptic Interfaces

The framework presented in this paper was based on impedance-type haptic interfaces. This was done as the energy exchange between the continuous and discrete domain can be determined according to (2.3). For admittance-type haptic interfaces, where a velocity is commanded by the virtual environment based on a measured force applied by the user, (2.3) does not hold.

Taking into account that the sampling frequency of the virtual environment will be relatively high compared to the changes in applied force by the user, the exchanged energy might be approximated using the trapezoidal rule

$$\begin{aligned} \overline{F}_U(\overline{k}) &= \frac{F_U(k) + F_U(k-1)}{2} \\ \Delta H_I(k) &= \overline{F}_U(\overline{k})\dot{q}_I(\overline{k})\Delta T, \end{aligned} \tag{2.46}$$

where F_U is the measured force applied by the user, $\overline{F}_U(\overline{k})$ an estimation of the average force applied by the user during sample period $\overline{k}$, and $\dot{q}_I(\overline{k})$ the velocity commanded by the virtual environment with which the haptic interface moves at the interaction point during sample period $\overline{k}$. As (2.46) is only a rough approximation of the physically exchanged energy and is not guaranteed to be conservative with respect to that energy, passivity of the virtual environment is not guaranteed.

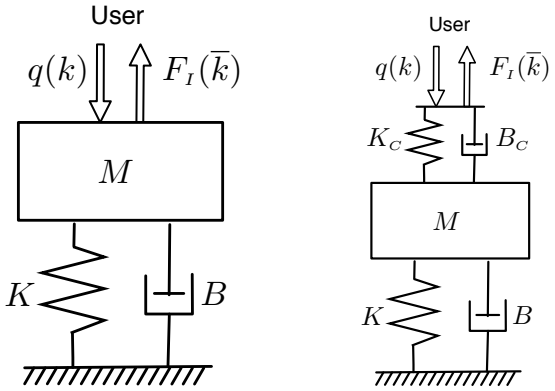

(a) 'Incorrect' Model (b) 'Correct' Model

Figure 2.13: **Modeling of a Mass-Spring-Damper system for impedance-type haptic interfaces:** without the contact model the mass-element will have a different causality depending on if the user is interacting with the system or not.

2.7.2 'Correct' Models

In Section 2.3 it was stated that any system composed of energy exchanging elements can be described as a port-Hamiltonian system. However, not every system is suitable to implement as a virtual environment. This is related to the causality of the energy storing components in relation to the causality of the haptic interface.

Consider as an example the mass-spring-damper of Fig. 2.13a. The intrinsic dynamic behavior of this model can be described as the acceleration of the mass which occurs due to the forces exerted on the mass by the spring and damper. When the user is interacting with this system with an impedance-type haptic interface this dynamic relation inside the model is changed. The user enforces a motion in the virtual environment and experiences a force feedback. Therefore, the motion of the mass is determined by the motion of the user and the constitutive relation of the mass element produces the force which was required to achieve this change of motion. This differential causality of the mass-element would require Dirac Impulse-like behavior of the virtual environment, which is physically not realizable given the discrete implementation of the virtual environment. Similarly, the interaction with a pure spring-element is problematic when an admittance-type haptic interface is used.

Such differential causalities are always due to too severe simplifications applied to the model describing the dynamic behavior of the physical system. In the mass-spring-damper system of Fig. 2.13a, an infinitely rigid contact model is assumed, whereas in reality the stiffness of every object is limited in some sense. A more accurate model describing the mass-spring-damper model would be the one given in Fig. 2.13b, where a spring-damper contact model, S_C and B_C, has been added to the model of Fig. 2.13a.

2.8 Conclusions and Future Work

In this paper the framework for implementing passive sampled port-Hamiltonian systems has been revisited. With respect to the original algorithm, a reformulation of how dissipated energy is computed is proposed. For multi-dimensional systems, this reformulation causes the entire port-Hamiltonian system to be broken down into several energy balances that need to be computed in a hierarchical order. The applicability of the approach, taking the proposed revisions into account, have been verified with various experiments.

The framework for PSPH systems offers a good compromise between the various desired goals as discussed in Section 2.2. The realism of the interaction is determined by the implemented model and the PSPH framework is capable of handling models of arbitrary size and complexity. The realism of the interaction with the implemented model is only decreased up to minimum level to maintain passivity of the interconnection of the various components. Finally, the framework is an explicit integration method so it is possible to derive an upper bound for the implementable sample frequency given the cost of computation of the model and the available computing resources.

Future work will focus on three issues related to the proposed approach. In the first place an extensive noise sensitivity analysis needs to be performed. Based on preliminary experience, viscous damping elements connected directly to the user's interaction point appear to be susceptible to measurement noise. A second issue is related to the scalability of the models. In the current implementation the number of calculations needed to compute the new state of the virtual environment increases rapidly with increasing size of the models. The third issue relates to the manner of implementing virtual environments. Complex models are usually composed of a limited number of possible combinations of a limited number of components. The resulting repetitive nature of the model structure is very suitable for automatic code generation.

CHAPTER 3

Bilateral Telemanipulation with Time Delays A Two-Layer Approach combining Passivity and Transparency

Franken, M., Stramigioli, S., Misra, S., Secchi, C. and Macchelli, A.
IEEE Transactions on Robotics

In this paper a two-layered approach is presented to guarantee a stable behavior of bilateral telemanipulation systems in the presence of time-varying destabilizing factors such as hard contacts, relaxed user grasps, stiff control settings, and/or communication delays. The approach splits the control architecture in two separate layers. The hierarchically top layer is used to implement a strategy that addresses the desired transparency and the lower layer ensures that no "virtual" energy is generated. This means that any bilateral controller can be implemented in a passive manner. Separate communication channels connect the layers at the slave and master side so that information related to exchanged energy is completely separated from information about the desired behavior. Furthermore, the proposed implementation does not depend on any type of assumptions about the time delay in the communication channel. By completely separating the properties of passivity and transparency each layer can accommodate any number of different implementations allowing for almost independent optimization. Experimental results are presented which highlight the benefit of the proposed framework.

3.1 Introduction

A telemanipulation chain is composed of a user, a master system, a communication channel, a slave system, and a remote environment for the user to act upon. The master and slave system both consist of a physical device and a controller (implemented on an embedded system). Typical applications of these chains are the interaction with materials in environments which are remote, difficult to reach, and/or dangerous for human beings. Bilateral telemanipulation occurs when the user is presented with force information about the interaction between the slave system and the remote environment, Fig. 3.1. Such a force feedback is likely to increase the performance of the user with respect to effectiveness, accuracy and safety in many practical applications, e.g. for robotic surgery as discussed by Bethea et al. (2004).

Two important criteria in bilateral telemanipulation are transparency and stability. Transparency is a performance measure of how well the complete system is able to convey to the user the perception of directly interacting with the environment (Lawrence, 1993). Many different control algorithms have been proposed in literature which try to obtain transparent bilateral teleoperation. Sheridan (1989, 1993) and Hokayem and Spong (2006) have written extensive survey papers discussing various approaches to implement bilateral telemanipulation.

Several factors can have a negative influence on the stability of bilateral controllers. Some of these factors are:

- a relaxed grasp of the user,
- stiff position and force control settings,
- hard contacts in the remote environment,
- and time delays in the communication channel between the master and the slave.

An elegant solution to prevent these factors from destabilizing the system is found in passivity theory. The interaction between passive systems is guaranteed to be stable and any proper combination of passive systems will again be a passive system (van der Schaft, 1999). As the environment can be assumed to be passive and humans can interact very well with passive systems (Hogan, 1989), guaranteeing passivity of the telemanipulation system itself ensures stability of the interactions between the user/environment and the telemanipulation system.

An interesting control problem is how to maintain passivity of the telemanipulation chain in the presence of time delays in the communication channel. As the master and slave system can be located at different sites, it is likely to assume that a certain amount of time delay will be present in the communication channel. Time delays can also occur due to various other processes other than physical distance, e.g. congestion of the network, and the coding and decoding of the signals exchanged through this network between the master and slave system. Passive control schemes that work in the presence of time delays have been developed, e.g. the scattering and wave variable approaches described by Anderson and Spong (1989) and Niemeyer and Slotine (2004). Arcara and Melchiorri (2002) and Lawn and Hannaford (1993) have compared several passivity-based algorithms to non-passive algorithms with respect to stability and the level of transparency

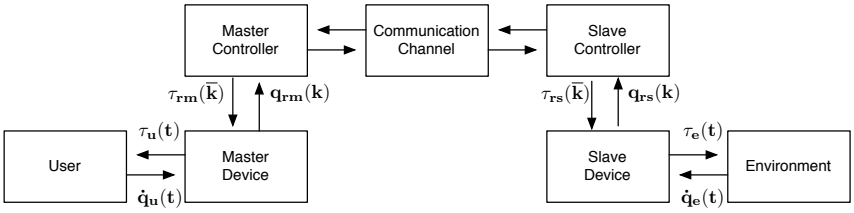

Figure 3.1: **Schematic overview of a bilateral telemanipulation chain.** Both the master and slave device are impedance-type displays. The information exchanged over the communication channel depends on the implemented controller. τ_* and $\dot{q}_*$ represent torques/forces and velocities, respectively. The subscript u, rm, rs, and e indicate the interaction between the user and the device, the actuators of the master device, the actuators of the slave device, and the interaction between the slave device and the environment, respectively.

that could be achieved for a range of communication delays. Passivity-based approaches are indeed found to be stable in the presence of even significant time delays, but the level of transparency that could be obtained was criticized.

The problem with current passivity-based methods is that they are specifically designed around a certain type of information exchange. This places strict limitations on the rest of the controller. As we will discuss there are a multitude of control architectures designed for transparency that do not fit within those passivity-based methods. Given the benefits of passivity with respect to guaranteed stability, we want to design a framework in which any controller can be implemented in a passive manner given arbitrary time delays.

In this paper we will present a new control framework for passive bilateral telemanipulation. The framework is composed of two layers placed in a hierarchically structure. Each layer is furthermore designed for a specific purpose, either to obtain transparency or to maintain passivity. In the top layer, the *Transparency Layer*, a control structure can be implemented to provide the best possible transparency of the telemanipulation chain, taking into account all available information about the system, the environment, and the task which the user is executing. The commands which are computed in this layer are passed to the bottom layer, the *Passivity Layer*. This layer contains an algorithm to maintain passivity of the total system. The key element of this algorithm is to define two communicating energy storage tanks from which the motions of both the slave and master are powered. The use of two control layers to combine passivity and transparency and the working of the *Passivity Layer*, in which energy is treated in the most general sense possible and completely free of any assumptions on the time delay in the communication channel, are the main contributions of this paper.

In the rest of this paper an impedance causality for both the master and slave systems (velocities as input and forces as output to the robotic devices) is assumed. For these devices the energy exchanged with the outside world can be precisely determined, which is a base assumption of the work presented in Section 3.4. The paper is organized as

follows: Section 3.2 introduces the concepts of passivity and also related work will be discussed. Section 3.3 further elaborates on the two-layered framework. Section 3.4 contains the theory of the *Passivity Layer*. Section 3.5 presents a full implementation and experimental results which were obtained with the proposed framework and demonstrate its effectiveness. A discussion about the proposed framework in relation to other proposed methods is presented in Section 3.6. The paper concludes and provides directions for future work in Section 3.7.

3.2 Passivity and Related Work

As mentioned in the previous section, a passive implementation of a bilateral controller ensures stable behavior of the system even in the presence of factors that could otherwise destabilize the system. We now provide a review of the important concepts pertaining to passive telemanipulation systems, which are essential for the derivations presented later in Section 3.4. Also four related approaches will be discussed. Each of these approaches constitutes a contribution to the research field, but in order to facilitate the comparison of those approaches with the framework proposed in this paper, we will indicate factors than can be considered, in the opinion of the authors, as structural limitations.

A system is said to be passive if the energy which can be extracted from it is bounded by the injected and initial stored energy. Any proper combination of passive systems will again be passive (van der Schaft, 1999). Independent of anything else, including the goal of the system, an energy balance of the telemanipulation system can be composed of the energy present in all of its components. The total energy present in the control system at instant t, $H_T(t)$, is

$$H_T(t) = H_M(t) + H_C(t) + H_S(t), \tag{3.1}$$

where $H_M(t)$, $H_S(t)$, and $H_C(t)$ represents the energy present at the master side, at the slave side, and in the communication channel, respectively. This is shown in Fig. 3.2. Assuming zero initially stored energy the passivity condition of the system is

$$H_T(t) \geq 0 \tag{3.2}$$

Physical energy exchange during operation is taking place between the user and the master system, and between the slave system and the environment. The only requirement therefore necessary to ensure a passive interconnection of the entire system with the physical world is

$$\dot{H}_T(t) \leq P_M(t) + P_S(t), \tag{3.3}$$

where $P_M(t)$ and $P_S(t)$ are respectively the power flowing from the master and slave robot into the master and slave controller and $\dot{H}_T(t)$ is the rate of change of the energy balance of the system. (3.2) ensures passivity of the system and (3.3) ensures a passive connection of the system with the physical world.

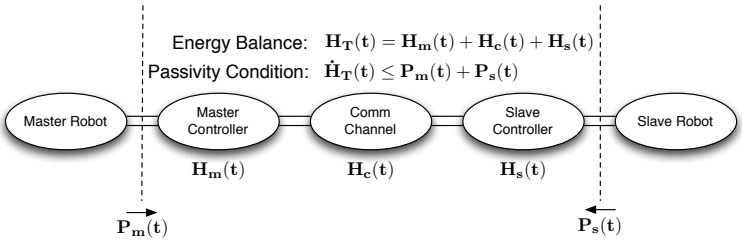

Figure 3.2: **Energy balance of the telemanipulation chain.** The double lines indicate an energetic connection.

3.2.1 Scattering/Wave Variable based approaches

It is well known that the direct exchange of power variables (velocities and forces) between the master and slave devices generates "virtual" energy in the presence of time delays in the communication channel. The scattering and wave variables approaches developed by Anderson and Spong (1989) and Niemeyer and Slotine (2004) apply a coding scheme to the power variables to turn the time delayed communication channel into a passive element. When the controllers at both the master and slave side are furthermore passive, the complete system is passive according to (3.3), such a complete approach is described by Secchi et al. (2006*a*).

A wave variable contains both information related to the energy exchange occurring at that side and the desired behavior to be displayed by the other device. Niemeyer (1996) describes a wave variable as a general "move/push" command to be interpreted by the receiving device and the returning wave describes the response of that device to the received command. This means that the motion performed by the user and the resulting force feedback are separated in time by the round-trip time of the communication channel. Other transparency related problems arise due to the nature of the (de)coding process and/or non-idealities in the communication channel (time-varying delay and package loss), e.g. position and force mismatch. Extensions to improve the performance include the use of Smith Predictors, e.g. (Ching and Book, 2006), the transmission of wave integrals, e.g. (Niemeyer and Slotine, 2004), and the combination of wave variables with the transmission of interaction measurements as discussed by Tanner and Niemeyer (2005)

3.2.2 Time Domain Passivity Control

A different solution to the passivity problem was proposed by Ryu et al. (2004*b*). There the Time Domain Passivity Control (TDPC) algorithm, developed by Hannaford and Ryu (2002) for passive interaction with virtual environments, was applied to bilateral telemanipulation. The TDPC approach introduces a Passivity Observer (PO) and a Passivity Controller (PC). This algorithm enforces (3.3) with $H_C = 0$ as no communication channel is considered. For this algorithm simultaneous information about the energy exchange at the master and the slave side is required and is as such not applicable to systems with time delays in the communication channel. Two extensions have been proposed to extend

the TDPC approach to the time-delayed situation.

Artigas et al. (2007) incorporate an energy reference algorithm. Artigas et al. (2008) further extended this approach to also include a passive coupling between the continuous and discrete domain. The reference algorithm applies a forward and backward PO which estimates the energy in the communication channel based on the locally transmitted and received power variables and an estimate of the fixed transmission delay. At each side of the communication channel a PC maintains passivity according to the PO at that side.

Ryu and Preusche (2007) split the energy interaction into an incoming and outgoing energy flow, E_{in} and E_{out}. Each side transmits its E_{in} to the other side where passivity of E_{out} with respect to the received value of E_{in} is maintained by a PC. As the transmitted packets symbolize an amount of energy, the passivity of this approach is perfectly robust against time-varying delays and even packet loss in the communication channel.

These approaches have merged into a single algorithm as proposed by Ryu et al. (2010). However, these approaches are not suitable for the implementation of Impedance Reflection (IR) algorithms, e.g. (Tzafestas et al., 2008), where the feedback force to the user is predicted based on a local, possibly adaptive, model of the remote environment. The work of Artigas et al. is centered around the transmission of power variables and cannot accommodate the transmission of model parameters. In the algorithm of Ryu et al. the problem is that with an IR algorithm the energy extracted by the user, E_{out} at the master side, is likely to occur before E_{in} actually occurs at the slave side. This means that the PC at the master side will prevent the computed feedback force to be applied to the user as it would force the PO to become negative. A first approach to use a TDPC algorithm with an IR algorithm was proposed by Kawashima et al. (2008*b*). A TDPC structure is used to adapt the locally computed feedback force based on the actual measured, but delayed interaction force to make the system passive. This approach requires exact knowledge about the time delay that is present in the communication channel.

3.2.3 Energy Bounding Algorithm

Another approach originating from research towards passive interaction with virtual environments is the Energy Bounding Algorithm (EBA) proposed by Kim and Ryu (2010). Seo et al. (2008) have applied the EBA to time-delayed bilateral telemanipulation. The EBA limits the generated "virtual" energy to the dissipated energy by friction at the master and slave side. For this it uses models of viscous friction in the devices, possibly extended with assumptions about the viscous friction in the user's arm and/or environment.

Deviations from the physical friction with respect to the modeled friction can jeopardize stability of the system for which reason a conservative lower bound of the friction needs to be selected. Due to the nature of the derived update rule, as indicated by the authors in (Kim and Ryu, 2010), the force applied by the control system cannot be adjusted when the devices are perfectly stationary. Finally, it appears, based on (Seo et al., 2008) that in the bilateral telemanipulation application it can only work when the force exerted by the slave device is used as feedback force to the user instead of the measured interaction force between the slave device and the remote environment. This can severely limit

the achievable transparency in the presence of time delays and limits the implementable bilateral controller to that specific implementation.

3.2.4 Passive Set-Position Modulation

A recent approach to deal with bilateral telemanipulation is the Passive Set-Position Modulation (PSPM) framework proposed by Lee and Huang (2008*b*, 2010). This approach is centered around a spring-damper controller. The energy dissipated by the "virtual" damper is stored in an energy tank. The jump in spring potential due to the discrete jump of the set-position by the control algorithm is limited to the available energy in the tank (a negative jump adds energy to the tank). In the bilateral telemanipulation application excess energy in the tank is transmitted to the other side, or dissipated.

There are several issues related to the working of the PSPM. Most notably, the underlying assumption is that part of the control system can be regarded as continuous-time. The set-position signal is a discrete signal, but the position of the device, as used in the servo control loop, is considered as a continuous signal. However, the control system is always sampled even though the update rate for the set-position might be much lower than the fundamental sampling rate of the servo control loop. It is well known that the description of a passive element in continuous-time can generate energy when implemented on a discrete medium. Therefore, an extended form of the passivity condition by Colgate et al. (1993) relating the parameters of the controller, the sample frequency, and the device friction is necessary to guarantee passivity of the system. Assuming a constant sampling time, ΔT_S, the condition described by Lee and Huang (2010) becomes:

$$B_{dev} \geq 2B_C + \frac{K_C \Delta T_S}{2} \tag{3.4}$$

where B_{dev}, B_C, and K_C indicate the physical viscous device friction, and the implemented viscous damping and stiffness in the PSPM-element, respectively. (3.4) states that the required physical viscous damping has to be at least twice as large as the implemented virtual damping for the system to be guaranteed to be passive.

The input to the controller is a set-position for the spring. This means that bilateral control algorithms that compute a desired force to be applied to the device(s) require intermediate data processing. This data processing transforms a desired control force into the required set-position. This appears elaborate, noise sensitive due to the inherent presence of the velocity estimate, and also requires the set-position signal to be updated at the same frequency as the velocity estimate. This last factor degrades the validity of the assumption that the servo control loop can be considered to be in continuous-time.

Finally, the PSPM relies on the use of a constant viscous damper to extract energy into the energy tanks. This means that the response will already always be damped even when there is enough energy in the tank. The excess extracted energy is artificially dissipated by thresholding the level of the energy tank. This constant damping also needs to be taken into account in any higher level control architecture that is connected through intermediate data processing to prevent an over-damped response of the system. With the PSPM it is

therefore difficult to separate the design of the controller to display the desired behavior and the manner in which passivity is maintained.

3.3 Proposed Two-Layer Framework

In the previous section several passivity-based control structures were discussed. Without making any assumptions about the type of controllers implemented we can formulate the control goals of a passive bilateral telemanipulation system as follows:
The slave device needs to display the behavior desired by the user, and the master device needs to accurately provide force feedback about the interaction between the slave device and the remote environment, unless this behavior violates the passivity condition of the telemanipulation system

This shows that a natural layering in control objectives arises. First a desired control action needs to be computed so that the master and slave device display the desired behavior/information. Then a "check" is to be performed of how this desired action will influence the energy balance of the system. If passivity will not be violated it can directly be applied to the physical system, but if passivity is expected to be lost due to the desired control action it should be modified before application to the physical system. Such an approach allows for the highest possible transparency given that passivity needs to be preserved.

This natural layering can also be directly transformed into a control structure. An algorithm that combines transparency and passivity in the discussed manner would be a two-layer structure as shown in Fig. 3.3. The *Transparency Layer* contains a control algorithm to display the desired behavior and obtain transparency. Ideally, this could be any type of bilateral control algorithm. The only requirement the framework presented in this paper places on the implemented controller is that it computes forces to be applied to the master and slave devices. In order to compute the desired control action, $\tau_{TL*}(k)$, access is required to a specific part of the measured interaction data, e.g. forces, positions, and/or velocities, where m and s instead of $*$ indicate the master and slave, respectively. The *Passivity Layer* on the other hand monitors and enforces the energy balance of the system according to the algorithm discussed in Section 3.4.

The benefit of the strict separation into layers is that the optimization of the strategy used to ensure optimal transparency does not depend on the strategy used to ensure passivity and vice versa. As passivity does not have to be considered in the design of the *Transparency Layer*, the whole range of control techniques which are non-passive, e.g. most filtering techniques, can be applied without problems. Also due to this strict separation into layers two two-way communication channels between the master and slave system can be defined. One channel is used to communicate energy exchange related information between the *Passivity Layers* and the second channel to communicate information related to the desired behavior to be displayed by the devices between the *Transparency Layers*. This means that no (de)coding process is required as with Wave Variable based approaches. Furthermore, no restrictions are necessary on the information exchanged between the *Transparency Layers*.

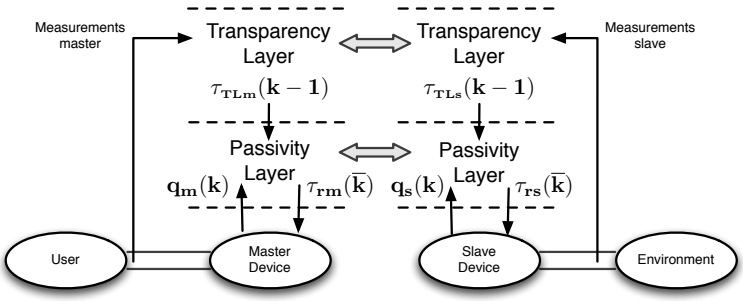

Figure 3.3: **Two layer algorithm for bilateral telemanipulation.** The double connections indicate an energetic interaction.

It should be noted that of the passivity-based control structures listed in the previous section the time-delayed TDPC approach by Ryu and Preusche (2007) and Ryu et al. (2010) and the PSPM framework by Lee and Huang (2010) can also be represented as a two-layered framework as depicted in Fig. 3.3. However, as mentioned in the previous section the implementation of the time-delayed TDPC approach restricts the types of bilateral controllers that can be implemented (no impedance reflection algorithms) and furthermore only acts upon a loss of passivity and was not intended to shape the interaction to prevent a loss of passivity. The time delayed TDPC approach is centered on the energy exchange that occurs in the communication channel. Any augmentation of the force feedback to the user in order to improve his performance during the execution of a task, e.g. by incorporating virtual fixtures as described by Abbott, Marayong and Okamura (2007), needs to be separately implemented with additional measures to ensure stability (Colgate et al., 1993). The PSPM approach can accommodate these features by means of the intermediate data processing capabilities, but requires an additional hardware-controller settings condition to be satisfied. Furthermore, although the intermediate data processing capability is there, its implementation might not be straightforward. In the next section we will introduce an implementation of the *Passivity Layer* that is in the opinion of the authors free of such limitations.

3.4 Passivity Layer

In this section we will discuss how the *Passivity Layer*, which was introduced in the previous section, works[1]. The only thing that is needed to know about the *Transparency Layer* is that it generates desired torques to be applied to the master and slave devices.

Assume that the slave device is operating under position control of the master device. Every movement the slave device makes will have an associated energetic cost. In order for the system to be passive this amount of energy will have to be present at the slave side

[1]The index k is used to indicate instantaneous values at the sampling instant k and the index $\overline{k}$ is used to indicate variables related to an interval between sampling instants $k-1$ and k.

at the moment the movement is executed. The passivity condition of (3.2), applied to the energy balance of the system (3.1), also requires that that same amount of energy will have had to be injected previously by the user at the master side and to be transported to the slave side through the communication channel. Depending on the implemented bilateral control algorithm the same can apply in reverse to energy extraction at the master side. This clearly requires the transport of energy between the master and the slave system.

Due to the time delays separating the master and slave system, it is not possible to simultaneously monitor the energy exchange at both interaction ports. This means that when the user commands a motion to be executed by the slave, it is not known *a priori* (exactly) how much energy is required by the slave device to execute that motion. To this end, the concept of a lossless energy tank is introduced in the *Passivity Layer* at both the master and the slave side, which can exchange energy. The level of these tanks can be interpreted as a tight energy budget from which controlled movements can be powered and which are being replenished by the user at the master side when necessary, or if possible/desired also at the slave side. If the energy level in the tanks is low, the controlled movements the system can make are restricted. An extreme situation occurs when the tank is completely empty in which situation the system cannot make a controlled movement at all. Passivity will always be maintained as all the energy present in the system has been injected by the user and each system cannot use more energy than is available in its energy tank.

Adjustments made by the *Passivity Layer* to the commands of the bilateral controller, implemented in the *Transparency Layer*, can have a negative influence on the achievable transparency by the telemanipulation system. This decrease however is minimized to the point where passivity is maintained and thus stable behavior guaranteed.

In the following sub-sections the four components of the *Passivity Layer* at each side are discussed. As these operations are implemented at both sides in the same manner, subscripts indicating the master and slave have been omitted for now. In order to illustrate the working of the *Passivity Layer*, a flow chart of all the steps in the *Passivity Layer* for either side of the telemanipulation system is presented in Fig. 3.6 at the end of this section.

3.4.1 Monitoring energy flows

At both the master and the slave side, the following three energy flows can be identified:

- an energy exchange with the physical world,
- an energy flow to the other system, and
- an energy flow from the other system.

We will now show how each of these flows can be monitored and regulated in order to maintain passivity according to (3.2) and (3.3).

On the master and slave side the controllers will have to control two robots which will interact with the user and the environment. As the controller is implemented on some sort of embedded processing unit there is a connection between the continuous and discrete domain. Let $\dot{q}(t)$ represent the velocity vector of the actuators at time t and $q(k)$ the sampled position vector of the actuators at sample instant k. Consider the sample period

$\overline{k}$. The torques exerted by the actuators on the robot during sample period $\overline{k}$ is given by $\tau_r(\overline{k})$, which is held constant during the sample interval. Thus, the energy exchange between the discrete time controller and the physical world, $\Delta H_I(k)$, during the sample interval between the time instants, $k-1$ and k is

$$\begin{aligned} \Delta H_I(k) &= \int_{(k-1)\Delta T_S}^{k\Delta T_S} \tau_r(\overline{k})\dot{q}(t)dt \\ &= \tau_r(\overline{k})(q(k)-q(k-1)) \\ &= \tau_r(\overline{k})\Delta q(k), \end{aligned} \tag{3.5}$$

where ΔT_S is the length of the sample period and $\Delta q(k)$ the computed position difference at sample instant k that occurred during sample period $\overline{k}$. Therefore, only a position measurement is required to determine the energy exchange, which was introduced by Stramigioli et al. (2005). The computation of (3.5) assumes a perfect servo-loop and noise-free position measurement. If bounds can be derived for the inaccuracies in both the servo-loop and the measurement, (3.5) can be adjusted to account for these imperfections. As (3.5) only holds for impedance type systems (force out causality) we require the entire control structure, and thus the *Transparency Layer*, to adhere to this causality.

As far as energy exchange between the master and slave is concerned, we can consider the possibility to send energy quanta from the master to the slave when energy is available in the energy tank at the master side and vice versa. These quanta can be transmitted in the form of packets containing the amount of energy send. Several possible communication protocols for this energy transfer will be discussed in Section 3.4.3. Both master and slave can implement completely asynchronously the following operations (3.6)-(3.8). When such an energy packet arrives at the other side it is stored in a receiving queue.

$$H_+(k) = \sum_{i \in Q(k)} \bar{H}(i), \tag{3.6}$$

where $Q(k)$ represents the set of all energy packets present in the receiving queue of the master at sample instant k, $\bar{H}(i)$ represents the i^{th} energy packet. Therefore, $H_+(k)$ represents the total amount of energy which is present in the receiving queue at that time instant. At each sample instant k the receiving queue is emptied, meaning that the energy present in the receiving queue, $H_+(k)$ is added to the level of the energy tank. The exchanged energy with the physical world during the previous sample period is computed according to (3.5) and subtracted from the level of the energy tank. The energy level of the tank after these operations, $H(k)$ is

$$H(k) = H(\overline{k}) + H_+(k) - \Delta H_I(k), \tag{3.7}$$

where $H(\overline{k})$ is the energy level of the tank before the operations at sampling instant k. Based on the chosen energy transport protocol an energy quantum, $H_-(k)$, is determined to transmit to the other side. This energy quantum is at least limited to $H(k)$ to preserve passivity. The amount of energy that is transmitted is extracted from the energy tank. The

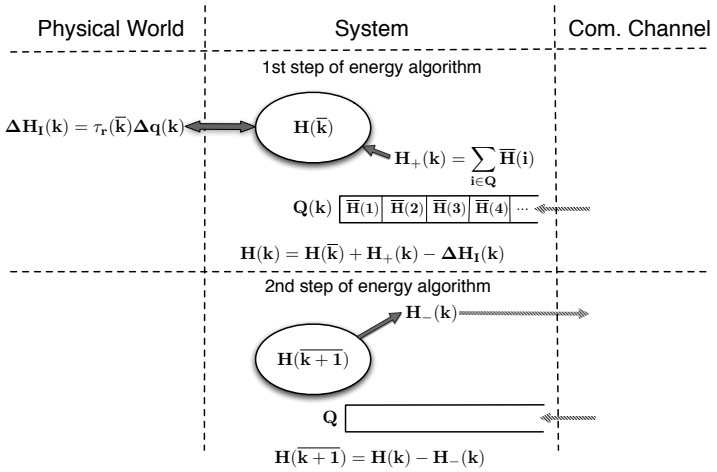

Figure 3.4: **Processing energy flows:** The energy received out of the communication channel is added to the level of the energy tank and the energy exchanged with the physical world is subtracted from the the energy level (1st step). An energy packet is transmitted to the other system (2nd step). The double arrow indicates that the energy exchange with the physical world can both be positive and negative.

energy which is left in the tank after these operations and thus available during the next sampling period, $H(\overline{k+1})$ is

$$H(\overline{k+1}) = H(k) - H_-(k). \tag{3.8}$$

With this algorithm we are therefore able to compute the exact energy balance at each instant of time when sampling occurs and passivity according to (3.1), (3.2), and (3.3) is guaranteed. The level of the energy tanks is the total energy present on the master and slave side, H_M and H_S respectively. The sum of all the energy packets in the communication channel gives the total energy present in the communication channel, H_C. A graphical representation of (3.5) through (3.8) is given in Fig. 3.4 indicating the two steps of the energy flow computation.

As each packet represents an amount of energy, the passivity of the communication channel is unaffected by any non-deterministic time delay, similar to Ryu et al. (2010) and Lee and Huang (2010). The change of energy in the communication channel at sample instant k, $\Delta H_C(k)$, can be expressed as

$$\Delta H_C(k) = H_{-M}(k) - H_{+M}(k) + H_{-S}(k) - H_{+S}(k), \tag{3.9}$$

where $H_{-M}(k)$ and $H_{+M}(k)$ are the energy flow into and from the communication channel at the master side and $H_{-S}(k)$ and $H_{+S}(k)$ the energy flows at the slave side. The

total energy in the communication channel, $H_C(k)$, is

$$\begin{aligned} H_C(k) &= \sum_{i=1}^{k} \Delta H_C(k) \\ &= \sum_{i=0}^{k} H_{-M}(i) - H_{+M}(i) + H_{-S}(i) - H_{+S}(i), \end{aligned} \tag{3.10}$$

Due to the time delay in the communication channel

$$\begin{aligned} H_{-S}(i) &= H_{+M}(i + d_{SM}(i)) \\ H_{-M}(i) &= H_{+S}(i + d_{MS}(i)), \end{aligned} \tag{3.11}$$

where $d_{SM}(i) \geq 0$ and $d_{MS}(i) \geq 0$ represent the, possibly non-deterministic, time delays in the communication channel, including possible package loss. Therefore

$$\begin{aligned} \sum_{i=0}^{k} H_{-M}(i) &\geq \sum_{i=0}^{k} H_{+S}(k) \\ \sum_{i=0}^{k} H_{-S}(i) &\geq \sum_{i=0}^{k} H_{+M}(k), \end{aligned} \tag{3.12}$$

so that

$$H_C(k) \geq 0 \quad \forall k, \tag{3.13}$$

which means that the communication channel can never produce energy as long as packet duplication is prevented. Duplicated packets can easily be handled by including a timestamp in each packet.

3.4.2 Energy tanks

In the previous section we have shown that there exist three energy flows at both the master and the slave side. The desired control actions determined by the *Transparency Layer* will influence the energy exchange with the physical world and thus how much energy is flowing into or out of the total system. In order to completely separate the *Passivity Layer* from the *Transparency Layer* a method is required to regulate the energy level independent of what the *Transparency Layer* is commanding.

To this end a Tank Level Controller (TLC) is defined in the *Passivity Layer* at the master side. The function of this TLC is to monitor the energy level of the local tank, $H_M(\overline{k+1})$, with respect to a desired level H_D. Whenever $H_M(\overline{k+1})$ is lower than H_D at sampling instant k, the TLC is to extract a small additional amount of energy from the user during the next sampling period $\overline{k+1}$ to replenish the tank. Using such a TLC will enable the control architecture to always recover from a deadlock situation in a passive manner when all the energy stored in the system is depleted.

Several TLC implementations are possible. In this paper, the TLC is a modulated viscous damper, which applies a small opposing torque, $\tau_{TLC}(k)$ to the user's movement to extract energy from the user into the energy tank

$$\begin{aligned} \tau_{TLC}(k) &= -d(k)\dot{q}_m(k) \\ d(k) &= \begin{cases} \alpha(H_D - H_M(\overline{k+1})) & \text{if } H_M(\overline{k+1}) < H_D \\ 0 & \text{otherwise} \end{cases}, \end{aligned} \tag{3.14}$$

where α is a parameter that can be used to tune the rate at which energy is extracted from the user and $\alpha > 0$. If α is set to a high value and/or the user moves very fast an overshoot of the energy level in the system with respect to the desired energy level can occur. The value to be set for α and H_D is highly dependent on the device characteristics.

It is important to note that although this strategy might appear similar at first glance to the TDPC strategy by Ryu et al. (2004*b*), its purpose is in fact very different. The PC element in the TDPC algorithm is used to dissipate virtually generated energy whereas in this application the modulated damper is primarily activated to make energy available in the system. It should also be noted that the presented strategy is only one way to extract energy from the user and that the framework can accommodate many alternatives.

3.4.3 Energy transport

The TLC will make energy available at the master side, but energy is required at the slave device for it to be able to perform its task. In this section various protocols are discussed that can be implemented to regulate the distribution of energy through the system, ranging from simple open loop protocols to more complex protocols.

Simple Energy Transfer Protocol

Energy can be distributed through the system using the Simple Energy Transfer Protocol (SETP). Both the master and slave system transmit a fixed fraction, β, of its energy level (when energy is available) to the other system. This will cause the total energy in the system to be distributed over the master and slave system and the communication channel. As this is a bilateral transfer protocol it is not dependent on where the energy is entering the system. This is illustrated in Fig. 3.5, where the energy tanks are depicted as water barrels, each packet as a glass, and the energy quanta of each packet as the water level inside the glass.

When the system can be described as a discrete Linear Time Invariant (LTI) system it can be proven mathematically that the energy levels in the two tanks will converge to the same value when there is no interaction with the physical world, irrespective of the initial energy distribution. The LTI model, Σ_1, of the system is

$$\Sigma_1 : x(\overline{k+1}) = \begin{bmatrix} 1-\beta & 0 \\ 0 & 1-\beta \end{bmatrix} x(\overline{k}) + \begin{bmatrix} 0 & \beta \\ \beta & 0 \end{bmatrix} x(\overline{k-d}), \tag{3.15}$$

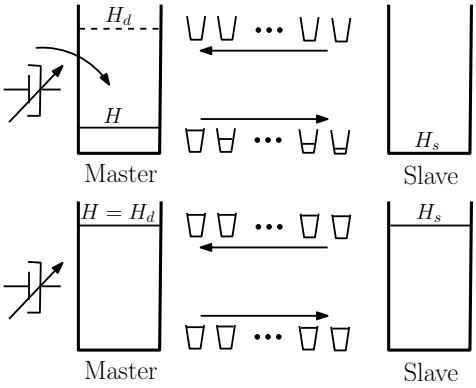

Figure 3.5: **Illustration of level synchronization between energy tanks:** The modulated damper extracts energy from the master and the implemented energy transport protocol forces the energy level in the master and slave tank to synchronize.

where $x = \begin{bmatrix} H_M \\ H_S \end{bmatrix}$ and d indicates the constant communication delay, respectively. From Σ_1 a new state, H_{dif} is derived that describes the dynamics of the difference between the tank levels

$$\begin{aligned} H_{dif}(\overline{k+1}) &= H_M(\overline{k+1}) - H_S(\overline{k+1}) \\ &= (1-\beta)H_{dif}(\overline{k}) - \beta H_{dif}(\overline{k-d}). \end{aligned} \tag{3.16}$$

The characteristic polynomial, $P(z)$, describing the dynamic behavior of just this new state is described as Ren et al. (2003)

$$P(z) = z^{d+1} - (1-\beta)z^d + \beta. \tag{3.17}$$

Investigating the stability of this system, without explicitly computing the roots of the polynomial, can be performed using the Jury Stability Criterion Jonckheere and Ma (1989). This criterion states that if certain terms, that are computed from the coefficients of the polynomial, are positive the system is asymptotically stable. Application of this criterion to $P(z)$ indicates the following terms have to be positive

$$\begin{aligned} \frac{4\beta(1-\beta)}{d\beta+1} &> 0 \\ \frac{-r\beta^2 + (r-1)\beta + 1}{(r-1)\beta+1} &> 0 \quad \forall r \in [0..d-1]. \end{aligned} \tag{3.18}$$

For $0 < \beta < 1$ and any d all the terms of (3.18) are positive. This indicates the tank level difference using the SETP is asymptotically stable and will converge to zero in the absence of external inputs, albeit that the settling time can be extremely large for large d and/or β. If the time in which the TLC extracts the energy to fill the master tank is small

compared to the settling time of the SETP an overshoot of the energy level of the tanks with respect to H_D can occur.

This derivation of asymptotic stability also holds for systems, Σ_2, with asynchronous delays as long as the total number of delay states, n, is even. Such a system has the same characteristic polynomial, $P_1(z)$ as Σ_1, given that $n = 2d$,

$$P_1(z) = z^{n+2} - 2(1-\beta)z^{n+1} + (1-\beta)^2 z^n - \beta^2. \tag{3.19}$$

Asymptotic stability of Σ_1 implies asymptotic stability of Σ_2.

Advanced Energy Transfer Protocols

The SETP implies that energy quanta are continuously being exchanged between the master and slave system. This indicates that the user besides filling both tanks with energy will also have to saturate the communication channel with energy packets. For Σ_1 there are $2d$ energy packets in the communication channel. Assume that the TLC has extracted precisely enough energy to let the energy level in both tanks converge to H_D and this convergence has taken place. In that situation each energy packet in the communication channel has the same value βH_d. So in this situation the total amount of energy in the communication channel, $\overline{H}_C$, is:

$$\overline{H}_C = 2d\beta H_D. \tag{3.20}$$

The total amount of energy in the communication channel can therefore become quite large for larger time delays and/or β.

More complex transfer protocols can be implemented, each with its own specific benefits and drawbacks. A transfer protocol that is still simple, but does not have constant energy exchange between master and system, is to change the positive energy quanta being sent from the slave to the master into energy requests. The transfer protocol at the master side will then send an initial amount of energy to the slave side to fill the tank and the slave will only send energy requests to the master when the level in the tank drops below that desired level due to energetic interaction with the physical world. The master side records the total energy request by the slave and will send a percentage of its available energy towards the slave until the energy request is satisfied. A drawback of this protocol is that the energy request and the subsequent delivery are separated in time by the round-trip time of the communication channel. This will have to be taken into account when selecting the desired energy level of both tanks.

Now assume that an IR algorithm is implemented in the *Transparency Layer*. As the interaction forces are now predicted at the master side, it is possible to record the energy exchange and transmit this energy directly to the slave side. The energy tanks are then solely used to deal with model inaccuracies and the delays in the communication channel.

The above shows that although the *Transparency Layer* and *Passivity Layer* are completely separated and can be tuned independently, the energy transfer protocols that can be implemented in the *Passivity Layer* are restricted by the chosen implementation of the *Transparency Layer*.

3.4.4 Saturation of controlled torque

The *Transparency Layer* computes a controlled torque, $\tau_{TL}(k)$ at each side, to be applied to the master and slave device during sampling period $\overline{k+1}$ to display the desired behavior. At both sides, the *Passivity Layer* enforces limits on this desired torque in order to maintain passivity. The resulting limited torque, $\tau_{PL}(k)$, will be applied to the actuators during sample period $\overline{k+1}$. It should be noted that although $H(\overline{k+1})$ indicates the energy level in the tank during the sample period $\overline{k+1}$ its value is known after the procedure of Section 3.4.1 has been performed at sample instant k. This procedure is performed before $\tau_{PL}(k)$ is computed so the value of $H(\overline{k+1})$ can be used to compute $\tau_{PL}(k)$.

The fundamental limit which the *Passivity Layer* enforces is that when no energy is available at a side, the controlled torque that can be applied at that side during the coming sampling period is zero

$$\tau_{max1}(k) = \begin{cases} 0 & \text{if } H(\overline{k+1}) \leq 0 \\ \tau_{TL}(k) & \text{otherwise} \end{cases}. \tag{3.21}$$

Between two sample instants there is no way to detect, act upon, and therefore prevent a possible loss of passivity. It is however possible to minimize the chance of such a loss by implementing additional saturation functions. We know that the interval before a next sample will last ΔT_S seconds and suppose the device is moving with velocity $\dot{q}(\overline{k})$. If the force applied during sample period $\overline{k+1}$ were to have a relatively small influence on the velocity with which the device is moving, an initial estimate of the energy exchange that will occur would be:

$$\Delta H_I(\overline{k+1}) = \tau(\overline{k+1})\dot{q}(\overline{k})\Delta T_S \tag{3.22}$$

so an upper bound for $\tau(\overline{k+1})$ to limit this energy exchange to the available energy would be

$$\tau_{max2}(k) = \frac{H(\overline{k+1})}{\dot{q}(\overline{k})\Delta T_S} \tag{3.23}$$

The applied force during $\overline{k+1}$ however will most often influence the velocity with which the device is moving. This influence might be approximated based on a competent dynamic model of the system so that the worst case velocity of the system can be expressed as function of the applied force, the current velocity, and the duration of the sample period $\dot{q}_{max}(\tau_{PL}(\overline{k+1}), \dot{q}(\overline{k}), \Delta T_S)$. $\dot{q}_{max}$ can then be used in (3.23) to derive $\tau_{max2}(k)$. This still neglects the influence the user and environment will have on the motion of each device. Therefore it is still possible that more energy is extracted at either side than is stored in the tank. If that were to happen, (3.21) shuts off the commands from the *Transparency Layer* and thus prevents the system from becoming unstable.

The above two saturation functions ensure that the system will remain passive, or at least minimize the chance of a momentary loss of passivity from occurring. Additional saturation methods can be thought of that not only maintain passivity, but shape the interaction in a beneficial way depending on the amount of energy available in the system.

An additional saturation method that can be useful is for instance to define a mapping, $g(H(\overline{k+1}))$, from the current available energy in the tank to the maximum torque that can be applied. Meaning:

$$\tau_{max3}(k) = g(H(\overline{k+1})). \tag{3.24}$$

This mapping can be designed in such a way that a safe interaction in complex situations is guaranteed. What a *safe interaction* is, depends on the task, the environment, and the circumstances under which the task has to be executed in the environment. Therefore no general implementations of (3.24) can be provided. Two examples where (3.24) might be useful will now be sketched. Assume that an impedance reflection algorithm has been implemented in the *Transparency Layer* and that the environment has not yet been properly identified. In such a situation the position controller in the *Transparency Layer* at the slave side could exert excessive forces on the environment to track the motions of the master. This is likely to damage the objects that are encountered in the environment. However, in such situations the amount of energy in the system is very limited (the user is not yet interacting with the virtual model) and so (3.24) could be designed to prevent excessive forces from being applied to the objects in the environment.

A second example where (3.24) could be useful is discussed by Franken et al. (2009). There a mapping is used in combination with the SETP to gently release objects which the slave is grasping when a communication blackout should occur.

The maximum allowable torque, $\tau_{max}(k)$, is the lower bound of all the various limiting/saturation functions

$$\tau_{max}(k) = \min(\tau_{max1}(k), \tau_{max2}(k), \tau_{max3}(k), ...), \tag{3.25}$$

where ... indicate other limiting/saturation functions that can be implemented. These additional functions for instance could be beneficial for a specific device, environment, and/or task to be executed. Note that all limiting functions except τ_{max1} are optional, although the exclusion of τ_{max2} and/or τ_{max3} can result in unwanted switching behavior of the *Passivity Layer*. It should also be noted that the limiting/saturation functions in the *Passivity Layer* at the master and slave side do not necessarily have to be identical.

The torque, $\tau_{PL}(k)$, which is the bounded version of the torque, $\tau_{TL}(k)$, requested by the *Transparency Layer* is computed as

$$\tau_{PL}(k) = \operatorname{sgn}(\tau_{TL}(k)) \min(|\tau_{TL}(k)|, \tau_{max}(k)). \tag{3.26}$$

The final torques to be applied to the master and slave devices during the sample period $\overline{k+1}$, $\tau_{rm}(\overline{k+1})$ and $\tau_{rs}(\overline{k+1})$, respectively, are

$$\begin{aligned} \tau_{rm}(\overline{k+1}) &= \tau_{PLm}(k) + \tau_{TLC}(k) \\ \tau_{rs}(\overline{k+1}) &= \tau_{PLs}(k), \end{aligned} \tag{3.27}$$

where $\tau_{PLm}(k)$ and $\tau_{PLs}(k)$ are the torques computed by the *Passivity Layer* at the master and slave side, respectively. At the master side $\tau_{TLC}(k)$, which results from the TLC of (3.14), is superimposed on $\tau_{PLm}(k)$ before application to the device.

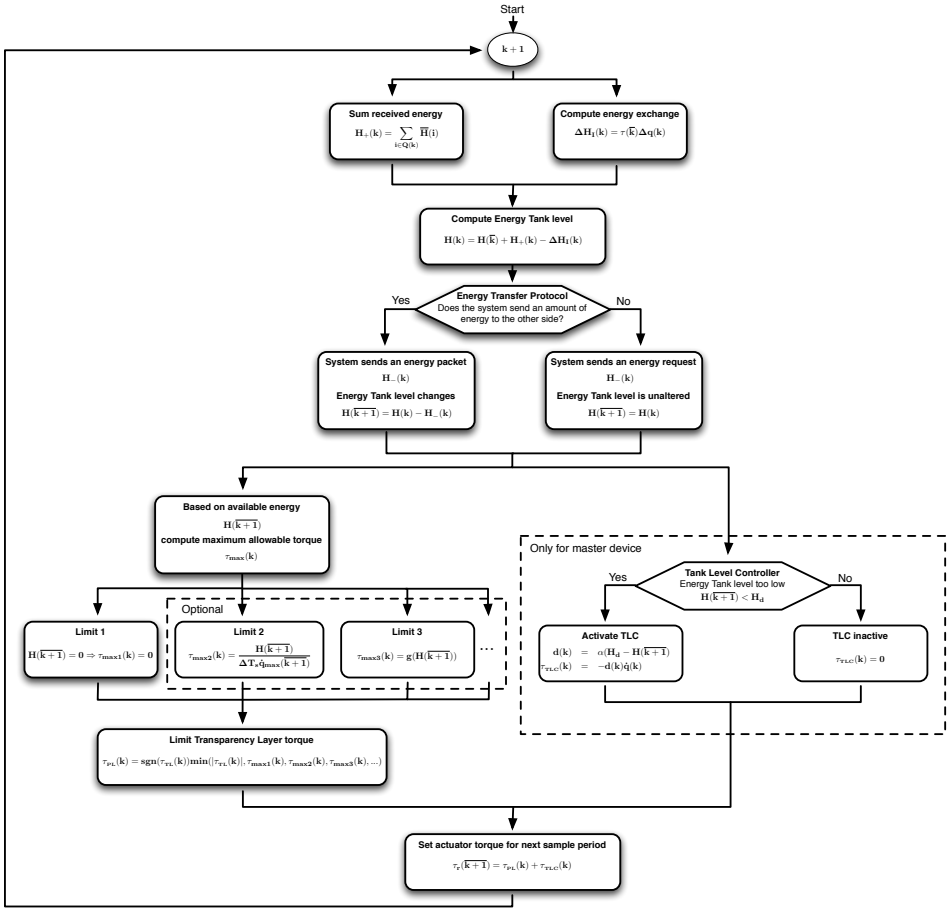

Figure 3.6: **Workflow of the complete *Passivity Layer* at either side of the telemanipulation system:** This workflow assumes that $\tau_{TL}(k)$ has already been computed. First, the incoming energy flows are evaluated. Afterwards the energy flow towards the other system is computed and handled. Finally, the limiting values for the torque originating from the *Transparency Layer* are computed. For the master system the Tank Level Controller is activated if necessary. The limited *Transparency Layer* torque and TLC torque combined form the feedback force to the user for the next sampling period.

3.5 Experimental Results

In this section we will provide experimental results that were obtained with the setup depicted in Fig. 3.7. The setup consists of two identical one degree of freedom devices powered by a DC motor without gearbox. A high-precision encoder with $65\,\mathrm{k}$ pulses per rotation is used to record the position of each device. The mechanical arm of each device

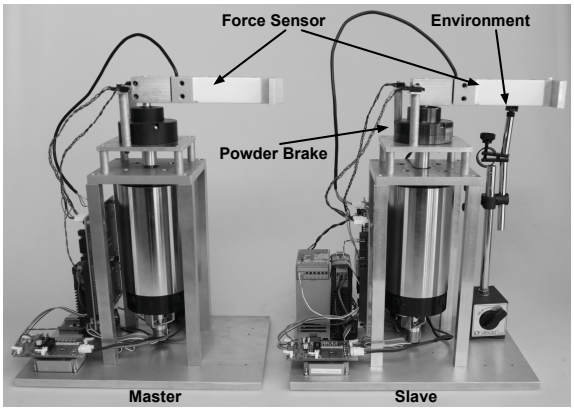

Figure 3.7: **Experimental setup:** The setup consists of two identical one degree of freedom devices powered by an electromotor without gearbox. The position of each motor is recorded with a high-precision incremental encoder and the mechanical arm consists of a linear force sensor to record the interaction force between the user/environment and the devices.

contains a linear force sensor to record the interaction force between the user/environment and the devices. Both devices are controlled from the same embedded controller running a real-time Linux distribution. The controllers are implemented in the program 20-sim (Controllab Products B.V., 2010) and real-time executable code specific for this setup is generated directly from 20-sim and uploaded to the embedded controller by means of the program 4C (Controllab Products B.V., 2010). The sampling frequency of the control loop is $1\,\mathrm{kHz}$. As environment a mechanical spring with a stiffness of approximately $1500\,{}^{\mathrm{N}}/_{\mathrm{m}}$ is used. The recorded position of this spring in the environment varies slightly between experiments as incremental position encoders are used and the initial position of the slave device is not perfectly equal for each experiment.

Two different bilateral controllers were implemented to show the benefits and flexibility of the Two-Layer approach. A regular Position-Force (PF) controller is implemented in a situation without and with time delay. In the second experiment the time delay is still present and the PF controller is replaced with an IR algorithm. The time delay implemented in the artificial communication channel between the master and slave device is $1\,\mathrm{s}$, constant, and without package loss. Both of the experiments are carried out using the same implementation of the *Passivity Layer*. Experimental results are shown both with the *Passivity Layer* turned on and off and for grasps of the user switching between hard, relaxed, and soft.

First the implementation of the *Passivity Layer* will be discussed and afterwards the implementations of the two different controllers combined with the experimental results. It should be noted that with the change from the PF controller to the IR algorithm only the implementation of the *Transparency Layer* changes and no adjustments to the *Passivity Layer* are required. There are even no changes needed to the *Passivity Layer* when

introducing the time delay in the communication channel.

The force sensors record the force at the interaction points between the user/ environment and the device. Therefore it is chosen to have the *Transparency Layer* compute a force to be exerted at the interaction point and not directly a torque to be applied by the motor. In the *Passivity Layer* the saturation functions are applied to this force after which it is transformed into a torque to be applied by the actuator using the length of the mechanical arm r of each device. For both devices $r = 0.15\,\mathrm{m}$. The TLC in the *Passivity Layer* at the master side also computes a torque.

3.5.1 Implementation Passivity Layer

The *Passivity Layer* is implemented as discussed in Section 3.4. As energy transfer protocol the SETP of Section 3.4.3 is chosen. The values for the various parameters are listed in Table 3.1. As saturation functions (3.21) and (3.24) and the maximum force that can be delivered by the actuators have been implemented. The mapping of (3.24) is implemented only at the slave side and in the form of a linear spring with stiffness K_s, so

$$|F_{max2}(k)| = \sqrt{2H_S(\overline{k+1})K_S} \tag{3.28}$$

and

$$|F_{max3}(k)| = 11.5\,\mathrm{N} \tag{3.29}$$

3.5.2 Position-Force Controller

As first implementation of the *Transparency Layer* a regular PF controller is implemented. Such a controller is characterized by a poor transparency as the proportional gain of the position controller acts as a spring with limited stiffness between the master and slave position. Although accurate force reflection can be achieved, the position tracking performance of the slave device will be limited during contact phases with the environment. However, the added benefit of the *Passivity Layer* with respect to the stability of the system can clearly be demonstrated. The PF controller is implemented as:

$$\begin{aligned} F_{TLm}(k) &= F_e(k) \\ F_{TLs}(k) &= -K_p(q_m(k) - q_s(k)) - K_d\dot{q}_s(k) \end{aligned} \tag{3.30}$$

where F_e is the measured interaction force between the slave device and the environment. K_p and K_d are the gains of the position controller.

Table 3.1: Parameter values of the *Passivity Layer*

Parameter	Value	Parameter	Value
H_D	0.075 J	β	0.01
α	$70\,{}^{\mathrm{Nm\cdot s}}/_{\mathrm{rad\cdot J}}$	K_S	$500\,{}^{\mathrm{N}^2}/_{\mathrm{J}}$

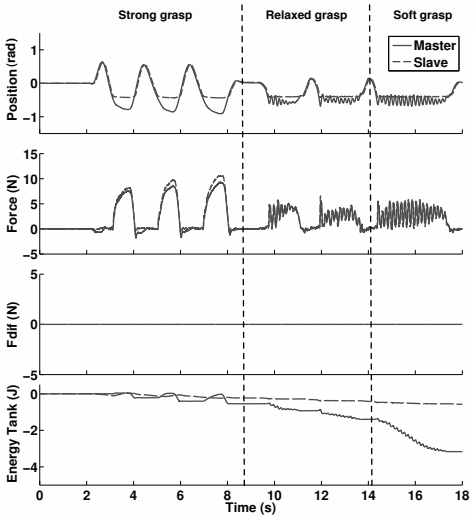

Figure 3.8: **Non-passive Position-Force Controller:** The contact between the slave device and the environment becomes unstable for more relaxed grasps by the user.

Several experiments have been carried out with the controller settings as given in Table 3.2. Each figure shows the position of the master and slave device, the force recorded by the force sensors in the master and slave device, the difference between the force computed by the PF controller and the force applied by the *Passivity Layer* at the master side (F_{dif}), and the level of the energy tanks at the master and slave side, respectively.

Fig. 3.8 shows the response when the *Passivity Layer* is not active. As long as the user has a strong grasp on the device the response is stable and the interaction forces are accurately reflected. However, when the user relaxes his grasp oscillations start to occur in the system response when contact is made with the environment. Finally for a soft grasp the contact is unstable and the slave system is bouncing on the environment. The system is producing "virtual" energy as indicated by the negative and decreasing tank level of both the master and slave system. The energy tank levels also shows that in this situation "virtual" energy is mostly generated at the master side as the level of that tank is decreasing much faster than the level of at the slave side.

Fig. 3.9 shows the same experiment but with the *Passivity Layer* activated. The initial extraction phase is indicated in which both energy tanks are filled. For all three grasps the system response is stable and the user is experiencing force feedback. The relative

Table 3.2: Parameter values of the *Transparency Layer*

Parameter	Value	Parameter	Value
K_p	$25\,^{\mathrm{N}}/_{\mathrm{rad}}$	K_v	$0.75\,^{\mathrm{Ns}}/_{\mathrm{rad}}$
γ	0.01	β_e	0.99

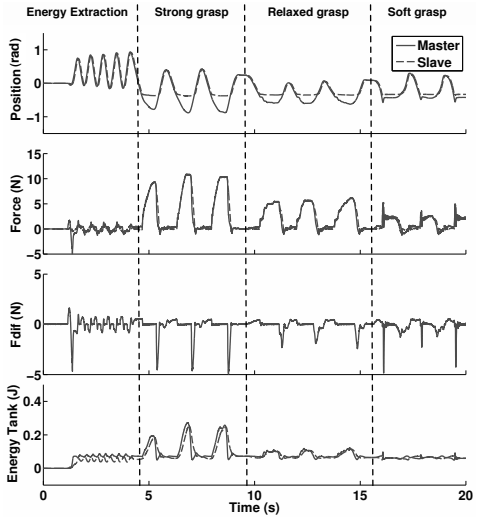

Figure 3.9: **Passive Position-Force Controller:** The contact between the slave device and the environment remains stable for all grasps by the user. The relative adjustment by the *Passivity Layer* is increasing for more relaxed grasps.

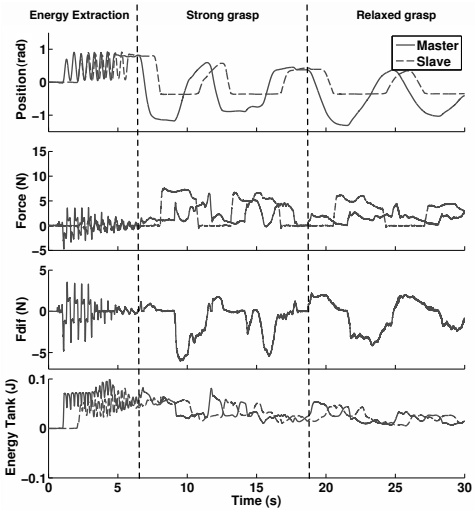

Figure 3.10: **Passive Position-Force Controller with** 1 s **Time Delay:** The transparency of the telemanipulation system is extremely low due to the time delay, but remains stable for even relaxed grasps by the user. Without the *Passivity Layer* violent jerks appear in the feedback force which require a strong grasp by the user to keep the system stable.

influence of the *Passivity Layer* on the feedback force to the user is increasing with more relaxed grasps by the user.

Fig. 3.10 shows the response of the system when a $1\,\mathrm{s}$ delay is introduced in the communication channel. In this case the transparency of the system is extremely low as action and reaction at the user side are separated in time by a round trip delay of $2\,\mathrm{s}$. Without the *Passivity Layer* a strong grasp is needed in order to keep the system stable as violent jerks frequently occur. Fig. 3.10 shows that with the *Passivity Layer* activated the system remains stable even with a relaxed grasp by the user.

3.5.3 Impedance Reflection

As second implementation of the *Passivity Layer* an IR algorithm has been implemented based on the scheme proposed by Tzafestas et al. (2008) and similar to the one used by Franken et al. (2009). A schematic drawing of this implementation of the *Transparency Layer* is depicted in Fig. 3.11. In the following four subsections the implementation of each element of Fig. 3.11 is discussed.

Virtual Environment

The virtual environment is implemented as a simple discretized linear spring model:

$$F_{TLm}(k) = -\hat{K}_e(k)(q_m(k) - \hat{x}_e(k))/r \tag{3.31}$$

where $\hat{K}_e(k)$ and $\hat{x}_e(k)$ are the estimated stiffness and position of the object in the environment. Due to the identification algorithm the mechanical spring in the environment is identified as a torsional spring. Therefore the length of the mechanical arm is used to transform the resulting torque into the desired force at the interaction point.

Adjustment

A simple smoothing function is implemented that limits the change in parameters to a percentage of the difference between the currently used and identified parameters:

$$\Delta p_m(k) = \gamma(p_I(k) - p_m(k-1)) \tag{3.32}$$

where p_I and p_m indicate the received identified parameters and the current parameters used at the master side, respectively.

Behavior Controller

The same position controller for the slave device as used in Section 3.5.2 is implemented. So:

$$F_{TLs}(k) = -K_p(q_m(k) - q_s(k)) - K_d\dot{q}_s(k) \tag{3.33}$$

The series spring of the position controller is removed from the feedback force to the user, but is still present in the position response of the slave device. This means that the

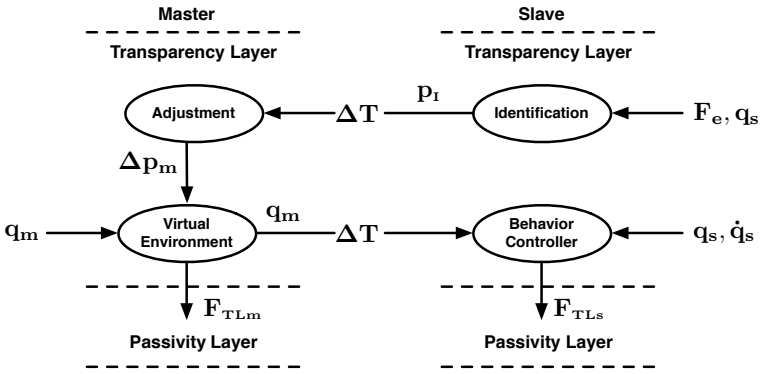

Figure 3.11: **Impedance Reflection algorithm based on Tzafestas et al. (2008)** Feedback force to the user is based on a local model of the remote environment of which the parameters are estimated online.

transparency of the system will still be limited as the position responses of the master and slave device can greatly differ when interacting with the environment. A solution to this problem could be to implement either an adaptive or robust control structure. Misra and Okamura (2006) for instance use the identified parameters of the environment to modify the position control gains.

Identification

The identification algorithm implemented here is a linear regression algorithm based on (Diolaiti et al., 2005). The estimator tries to minimize the cost function:

$$\begin{aligned} V_N(\hat{K}_e) &= \frac{1}{N}\sum_{k=1}^{N}\epsilon(k)^2 \\ \epsilon(k) &= rF_e(k) - (\hat{K}(k)(q_s(k) - \hat{x}_e) \end{aligned} \tag{3.34}$$

and is implemented by computing the following recursive equations during the estimation process:

$$\begin{aligned} \hat{K}_e(k) &= \hat{K}_e(k-1) + Q(k)\epsilon(k) \\ Q(k) &= R(k-1)(\hat{x}_s(k))(\beta_e + (\hat{x}_s(k))^2 R(k-1))^{-1} \\ R(k) &= \frac{1}{\beta_e}(1 - Q(k)\hat{x}_s(k))R(k-1) \\ \hat{x}_s(k) &= q_s(k) - \hat{x}_e(k) \end{aligned} \tag{3.35}$$

where β_e is a forgetting factor to limit the estimation to more recent measurements. R is initialized as 1 and no prior information about the parameters is assumed. $\hat{x}_e$ is determined

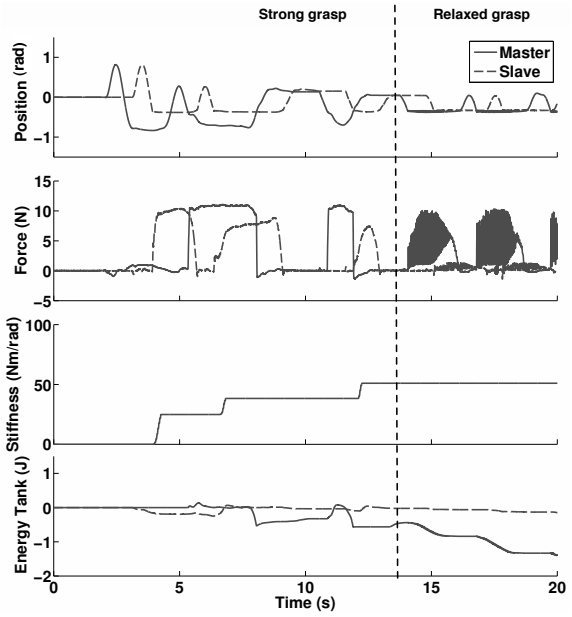

Figure 3.12: **Non-passive Impedance Reflection:** The interaction force is now predicted based on the local model which increases the transparency of the system with respect to the PF controller. The initial contact between the slave and environment is a very hard collision and only limited due to the saturation of the motor amplifiers. For a relaxed grasp of the user the contact with the virtual model is unstable.

as the position of the slave device where a certain force threshold is exceeded. This is done to prevent the dynamics of the force sensor with the slave device moving in free space to activate the activation algorithm. $\hat{x}_e$ is therefore a rough approximation of x_e. This results in an unwanted effect that the estimated stiffness drops to zero when the environment force decreases. Therefore (3.35) is only executed when the environment force is increasing. This rough approximation of x_e can also results in the stiffness of the environment to be overestimated.

Experimental results

This scheme improves the transparency of the system with respect to the PF controller in the presence of time delays in the communication channel as the feedback force to the user is predicted based on a local virtual model of the environment. However, the transparency is still limited due to the fixed position controller, as indicated in Section 3.5.3, and visualized in Fig. 3.12 and Fig. 3.13 by the large position difference between the master and slave device.

The settings for the IR algorithm are listed in Table 3.2. The time delay in the communication channel is again $1\,\mathrm{s}$. Each figure shows the position of the master and slave

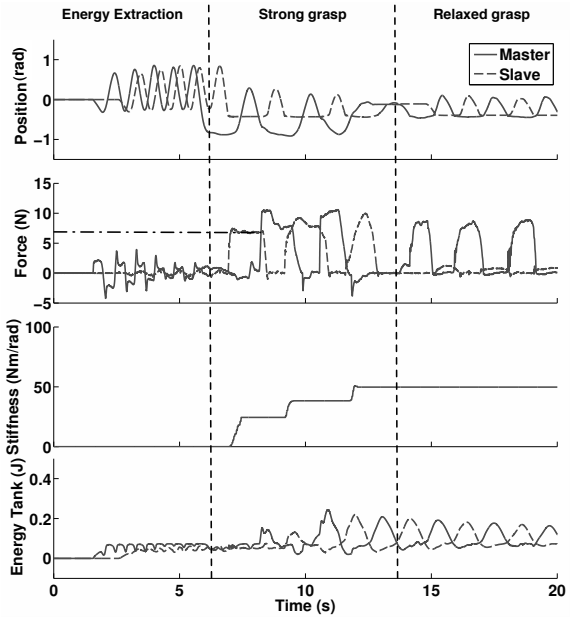

Figure 3.13: **Passive Impedance Reflection:** The increase in transparency with respect to the PF controller remains. With respect to the non-passive implementation the initial contact can be shaped by means of the saturation functions in the *Passivity Layer*. Due to the added damping by the *Passivity Layer* the contact with the virtual model is stable also for a relaxed grasp of the user.

device, the force recorded by the force sensor in each device, the estimated stiffness by the identification algorithm of Section 3.5.3 expressed as radial stiffness, and the level of the energy tanks at the master and slave side, respectively.

Fig. 3.12 shows the system response when the *Passivity Layer* is not activated. While the slave device is interacting with the environment the identification algorithm is estimating the stiffness of the environment. The user is subsequently presented with a predictive force feedback based on the implemented model and identified parameters. The initial force exerted by the slave device on the environment is $12\,\mathrm{N}$. This force is only limited due to the limitations of the motor amplifiers and would have been much higher. It should be noted that the force computed by the local model, for the identified stiffness, in the *Transparency Layer* is saturating the motor amplifiers. This means that the environment can only be accurately reflected within a certain position range of the master device. When the user relaxes his grasp on the device the interaction with the local virtual model is no longer stable and large oscillations in the feedback force occur. This means the system is generating energy as is visible from the negative and rapidly decreasing tank level of the master device. This oscillatory behavior is subsequently also exhibited by the slave device.

Fig. 3.13 shows the response with the *Passivity Layer* activated. Two major differ-

ences are visible with respect to Fig. 3.12. The initial impact force between the slave device and the environment is limited due to the saturation functions in the *Passivity Layer*. The impact force in Fig. 3.13 is about $7\,\mathrm{N}$ whereas it is $12\,\mathrm{N}$ in Fig. 3.12. When the user is interacting with the properly identified local model he is injecting energy into the system, which allows the *Passivity Layer* at the slave system to exert higher forces on the remote environment as the user clearly intends to exert these forces on the object. The second difference is the absence of the vibrations when the user is relaxing his grasp. The interaction with the virtual environment is kept stable due to the added damping in the *Passivity Layer* to keep the system passive.

It should be noted that there exists a lower bound of the user's grasp for this latter effect. The *Passivity Layer* only adds enough damping to maintain passivity of the system. As the virtual environment is a pure undamped spring it will exhibit an oscillatory response when there is no damping added by the user's grasp. This oscillatory behavior is simply stable, it does not grow in magnitude, as the *Passivity Layer* will enforce passivity of the system. In the absence of the *Passivity Layer* the system will be unstable for the same soft grasp by the user.

3.6 Discussion

With respect to each of the passivity-based control structures treated in Section 3.2 the proposed Two-Layer Framework with the implementation of the *Passivity Layer* treated in Section 3.4 has at least some of the following benefits:

- **Hardware independent:** No additional relation between the implementation of the controller and the hardware parameters is needed to ensure stable behavior.
- **Wide variety of bilateral controllers:** The only restriction placed on the implemented bilateral controller is that it computes a force to be applied to each device.
- **Almost independent optimization of each layer:** The manner in which the *Passivity Layer* is implemented monitors the energy exchange and only intervenes when necessary. This means that if the bilateral controller in the *Transparency Layer* is displaying passive behavior, the *Passivity Layer* does nothing. This allows almost independent optimization of each layer. The only dependency between the layers is that the Energy Transfer Protocols that can be implemented are restricted by the chosen implementation of the *Transparency Layer*.
- **Flexibility:** The *Passivity Layer* is centered around the communicating energy tanks and the monitoring of the energy exchange with the physical world. Any number of saturation functions can be designed, implemented and optimized independently of each other to shape that physical interaction based on the available energy in the tank.

As has been pointed out in Section 3.4 it is possible for the system to be momentarily active. This is inherent to the fact that the energy exchange during the sample period cannot be monitored and its value can only be computed *a posteriori*. All Time Domain Passivity structures that are centered around monitoring the energy exchange share

this effect. However, in this framework the active behavior of the system is limited to a single sample period, because the *Passivity Layer* will shut off the commands of the *Transparency Layer* until passivity of the system is restored. Other approaches like the EBA and PSPM can prevent energy from being generated at all times, but only as long as the models of the hardware that are being used are accurate lower bounds.

3.7 Conclusions and Future Work

In this paper a new framework for bilateral telemanipulation was presented. The two-layered approach allows the combination of passivity and transparency in a very intuitive manner. Using this framework any control architecture with an impedance causality can be implemented in a passive manner. Furthermore the framework allows many of its features to be tuned for specific devices and/or tasks. Especially the energy transfer protocol and saturation functions can be designed and optimized for a specific device, environment, and/or task. The presented experimental results show the benefits of the two-layered implementation. A single implementation of the *Passivity Layer* was able to maintain stability of two different implementations of the *Transparency Layer* even in the presence of large time delays, hard contacts, and a variety of user grasps. The transparency properties of the bilateral controllers, implemented in the *Transparency Layer*, were maintained and their commands were only adjusted by the minimum to maintain passivity of the system.

Future work will focus on the systematic implementation of the various design options and tuning of the parameters in the *Passivity layer*. Also the implementation of the framework on systems with multiple degrees of freedom will be analyzed.

The passivity layer presented in this paper makes the system passive with respect to the actuators at both the master and slave side. All the energy spent by the actuators at the slave side is extracted from the user. This means that transparency is adversely influenced by friction in the slave device. Therefore future research will also be directed to friction compensation techniques to extend this approach to manipulators with high internal friction. Preliminary results of such a friction compensation technique were presented by Franken et al. (2010*a*).

CHAPTER 4

Improved Transparency in Energy-Based Bilateral Telemanipulation

Franken, M., Misra, S. and Stramigioli, S.
Under review with Mechatronics

In bilateral telemanipulation algorithms based on enforcing time-domain passivity, internal friction in the devices poses an additional energy drain. This can severely decrease the obtainable transparency of these algorithms when high amounts of friction are present in the slave device. Based on a model of the friction, the dissipated energy can be estimated and reclaimed inside the energy balance of the control algorithm. Extending the energy balance which is monitored, decreases the net passivity of the telemanipulation system enforced by the control algorithm, which usually enforces passivity of just the bilateral controller. Experimental results are provided that demonstrate the effectiveness of the proposed approach in increasing the obtainable transparency. As long as the physically dissipated energy is underestimated, the telemanipulation system as a whole will remain passive. Thus the guaranteed stability property of the time-domain passivity algorithm is maintained.

4.1 Introduction

A bilateral telemanipulation system presents the user with haptic feedback about the interaction between the slave device and the remote environment. The transparency of the telemanipulation system is defined as the degree to which it is able to convey to the user the perception of direct interaction with the environment (Lawrence, 1993). One of the factors that determine the achievable transparency is the implemented bilateral control algorithm. Various control algorithms for bilateral telemanipulation have been proposed/applied with different stability and transparency properties, amongst others Position-Force controllers e.g. (Kim et al., 2005), Four Channel control (Lawrence, 1993), Impedance Reflection algorithms e.g. (Goethals et al., 2007), and Coupled Impedance controllers, e.g. (Lee and Li, 2005). A recent overview can be found in (Hokayem and Spong, 2006).

Stability issues can arise in bilateral telemanipulation systems due to e.g. hard contacts in the environment and time delays in the communication channel connecting the master and slave system. The concept of passivity is often used in the design of bilateral telemanipulation systems as the interaction between passive systems is guaranteed to be stable. Both the user and the environment can be assumed to be passive, or to interact at least with passive systems in a stable manner (Hogan, 1989). Thus guaranteeing passivity of the telemanipulation system ensures stability of the interaction between the user/environment and the telemanipulation system.

Non-linear control architectures have been proposed in literature that can be combined with regular bilateral control algorithms to ensure passivity of the system. These algorithms adapt the commanded forces computed by the bilateral control algorithm to ensure that the telemanipulation system remains passive. Due to the adaptation of the command signals the interaction with this system is guaranteed to be stable, even though the bilateral control algorithm itself would result in unstable behavior of the system. Examples include the work of Ryu et al. (2004*b*), Ryu et al. (2010), Kim and Ryu (2010), Lee and Huang (2010), and Franken et al. (2009). Of these approaches we will focus on Time Domain Passivity (TDP) algorithms, e.g. (Ryu et al., 2004*b*), (Ryu et al., 2010), and (Franken et al., 2009). In TDP algorithms an energy balance of the system is monitored. This balance is based based on the energy exchange between the physical world and the bilateral control algorithm. Passivity of that interaction is enforced with modulated dampers.

Perfect transparency means that the user should not be able to discern the dynamic behavior of the mechanical master and slave device, and the bilateral control algorithm during operation. When left uncompensated, mechanical friction at both the master and slave side can decrease the obtained transparency (De Gersem and Van Brussel, 2004). In this paper we will consider bilateral telemanipulation systems that consist of impedance-type displays (force output causality). For such devices mechanical friction can decrease the tracking performance with respect to the desired position at the slave side and the desired force at the master side. At the master side the mechanical friction will distort the force feedback experienced by the user, which is most apparent during free space motion.

Extensive research has been performed with respect to friction compensation in motion and force control. Methods have been proposed that use observer-based compen-

sators, e.g. (Friedland and Park, 1992) and (Vedagarbha et al., 1999), adaptive controllers, e.g. (Feemster et al., 1999) and (Tomei, 2000) force feedback control, e.g. (Kwon and Woo, 2000) and (Bernstein et al., 2005), and model-based feedforward compensation, e.g. Ando et al. (2002), (Liu et al., 2004), (Mahvash and Okamura, 2007), and (Khayati et al., 2009). Overviews of various sources of friction, applicable models and various compensation methods applied to systems with friction are published by Armstrong-Helouvry et al. (1994) and Bona and Indri (2005).

Examples of friction compensation specifically applied to bilateral telemanipulation systems and haptic feedback devices include the work of Kwon and Woo (2000), Bernstein et al. (2005), Bi et al. (2004), and Mahvash and Okamura (2007). Mahvash and Okamura (2007) discuss that not every compensation method is suitable to be applied in bilateral telemanipulation systems depending on the chosen bilateral control algorithm and available sensors.

So far the effect of physical friction on the performance of TDP algorithms has been mostly neglected. Monfaredi et al. (2006) recognized that TDP algorithms provide better results when applied to lightweight devices with low internal friction. Increased amounts of internal friction in the slave device were found to reduce the obtainable transparency with the telemanipulation system. Therefore they proposed to apply a stiffness observer to the interaction with the environment and make the damping applied at the user side dependent on the identified stiffness instead of the energy balance when slave devices with higher internal friction are used. In their approach the energy balance is no longer monitored, making the approach similar to the one proposed by Love and Book (2004). However, the required amount of damping to enforce passive behavior of the system is not solely dependent on the stiffness of the environment, e.g. the influence of the grasp of the user, the parameters of the bilateral controller, the device impedances, and the type of motion is neglected. Furthermore, the stability properties of the system become dependent on the convergence of the applied stiffness identification algorithm. Although an interesting approach, it fails to address the underlying problem of TDP algorithms.

In this paper, the influence of friction on TDP algorithms is analyzed. The analysis is performed based on the two-layer framework introduced by Franken et al. (2009). It will be shown that friction influences the system in two distinct ways, which can each be separately handled in one of the layers. In the *Transparency Layer* one of the aforementioned compensation methods can be applied to increase the performance with respect to motion and force tracking. In the *Passivity Layer* an energy-based compensation method is proposed. The focus of the paper lies on this last compensation method. Furthermore, the proposed approach is applicable in any TDP algorithm, e.g. (Ryu et al., 2004*b*) and (Ryu et al., 2010). The contribution of this paper are the proposed friction compensation technique in the monitored energy balance of the TDP algorithm and its experimental validation.

The paper is organized as follows: Section 4.2 introduces the two-layer approach to bilateral telemanipulation. Section 4.3 discusses the influence of friction within the two-layer framework and the proposed compensation strategy. Section 4.4 describes an implementation of such a friction compensation technique in the two-layer framework. Experimental results with this implementation showing the obtainable increase in trans-

parency are presented in Section 4.5. A discussion on the proposed approach is contained in Section 4.6. The paper concludes and provides direction for future work in Section 4.7.

4.2 Energy-based Bilateral Telemanipulation

In this section we will summarize the working of the two-layered framework proposed by Franken et al. (2009)[1]. Two layers are defined that each address a distinct goal. The *Transparency Layer* contains the bilateral control algorithm that makes the system display the desired behavior, whereas the *Passivity Layer* enforces passivity of the system, see Fig. 4.1.

The *Transparency Layer* can contain any control algorithm that delivers the desired transparency, as long as it results in a desired torque/force to be applied to the devices at both sides, e.g. (Lawrence, 1993), (Kim et al., 2005), (Goethals et al., 2007), and (Lee and Li, 2005). The generalized forces to be applied at the master and slave side are τ_{TLm} and τ_{TLs}, respectively. These desired forces are the inputs to the *Passivity Layer* of which the working is summarized below.

A system is passive when the energy that can be extracted from the system is bounded by the energy that was injected into the system and the energy initially stored in the system, $E(0)$:

$$\int_{t_0}^{t_1} -\tau_I(t)\dot{q}_I(t)dt \geq -E(0), \tag{4.1}$$

where τ_I and $\dot{q}_I$ are the force and velocity associated with the interaction point of the system. $E(0)$ is assumed to be zero. Non-passive systems are said to generate "virtual" energy and it is this additional energy that can potentially destabilize the system.

For impedance-type systems (force output causality) the energy exchange between the control system and the physical world during sample period $\overline{k}$, $\Delta H_I, (k)$ can exactly be determined *a posteriori* as:

$$\begin{aligned} \Delta H_I(k) &= \int_{(k-1)\Delta T}^{k\Delta T} -\tau_I(t)\dot{q}_I(t)dt \\ &= -\tau_I(\overline{k}) \int_{(k-1)\Delta T}^{k\Delta T} \dot{q}_I(t)dt \\ &= -\tau_I(\overline{k})\Delta q_I(k), \end{aligned} \tag{4.2}$$

where $\Delta q_I(k)$ is the position difference of the interaction point that occurred during sample period $\overline{k}$. Using (4.1) and (4.2) an energy balance, H_T, of the bilateral controller can

[1] With respect to the mathematical notation used in this paper we would like to point out the following. The index k is used to indicate instantaneous values at the sampling instant k and the index $\overline{k}$ is used to indicate variables related to an interval between sampling instants $k-1$ and k. The symbol τ is used to indicate a generalized force vector which can contain both forces and torques.

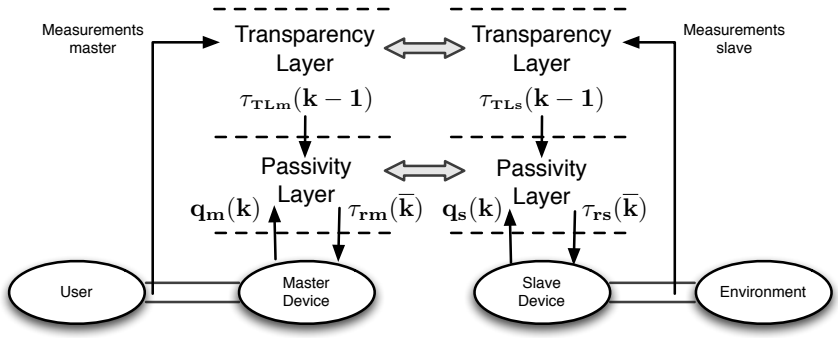

Figure 4.1: **Two-layer framework for bilateral telemanipulation.** The double connections indicate an energy exchange interaction. Franken et al. (2009)

be composed as

$$\begin{aligned} H_T(\overline{k}) &= \int_{t_0}^{t_1} -\tau_{PLm}(t)\dot{q}_M(t) - \tau_{PLs}(t)\dot{q}_S(t)dt \\ &= \sum_{i=0}^{(k-1)\Delta T} \Delta H_{Im}(i) + \Delta H_{Is}(i), \end{aligned} \tag{4.3}$$

where τ_{PLm} and τ_{PLs} are the forces exerted by the *Passivity Layer* on the master and slave device, respectively. Under the assumption of rigid body dynamics for the master and slave device, $\dot{q}_M$ and $\dot{q}_S$ are the velocities of the master and slave device, respectively. $\Delta H_{Im}(k)$ and $\Delta H_{Is}(k)$ are computed according to (4.2) and represent the energy exchanged between the physical world and the control system, operating in discrete time, at the master and slave side, respectively. (4.3) represent the amount of energy 'stored' in the bilateral control algorithm. If (4.3) is enforced to be positive always, the telemanipulation system is passive and thus stability will be guaranteed.

To account for time delays in the communication channel the *Passivity Layer* splits (4.3) into three parts:

$$H_T(\overline{k}) = H_M(\overline{k}) + H_C(\overline{k}) + H_S(\overline{k}), \tag{4.4}$$

where H_M, H_C, and H_S represent the energy at the master side, in the communication channel, and at the slave side. The energy at the master and slave side, H_M and H_S, are stored in energy tanks. The energy levels in these tank can be regarded as energy budgets from which controlled movements can be powered. An energy transfer protocol is required to make energy available in the system where needed. An example is the Simple Energy Transfer Protocol (SETP), where each side transmits each iteration a fraction, β, of its energy level to the other side. This guarantees $H_C \geq 0$ for arbitrary time delays and ensures asymptotic stability of the difference of the tank levels for arbitrary constant time delays. The proof of the latter is obtained by a straightforward application of the Jury

Stability Criterion to the linear time invariant description of the tank level difference.

With the SETP there are three energy flows connected to each energy tank, the energy exchange that occurs with the physical world and both an incoming and outgoing energy flow from the communication channel. The energy tank levels are given as

$$\begin{aligned} H_M(\overline{k}) &= \sum_{i=0}^{(k-1)\Delta T} \Delta H_{Im}(k) + \Delta H_{SM+}(k) - \Delta H_{MS-}(k) \\ H_S(\overline{k}) &= \sum_{i=0}^{(k-1)\Delta T} \Delta H_{Is}(k) + \Delta H_{MS+}(k) - \Delta H_{SM-}(k), \end{aligned} \tag{4.5}$$

where ΔH_{MS-} and ΔH_{MS-} are the energy packets send each iteration into the communication channel at the master and slave side. ΔH_{MS+} and ΔH_{SM+} are the amounts of energy received at each side out of the communication channel. The energy flow out of the communication channel at each side is the time-delayed energy flow into the communication channel at the other side. A thorough treatment of the two-layer framework is contained in Franken et al. (2011b).

When the energy level at either the master or slave side is low, the force that can be exerted by the bilateral control algorithm at that side is restricted to maintain passivity. Saturation functions can be implemented that guarantee

$$\begin{aligned} H_M(\overline{k}) &\geq 0 \\ H_S(\overline{k}) &\geq 0. \end{aligned} \tag{4.6}$$

Examples of such saturation functions are discussed in (Franken et al., 2009). The various saturation functions that are implemented compute maximum torques, $\tau_{Mmax}(k)$ and $\tau_{Smax}(k)$ that can be applied at the master and slave side by the *Passivity Layer* during sample period $\overline{k+1}$ so that passivity will be maintained. The forces applied by the *Passivity Layer* are computed as

$$\begin{aligned} \tau_{PLm}(\overline{k+1}) &= \operatorname{sgn}(\tau_{TLm}(k)) \min(|\tau_{TLm}(k)|, \tau_{Mmax}(k)) + \tau_{TLC}(k) \\ \tau_{PLs}(\overline{k+1}) &= \operatorname{sgn}(\tau_{TLs}(k)) \min(|\tau_{TLs}(k)|, \tau_{Smax}(k)), \end{aligned} \tag{4.7}$$

where τ_{TLC} is the force exerted by the Tank Level Controller (TLC). The TLC is defined at the master side to regulate the energy level in the system independent of the bilateral control algorithm in the *Transparency Layer*. The TLC is activated in order to extract an initial amount of energy, and further additionally required energy, from the user to maintain a desired energy level in the system. The TLC is implemented as a modulated viscous damper:

$$\begin{aligned} \tau_{TLC}(k) &= -d(k)\dot{q}_M(k) \\ d(k) &= \begin{cases} \alpha(H_D - H_M(\overline{k+1})) & \text{if } H_M(\overline{k+1}) < H_D \\ 0 & \text{otherwise} \end{cases}, \end{aligned} \tag{4.8}$$

where H_D is the desired energy level of the tank and $d(k)$ is the modulated viscous damping coefficient and α is a tuning parameter for the rate at which the user will replenish the energy tank given a certain motion. The selection of H_D and α dependents on the device characteristics, the implemented energy transfer protocol, and the properties of the communication channel (Franken et al., 2011b). Systematic tuning of the parameters in the *Passivity Layer* is the topic of ongoing research.

The algorithm implemented in the *Passivity Layer* maintains the energy balance:

$$H_T(\overline{k}) = \sum_{i=0}^{k-1} \Delta H_{Im}(i) + \Delta H_{Is}(i) \geq 0, \tag{4.9}$$

which guarantees passivity of the bilateral control algorithm and thus of the telemanipulation system as a whole.

4.3 Friction

In the previous section the two-layer approach to bilateral telemanipulation was described. In this section the influence of friction on the performance of each layer will be analyzed. It will be shown that in each layer compensation methods of a different nature need to be implemented to achieve the highest possible level of transparency while guaranteeing stability.

4.3.1 Transparency Layer

The bilateral control algorithm in the *Transparency Layer* is intended to provide the user with the desired level of transparency. For most bilateral control algorithms this translates into the following goals:

- accurate reflection of the environment force to the user,
- accurate position tracking by the slave device with respect to the motion of the master device.

Mechanical friction in the master and slave device can reduce the performance of the system with respect to these two goals. The rigid-body dynamic equations of the master and slave system are:

$$\begin{aligned} \tau_{PLm}(t) + \tau_H(t) + \tau_{Rm}(t) &= M_M(q_M)\ddot{q}_M(t) \\ \tau_{PLs}(t) + \tau_E(t) + \tau_{Rs}(t) &= M_S(q_S)\ddot{q}_S(t), \end{aligned} \tag{4.10}$$

where τ_H and τ_E are the forces exerted by the user and the environment, respectively. τ_{Rm} and τ_{Rs} are the non-linear mechanical friction forces in the master and slave device and M_M and M_S are the configuration dependent inertia matrices of the master and slave device, respectively.

In order to achieve the desired goals τ_{TLm} and τ_{TLs} need to be designed such that the negative influence of friction, τ_{Rm} and τ_{Rs}, with respect to the desired goal is removed.

If force/torque sensors are available force feedback control can be applied at the master side, e.g. (Kwon and Woo, 2000). If a sufficiently accurate model of the friction can be derived, model-based feedforward control can be applied, e..g. (Ando et al., 2002). Bernstein et al. (2005) conclude that a hybrid implementation of these two approaches offers superior performance when compared to the performance of the separate approaches. At the slave side, an adaptive position controller can be used to change the parameter gains to achieve a desired measure of position tracking, e.g. (Tomei, 2000), or model-based feedforward control can be applied to obtain the same goal, e.g. (Mahvash and Okamura, 2007). Mahvash and Okamura (2007) discuss that for a position-position control architecture, adaptive techniques based on a pure position tracking error cannot be applied as the tracking error is also influenced by the interaction with the environment. Force-feedback control cannot be applied as the slave device can also be operating in free space.

4.3.2 Passivity Layer

The algorithm described in Section 4.2 guarantees stability of the telemanipulation system by enforcing passivity of the bilateral control algorithm, (4.9). The rigid-body dynamic equations of (4.10) can be transformed into energy balances as:

$$\begin{aligned} \int_{(k-1)\Delta T}^{k\Delta T} -\tau_{PLm}(t)\dot{q}_M(t)dt &= \int_{(k-1)\Delta T}^{k\Delta T} (\tau_H(t) + \tau_{Rm}(t) - M_M(q_M)\ddot{q}_M(t))\dot{q}_M(t)dt \\ \Delta H_{Im}(k) &= -\Delta H_H(k) - \Delta H_{Rm}(k) - \Delta H_{Km}(k), \end{aligned} \tag{4.11}$$

where $\Delta H_H(k)$, $\Delta H_{Km}(k)$ and $\Delta H_{Rm}(k)$ are the amount of energy exchanged between the master system and the user, the change of kinetic energy in the master device, and the energy dissipated due to friction in the master device during sample period $\overline{k}$. Similarly for the slave device:

$$\Delta H_{Is}(k) = -\Delta H_E(k) - \Delta H_{Rs}(k) - \Delta H_{Ks}(k), \tag{4.12}$$

where $\Delta H_E(k)$, $\Delta H_{Ks}(k)$ and $\Delta H_{Rs}(k)$ are the amount of energy exchanged between the slave system and the environment, the change of kinetic energy in the slave device, and the energy dissipated due to friction in the slave device during sample period $\overline{k}$. The signs in (4.11) and (4.12) are due to the definition of the positive energy flow direction according to (4.10).

It immediately follows from (4.12) that physical friction in the slave device not only influences the position tracking performance of the slave device, but also the energy balance as enforced by the *Passivity Layer*. This influence is independent of possible friction compensation methods implemented in the *Transparency Layer* to achieve proper position and force tracking. Consider the situation where the slave device is moving at a constant velocity in free space ($\Delta H_E(k) = 0$ and $\Delta H_{Ks}(k) = 0$). The energy balance of (4.12) reduces to:

$$\Delta H_{Is}(k) = -\Delta H_{Rs}(k). \tag{4.13}$$

This means that due to (4.9) the energy dissipated in the slave device will have to be injected by the user. As the slave device is moving in free space it is likely to assume that the commanded torque/force by the control algorithm in the *Transparency Layer* at the master side is zero, $\tau_{TLm}(k) = 0$. Therefore, the TLC will be activated so that the user injects energy into the system to compensate for ΔH_{Rs}. Subsequently, due to the activation of the TLC the user will not experience free space motion as such.

Similar arguments can be applied to the master system. Consider the situation where the user is moving at a constant velocity and that at the slave side $\Delta H_{Is}(k) = 0$. Assume that the user needs to experience free space motion ($\Delta H_{H}(k) = 0$) and that adequate friction compensation techniques have been applied in the *Transparency Layer* to achieve that free space motion sensation. From (4.11) it follows that

$$\Delta H_{Im}(k) = -\Delta H_{Rm}(k), \tag{4.14}$$

which means that without additional measures in the *Passivity Layer* the TLC will again be activated. It can also be argued that without friction compensation in the *Transparency Layer* the user is injecting energy into the system to overcome the friction in the master device, ΔH_{Rm}, which can be used as partial fulfillment of the energy that would need to be extracted by the TLC.

A sufficient condition for stability of the telemanipulation system is that no energy can be extracted from the system as a whole, meaning that

$$\int_{t_0}^{t_1} \tau_{H}(t)\dot{q}_{M}(t) + \tau_{E}(t)\dot{q}_{S}(t)dt \geq 0. \tag{4.15}$$

By implementing the *Passivity Layer* as described in Section 4.2, passivity of the bilateral controller is enforced. This means that (4.15) becomes

$$\int_{t_0}^{t_1} \tau_{H}(t)\dot{q}_{M}(t) + \tau_{E}(t)\dot{q}_{S}(t)dt \geq H_{Rm}(t_1) + H_{Rs}(t_1), \tag{4.16}$$

where $H_{Rm}(t_1)$ and $H_{Rs}(t_1)$ are the energy dissipated by friction in the master and slave device between t_0 to t_1, respectively. (4.16) indicates net passivity, which can be quite significant based on the amount of physical friction present in the master and slave device. This leads to the conclusion that the implementation of the *Passivity Layer* of Section 4.2 and TDP approaches in general are conservative as more friction is added to the system than strictly necessary to guarantee passivity of the telemanipulation system as a whole.

A solution to this conservatism in the *Passivity Layer* is to account for the dissipated energy in the monitored energy balance. Assume that a model of the friction in the master and slave device is available. Based on the implemented models and the position measurements, the amount of energy dissipated by friction during each sample period in the devices can be estimated. This would yield $\Delta\tilde{H}_{Rm}(k)$ and $\Delta\tilde{H}_{Rs}(k)$ at the master and slave side. Any model that is suitable to describe the friction can be implemented, see e.g. (Armstrong-Helouvry et al., 1994) for an overview of various models.

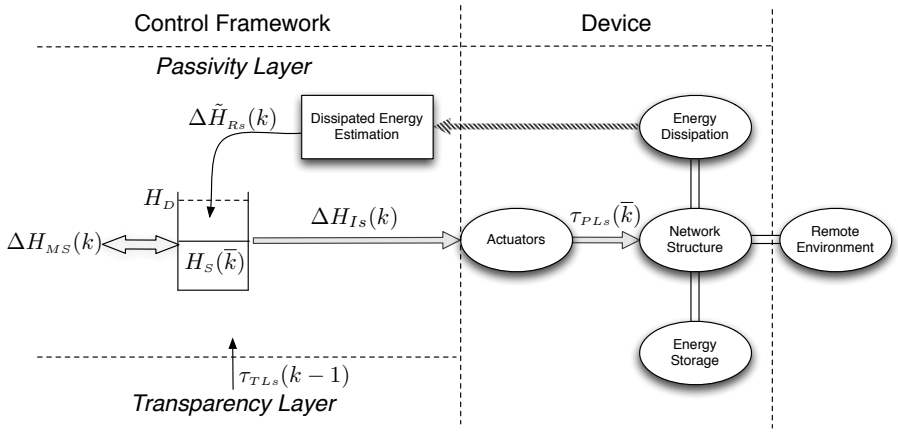

Figure 4.2: **Dissipated energy compensation at the slave side in the *Passivity Layer*:** For clarity only the energy flows are depicted in the *Passivity Layer*, $\Delta H_{MS}(k)$ represents the energy exchange between the master and slave system through the communication network.

In the *Passivity Layer* the estimated amounts of energy are subsequently added to the energy tanks. This is sketched in Fig. 4.2 for the slave side. The energy balance that is enforced by the two-layer framework becomes:

$$H_T(\bar{k}) = \sum_{i=0}^{k-1} \Delta H_{Im}(i) + \Delta\tilde{H}_{Rm}(i) + \Delta H_{Is}(i) + \Delta\tilde{H}_{Rm}(i) \geq 0. \tag{4.17}$$

This prevents the TLC from being activated to compensate for the energy dissipated internally in the master and slave device, which would result in net passivity of the system. Stability is still guaranteed as the telemanipulation system as a whole remains passive according to (4.15). The only requirement to achieve (4.15) is

$$\sum_{i=0}^{k} \Delta\tilde{H}_{Rm}(i) + \Delta\tilde{H}_{Rs}(i) \leq \int_{t=0}^{k\Delta T} -\tau_{Rm}(t)\dot{q}_M(t) - \tau_{Rs}(t)\dot{q}_S(t), \tag{4.18}$$

which simply means that the estimate of the dissipated energy should be smaller than the physically dissipated energy so that a small amount of net passivity remains in (4.15).

An important difference with the friction compensation method in the *Transparency Layer* is that friction compensation in the *Passivity Layer* does not directly result in a force to be applied to the physical device. Assume that a model-based feedforward compensation method is implemented in the *Transparency Layer*. The computed feedforward force is physically applied to the device and will as such influence the motion of the device directly. The performance of friction compensation methods in the *Transparency Layer* can be reduced due to e.g. ignored non-linear effects such as stiction, the Stribeck effect, stick-

slip, measurement noise, and phase-lag due to possible filtering operations. These factors can significantly reduce the performance of the friction compensation method when the devices are moving at low velocities, especially near zero-crossings (Bi et al., 2004). A possible consequence of such neglected effects is chattering of the device. By using more advanced compensation methods this can be mitigated, e.g. Suraneni et al. (2005) apply online identification and adaptation and Mahvash and Okamura (2007) implement a passive compensation method.

With respect to the friction compensation method in the *Passivity Layer* the only requirements are (4.18) and a certain smoothness of $\Delta\tilde{H}_{Rm}$ and $\Delta\tilde{H}_{Rs}$. Non-smoothness of $\Delta\tilde{H}_{Rm}$ and ΔH_{Rs} can cause non-smoothness in the TLC, which can be experienced by the user as disturbing. This means that the requirements on the competence of the model are much less strict in the *Passivity Layer* compared to the *Transparency Layer*. The inclusion of any friction model that adheres to these two conditions will reduce the net passivity of the telemanipulation system as enforced by the *Passivity Layer*. Thus the obtainable transparency will be increased by any such friction model.

A final aspect with respect to the proposed model-based friction compensation in the *Passivity Layer* that needs to be taken into account is the possible occurrence of a build up effect in the energy tanks. Consider the situation where the slave system is moving in free space, no friction compensation has been applied in the *Transparency Layer* at the master side, and perfect friction models are implemented in the *Passivity Layer*. Continuous compensation of the dissipated energy in the master device in the *Passivity Layer* will cause a build up effect. Energy is continuously added to the tank at the master side, $\Delta\tilde{H}_{Rm}(k) \geq 0$, whereas no energy is spend from the tank at the slave side, $\Delta H_{Is}(k)+\Delta\tilde{H}_{Rs}(k) = 0$. This build up effect will prevent the *Passivity Layer* from adequately suppressing unstable behavior of the telemanipulation system. The build up of energy will first have to dissipated by generated "virtual" energy that is associated with non-passive behavior of the bilateral control algorithm in the *Transparency Layer* before the *Passivity Layer* can stabilize the system. This means that the system can temporarily display unstable behavior due to this build up effect. This problem due to energy build up is associated with TDP algorithms in general and ad-hoc resetting schemes have been proposed for the TDPC approach by e.g. Hannaford et al. (2002) and Artigas et al. (2006). It should be noted that the mentioned unstable behavior is actually potentially unstable behavior, as non-passive behavior (generation of "virtual" energy) is a required, but not sufficient condition for instability.

In the situation described above the build up effect in the *Passivity Layer* is caused by the continuous inclusion of the dissipated energy at the master side. For the compensation algorithm the circumstances need to be identified under which the dissipated energy can be safely compensated. Two possible methods are:

1. Always include $\Delta\tilde{H}_{Rs}(k)$ and only include $\Delta\tilde{H}_{Rm}(k)$ when $H_M(\overline{k}) < H_D$.
2. Only include $\Delta\tilde{H}_{Rs}(k)$ when $H_S(\overline{k}) < H_D$ and only include $\Delta H_{Rm}(k)$ when $H_M(\overline{k}) < H_D$.

where H_M, H_S, and H_D are again the energy levels of the tank at the master and slave side and the desired energy level for the tanks, respectively. The first approach is less

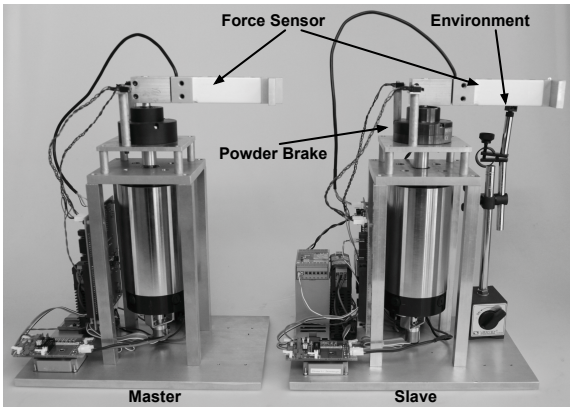

Figure 4.3: **Experimental setup:** The setup consists of two one degree of freedom devices powered by an electromotor without gearbox. The position of each motor is recorded with a high-precision incremental encoder and the mechanical arm consists of a linear force sensor to record the interaction force between the user/environment and the devices. A powder brake is attached to the motor axis of the slave device which allows the amount of friction in the slave device to be controlled.

conservative as more of the dissipated energy due to physical friction in the slave device is reclaimed in the energy balance enforced by the *Passivity Layer*. This approach is suitable to be applied under a forward energy-flow assumption, where motions can only be initiated by the user. If motions can be initiated from the environment a build up of energy in the *Passivity Layer* is still possible. The second strategy never leads to a build up of energy, but will result in a higher net passivity of the system to be enforced by the TDP algorithm due to the higher amount of neglected energy. Depending on the assumptions made about the environment one of these strategies should be selected.

4.4 Implementation

In this section the test setup used in the experiments will be introduced. A specific implementation of the two-layer framework will be presented along with an implementation of the proposed friction compensation method specific for the used test setup.

4.4.1 Test setup

The setup, Fig. 4.3, consists of two one degree of freedom devices powered by a DC motor without gearbox. The maximum continuous torque that these motors can exert is $1.38\,\mathrm{Nm}$. A high-precision encoder with $65\,\mathrm{k}$ pulses per rotation is used to record the position of each device. The mechanical arms of the devices rotate in the plane parallel to the base plate. The mechanical arms contain a linear force sensor to record the force which is applied at the interaction point perpendicular to the arm in the plane of motion.

The interaction point between the user/environment and the devices is at the end of each mechanical arm.

Both devices are controlled from the same controller running on a real-time Linux distribution. The controllers are implemented in the program 20-sim (Controllab Products B.V., 2010) and real-time executable code specific for this setup is generated directly from 20-sim and uploaded to the controller by means of the program 4C (Controllab Products B.V., 2010). The sampling frequency of the control loop is $1\,\mathrm{kHz}$. As environment a mechanical spring with a stiffness of approximately $1500\,{}^{\mathrm{N}}/_{\mathrm{m}}$ is used. The recorded position of this spring in the environment varies slightly between experiments as only incremental position encoders are used and the initial position of the slave device is not perfectly equal for each experiment.

In order to demonstrate the effectiveness of the approach of Section 4.3 the level of friction in the slave device needs to be adjustable. To this end a powder brake (Merobel FAT 20) is incorporated in the slave device. A powder brake is essentially a bearing with a coil integrated in the component. When a current runs through the coil, the resulting electromagnetic field attracts ferromagnetic powder in between the running surfaces of the bearing creating coulomb friction. The amount of coulomb friction is approximately linearly dependend on the applied current.

4.4.2 Two-Layer Framework

In the *Transparency Layer* a regular Position-Force controller is implemented as given by:

$$\begin{aligned} \tau_{TLm}(k) &= rF_e(k) \\ \tau_{TLs}(k) &= K_p(q_M(k) - q_S(k)) - K_d\dot{q}_S(k) \end{aligned} \tag{4.19}$$

where F_e is the measured interaction force between the slave device and the environment, $r = 0.15\,\mathrm{m}$ is the length of the mechanical arm of each device, and K_p and K_d are the proportional and derivative gain of the PD-type position controller, respectively.

The focus of this paper is the effect of friction compensation with respect to the obtainable transparency in the two-layer framework. The proposed approach of Section 4.3 consists of local procedures at the master and slave side. Due to this locality their performance is not dependent on possible time delays in the communication channel. Therefore, in this paper a non-delayed implementation is considered. In this non-delayed implementation the energy tanks in the *Passivity Layer* at the master and slave side, H_M and H_S, are merged into a single energy tank H_T. Furthermore, to show the effectiveness of the friction compensation no additional saturation functions have been implemented. This implementation of the two-layer framework is comparable to the standard TDPC algorithm as proposed by Ryu et al. (2004*b*) with a non-zero positive value to be maintained in the energy balance.

The TLC is implemented as (4.8). Both the tuning parameter of the TLC and the tank level are chosen such that the energy tank is never depleted during normal operation for the various operating conditions of all experiments.

The parameters used for all elements of the control structure are listed in Table 4.1.

4.4.3 Friction Compensation

Device identification experiments showed that the mechanical friction in the slave device can be approximated by coulomb friction and that the amount of viscous friction is neglible. The coefficient for the coulomb friction, $\tilde{B}_C$ of the slave device was determined to be approximately $0.06\,\mathrm{Nm}$, of which most is due to the residual torque of the powder brake. Actuation of the powder brake will increase the amount of coulomb friction in the slave device. Three different levels of friction added by the powder brake have been used. The estimated levels of coulomb friction in the slave device were low friction ($\tilde{B}_C = 0.06\,\mathrm{Nm}$), medium friction ($\tilde{B}_C = 0.4\,\mathrm{Nm}$), and high friction ($\tilde{B}_C = 1\,\mathrm{Nm}$). The amount of friction in the master device is negligible.

It is chosen not to include friction compensation in the *Transparency Layer*. Due to mechanical play in the slave device, feedforward friction compensation based on a simple coulomb friction model, Fig. 4.4, causes chattering. The use of adaptive position controllers has also been neglected as the focus of this paper lies on the friction compensation applied in the *Passivity Layer*. This means that the position tracking performance of the slave device with respect to the master device will decrease when the amount of friction in the slave device is increased.

It is assumed that no movements can be initiated from the environment, so that continuous friction compensation in the *Passivity Layer* of $\Delta\tilde{H}_{Rs}$ at the slave side can be implemented. As the friction in the master device is negligible no friction compensation is included in the *Passivity Layer* at the master side.

The coulomb friction model, Fig. 4.4, is given by

$$\tilde{\tau}_{Rs}(t) = -\tilde{B}_C\,\mathrm{sgn}(\dot{q}_S(t)). \tag{4.20}$$

The energy dissipated, $\Delta\tilde{H}_{Rs}(k)$, during a sample period, $\overline{k}$, can be computed *a posteriori* at sample instant k. The input for this computation is the displacement of the slave device that has occurred during the sample period, $\overline{k}$. As this computed energy is added to the energy tank in the *Passivity layer* overestimation of the physically dissipated energy needs to be prevented. This not only concerns the used model parameters, but also the presence of possible measurement noise needs to be taken into account. Franken et al. Franken et al. (2010*a*) show how the energy function described below can be adjusted based on the stochastic characteristics of the measurement noise.

Table 4.1: Control structure parameter values

Parameter	Value	Parameter	Value
K_p	$3.75\,{}^{\mathrm{Nm}}/_{\mathrm{rad}}$	K_d	$0.11\,{}^{\mathrm{Nm\cdot s}}/_{\mathrm{rad}}$
H_D	$1\,\mathrm{J}$	α	$50\,{}^{\mathrm{Nm\cdot s}}/_{\mathrm{rad\cdot J}}$

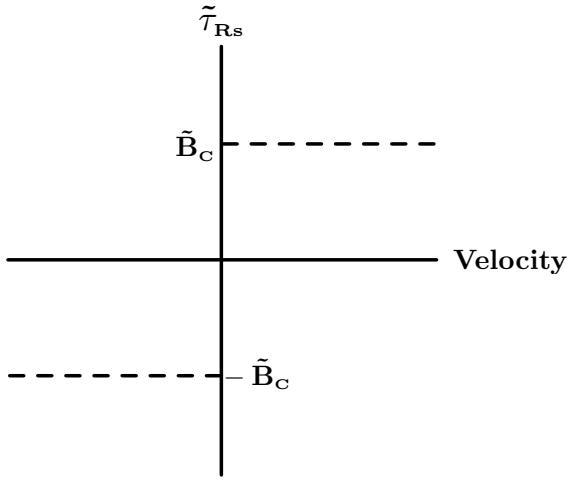

Figure 4.4: **Friction model:** The used friction model consists purely of coulomb friction. The friction compensation technique can accommodate any type of friction model that (partially) describes the physical friction in the device.

The estimated power, $\tilde{P}_C(t)$, dissipated due to coulomb friction is

$$\tilde{P}_C(t) = \tilde{B}_C|\dot{q}_S(t)| \tag{4.21}$$

The integral of (4.21) during a sample period gives the estimated dissipated energy. However, it is not possible to detect a change of direction during a sample period. Therefore the estimated energy dissipated by the coulomb friction, $\Delta\tilde{H}_{Rs}(k)$, directly from the measured displacement, $\Delta q_S(k)$, as

$$\begin{aligned} \Delta\tilde{H}_{Rs}(k) &= \tilde{B}_C|\Delta q_S(k)| \\ &\leq \int_{(k-1)T}^{kT} B_C|\dot{q}_S(t)|dt \end{aligned} \tag{4.22}$$

which is a lower-bound of the physically dissipated energy as long as $\tilde{B}_C < B_C$, where B_C is the physical coulomb friction coefficient.

4.5 Experiments

In this section we will demonstrate that the compensation method of Section 4.3 increases the transparency obtainable with TDP algorithms. The stability properties of the TDP algorithm are unaffected as long as the used friction model underestimates the physical friction.

Three different levels of friction added by the powder brake were used. The estimated

levels of coulomb friction in the slave device were low friction ($\tilde{B}_C = 0.06\,\mathrm{Nm}$), medium friction ($\tilde{B}_C = 0.4\,\mathrm{Nm}$), and high friction ($\tilde{B}_C = 1\,\mathrm{Nm}$). These friction coefficients are conservative enough so that the physically dissipated energy is not overestimated. The position controller at the slave device is not optimized to cope with increased amounts of friction in the slave device. This means that the position tracking performance will decrease when the friction is increased.

For all friction levels three different implementations of the *Passivity Layer* were tested:

- *Passivity Layer* switched off,
- regular *Passivity Layer*,
- extended *Passivity Layer* with friction compensation at the slave side.

During each experiment a repetitive motion pattern was carried out (movement in free space, 2 contact phases with a stiff user grasp, movement in free space, and finally 2 contact phases with a soft user grasp). During the stiff user grasp phase the user is firmly holding the device, whereas during the soft grasp phase the fingertips of the user are lightly touching the device. For each experiment the positions of the master and slave device are plotted together with the interaction forces between the user and the master device F_h and between the slave device and the environment F_e, and the level of the energy tank H_T in the *Passivity Layer*. Contact phases and free space motion are depicted by C and F, respectively.

Fig. 4.5 show the obtained results for the situation when the *Passivity Layer* is turned off. For all three friction levels excellent free space behavior is obtained, only the inertial effects of the force sensor are discernible in the feedback force to the user. The magnitude of these inertial effects increases for higher friction levels added by the powder brake due to stick-slip effects and the presence of a small amount of mechanical play in the slave device. Fig. 4.5 shows that the contact with the environment is unstable for a relaxed user grasp irrespective of the friction at the slave side.

When the standard *Passivity Layer* is activated, Fig. 4.6, these contact instabilities are prevented. However, a significant decrease in transparency is visible when the friction level in the slave device is increased. Already for the situation without additional friction supplied by the powder brake, Fig. 4.6a, an additional force is computed by the TLC in the *Passivity Layer* at the master side to maintain passivity of the monitored energy balance. This force is noticeable and the user does not experience free space motion as such. Finally, for higher amounts of friction the interaction force between the slave device and the environment is completely masked by the force added by the TLC. In this situation the user is not able to discriminate between contact phases and free space motion phases while moving the device. Only in static situations the user accurately experiences the interaction force between the slave device and the remote environment.

Fig. 4.7 shows the improvement in free space behavior when the standard *Passivity Layer* is extended with the friction compensation technique proposed in Section 4.3 and detailed in Section 4.4.3. The energy dissipated by the friction in the slave device is now estimated based on the identified coulomb friction model and added to the energy tank in the *Passivity Layer*. This means that the bilateral control algorithm is allowed to generate

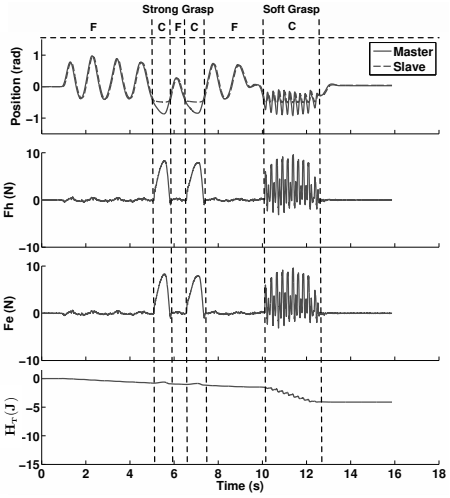

(a) Low friction

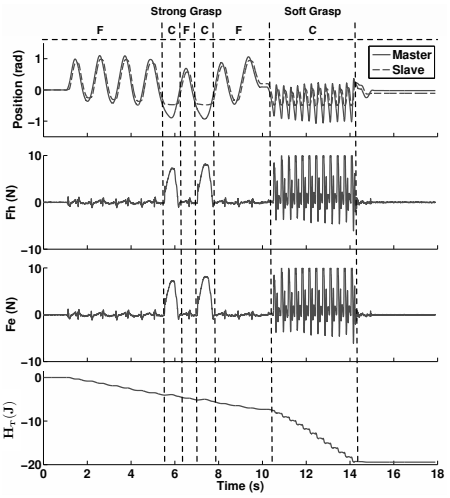

(b) Medium friction

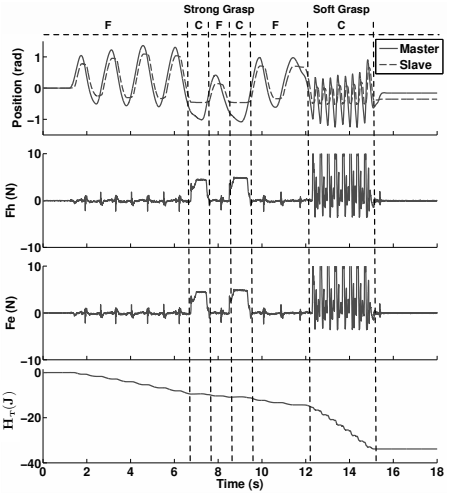

(c) High friction

Figure 4.5: **Experimental results with *Passivity Layer* switched off:** F and C indicate free space motion and contact phases, respectively. For all three friction levels excellent free space behavior is obtained, only inertial effects of the force sensor in the slave device are discernible in the feedback force to the user. However, this non-passive implementation results in an unstable interaction with the remote environment when the user applies a soft grasp.

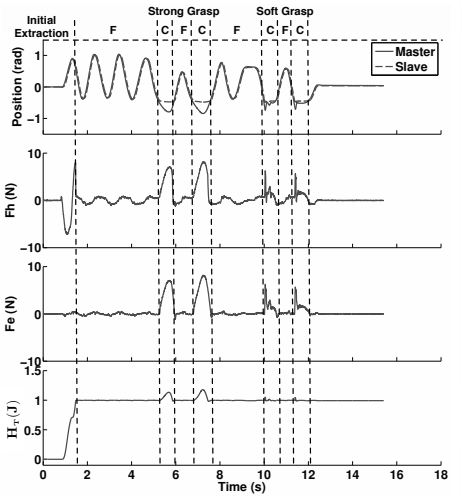

(a) Low friction

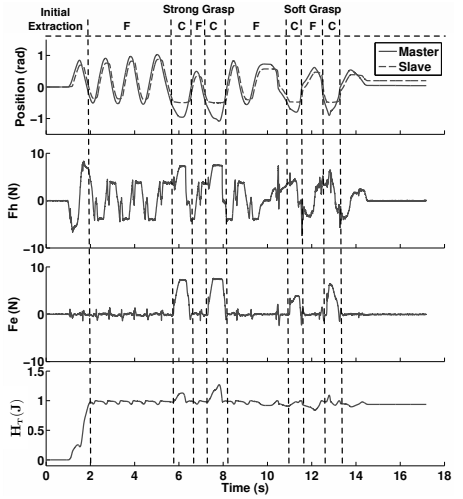

(b) Medium friction

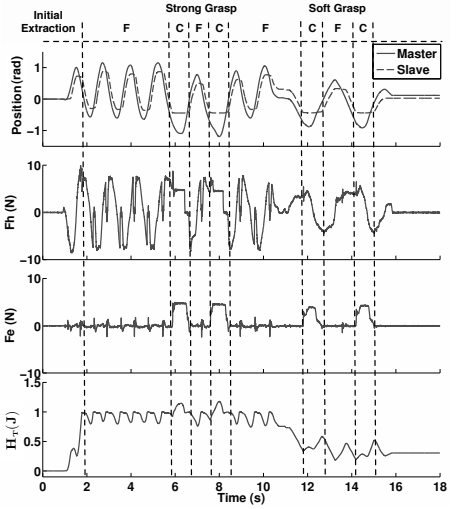

(c) High friction

Figure 4.6: **Experimental results with standard *Passivity Layer*:** F and C indicate free space motion and contact phases, respectively. The passivity condition which is enforced prevents instability of the interaction with the remote environment even when the user applies a soft grasp. However, for increasing friction levels in the slave device the transparency of the telemanipulation decreases due to the continuous activation of the *Passivity Layer*.

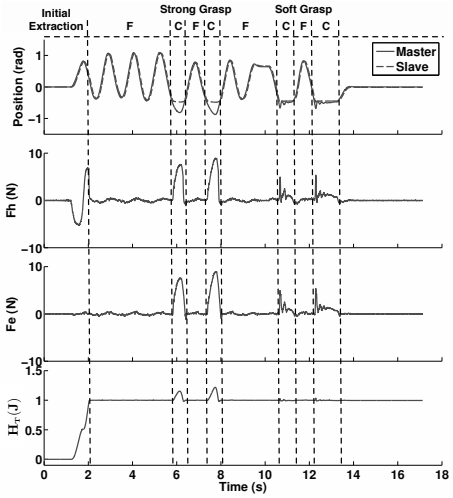

(a) Low friction

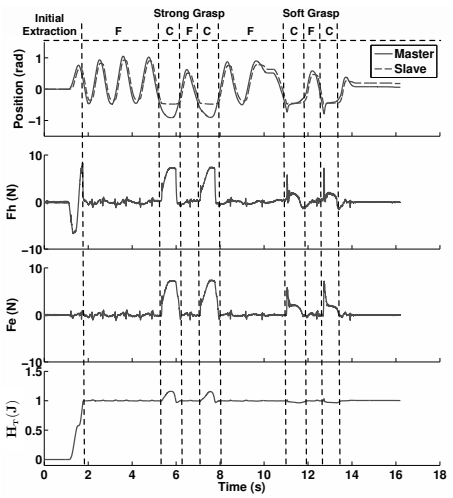

(b) Medium friction

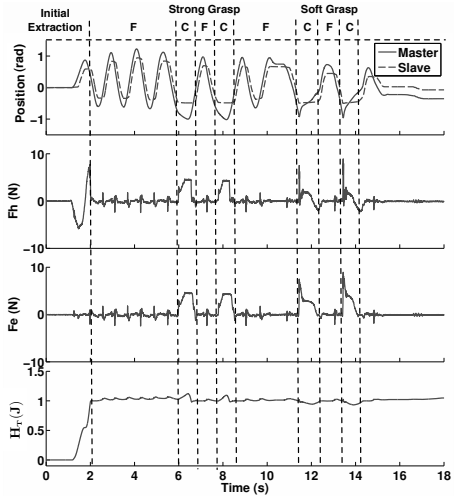

(c) High friction

Figure 4.7: **Experimental results with extended *Passivity Layer*:** F and C indicate free space motion and contact phases, respectively. Extending the energy balance in the *Passivity Layer* to incorporate the device friction reduces the conservatism of the algorithm. The user experiences free space motion even for high friction levels and stability of the interaction is still guaranteed even for a soft grasp by the user.

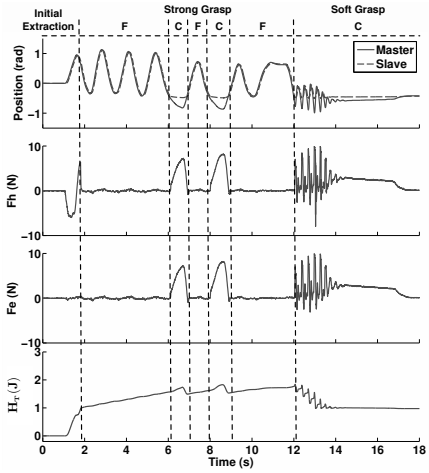

Figure 4.8: **Effect of overestimating dissipated energy:** F and C indicate free space motion and contact phases, respectively. During free space motion "virtual" energy is generated in the model-based feedback loop which results in a rising level of the energy tank. This build up of energy prevents the *Passivity Layer* from acting immediately on non-passive behavior of the system, which can result in temporary unstable behavior.

the energy that is needed to overcome the device friction. Non-passive behavior that could potentially destabilize the system is still suppressed by the *Passivity Layer*. This is demonstrated by the stability of the contact phases for both grasps by the user.

Fig. 4.7 shows that the extension to the *Passivity Layer* proposed in Section 4.3 can increase the transparency of the TDPC algorithm. This effect is especially noticeable during free space motion and is obtained by incorporating a model-based feedback loop in the *Passivity Layer*. However, the use of a model means that the energy balance is no longer solely based on measured energy exchanges, but also on an estimated quantity (the dissipated energy). When this model overestimates the physically dissipated energy, the TDP algorithm no longer guarantees passivity as "virtual" energy is generated in the established feedback loop. This is demonstrated in Fig. 4.8 where the friction coefficient used in the model, $\tilde{B}_C = 0.24\,\mathrm{Nm}$ is chosen four times larger as physically present, $B_C \approx 0.06\,\mathrm{Nm}$. A build up of energy occurs during free space motion. This excess energy in the energy-balance prevents the *Passivity Layer* from acting immediately on non-passive behavior of the bilateral controller in the *Transparency Layer* and results in momentary unstable behavior when the user applies a soft grasp. The *Passivity Layer* stabilizes the interaction as soon as the "virtual" energy generated by the non-passive behavior of the *Transparency Layer* has

dissipated the "virtual" energy generated in the model-based feedback loop. This shows that a transparency versus stability trade-off is present in TDP algorithms. The transparency of the approach can be increased by incorporating more knowledge about the physical devices, but at the cost of robustness against modeling errors.

4.6 Discussion

In Section 4.3 it was discussed that in order to obtain the highest possible transparency friction compensation has to be included in both the *Transparency*- and *Passivity Layer*. It could be argued that this can be circumvented by compensating for friction outside the two-layer framework. In Section 4.3.1 force feedback control and model-based feedforward control were indicated as possible friction compensation techniques suitable for application at the master side. Either of these approaches, or a hybrid implementation as by Bernstein et al. (2005), could indeed be implemented outside the two-layer framework and would effectively compensate for the friction at the master side.

At the slave side however, only model-based feedforward control can be implemented adequately outside the two-layer framework. A sufficiently accurate model might not be derivable to implement in a feedforward controller. However, if the derived model underestimates the physical friction, it can still be used in the *Passivity Layer* to reduce the net passivity of the system that is enforced by the TDP algorithm. This will not increase the position tracking performance of the slave device, but will prevent the force reflection to the user to be adversely influenced by the TDP algorithm. Possible adaptive position control techniques that could be applied are necessarily implemented in the *Transparency Layer*. Thus friction compensation should also be implemented in the *Passivity Layer*.

4.7 Conclusions and Future Work

In this paper a method is proposed and experimentally validated to improve the transparency obtainable with TDP algorithms when applied to devices with non-negligible mechanical friction. The friction in the slave device was recognized as a major limiting factor in the obtainable transparency with TDP algorithms as it forms a continuous drain of energy that needs to be compensated by the user. Extending the energy balance monitored by the TDP algorithm to incorporate the device friction decreases the net passivity enforced by the TDP algorithm of the telemanipulation system. This decreases the influence that the TDP algorithm exerts on the commands computed by the bilateral control algorithm in the *Transparency Layer*. Thus the obtainable transparency with the telemanipulation system as a whole is increased. The desired stability properties of the TDP algorithm are maintained as long as the implemented friction model underestimates the physical friction. The results in this paper were specific to the two-layer framework, but the approach is applicable to any TDP algorithm, e.g. Ryu et al. (2004*b*, 2010).

Future work will focus on further validation of the proposed approach. Experiments with devices containing multiple degrees of freedom and friction effects other than mere coulomb friction have to be conducted. The use of online friction identification methods, e.g. observer-based and delineated feature identification methods, will be explored.

Imperfections in the test setup (mechanical play and measurement noise) thus far prevented the use of a friction compensation method in the *Transparency Layer*. Compensation methods that are robust with respect to these imperfections will be investigated and/or mechanical parts of the setup itself will be redesigned and fabricated.

The practical significance of the proposed friction compensation technique also needs to be demonstrated. To that end human subject studies will need to be performed focusing on the performance with respect to tasks such as stiffness discrimination. A performance increase with respect to this task is expected when the proposed friction compensation is implemented.

Extending the energy balance in the TDP algorithm can also be used to increase the complimentarity of TDP algorithms with passivity based design approaches in the frequency domain, e.g. Absolute Stability (Hashtrudi-Zaad and Salcudean, 2001) and Bounded Environment Passivity (Willaert et al., 2010a). Preliminary results with a combination of both types of approaches are reported by Franken et al. (2011).

Acknowledgements

The authors wish to thank Roel Metz and Marcel Schwirtz for their contribution in the realization of the experimental test setup.

CHAPTER 5

Bilateral Telemanipulation: Improving the Complementarity of the Frequency- and Time-Domain Passivity Approaches

Franken, M., Willaert, B., Misra, S. and Stramigioli, S.
Proceedings of the IEEE International Conference on Robotics and Automation 2011

Passivity of bilateral telemanipulation systems ensures stability of the interaction with such systems. In the frequency domain, passivity of a linear time invariant approximation of the system can be designed for a considered set of operating conditions. Non-linear control structures have been proposed that enforce passivity of the system in the time domain. In this paper, extensions are proposed that increase the complimentarity of the frequency- and time-domain approaches. The combination of both approaches allows a guaranteed measure of transparency to be designed in the frequency domain for a desired set of operating conditions. For operating conditions outside the desired set, stable interaction is guaranteed by the non-linear passivity enforcing control structure. Simulation results of the combined approach are presented that show that the stability properties of the bilateral controller designed in the frequency domain are improved and the transparency properties are improved with respect to those of the standard passivity-enforcing algorithm in the time-domain.

5.1 Introduction

Bilateral telemanipulation systems reflect force information about the remote interaction between the slave system and the environment to the user. This bidirectional coupling between the user and the environment comprises a closed chain with multiple possible unknown and time-varying components, e.g. the user and environment impedance. A major research topic is therefore how to optimize transparency, (Lawrence, 1993), while guaranteeing stability of the coupled system under all operating conditions. With respect to the stability issue various passivity-based approaches have been introduced in literature. A passive system cannot generate energy and the interconnection of a passive system with any other passive system is guaranteed to be stable (van der Schaft, 1999). As the environment can be assumed to be passive and humans can interact very well with passive systems (Hogan, 1989), a passivity-based approach is an elegant solution to the stability problem.

We identify two major categories in the control of bilateral telemanipulation systems which are centered around the concept of passivity of the system:

1. Approaches that design bilateral controllers in the frequency domain, based on Linear Time Invariant (LTI) models of the system, e.g. (Lawrence, 1993), (Haddadi and Hashtrudi-Zaad, 2010), (Hashtrudi-Zaad and Salcudean, 2001), and (Willaert et al., 2010a)
2. Approaches that implement non-linear control structures that enforce passivity of the bilateral controller in the time domain, e.g. (Ryu et al., 2004*b*), (Artigas et al., 2008), (Franken et al., 2009), and (Lee and Huang, 2010).

Naturally, each approach has its benefits and drawbacks, making it more or less suited to deal with specific problems. For instance, the frequency domain approaches result in linear controllers of which the stability and transparency properties are easier to compute. Whereas the time domain approaches can better deal with all kinds of non-linear and time-varying effects, e.g. non-linear device dynamics, time-varying communication delays including package loss, and can accommodate a wide range of bilateral controllers (Franken et al., 2009), of which the passivity-properties can not necessarily be analyzed in the frequency domain.

In this paper we want to show that both approaches can be complimentary to a large extent when considering LTI systems. In the frequency domain design phase normally all possible operating conditions need to be taken into account, which results in restrictions on the control parameters of the system and thus limits the achievable transparency. The combination with a passivity enforcing control structure in the time domain alleviates this restriction as it guarantees stability and allows a restricted set of operating conditions to be taken into account in the frequency domain design phase. In reverse the combination with a frequency domain design phase allows to better quantify the transparency properties of the time domain algorithm as it will provide insight in the operating conditions that activate the time domain algorithm.

The paper is organized as follows: The model of the system which we will use for the analysis and numerical simulations is introduced in Section 5.2. The concept of passivity

will be discussed in Section 5.3 and also recent work on frequency domain and time domain passivity-based approaches will be discussed. Section 5.4 describes the desired complimentary effect of the two passivity-based approaches of Section 5.3. Section 5.5 introduces the extensions to the time domain passivity-based approach needed to establish that complimentary effect. An example in which the frequency domain and time domain approaches are combined will be discussed in Section 5.6. In Section 5.7, trade-offs between transparency and stability that persist are indicated. The paper concludes in Section 5.8.

5.2 System description

In this section, we will present the description of the telemanipulation chain that we will use throughout the paper. For our analysis we will assume that both the master and the slave system are one degree of freedom rigid bodies with mass M and subjected to viscous friction B:

$$\begin{aligned} F_h(t) + F_m(t) &= M_m \ddot{q}_m(t) + B_m \dot{q}_m(t) \\ F_e(t) + F_s(t) &= M_s \ddot{q}_s(t) + B_s \dot{q}_s(t) \end{aligned} \tag{5.1}$$

where F and q represent forces and positions, respectively. The subscripts h, m, s, and e indicate the human operator, the master device, the slave device, and the environment, respectively.

The implemented bilateral controller is a Position-Force (P-F) controller. A perfect communication network is assumed (no time delay and losses). This choice is made as the frequency domain passivity analysis of this controller can still be relatively easy performed analytically. However, the results presented in this paper can be established for any LTI bilateral controller. The P-F controller is:

$$\begin{aligned} F_m(t) &= \lambda F_e(t) \\ F_s(t) &= K_p(\mu q_m(t) - q_s(t)) - K_v \dot{q}_s(t) \end{aligned} \tag{5.2}$$

where K_p, K_v are the parameters of the position controller at the slave side and μ, λ the scaling factors applied to the position and force commands.

5.3 Passivity

The underlying condition for passivity is that the energy that can be extracted from the system at any time is bounded by the energy that was injected into the system and the energy that was initially stored in the system (van der Schaft, 1999):

$$\int_0^t -F(t)^T \dot{q}(t) dt \geq -E(0), \tag{5.3}$$

where $F(t)$ and $\dot{q}(t)$ are the forces and velocities at the interaction points, respectively. $E(0)$ is the energy initially stored in the system and assumed to be zero. The telemanipulation system is a two-port system so (5.3) can be written as:

$$\int_0^t F_h(t)^T \dot{q}_m(t) + F_e(t)^T \dot{q}_s(t) dt \geq 0. \tag{5.4}$$

where the sign change is due to the use of $F_h(t)$ and $F_e(t)$ according to (5.1). If a system is non-passive it is said to generate "virtual" energy and this energy can potentially destabilize the system.

5.3.1 Frequency Domain Passivity-Based Design

Passivity of a two-port LTI-system can be checked in the frequency domain using Raisbeck's passivity criterion (Haykin, 1970). However, for many LTI bilateral controllers the range of allowed parameter settings based on this criterion is extremely limited if at all existing. For the system of Section 5.2 Willaert et al. (2010a) proof that it can never comply with Raisbeck's passivity criterion. Consequently, two-port passivity of telemanipulation systems is not very useful as a design tool in the frequency domain due to too restrictive sufficient conditions given by the used criterion.

However, the guaranteed stability due to passivity remains an attractive property for bilateral systems. This inspired researchers, e.g. Hashtrudi-Zaad and Salcudean (2001), Haddadi and Hashtrudi-Zaad (2010), and Willaert et al. (2010a), to incorporate more information about the application of the system in the design phase and apply passivity-based designs on these extended models.

The operating conditions of a telemanipulation system specify everything that is related to the interaction between the telemanipulation system and the user/
environment, e.g. control parameters, device impedances, time-variant impedances of the user/environment. A set of operating conditions, e.g. the range of impedances of the environment, can be composed of all operating conditions that can/will occur. The frequency domain approaches discussed below analyze the passivity of part of the telemanipulation system for a considered set of operating conditions. Transparency of the system is optimized given the boundary condition of passivity.

The Absolute Stability approach, based on the work of Llewellyn (1952), derives control parameters that result in a passive one-port system when the telemanipulation system is terminated by any passive impedance at either side. Such a system is guaranteed to be stable as long as there is no direct interaction between the user and the environment. Willaert et al. (2010a) calculated that the system of Section 5.2 is absolute stable if the hardware and control parameters comply with the following two conditions:

$$\begin{aligned} \mu\lambda &\leq \frac{4B_m}{B_s + K_v} \\ \mu\lambda &\leq \frac{B_m(B_s + K_v)}{M_s K_p} \end{aligned} \tag{5.5}$$

The Absolute Stability approach alleviates the restrictions on the control parameters with respect to the two-port LTI passivity condition. This is possible as it assumes the absence of a secondary interaction path between the user and the environment and is an example of a restricted set of operating conditions for the design phase. However, the Absolute Stability approach still considers an infinite range for the impedance of the human operator as well as for the environment. In real applications, the range of impedances that can/will be encountered will always be restricted/bounded in some way. Recent work has focussed on including such bounds in the design phase, e.g. (Cho and Park, 2005), (Haddadi and Hashtrudi-Zaad, 2010), and (Willaert et al., 2010a).

The Bounded Environment Passivity approach (Willaert et al., 2010a) can be used to compute control parameters for which the one-port system composed of the telemanipulation system and environment is passive. In the analysis a class of impedances is considered and bounds can be incorporated on the magnitude of each element. For the system of Section 5.2, the following bounds (Willaert et al., 2010a) can be derived for environments characterizable as a pure spring model by considering the maximum stiffness, K_e^{max}, of the environment:

$$
\begin{aligned}
& B^{lim} = min[\sqrt{2(K_p + K_e^{max})M_s}, 2\sqrt{K_p M_s}] \\
& 0 \leq (B_s + K_v) \leq B^{lim} \quad \Rightarrow \quad \mu\lambda \leq \frac{B_m(B_s + K_v)}{M_s K_p}[1 + \frac{K_p}{K_e^{max}} - \frac{(B_s + K_v)^2}{4K_e^{max} M_s}] \\
& (B_s + K_v) \geq B^{lim} \text{ and } K_e^{max} \leq K_p \quad \Rightarrow \quad \mu\lambda \leq \frac{B_m(K_p + K_e^{max})^2}{(B_s + K_v)K_p K_e^{max}} \qquad (5.6) \\
& (B_s + K_v) \geq B^{lim} \text{ and } K_e^{max} > K_p \quad \Rightarrow \quad \mu\lambda \leq \frac{4B_m}{(B_s + K_v)}
\end{aligned}
$$

where the ratio between the viscous friction $B_s + K_v$ in the slave system and B^{lim} and the ratio between K_p and K_e^{max} are used to select a boundary condition for $\mu\lambda$. As detailed by Willaert et al. (2010a), comparing (5.6) with (5.5) shows that assuming a maximum stiffness of the environment can have a relaxing effect on the allowed parameter settings of the bilateral controller.

However, a system designed using these approaches is only passive when all physical environments that can be encountered during operation comply with the assumed classes and/or bounds. When other environments can be encountered, the system is not guaranteed to be passive, e.g. when interacting with stiffnesses higher than the assumed K_e^{max}, and is thus potentially unstable.

5.3.2 Time Domain Passivity Control

A different approach to ensure passivity of a telemanipulation system would be to apply a non-linear control algorithm that prevents non-passive behavior of the bilateral controller. The class of possible solutions we focus on here are based on Time Domain Passivity Control (TDPC) by damping injection. This was initially proposed by Ryu et al. (2004*b*) and extended/different implementations have been proposed to extend the application of

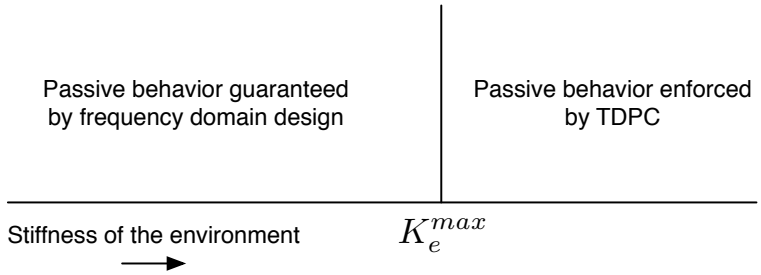

Figure 5.1: **Complimentarity of Bounded Environment Passivity and Time Domain Passivity Control:** Up to environment stiffness K_e^{max} the bilateral system displays passive behavior guaranteed by the design in the frequency-domain. For stiffnesses higher than K_e^{max} the Time Domain Passivity Control algorithm enforces passive behavior of the bilateral system.

this approach by e.g. Artigas et al. (2008) and Franken et al. (2009).

The basic concept of this class of TDPC is to monitor an appropriate energy balance for the system controlled by a bilateral controller. Non-passive behavior of the system is detected by the monitored balance becoming negative and a modulated damper at the master side is activated to modify the commands of the bilateral controller to maintain a neutral energy balance.

This class of TDPC algorithms is highly applicable to impedance type displays (velocity input, force output causality). For this class of systems, the energy exchange between the bilateral control algorithm and the master and slave devices can be exactly computed as (Stramigioli et al., 2005):

$$\Delta H_I(k) = -F_a(\overline{k})\Delta q_a(k) \tag{5.7}$$

where $\Delta H_I(k)$ is the energy exchanged between the control algorithm and the physical device during sample period $\overline{k}$, $F_a(\overline{k})$ is the force applied by the actuators during the sample period, and $\Delta q_a(k)$ is the measured change in position of the actuators.

The energy balance, H, which is then enforced is implemented as

$$H = \sum_{k=1}^{n} \Delta H_{Im}(k) + \Delta H_{Is}(k) \geq 0 \tag{5.8}$$

where $\Delta H_{Im}(k)$ and $\Delta H_{Is}(k)$ are the exchanged amounts of energy at the master and slave side during sample period $\overline{k}$, respectively. (5.8) is a discrete version of (5.3) with the interaction points chosen as the actuators of the master and slave device. Enforcing (5.8) guarantees (5.4).

5.4 Complimentarity

The aim of each of the two approaches discussed in the previous section is complimentary with respect to the aim of the other. The TDPC algorithm enforces passivity of the bilateral controller under all possible operating conditions. In the design phase the transparency of the system is optimized for a set of operating conditions given the boundary condition of passive behavior. The complimentary effect that we wish to establish is to have minimal interference of the TDPC algorithm as long as the operating conditions of the system are within the considered set in the frequency domain design phase. However, when the operating conditions are outside that considered set, the TDPC algorithm should enforce passivity and therefore guarantee stability although the bilateral controller itself is potentially unstable according to the frequency domain-analysis.

This allows optimization of the bilateral controller for a specific set of desired operating conditions. For example in robotic surgery interaction can occur with both soft and hard materials, e.g. tissue and bone, respectively. When the TDPC algorithm is not implemented these hard contacts need to be taken into account in the design phase in the frequency domain. This can impose severe restrictions on the allowable parameter settings and limit the transparency of the system. If a properly matched TDPC algorithm is applied, the considered set of operating conditions in the design phase can be limited to the interaction with soft materials. The stability during hard contacts is then guaranteed by the TDPC algorithm.

In reverse, the application of a TDPC algorithm will by its nature guarantee stable behavior. It does not however convey information about the set of operating conditions that will trigger the TDPC algorithm. To estimate the set of environments that can be accurately displayed by the system without interference, a frequency domain-analysis can be performed.

An example of this desired complimentarity of the two approaches is sketched in Fig. 5.1. Up to stiffness K_e^{max} passivity of the telemanipulation system is guaranteed by the design of the controller in the frequency domain. For contact stiffnesses higher than K_e^{max} the telemanipulation system as designed in the frequency domain is potentially unstable, but passivity of the system is enforced by the non-linear TDPC algorithm.

5.5 Time Domain Passivity Control Extension

The complimentary effect described in the previous section is not possible with the standard TDPC algorithm. An immediate difference between the approaches of Sections 5.3.1 and 5.3.2 is that in the frequency domain the device dynamics are incorporated whereas these are neglected in the standard TDPC algorithm. This means that the boundaries of the system between which passivity is designed in the frequency domain differ from those between which passivity is enforced in the time domain, Fig. 5.2. (5.8) is a more restrictive condition than (5.4) which means that (5.8) can indicate that the system is supposedly non-passive, although the system as a whole is still passive.

The TDPC algorithm needs to be adapted to reduce its conservatism. The energy

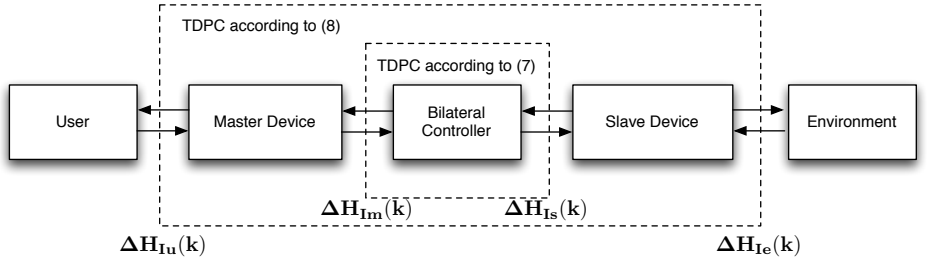

Figure 5.2: **Schematic overview of energy exchange:** Standard TDPC algorithms neglect the device dynamics, whereas these are taken into account in the design phase in the frequency domain.

balance which is monitored by the TDPC algorithm could be adapted to correspond with (5.4) as

$$\sum_{k=1}^{n} \Delta H_{Ih}(k) + \Delta H_{Ie}(k) \geq 0 \tag{5.9}$$

where ΔH_{Ih} and ΔH_{Ie} are the energies exchanged between the user and the master device and between the slave device and the environment, respectively. However, this energy balance when implemented in a TDPC-algorithm will not produce the desired result, which is guaranteed stability of the interaction with the system. An important difference is that in the frequency domain design phase the passivity of the system is checked when interacting with each considered environment independently. In the time domain on the other hand the passivity of the system is monitored online and thus for the interaction with a number of environments and users (e.g. different grasps and/or motions) in series. The history of the interaction can influence the performance of the TDPC algorithm.

The passivity condition of (5.9) is an inequality, which means that a net amount of energy can be stored in the system when interacting with certain environments. This net injected energy leads to a build-up of energy in (5.9). When the system starts to interact with an environment for which the frequency domain-analysis showed that the system is non-passive, and thus potentially unstable, this might not be detectable by the TDPC algorithm due to e.g. the prior interaction with other environments. The TDPC algorithm will not be activated until the generated "virtual" energy, due to the non-passivity of the system, has fully compensated the build-up of energy in (5.9). Therefore, the interaction with the system could temporarily be unstable. The duration of this temporary potential instability depends on the size of the build up of energy and can be quite significant. An example will be treated in Section 5.6.

Fig. 5.3 shows the value for three types of energy balances for a sinusoidal motion with the slave device moving in free space. Fig. 5.3 shows that the standard TDPC algorithm, based on (5.8), will be activated even with the slave device moving in free space. However, for a TDPC algorithm based on (5.9) indeed a build up of energy will occur, which is undesirable with respect to the guaranteed stability of the system. In the

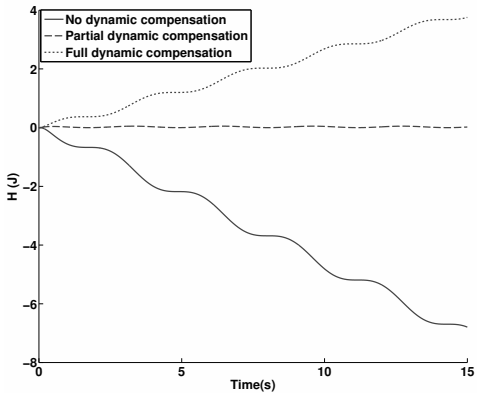

Figure 5.3: **Three energy balances of the same system moving in free space:** without dynamic compensation (5.8), with full compensation of the device dynamics (5.9), and the energy exchange at the motors with partial compensation of the device dynamics.

following subsections, three extensions to the standard TDPC algorithm will be discussed that will enable the TDPC algorithm to immediately detect non-passive behavior of the system while minimizing its influence when the system itself is passive according to the frequency domain-analysis. The value of this adapted energy balance is also depicted in Fig. 5.3.

A first extension of the TDPC algorithm was proposed by Franken et al. (2010*a*) which incorporate the device friction of the slave device to improve the performance of a TDPC algorithm when applied to telemanipulation systems with significant internal friction at the slave side.

5.5.1 Extending the Energy Balance

The energy balance monitored by the TDPC algorithm can be extended based on the LTI model of the hardware of the telemanipulation system that is used in the frequency domain design phase. An energy function of each element, e.g. masses, springs, and dampers, can be formulated based on their LTI model. The amount of energy absorbed/dissipated by that element is then a function of the measured displacement. By extending the energy balance of (5.8) with these additional energy functions the boundaries of the system between which passivity is enforced can be shifted.

In the system given in Section 5.2 the master and slave device are both considered to be perfectly rigid arms with a certain mass M and internal friction B. This means that the energy exchange of (5.7) is seperated from the energy exchange between the master and slave device and the slave device and environment as

$$\begin{aligned} \Delta H_{Im}(k) &= \Delta H_{Ih}(k) - \Delta H_{Km}(k) - \Delta H_{Rm}(k) \\ \Delta H_{Is}(k) &= \Delta H_{Ie}(k) - \Delta H_{Ks}(k) - \Delta H_{Rs}(k) \end{aligned} \tag{5.10}$$

where $\Delta H_{Km}(k)$ and $\Delta H_{Ks}(k)$ indicate the change in kinetic co-energy of the master and slave device, respectively. $\Delta H_{Rm}(k)$ and $\Delta H_{Rs}(k)$ indicate the dissipated energy due to viscous friction in the master and slave device, respectively. These energy functions can be derived from the LTI model. A change in kinetic co-energy, $\Delta H_K(k)$, can be computed as:

$$\begin{aligned} H_K(k) &= \frac{1}{2} M \dot{q}(k)^2 \\ \Delta H_K(k) &= H_K(k) - H_K(k-1) \end{aligned} \tag{5.11}$$

where $H_K(k)$ is the kinetic co-energy of the system at sample instant k. With the assumption of constant velocity during the sample period, the energy dissipated by viscous friction, $\Delta H_R(k)$, becomes

$$\Delta H_R(k) = \frac{B \Delta q(k)^2}{\Delta T} \tag{5.12}$$

where ΔT indicates the duration of the sample period. (5.12) is a conservative estimate of the physically dissipated energy as can be shown using the Cauchy-Schwarz inequality (Franken et al., 2010*a*).

It should be noted that although this process improves performance (transparent behavior without interference over a larger set of operating conditions), the robustness against modeling inaccuracies is decreased. Underestimating the physical parameters will prevent "virtual" energy from being generated.

5.5.2 Energy Build-up

Fig. 5.3 shows that when the device dynamics are fully compensated according to the previous section, a build up can occur in the monitored energy balance. This is due to the full compensation of the dissipative elements in the system.

As we are extending the energy balance to incorporate the device dynamics, we can choose to not always compensate for the dissipated energy to prevent a build-up. For the compensation algorithm the circumstances need to be identified under which the dissipated energy can be safely compensated. Two methods have been considered, of which one is susceptible to build up under a specific circumstance:

1. Always compensate $\Delta H_{Rs}(k)$ and only include $\Delta H_{Rm}(k)$ when $H(k) < 0$.
2. Compensate $\Delta H_{Rs}(k)$ and $\Delta H_{Rm}(k)$ only when $H(k) < 0$.

where $H(k)$ is the value of the energy balance, and $\Delta H_{Rm}(k)$, and $\Delta H_{Rs}(k)$ are the dissipated energies in the master and slave device, respectively. The first approach is less conservative as more of the dissipated energy due to physical friction is reclaimed in the energy balance. The first approach works fine for passive environments, but can lead to a build up of energy when motions can be initiated from the environment. The second strategy never leads to a build up, but will cause the TDPC algorithm from being activated more frequently due to the higher amount of neglected energy. Depending on the assumptions made about the environment one of these strategies should be selected.

5.5.3 Energy Scaling

The telemanipulation system is used to interact with the remote environment. It can be beneficial to not display the forces/velocities in a one-to-one ratio at the master and slave side. Motion scaling can be used to enable high precision micro manipulation capabilities in the remote environment. Motion and force scaling can also be used to design passive behavior of the system, e.g. the use of $\mu\lambda$ in (5.6) and (5.5).

When motion and/or force scaling is included in the design of the bilateral controller, the ideal behavior of (5.1) can be expressed as

$$\begin{aligned} \dot{q}_s(t) &= \mu\dot{q}_m(t) \\ F_h(t) &= -\lambda F_e(t) \end{aligned} \tag{5.13}$$

This scaling of the power port variables will also effect the energy balance of the system. Taking the scaling values into account the energy balance of the ideal behavior (5.13) of the two-port system becomes

$$\int_{t=0}^{t_1} -\lambda F_e(t)\dot{q}_m(t) + \mu F_e(t)\dot{q}_m(t)dt \geq 0 \tag{5.14}$$

This shows that unless $\mu = \lambda$ an energy mismatch between the two interaction ports arises. This can either lead to a build up effect as discussed earlier, or cause the modulated damper of the TDPC algorithm to be activated continuously even though the system would be demonstrating the ideal energy behavior.

The solution to this problem is to not enforce two-port passive behavior on the energy balance of the system given by (5.14). The system does not display two-port passive behavior when scaling is present, but the behavior is passive with respect to a storage function and therefore still mimics a dissipative system, which are thoroughly treated by Willems (1972). That storage function is a transformed energy balance that takes the scaling into account (5.15). Passivity is being enforced by a modulated damper at the master side, so the energy exchange is normalized with respect to the master side

$$\int_{t=0}^{t_1} F_h(t)\dot{q}_m(t) + \frac{\lambda}{\mu}F_e(t)\dot{q}_s(t)dt \geq 0 \tag{5.15}$$

Naturally this energy balance needs to be adjusted for the build up effect as described earlier. Secchi et al. (2005) have similarly applied scaling to haptic interfaces and in a scattering-based telemanipulation algorithm.

5.6 Example

In the previous section we have discussed three required extensions to the TDPC algorithm in order to establish complimentarity with the design of the bilateral controller in the frequency domain. To demonstrate the increase of performance of the combined ap-

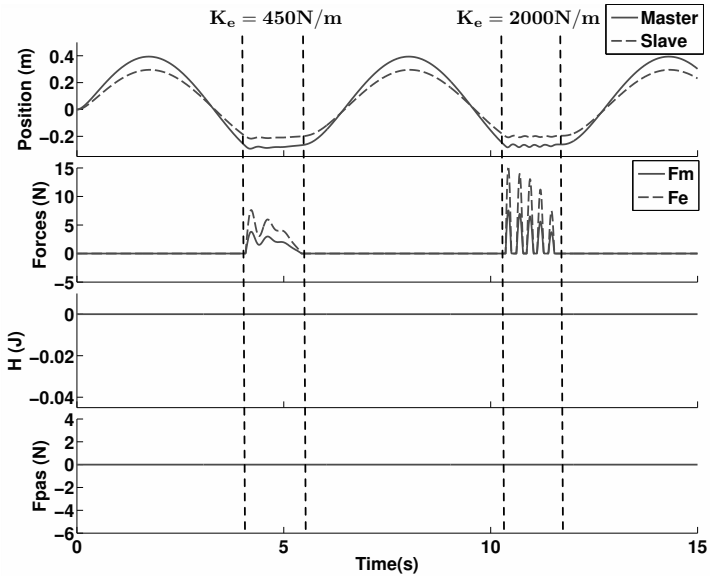

Figure 5.4: **Position-Force control without TDPC:** Stable interaction is not guaranteed with all environments.

proach several simulations have been performed using the program 20-sim (Controllab Products B.V., 2010).

The system model of Section 5.2 is used with the parameters listed in Table 5.1, which are based on the setup described by Willaert et al. (2010a). The environment consists of a material characterized by a simple spring model with stiffnesses K_e located at position $q_w = -0.2m$. The user is modeled as a spring-damper controller with parameters $K_p = 20N/m$ and $K_v = 4Ns/m$ with as set-point a sinusoidal motion with an amplitude of $0.4m$ and frequency of $0.16Hz$.

The modulated damper is implemented as:

$$\begin{aligned} F_{pas}(k) &= -d(k)\dot{q}_m(k) \\ d(k) &= \begin{cases} -\alpha H(k) & \text{if } H(k) < 0 \\ 0 & \text{otherwise} \end{cases} \end{aligned} \tag{5.16}$$

Table 5.1: Parameter values of physical setup

Parameter	Value	Parameter	Value
M_m	0.64 kg	M_s	0.61 kg
B_m	3.4 Ns/m	B_s	11 Ns/m
K_p	4000 N/m	K_v	80 Ns/m

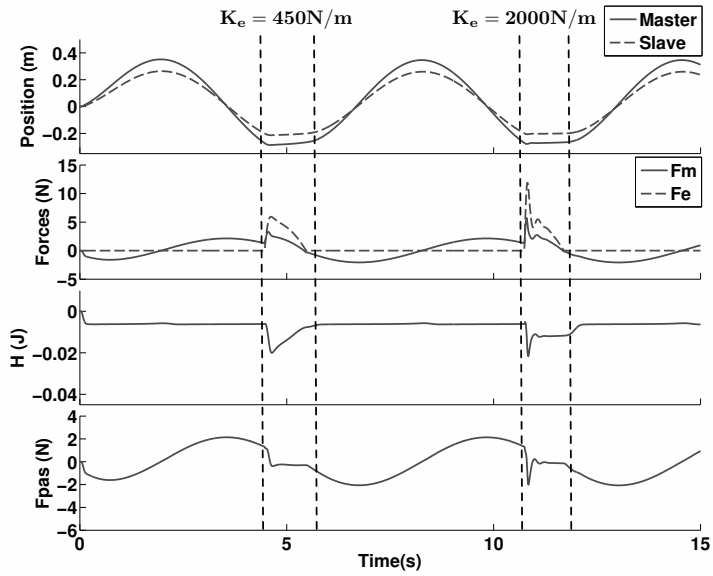

Figure 5.5: **Position-Force control with standard TDPC:** Stability is always guaranteed, but TDPC is also active when stability is already guaranteed by the design of the bilateral controller.

where F_{pas}, $d(k)$, and α are the additional force applied to the user to restore passivity, the value of the modulated damper, and α is a tuning parameter for the rate at which the additional required energy is extracted from the user, respectively. α is set to 1000 for these simulations to produce a stable contact phase. The sample frequency at which the discrete control loop is computed is $1kHz$.

Suppose that based on the task and the particular environment the maximum stiffness that we wish to accurately reflect is $500N/m$. In that case, using the device parameters in Table 5.1 and (5.6), a maximum value holds of $\mu\lambda = 0.38$. We select $\mu = 0.75$ and $\lambda = 0.5$ for good transparency of the telemanipulation system for stiffnesses up to $K_e = 500N/m$. However, assume that the hardest contact in the environment has a stiffness of $2000N/m$. Based on the Bounded Environment Passivity approach a maximum value of $\mu\lambda = 0.17$ holds for this worst case stiffness. With the selected settings the telemanipulation system is potentially unstable for certain contacts that can occur during operation.

Several simulations have been performed. In each simulation during the first contact phase the environment stiffness is $K_e = 450N/m$ and during the second contact phase the stiffness is $K_e = 2000N/m$. Each plot shows the positions of the master and slave device, the force applied to the user F_m by the controller and the interaction force at the environment side F_e. For clarity the level of the monitored energy balance, H, and the force exerted by the modulated damper of the TDPC, $Fpas$, are also plotted separately.

Fig. 5.4 shows the response of the system when only the designed P-F controller

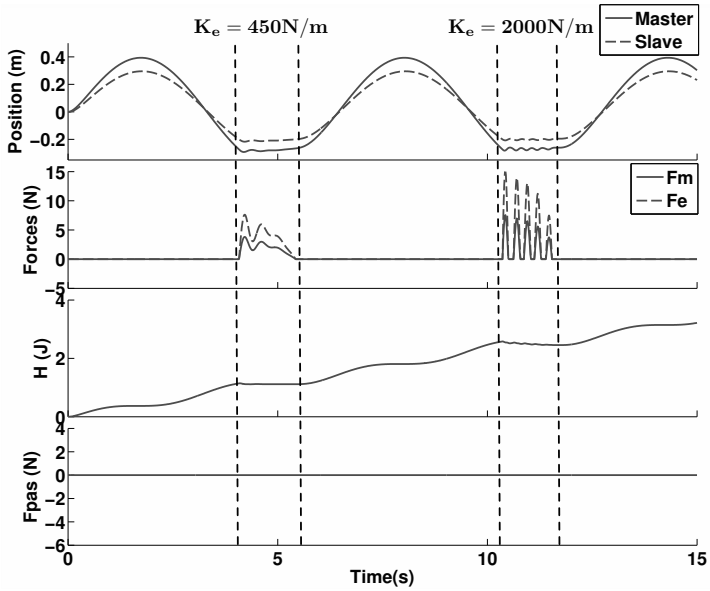

Figure 5.6: **Position-Force control with incorrect Extended TDPC:** Due to an energy build up the algorithm fails to suppress contact instabilities due to active behavior of the bilateral controller.

is implemented. The plot demonstrates that for stiffnesses above K_e^{max} stability of the contact between the slave and the environment is not guaranteed by the bilateral controller and the slave device bounces on the surface of the material.

In the second simulation, Fig. 5.5, the bilateral controller is combined with the standard TDPC algorithm of Section 5.3.2. Fig. 5.5 shows that the contact stability is improved for $K_e > K_e^{max}$, the slave does not bounce on the surface of the material. However, the modulated damper is also highly active during the free space motion and the first contact phase for which stability of the interaction is guaranteed by the frequency domain design phase. This unnecessary additional damping limits the transparency of the telemanipulation system.

In the third simulation the extended TDPC algorithm is used. Fig. 5.6 shows the system response when the dissipated energy in both the master and slave device is continuously compensated. When the system starts to display non-passive behavior during the second contact phase the modulated damper is not activated due to the positive value of the monitored energy balance. During this period where the bilateral controller generates "virtual" energy the energy balance is decreasing (from $t \approx 10s$), but remains positive.

Fig. 5.7 finally shows the response of the system with the extended TDPC algorithm as proposed in Section 5.5. As no movements can be initiated from the environment, the dissipated energy in the slave device is continuously compensated, see Section 5.5.2. The dissipated energy in the master device is only used when the energy balance is negative. Comparing Fig. 5.7 with Fig. 5.4 shows that also with the extended TDPC algorithm

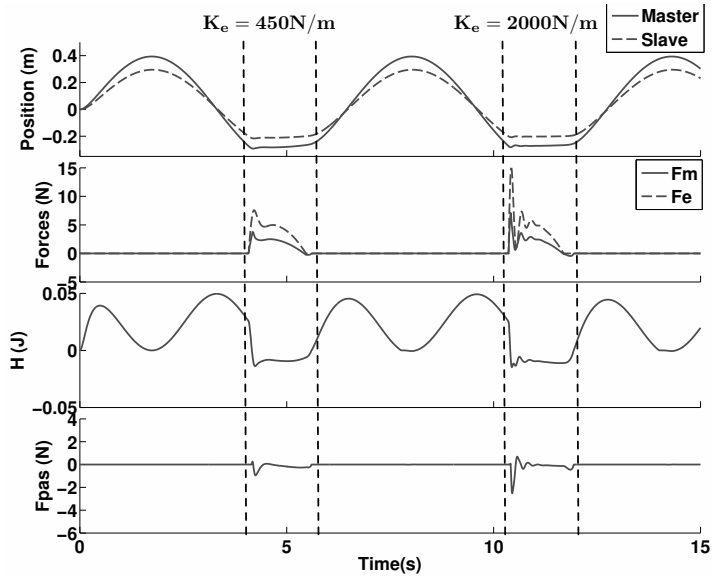

Figure 5.7: **Position-Force control with correct Extended TDPC:** Stability is always guaranteed and the influence of TDPC is minimized when stability is guaranteed by the design of the bilateral controller.

the contact stability is guaranteed for environments with $K_e > K_e^{max}$. Comparing Fig. 5.7 with Fig. 5.5 shows that the influence of the extended TDPC algorithm is minimal compared to the standard TDPC algorithm during the free space motion and first contact phase, where $K_e < K_e^{max}$. This indicates an increase in the transparency of the telemanipulation system when the extended TDPC algorithm is used.

5.7 Discussion

In the previous section simulation results were presented that show that a better complimentarity between the design of the bilateral controller in the frequency domain and an extended TDPC algorithm can be achieved. However, a perfect complimentarity cannot be established. This is visible in Fig. 5.6. Even though $K_e < K_e^{max}$, the extended TDPC algorithm is active, albeit very lightly.

An important cause for the TDPC algorithm to be activated before the theoretical boundary of K_e^{max}, is the neglecting of dissipated energy. This is done to prevent the build up effect. A second cause can be found in the inherent difference between the frequency domain-analysis and time domain-implementation. In the frequency domain, a continuous time model of the controller is used, whereas this controller is actually implemented in discrete-time. It is well known that a continuous-time passive model can become non-passive when discretized (Colgate et al., 1993). However, this effect, given a high enough sample frequency, will only be a minor cause with the used bilateral con-

troller.

Besides the above two causes, which are inherent to the method, a third cause is in this particular example due to the nature of the Bounded Environment Passivity approach. This approach focuses on one-port passive behavior of the interaction between the user and the master device. For light grasps of the user an internal damped resonance mode exists that when excited cause the telemanipulation system to be momentarily two-port non-passive. In that situation the interaction between the user and the master device can remain one-port passive. This difference can be circumvented by applying a frequency domain design method that analyzes passive behavior of both interaction ports, e.g. extending the Bounded Environment Passivity approach with a Bounded Operator approach (Willaert et al., 2010a), a similar approach using a different analysis method was proposed by Haddadi and Hashtrudi-Zaad (2010).

Time-delays in the communication channel have not been considered in this paper. Physical, varying time-delays cannot be taken into account in the frequency domain and even constant time-delays turn any LTI-model into an infinite-dimensional system. The negative influence time-delays have on the stability of bilateral controllers designed for a no-delay situation can be handled effectively by a TDPC algorithm, see e.g. (Franken et al., 2009), (Artigas et al., 2008), and (Ryu et al., 2010). The transparency properties of the system will be lower compared to the no-delay situation, but stable interaction will still be guaranteed.

5.8 Conclusions

In this paper it was shown that it is possible to improve the complimentary effect between passivity-based approaches for the design of bilateral controllers in the frequency domain and the enforcing of passive behavior in the time domain by means of a TDPC algorithm. Several required extensions to the TDPC algorithm were the addition of the device dynamics to the monitored energy balance, methods for the prevention of an energy build up, and the inclusion of energy scaling. Using these extensions the influence of the TDPC algorithm can be minimized for the set of operating conditions that were considered in the frequency domain design phase. For operating conditions outside this set, and which can potentially destabilize the system, passivity and thus stability is enforced by the TDPC algorithm. Future work will focus on establishing this complimentary effect in physical experiments.

CHAPTER 6

Internet-Based Two-Layered Bilateral Telemanipulation: An Experimental Study

Franken, M., Misra, S. and Stramigioli S.
In preparation for IEEE International Conference on Robotics and Automation 2012

Enforcing passive behavior of a telemanipulation system guarantees stability of the interaction between the user/environment and the system. Stability is guaranteed even in the presence of factors that could otherwise destabilize the system, e.g. time delays and hard contacts in the environment. In this paper the two-layer framework for bilateral telemanipulation introduced by Franken et al. (2009) is applied in a series of bilateral telemanipulation experiments conducted over the internet. These experiments validate the ability of the approach to guarantee stable behavior of the system in the presence of time-varying delays and package loss. Two extensions to the two-layer framework are discussed that increase the transparency properties of the approach. The increase in transparency that can be obtained is demonstrated by experimental data.

6.1 Introduction

A fundamental requirement for bilateral telemanipulation is the guaranteed stability of the system under all possible circumstances. Therefore, passivity-based arguments are often applied in the design of bilateral control algorithms. A passive system is a system that cannot generate energy by itself. The interaction between passive systems is guaranteed to be stable and any proper combination of passive systems will again be a passive system (van der Schaft, 1999). Both the operator and the environment can be assumed to be passive, or at least to interact in a stable manner with passive systems. Thus ensuring passivity of the telemanipulation system itself, ensures stability of the interaction between the user/environment and the telemanipulation system.

Many different approaches have been proposed on how the concept of passivity can be applied to telemanipulation systems, see e.g. (Hokayem and Spong, 2006). In this paper we will focus on a class of algorithms that enforce passivity of the telemanipulation system by monitoring an energy balance of the system, Time Domain Passivity (TDP) algorithms. The first example of a TDP algorithm was proposed by Ryu et al. (2004*b*), Time Domain Passivity Control (TDPC). They applied a Passivity Observer (PO) and Passivity Controller (PC) algorithm to bilateral telemanipulation. This scheme was originally introduced by Hannaford and Ryu (2002) to guarantee stable interaction with virtual environments. The energy exchange between the user/environment and the telemanipulation system is monitored and when necessary a modulated damper is activated to dissipate any generated "virtual" energy.

A telemanipulation system allows the user to project his presence at a remote site. Therefore it is likely that there will exist time delays in the communication channel connecting the master and slave system. An interesting control problem is how to ensure passivity of the telemanipulation system in the presence of time-delays as the energy exchange at both interaction points can no longer be monitored simultaneously, which is an underlying assumption of the standard TDPC algorithm.

Extended implementations of the TDPC algorithm to allow for time delays were proposed by Ryu and Preusche (2007), Ryu et al. (2010), and Artigas et al. (2007, 2010*a*). Other approaches that maintain passive behavior of time-delayed telemanipulation systems in the time domain were introduced by Lee and Huang (2010) and Franken et al. (2009). Lee and Huang (2010) proposed the Passive Set Position Modulation framework, while Franken et al. (2009) introduced a two-layer framework in which the passivity properties and transparency properties were separated into different hierarchical control problems.

In this paper we will demonstrate the effectiveness of the two-layer approach in a series of internet-based telemanipulation experiments. Furthermore we will discuss two extensions that will improve the transparency properties of any control approach that is based on monitoring the physical energy exchange with the system. One of these extensions has been proposed by Franken et al. (2010*a*).

The paper is organized as follows: Section 6.2 discusses the two-layer framework for bilateral telemanipulation. The influence of a non-perfect communication channel is discussed in Section 6.3. In Section 6.4 the two transparency-enhancing extensions are

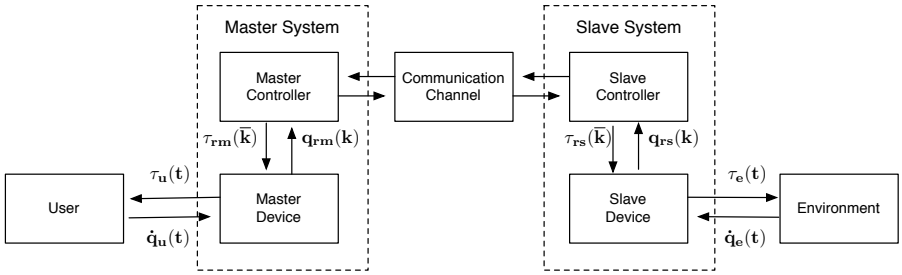

Figure 6.1: **Schematic overview of a bilateral telemanipulation chain:** τ_* and $\dot{q}_*$ represent torques/forces and velocities, respectively. The subscript u, rm, rs, and e indicate the interaction between the user and the master device, the actuators of the master and slave device, and the interaction between the slave device and the environment, respectively.

discussed. Experimental results are presented in Section 6.5. The paper concludes and provides directions for future work in Section 6.6.

6.2 Two-Layer Bilateral Telemanipulation

In this section we will treat the working of the two-layer framework for (time-delayed) bilateral telemanipulation first introduced by Franken et al. (2009). The framework consists of two control layers in a hierarchical structure, the *Transparency Layer* and the *Passivity Layer*, see Fig. 6.2.

6.2.1 Transparency Layer

The *Transparency Layer* can contain any control algorithm that delivers the desired transparency, as long as it results in a desired torque/force to be applied to the devices at both sides. In Section 6.5 experimental results will be shown with a Position-Force controller implemented in the *Transparency Layer*, while simulation results with a simple Impedance Reflection algorithm have been shown in Franken et al. (2009). The desired torques computed by the *Transparency Layer* are the inputs to the *Passivity Layer*.

6.2.2 Passivity Layer

This layer enforces passivity of the bilateral telemanipulation system [1]. When necessary the commands originating from the *Transparency Layer* are adjusted to maintain passivity. The *Passivity Layer* is centered around two communicating energy tanks. A tank is defined at both the master and slave side, and there are three energy flows connected to each tank:

[1] Notation used in this paper: The index k is used to indicate instantaneous values at the sampling instant k and the index $\overline{k}$ is used to indicate variables related to an interval between sampling instants $k-1$ and k.

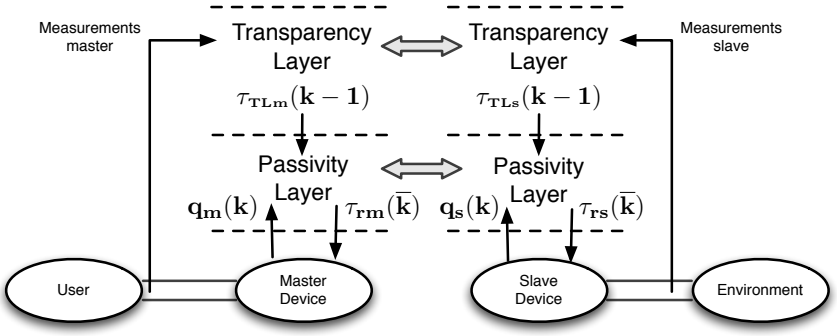

Figure 6.2: **Two-layer algorithm for bilateral telemanipulation.** The double connections indicate physical energy exchange.

- Energy exchanged with the physical world, ΔH_{Im} and ΔH_{Is}
- Energy received from the communication channel, $\Delta H_{SM+}(k)$ and $\Delta H_{MS+}(k)$
- Energy send into the communication channel, $\Delta H_{MS-}(k)$ and $\Delta H_{SM-}(k)$

where the subscript Im, $SM+$, and $MS-$ are related to the master side and Is, $MS+$, and $SM-$ to the slave side, respectively. The energy flow received from the communication channel at the master side, ΔH_{SM+}, is the time-delayed energy flow send into the communication channel at the slave side, ΔH_{SM-}, and vice versa. The level of the energy tank at each side is corrected each sampling instant with respect to these three energy flows, which means that the change of the energy level in each tank is given as

$$\begin{aligned} \Delta H_M(k) &= \Delta H_{Im}(k) + \Delta H_{SM+}(k) - \Delta H_{MS-}(k) \\ \Delta H_S(k) &= \Delta H_{Is}(k) + \Delta H_{MS+}(k) - \Delta H_{SM-}(k) \end{aligned} \tag{6.1}$$

where $\Delta H_M(k)$ and $\Delta H_S(k)$ are the change of the energy levels in both tanks, and thus

$$\begin{aligned} H_M(\overline{k+1}) &= H_M(\overline{k}) + \Delta H_M(k) \\ H_S(\overline{k+1}) &= H_S(\overline{k}) + \Delta H_S(k) \end{aligned} \tag{6.2}$$

where H_M and H_S are the levels of the energy tank at the master and slave side, respectively.

The first of these flows can be exactly quantified *a posteriori* according to (Stramigioli et al., 2005):

$$\begin{aligned} \Delta H_I(k) &= \int_{(k-1)\Delta T_S}^{k\Delta T_S} \tau_r(\overline{k})\dot{q}(t)dt \\ &= \tau_r(\overline{k})\Delta q(k) \end{aligned} \tag{6.3}$$

where τ_r and $\dot{q}$ are the force and velocity associated with the interaction point between the physical world and the controller in discrete time. (6.3) represents the energy which

is supplied by the actuators at that side.

The energy exchange between the two tanks is determined by the implemented Energy Transfer Protocol. Depending on the implementation of the *Transparency Layer* and the application of the system various protocols are possible. In this paper we will use the Simple Energy Transfer Protocol (SETP) in which each side transmits each iteration a fraction, β, of its available energy to the other side. The properties and implications of the SETP will be analyzed in Section 6.3.

A Tank Level Controller (TLC) is defined at the master side to regulate the energy level in the system. It is activated in order to extract an initial amount of energy, and further additionally required energy, from the user to maintain passivity. The TLC is located at the master side as the user has to inject energy into the system for the slave device to be able to execute the commanded task. The TLC is implemented as a modulated viscous damper, that is activated when the energy level in the tank available during sample period $\overline{k+1}$, $H_m(\overline{k+1})$, drops below the desired level of the tank, H_d. The additional force, τ_{TLC}, exerted by this modulated damper will extract additional energy from the user during sample period $\overline{k+1}$ to replenish the energy tank, and is given by:

$$\begin{aligned} \tau_{TLC}(k) &= -d(k)\dot{q}_m(k) \\ d(k) &= \begin{cases} \alpha(H_d - H_m(\overline{k+1})) & \text{if } H_m(\overline{k+1}) < H_d \\ 0 & \text{otherwise} \end{cases} \end{aligned} \tag{6.4}$$

where $d(k)$ is the modulated viscous damping coefficient, $\dot{q}_m(k)$ is the velocity of the master device at sample instant k and α is a tuning parameter for the rate at which the additional required energy is extracted from the user.

The energy tanks in this scheme can be regarded as energy budgets from which controlled motions of the devices can be powered. When the available energy is low, the forces that can be exerted by the devices are restricted. The manner in which the forces are restricted when the available energy is low can be designed to suit a specific device, environment, and/or task.

At each side passivity is enforced with respect to the energy tank at that side, which means

$$\begin{aligned} H_M(\overline{k}) &\geq 0 \quad \forall k \\ H_S(\overline{k}) &\geq 0 \quad \forall k \end{aligned} \tag{6.5}$$

This means that passivity of the entire telemanipulation system is enforced, independent of the time delay, as the amount of energy in the communication channel, H_C, due to the SETP can only be positive and thus

$$H_T(\overline{k}) = H_M(\overline{k}) + H_C(\overline{k}) + H_S(\overline{k}) \geq 0 \tag{6.6}$$

where (assuming zero initial energy in the communication channel)

$$\begin{aligned} H_C(\overline{k}) = \sum_{i=0}^{k-1} \Delta H_{MS-}(i) + \Delta H_{SM-}(i) \\ -\Delta H_{SM+}(i) - \Delta H_{MS+}(i) \geq 0 \end{aligned} \tag{6.7}$$

6.3 Non-Ideal Communication Networks

In this section we will analyze the influence a non-ideal communication network (varying time-delay and packet loss) has on the *Passivity Layer* of the two-layer framework. Problems can occur in the *Transparency Layer* when time-dependent operations, e.g. differentiations, are applied to the received signals, or incremental data is transmitted. Both these problems can be handled by a proper choice of communication protocol and transmission data.

6.3.1 Constant Time-Delay

When the time-delay in the communication channel is constant the SETP will force the levels of the two tanks to converge to the same level when no energy exchange occurs with the physical world. The LTI model, Σ_1, of the system is

$$\Sigma_1 : x(\overline{k+1}) = \begin{bmatrix} 1-\beta & 0 \\ 0 & 1-\beta \end{bmatrix} x(\overline{k}) + \begin{bmatrix} 0 & \beta \\ \beta & 0 \end{bmatrix} x(\overline{k-d}) \tag{6.8}$$

where $x = \begin{bmatrix} H_M \\ H_S \end{bmatrix}$ and d indicates the constant communication delay, respectively. From Σ_1 a new state, H_{dif} is derived that describes the difference between the tank levels

$$\begin{aligned} H_{dif}(\overline{k+1}) &= H_M(\overline{k+1}) - H_S(\overline{k+1}) \\ &= (1-\beta)H_{dif}(\overline{k}) - \beta H_{dif}(\overline{k-d}) \end{aligned} \tag{6.9}$$

The characteristic polynomial, $P(z)$, describing the dynamic behavior of just this new state is described as (Ren et al., 2003)

$$P(z) = z^{d+1} - (1-\beta)z^d + \beta \tag{6.10}$$

Investigating the stability of this system, without explicitly computing the roots of the polynomial, can be performed using the Jury Stability Criterium (Jonckheere and Ma, 1989). This criterium states that if certain terms, that are computed from the coefficients of the polynomial, are positive the system is asymptotically stable. Application of this

criterium to $P(z)$ indicates the following terms have to be positive

$$\begin{aligned} \frac{4\beta(1-\beta)}{d\beta+1} &> 0 \\ \frac{-r\beta^2+(r-1)\beta+1}{(r-1)\beta+1} &> 0 \quad \forall r \in [0..d-1] \end{aligned} \tag{6.11}$$

For $0 < \beta < 1$ and any d all the terms of (6.11) are positive. This indicates the tank level difference is asymptotically stable and will converge to zero in the absence of external inputs, albeit that the settling time can be large for large d and/or β.

During normal operation energy exchange with the physical world will take place. In that case the performance of the SETP is determined by the selection of the desired tank level, H_d, the transmitted fraction of the energy level, β, and the rate at which additional energy is extracted from the user by the TLC, α. The tuning of these parameters depends on the characteristics of the devices, the environment, and the executed motion.

6.3.2 Varying Time-Delay

When varying time-delays are present in the communication channel the performance of the SETP will worsen. The levels of the two tanks will not converge even when there is no energy exchange with the physical world, but will be subject to ripple. Theoretically this means that due to the presence of the TLC the amount of energy in the system could keep on increasing when the slave system is stationary. In practice this will not occur as energy will flow out of the system due to movements of the slave device and the variation of the time delay is assumed to be relatively small.

A more disturbing influence of a varying time-delay is thought to be the varying activation of the TLC that is likely to happen due to the ripple on the tank level. Assume that for a number of samples no energy arrives at the master side from the slave system due to varying delays. Each iteration energy will be send to the slave system causing the energy level of the tank to decrease, which in turn activates the TLC to extract energy from the user. When energy does arrive from the slave system, the energy level in the tank will show a discrete jump due to the received energy packet(s). When this jump causes the level of the tank to rise above the desired level, the TLC will be deactivated. This effect will occur more frequently for larger variations in the delay. Should this effect become noticeable it might be necessary to include a decaying function to the TLC which would prevent the TLC from switching off abruptly even when the desired amount of energy is present in the tank. Any energy extracted by such a decaying function would have to be dissipated in order to prevent a build-up of energy in the *Passivity Layer*.

6.3.3 Packet loss

Depending on the chosen implementation of the communication protocol packet loss might arise in the communication between master and slave device, e.g. communication based on UDP Kurose and Ross (2006). The SETP transmits quanta of energy through the

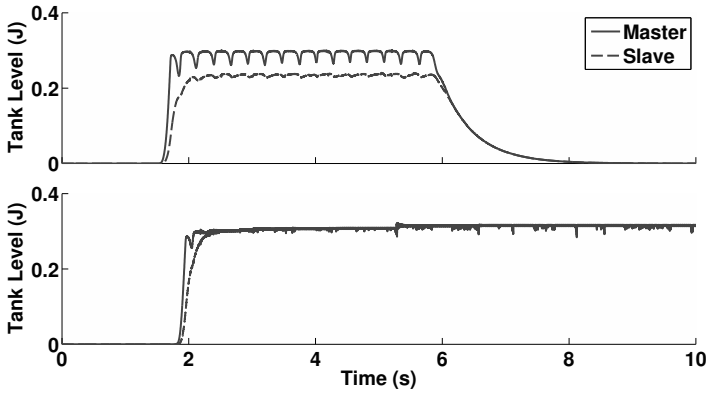

Figure 6.3: **SETP with packet loss in the communication channel:** Transmitting the sum of the energy prevents dissipative behavior due to packet loss in the communication channel.

communication channel. If a packet is lost, the energy is dissipated. The communication channel will be strictly passive as less energy can be extracted from it than was injected.

This dissipation of energy will affect two processes in the *Passivity Layer*. First the TLC will be activated more frequently to extract additional energy from the user to compensate for the energy lost in the communication channel. Secondly, the lower amount of energy present in the energy tank due to dissipation in the communication channel can trigger any implemented saturation function. This will adversely influence the tracking behavior of the slave device and the force reflection to the user.

The solution to this problem is to not send energy quanta directly, but rather the summation of all send packets over time. As each packet represents a positive (possibly zero) amount of energy, the summation over time can only remain constant or increase. Subtracting two subsequent received sums therefore gives exactly the amount of energy that was transmitted in the period between their transmissions irrespective of how many packets in between were lost. Out of order packages are immediately discarded as their information is fully contained in the received sum that was transmitted latest.

This effect is demonstrated in Fig. 6.3 were the master and slave are connected by means of a communication channel without time delay, but with an artificial packet loss of 20%. The TLC is activated in order to extract enough energy to fill the tanks. With the standard SETP the energy tanks are soon depleted as soon as the user stops moving due to the dissipative behavior of the communication channel. However, with the transmission of the sum of transmitted energy this problem is circumvented. As the energy of lost packets is now added to the tank later, the level of the energy tanks will be subject to some disturbance.

6.4 Improved Transparency

In the previous sections the basic principle of the two-layer framework has been explained. In this section we will discuss two extensions that when implemented can significantly decrease the adjustments made by the *Passivity Layer* to the desired torques originating from the *Transparency Layer*. As will be demonstrated in Section 6.5 this increases the obtainable transparency of the telemanipulation system while maintaining the stability properties of the basic approach.

The extensions when implemented only affect the energy tank at the side where they are implemented. As such their performance is unaffected by the time delay in the communication channel.

6.4.1 Friction compensation

The *Passivity Layer* monitors the energy exchange through the actuators between the physical world and the control algorithm executed in the discrete domain. As such two-port passive behavior of the bilateral control algorithm is enforced. This guarantees stability, but is overly conservative. Energy is dissipated in both the master and slave device due to mechanical friction. The actuators need to exert forces and thus spend energy to move the slave device, even when it is moving in free space. Due to the two-port passivity condition this energy needs to be injected by the user. With the slave device moving in free space the *Transparency Layer* will likely not command any force to be applied and as such the TLC will be activated to extract the required energy from the user. The user will therefore not experience free space motion. This degradation of the transparency depends on the amount of mechanical friction present in the slave device.

Franken et al. (2010*a*) proposed to compensate for this effect by constructing a model-based feedback loop for dissipated energy due to friction. Based on a model of the friction the amount of dissipated energy in the slave device is estimated and added to the energy tank at the slave side, Fig. 6.4. This process allows the control system to generate an amount of "virtual" energy to overcome the physical friction, which means that the boundaries between which passivity is enforced are extended to include the mechanical friction. The conservatism of the two-port passivity condition is reduced and the obtainable transparency of the complete system will be increased. As long as the model (and thus the estimate of the dissipated energy) is conservative with respect to the physical friction, stability of the total telemanipulation system is still guaranteed.

6.4.2 Energy scaling

The standard *Passivity Layer* will enforce two-port passive behavior of the bilateral control algorithm irrespective of the implementation of the *Transparency Layer*. However, certain applications of the telemanipulation system will involve scaling in the *Transparency Layer*, e.g. scaling down the motions of the user or increasing the interaction forces. These scaling properties do influence the energy exchange that is occuring. Assuming μ and λ represent the possible scaling factors for the motions and forces, we have

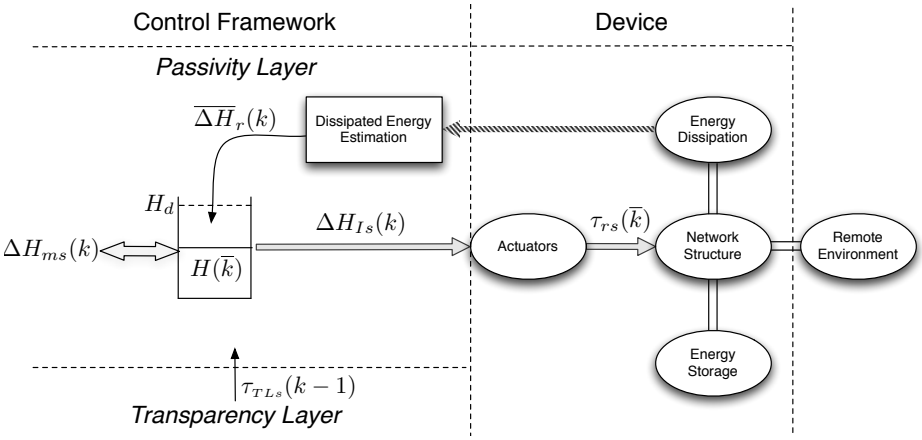

Figure 6.4: **Compensation of dissipated energy:** based on a model the dissipated energy due to mechanical friction can be estimated and added to the energy tank.

for a perfectly transparent system:

$$\begin{aligned} \dot{q}_S &= \mu \dot{q}_M \\ \tau_{TLm} &= \lambda \tau_e \end{aligned} \tag{6.12}$$

This means that in the ideal case the exchanged energy at the master side will be:

$$\int_{t_0}^{t_1} \tau_{TLm} \dot{q}_M dt = \int_{t_0}^{t_1} \lambda \tau_e \frac{1}{\mu} \dot{q}_S dt = \frac{\lambda}{\mu} \int_{t_0}^{t_1} \tau_e \dot{q}_S dt \tag{6.13}$$

With $\lambda \neq \mu$ the ideal system is no longer two-port passive, but still a dissipative system. Dissipative systems theory was introduced by Willems (1972) and showed that passive systems are a special class of dissipative systems. Dissipative systems are passive with respect to a supply function and thus also guaranteed to be stable. However, the difference is that the supply function is not necessarily physical energy.

Therefore in order for the *Passivity Layer* to produce the best results this scaling needs to be taken into account. We propose to scale the energy exchanged at the slave side as:

$$\Delta H *_{Is}(k) = \frac{\lambda}{\mu} H_{Is}(k) \tag{6.14}$$

so that the system is two-port passive with respect to the supply function

$$\Delta H *_T = \Delta H_{Im} + \Delta H *_{Is} \tag{6.15}$$

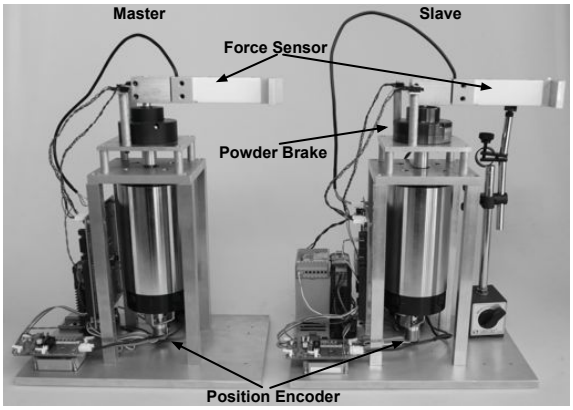

Figure 6.5: **Experimental setup:** The setup consists of two identical 1 d.o.f. devices.

6.5 Experiments

In this section experimental results obtained with the described two-layer control algorithm are presented. First the used test setup will be introduced with the specific implementation of the internet communication and control algorithms.

6.5.1 Test setup

The setup, Fig. 6.5, consists of two identical one degree of freedom devices powered by a DC motor without gearbox. The maximum continuous torque that these motors can exert is $1.38\,\mathrm{Nm}$. A high-precision encoder with $65\,\mathrm{k}$ pulses per rotation is used to record the position of each device. The mechanical arm of each device contains a linear force sensor to record the interaction force between the user/environment and the devices.

Both devices are controlled from the same embedded controller running a real-time Linux distribution. The controllers are implemented in the program 20-sim (Controllab Products B.V., 2010) and real-time executable code specific for this setup is generated directly from 20-sim and uploaded to the embedded controller by means of the program 4C (Controllab Products B.V., 2010). The sampling frequency of the control loop is $1\,\mathrm{kHz}$. As environment a mechanical spring with a stiffness of approximately $1500\,\mathrm{N/m}$ is used.

In order to demonstrate the effectiveness of the approach of Section 6.4 the level of friction in the slave device needs to be adjustable. To this end a powder brake (Merobel FAT 20) is incorporated in the slave device. A powder brake is essentially a bearing with a coil integrated in the component. When a current runs through the coil, the resulting electromagnetic field attracts ferromagnetic powder in between the running surfaces of the bearing, creating coulomb friction.

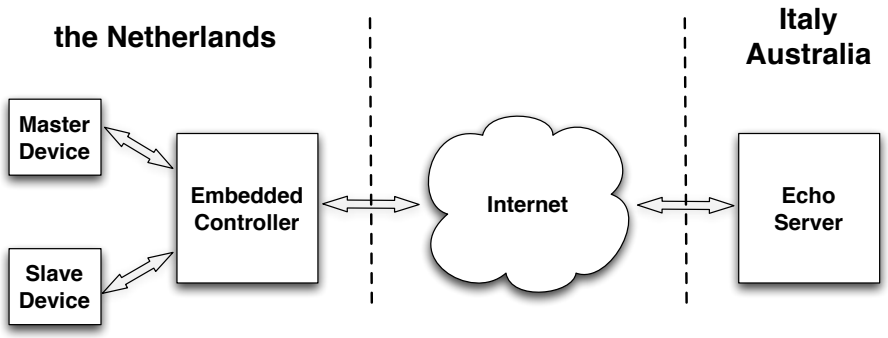

Figure 6.6: **Communication setup for the time delay experiments:** All communication between the control algorithms for the master and slave device takes place over the internet.

6.5.2 Internet Connection

For the time-delay experiments an internet connection has been established with two echo-servers. The first server is located in Italy and the second server in Australia. The data to be exchanged between master and slave device was transmitted from the Netherlands to either Italy or Australia, Fig. 6.6. Upon reception from the echoed package the data was used in the control algorithm of the intended system.

The code generation process of 4C has been extended to establish socket communication over the internet by means of the TCP/IP or UDP communication protocols (Kurose and Ross, 2006). For the time-delay experiments UDP is chosen as communication protocol as the obtainable transmission rate with TCP/IP was found to be insufficient for proper haptic feedback. Fig. 6.7 shows typical time-delays that were encountered during these experiments. It should be noted that these time-delays are one-way delays and occur both in the communication between master and slave, and vice versa, during the experiments.

Specifications of these connections representative for the connections during the experiments is given in Table 6.1. Each sampling instant the packet in the receiving buffer that was transmitted the latest was used and other packages were discarded. A package loss of 27% was recorded in the communication with Australia. According to Section 6.3 this would require the transmission of the sum of transmitted energy by the SETP as otherwise the communication channel would become extremely dissipative due to the package loss. However, in the *Passivity Layer* no packages are discarded and the information of all received packages is used. For the standard SETP this means that the energy content of

Table 6.1: Specification of internet connections

Connection	Mean Delay	Std Delay	Package Loss
Italy	40ms	1ms	0.04%
Australia	351ms	5ms	27%

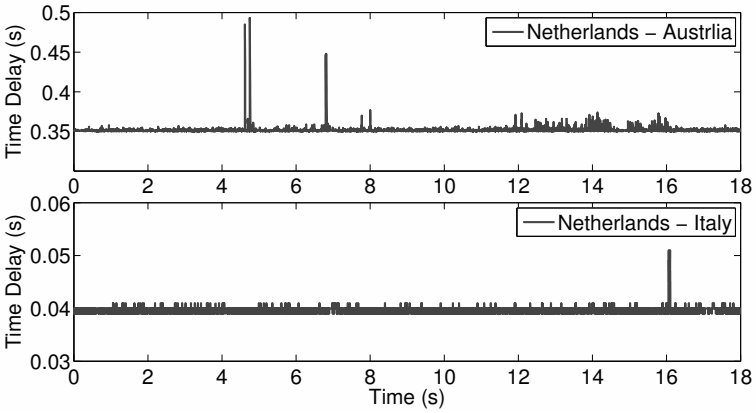

Figure 6.7: **Typical communication delay during experiments:** The delay time is the recorded Round Trip Time.

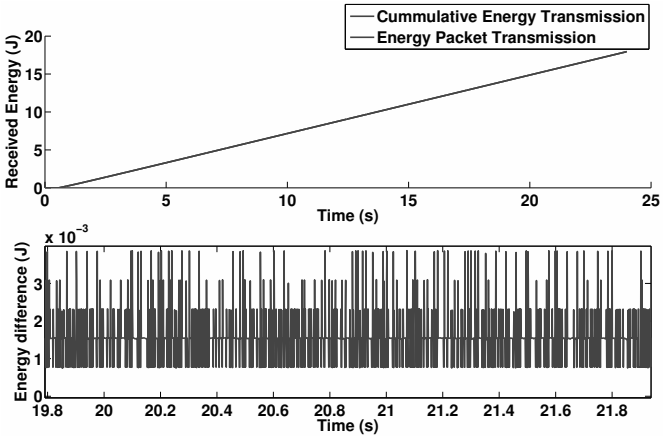

Figure 6.8: **Cumulative and Packet Energy Transfer:** In this experiment (communication with Australia) the energy transfer is not hampered due to packet loss.

all received packages is summed. Fig. 6.8 shows the received energy at the slave side for a typical experiment with both types of transmission. Even though the recorded package loss was 27% the number of packages actually dropped in the communication channel is extremely low. This is indicated by the very small difference between the two approaches. Even with UDP as transmission protocol this particular connection at 1 kHz was reliable in the sense that almost all data did arrive, however due to the varying time-delays multiple packages arrived between consecutive sampling instants instead of a single package per sampling instant.

6.5.3 Experimental Data

As implementation of the *Transparency Layer* a regular Position-Force Controller is implemented:

$$\begin{aligned} \tau_{TLm}(k) &= rF_e(k) \\ \tau_{TLs}(k) &= K_p(q_m(k) - q_s(k)) - K_d\dot{q}_s(k) \end{aligned} \tag{6.16}$$

where $r = 0.15\,\mathrm{m}$ is the length of the mechanical arm of each device and K_p and K_d are the proportional and derivative gain of the PD-type position controller, respectively.

In the *Passivity Layer* the cumulative version of the SETP is implemented. As saturation functions the maximum force that can be delivered by the actuators has been implemented and a mapping of the available energy to a maximum force is implemented only at the slave side and in the form of a linear spring with stiffness K_s, so

$$\begin{aligned} \tau_{max1}(k) &= \begin{cases} 0 & \text{if } H(\overline{k+1}) \leq 0 \\ \tau_{TL}(k) & \text{otherwise} \end{cases}, \\ |\tau_{max2}(k)| &= 1.38\,\mathrm{Nm} \\ |\tau_{max3}(k)| &= \sqrt{2H_s(\overline{k+1})K_S} \end{aligned} \tag{6.17}$$

The value of each parameter in the control algorithm is listed in Table 6.2.

In the first experiment there is no significant amount of friction in the slave device and/or mapping in the *Transparency Layer*. In the second set of experiments the powder brake is actuated to deliver an additional amount of coulomb friction of approximately $0.3\,\mathrm{Nm}$ and a position mapping of $\mu = 2$ is applied in the *Transparency Layer*. The actuators are not powerful enough to effectively apply an increased force mapping. Each experiment is carried out for each of the three time delays (no delay, communication through Italy, and communication through Australia).

Fig. 6.9 shows the performance of the system with the *Passivity Layer* deactivated. For a strong grasp by the user the system is stable for all three time delays. However, when the user applies a relaxed grasp contact instabilities occur immediately. These contact instabilities becomes more violent for larger time delays. The transparency of the Position-Force controller, even for a stiff grasp by the user, is extremely poor in the high-delay case as the mean of the RTT is 702ms, which is too large for the link between intended motion and resulting force to be cognitively perceivable by the user. This is an inherent property of this particular implementation of the *Transparency Layer*.

Fig. 6.10 shows that with the *Passivity Layer* activated the system remains stable

Table 6.2: Control structure parameter values

Parameter	Value	Parameter	Value
K_p	$3.75\,\mathrm{Nm}rad$	K_d	$0.11\,\mathrm{Nms}rad$
H_d	$0.3\,\mathrm{J}$	α	70
β	0.01	K_S	$16.8\,\mathrm{Nm}^2/\mathrm{J}$

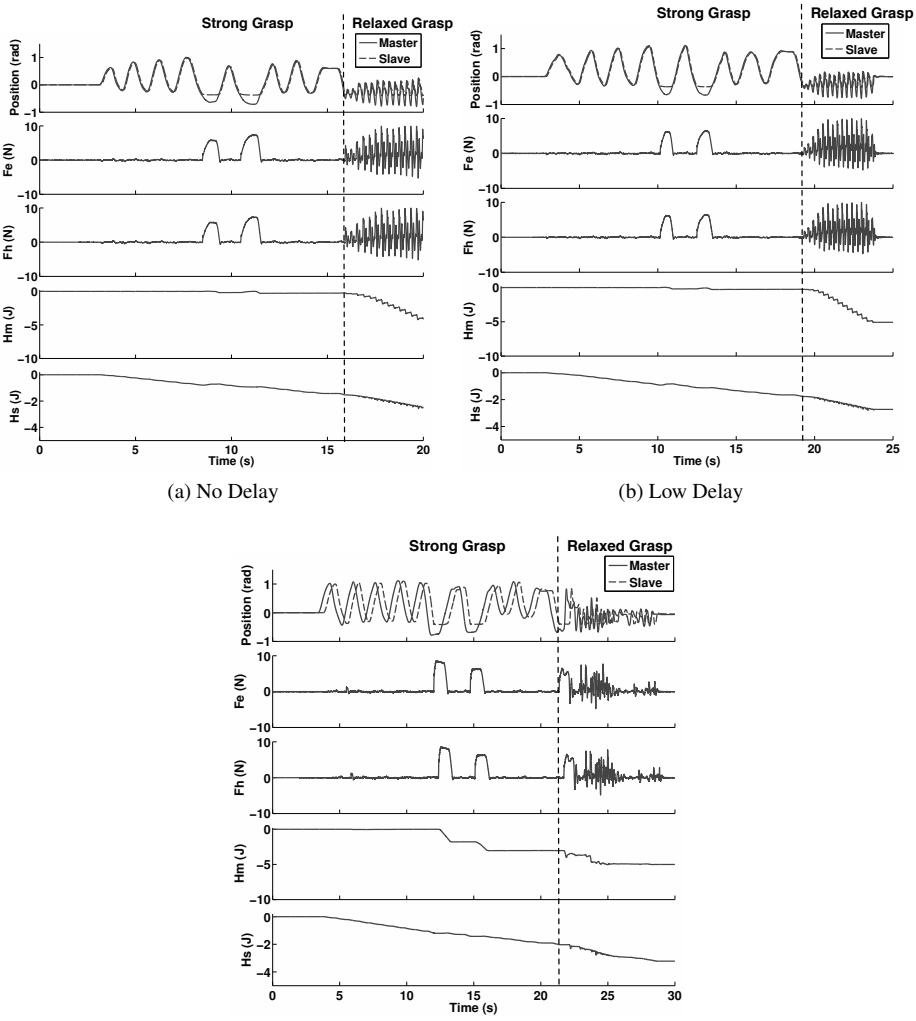

(a) No Delay

(b) Low Delay

(c) High Delay

Figure 6.9: **Non Passive Position-Force Control:** Contact instabilities (oscillations) occur when the user applies a relaxed grasp.

both for all time delays and all grasps applied by the user. In free-space motion a small residual feedback force to the user is already visible to compensate for the mechanical friction in the slave device. The transparency of the system is acceptable for the no- and low-delay cases. In the high-delay case the *Passivity Layer* needs to performs large adjustments to the commands of the Position-Force controller in order to maintain passivity. For this high-delay the transparency of the system remains extremely poor as the *Passiv-*

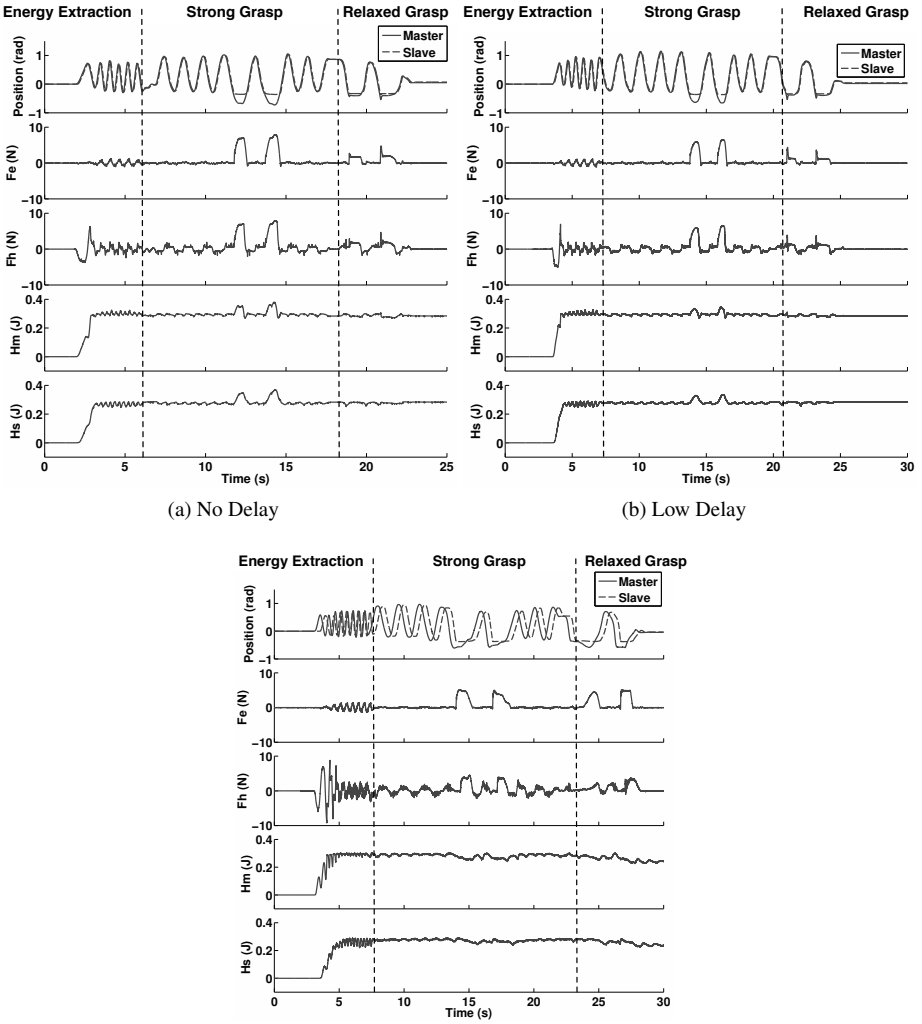

(a) No Delay

(b) Low Delay

(c) High Delay

Figure 6.10: **Passive Position-Force Control:** Stable interaction with the remote environment is established for all user grasps.

ity Layer does not improve the inherent transparency properties of the controller in the *Transparency Layer*, but only ensures stability. Fig. 6.10c shows that a high-frequent vibration starts to appear on the feedback force to the user due to the ripple in the tank level, which is caused by the varying time-delay in the communication channel. This vibration was not yet of such a magnitude that it was experienced by the user.

Fig. 6.11 shows the performance when the regular *Passivity Layer* is applied when

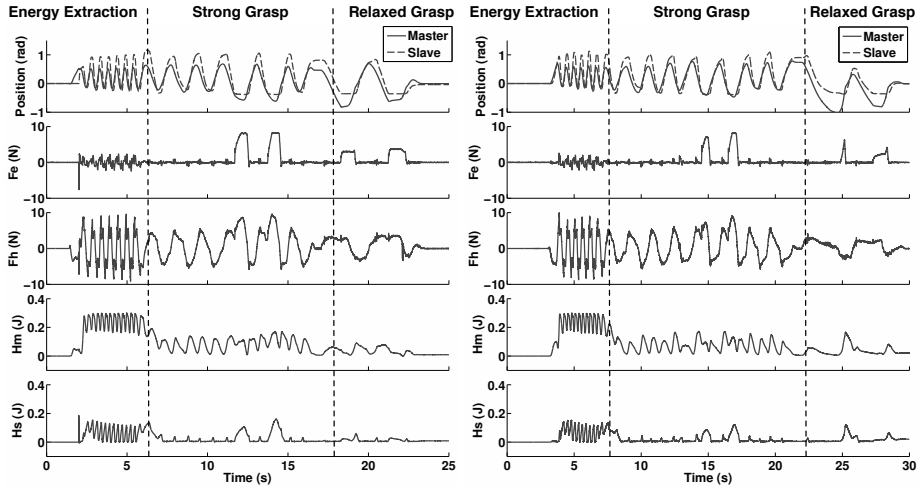

(a) No Delay

(b) Low Delay

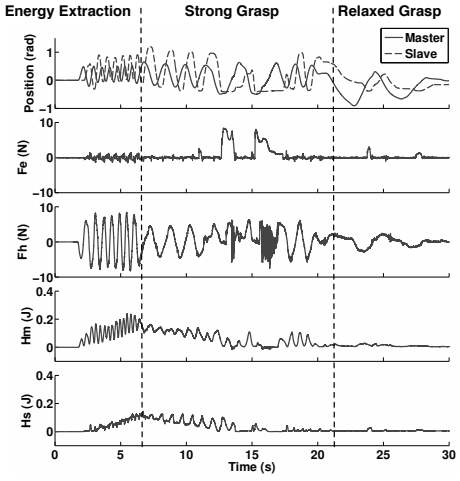

(c) High Delay

Figure 6.11: **Passive Position-Force Control with additional friction and motion scaling:** The transparency of the system is greatly reduced and becomes worse for increasing time delays.

both additional coulomb friction ($0.3\,\mathrm{Nm}$) is present in the slave device and a position mapping in the *Transparency Layer* ($\mu = 2$). The tracking performance of the slave system will decrease as the position-controller in the *Transparency Layer* is not optimized with respect to the increased mechanical friction. Already in the no-delay situation the transparency of the system is extremely low due to the continuous activation of the TLC.

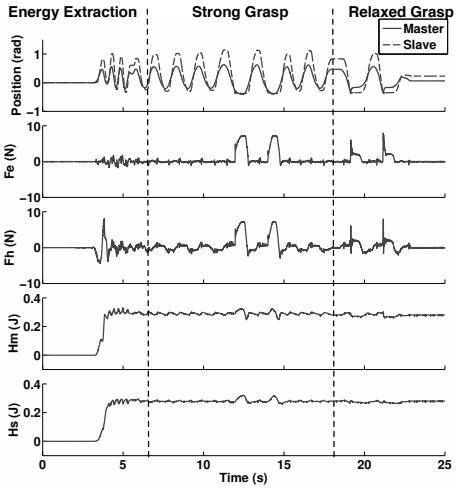

(a) No Delay

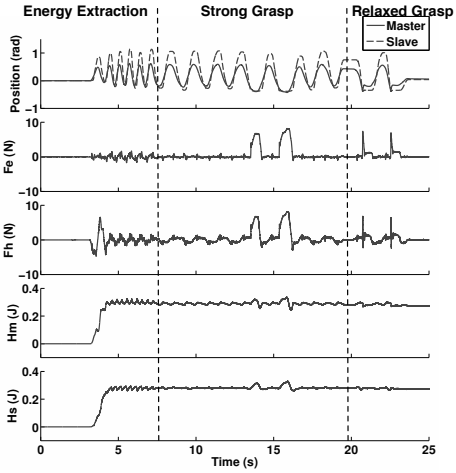

(b) Low Delay

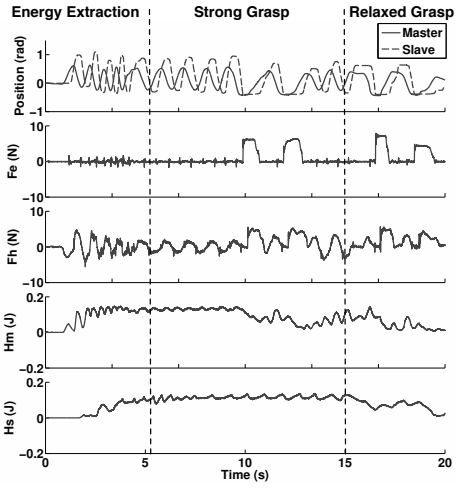

(c) High Delay

Figure 6.12: **Extended** *Passivity Layer* **Position-Force Control with additional friction and motion scaling:** Transparency of the system is greatly increased by compensating for the mechanical friction and motion scaling.

For the high-delay case the position tracking of the slave device has degraded significantly due to the low amount of energy available in the tank in combination with (6.17). Furthermore, in the high-delay case switching effects are visible in the feedback force to the user. This is caused by the depletion of the energy tank at the master side, which causes the commands of the *Transparency Layer* to be switched off according to (6.17). These

effects could be mitigated by increasing the desired tank level, the amount of energy transmitted, the rate of extraction and the inclusion of saturation functions at the master side, but would significantly increase the damping force experienced by the user which would also diminish the transparency of the system.

Fig. 6.12 shows the performance when the measures proposed in Section 6.4 are implemented. A significant reduction in the activation of the TLC is visible in the feedback force to the user and the position tracking of the slave system is improved for the high-delay case. The transparency improvement is especially noticeable when comparing the force feedback during free-space motions for the no- and low-delay case in Fig. 6.11 and Fig. 6.12. The transparency properties are at the same level as in Fig. 6.10 and stability is still guaranteed for all time-delays and grasps of the user.

6.6 Conclusion

In this paper experimental results obtained with the two-layer framework for time-delayed bilateral telemanipulation were presented. The efficacy of the framework applied to bilateral telemanipulation over the internet was demonstrated. Two extensions were discussed and experimentally validated to improve the performance of the framework when applied to slave devices with high amounts of internal friction and/or scaling factors in the control algorithm in the *Transparency Layer*. These extensions significantly improve the transparency of the system while maintaining the guaranteed stability properties of the original formulation.

Future work will focus on the investigation of other implementations of the *Transparency Layer* to improve the performance of the system in the presence of extreme time-delays as encountered in the time-delay experiments between the Netherlands and Australia.

Acknowledgment

The authors gratefully acknowledge the assistance of Hubert Flisijn, Rob Reilink, and Lorenzo Sabattini for their assistance in setting up the internet connections.

CHAPTER 7

Stability of Position-Based Bilateral Telemanipulation Systems by Damping Injection

Franken, M., Misra, S. and S. Stramigioli

Under review for the IEEE/RSJ International Conference on Intelligent Robots and Systems 2011

In this paper two different approaches to guarantee stability of position-based bilateral telemanipulation systems based on the concept of passivity are discussed. Both approaches inject damping into the system to guarantee passivity of the interaction with the device in the presence of time delays in the communication channel. The first approach derives tuning rules for a fixed viscous damper, whereas the second approach employs modulated dampers based upon the measured energy exchange with the device and enforce passivity in the time domain. A theoretical minimum damping injection scheme is sketched that shows that the fixed damping approach is inherently conservative with respect to guaranteeing stability. Experimental results show that both the theoretical minimum damping scheme and a time domain passivity algorithm are successful in stabilizing the telemanipulation system for large time delays with lower gains of the damping elements than derived by the fixed damping injection approach. However, as damping is inherently present in the system the tuning rules derived from the fixed damping injection approach can be used to identify if a time domain passivity algorithm is needed given boundary conditions on the actual time delays.

7.1 Introduction

Bilateral telemanipulation systems allow users to interact with remote environments and experience some notion of the interaction forces (haptic feedback). The realism of this reflected interaction is called the transparency of the system (Lawrence, 1993). The obtainable transparency is amongst others determined by the implemented bilateral control algorithm. A fundamental requirement for a useful telemanipulation system is that it is guaranteed to be stable given all possible circumstances that can be encountered during operation.

There are many different bilateral control algorithms proposed in literature, see e.g. (Hokayem and Spong, 2006) for a recent overview. Each control algorithm is characterized by different transparency and stability properties. In this paper we will compare two methods to ensure stability of a position-position (P-P) bilateral controller, Fig. 7.1.

When no time delays are present in the communication channel the P-P controller of Fig. 7.1 is guaranteed to be passive (Lee and Spong, 2006) (neglecting the destabilizing influence of sampling (Colgate et al., 1993)). The passivity of the bilateral controller is an attractive property as the interaction between passive systems is guaranteed to be stable. The user and the environment can both be assumed to be passive, or to interact at least in a stable manner with passive systems (Hogan, 1989). It is well-known that time delays can transform passive bilateral controllers that exchange power variables (e.g. velocities and/or forces) into controllers that generate "virtual" energy. This "virtual" energy can in turn potentially destabilize the system. For the P-P controller this has been shown by Artigas et al. (2010*b*).

Preventing this "virtual" energy from being generated, or to ensure that it is properly dissipated, ensures the passivity of the total telemanipulation system. A major breakthrough in time-delayed bilateral telemanipulation has been the introduction of the scattering/wave-variables technique by Anderson and Spong (1989) and Niemeyer and Slotine (2004). Applying this coding scheme to the exchanged power variables turns the communication channel itself into a passive element for any constant time delay. However, the inherent nature of the coding operation implies that information is mixed and/or lost and consequently the transparency of the system is reduced (Lawn and Hannaford, 1993).

A different approach that is being applied more often is to ensure the stability of bilateral controllers by means of appropriate damping injection. We distinguish two major groups of approaches. The first group applies Lyapunov theory to derive the fixed amount of viscous damping required in the control algorithm to ensure passivity of the bilateral controller under all circumstances, e.g. (Lee and Spong, 2006), (Nuno et al., 2009), and (Hua and Liu, 2010). The other group applies damping elements which are modulated based on a monitored energy balance of the system. These approaches only add additional damping to the system to maintain passivity according to the energy balance, Time-Domain Passivity (TDP) algorithms e.g. (Ryu et al., 2010) and (Franken et al., 2009). The applicability of these two approaches to the guaranteed stable interaction with the telemanipulation system will be compared in this paper. For that reason a theoretical Minimal Damping Injection (MDI) scheme is derived.

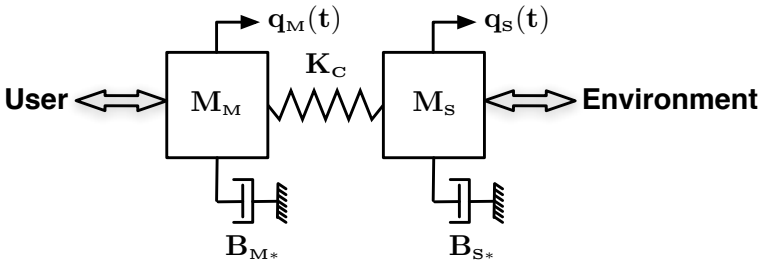

Figure 7.1: **Position-based bilateral control:** in the non-delayed situation a single spring is connecting the master and slave device.

The paper is organized as follows; Section 7.2 introduces the system model. Examples of the fixed damping approach are treated in Section 7.3.1. The MDI scheme is derived in Section 7.3.2 and a particular implementation of a TDP algorithm is discussed in Section 7.4. Section 7.5 contains experimental results obtained with the three approaches. A discussion on the applicability of each approach is contained in Section 7.6. Finally, conclusions are drawn in Section 7.7.

7.2 System model

In this paper we will examine two 1 degree of freedom (DOF) devices that are coupled by means of a P-P bilateral controller. Each device consists of a mass, M, and has internal viscous friction, B:

$$\begin{aligned} F_{U}(t) + F_{Cm}(t) &= M_{M}\ddot{q}_{M}(t) + B_{M}\dot{q}_{M}(t) \\ F_{E}(t) + F_{Cs}(t) &= M_{S}\ddot{q}_{S}(t) + B_{S}\dot{q}_{S}(t), \end{aligned} \tag{7.1}$$

where $q(t)$ and $\dot{q}(t)$ indicate a position and velocity and the subscripts $_M$ and $_S$ indicate the master and slave device, respectively. $F_U(t)$ and F_E indicate the force exerted by the user and the environment on the devices, respectively. Finally, $F_{Cm}(t)$ and $F_{Cs}(t)$ indicate the forces exerted by the P-P bilateral controller and are defined as:

$$\begin{aligned} F_{Cm}(t) &= -K_{Cm}(q_{M}(t) - q_{S}(t)) - B_{Cm}\dot{q}_{M}(t) \\ F_{Cs}(t) &= K_{Cs}(q_{M}(t) - q_{S}(t)) - B_{Cs}\dot{q}_{S}(t), \end{aligned} \tag{7.2}$$

where K_C, B_{Cm}, and B_{Cs} are the proportional and derivative gains of the applied position controllers, respectively. This system is depicted in Fig. 7.1, where for brevity the viscous damping in the devices and the controllers have been combined into B^*_M and B^*_S, respectively.

7.3 Stabilization by Damping Injection

The system introduced in the previous section is guaranteed to be stable when no time delays are present in the communication between the master and slave system (Lee and Spong, 2006). The destabilizing influence of time delays can be removed by including an appropriate amount of damping in the system.

The amount of additional damping which is apparent to the user has a large influence on the experienced transparency of the system. De Gersem et al. (2005) have already shown that damping experienced by the user significantly reduces the transparency of the telemanipulation system. In order to obtain the highest amount of transparency, the amount of damping added to stabilize the system should be as low as possible. In order to compare both of the approaches mentioned in Section 7.1, the theoretical minimum amount of damping required for passivity of the system is derived in this section.

7.3.1 Fixed Damping Injection

Various people have looked into how to stabilize bilateral controllers by means of fixed damping injection. Using a Lyapunov analysis tuning conditions are derived. These conditions link the required damping to the implemented stiffness of the position-controllers and the time delay in the communication channel. Some conditions that have been published in literature are discussed below.

Lee and Spong (2006) considered the situation in which the implemented stiffness, K_C, and damping, B_C, in the position-controllers and the time delays, T, in the communication channel are constant and symmetric. They derived that the bilateral controller would be guaranteed stable when the following condition was satisfied

$$B_C \geq 2TK_C. \tag{7.3}$$

Nuno et al. (2008, 2009) presented a different derivation that removed the necessity of certain assumptions in the work of Lee and Li (2005) and relaxed the parameter condition. In their work the following bound was derived:

$$4B_{Cm}B_{Cs} > (\overline{T}_{MS}^2 + \overline{T}_{SM}^2)K_{Cm}K_{Cs}, \tag{7.4}$$

where $\overline{T}_{MS}$ and $\overline{T}_{SM}$ are the upper bounds for the time delays in the communication from the master to the slave and vice versa, respectively.

Hua and Liu (2010) also incorporated asymmetric varying time delays and derived the following linear matrix inequalities:

$$\begin{aligned} -2B_{Cm}I + \overline{T}_{MS}Z + \overline{T}_{SM}K_{Cm}^2S^{-1} &< 0 \\ -\frac{K_{Cm}B_{Cs}}{K_{Cs}}I + \overline{T}_{SM}S + \overline{T}_{MS}K_{Cm}^2Z^{-1} &< 0, \end{aligned} \tag{7.5}$$

where S and Z are positive-definite matrices and I the identity matrix, respectively. For a one DOF system (7.5) can be simply rewritten in the form of (7.4) as

$$2B_{Cm}B_{Cs} > (\overline{T}_{MS} + \overline{T}_{SM})^2 K_{Cm}K_{Cs}, \tag{7.6}$$

by first isolating B_{Cm} and B_{Cs} in (7.5) and multiplying those expressions. Evaluating the derivative of the obtained inequality with respect to SZ and taking into account the positive definiteness of both S and Z it follows that the inequality is minimized for $SZ = K_{Cm}^2$ resulting in (7.6). It follows immediately from (7.4) and (7.6) that in this case the result obtained by Hua and Liu (2010) is more restrictive than that obtained by Nuno et al. (2008, 2009).

7.3.2 Minimal Damping Injection

In the previous section several parameter conditions have been discussed that stabilize the P-P controller of Fig. 7.1 in the presence of time delays. In the Lyapunov-based analysis the motions of the master and slave device are considered to be independent and arbitrary. Furthermore, the resulting parameter conditions only consider the time delays and the parameters of the control algorithm.

In this section, the amount of damping theoretically needed to implement a passive P-P controller, in the presence of arbitrary time delays in the communication channel, will be investigated. For this derivation a P-P controller with symmetric stiffness term is considered, $K_{Cm} = K_{Cs} = K_C$ in (7.2).

The time delays in the communication channel separate the master and slave system. Instead of a single spring connecting the master and slave system, we obtain two springs, Fig. 7.2. One spring connects the master device to the time-delayed position of the slave system and the other spring connects the slave device to the time-delayed position of the master system. Due to the time delays the energy content of these two springs

$$H_{Cm}(t) = \frac{1}{2}K_C(q_M(t) - q_S(t - T_{SM}))^2 \tag{7.7}$$

$$H_{Cs}(t) = \frac{1}{2}K_C(q_M(t - T_{MS}) - q_S(t))^2, \tag{7.8}$$

can differ with respect to the energy content of the single spring that would connect the master and slave system in the situation without time delays

$$H_C(t) = \frac{1}{2}K_C(q_M(t) - q_S(t))^2. \tag{7.9}$$

We will consider the difference of (7.7) and (7.8) with (7.9) as “virtual” energy which is generated by the time delays.

This difference in energy content will affect the force exerted by the bilateral con-

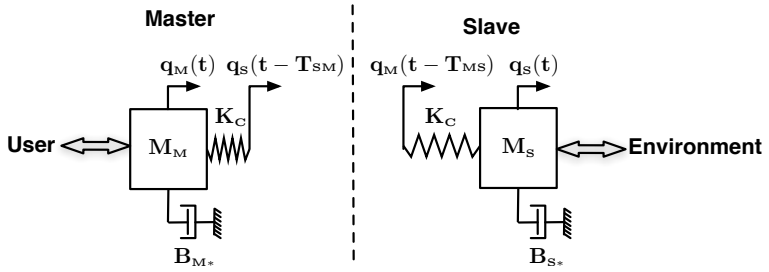

Figure 7.2: **Position-based bilateral control with time delay:** Due to the time delay two springs are present (one at each side) of which the energy content differs.

troller

$$\begin{aligned} F_{Cm}(t) &= -K_C(q_M(t) - q_S(t - T_{SM}) - B_{Cm}\dot{q}_M(t) \\ F_{Cs}(t) &= K_C(q_M(t - T_{MS}) - q_S(t)) - B_{Cs}\dot{q}_S(t). \end{aligned} \tag{7.10}$$

The time-delayed position signals can be expressed as the true positions with time-varying difference terms

$$\begin{aligned} q_M(t - T_{SM}) &= q_M(t) + \Delta q_M(t) \\ q_S(t - T_{MS}) &= q_S(t) + \Delta q_S(t). \end{aligned} \tag{7.11}$$

Thus, using (7.11), (7.10) can be written as

$$\begin{aligned} F_{Cm}(t) &= -F_C(t) + K_C\Delta q_S(t) - B_{Cm}\dot{q}_M(t) \\ F_{Cs}(t) &= F_C(t) + K_C\Delta q_M(t) - B_{Cm}\dot{q}_S(t), \end{aligned} \tag{7.12}$$

where

$$F_C = K_C(q_M(t) - q_S(t)), \tag{7.13}$$

is the force exerted by the single spring in the no-delay case. Comparing (7.2) and (7.10) shows that the influence of the time delays can be represented as an additional component in the force exerted by the bilateral controller on both the master and slave device, $K_C\Delta q_S(t)$ and $K_C\Delta q_M(t)$, respectively.

It is now important to note that the "virtual" energy present in each spring can either be positive or negative depending on the particular motions of the master and slave device and the time delay in the communication channel. If both systems are stationary the "virtual" energy in each spring will eventually become zero (as soon as the value of the stationary position has passed through the communication channel). Only when the "virtual" energy is positive in a spring and energy is injected by that spring into the physical world (the user/environment), "virtual" energy is leaking into the physical world which might destabilize the system.

Positive "virtual" energy is present when:

$$\frac{1}{2}K_C(q_M(t)-q_S(t))^2 < \begin{cases} \frac{1}{2}K_C(q_M(t)-q_S(t-T_{SM}))^2 \\ \frac{1}{2}K_C(q_M(t-T_{MS})-q_S(t))^2 \end{cases}, \tag{7.14}$$

which can be expressed in the following two conditions:

$$\Delta q_S(t)(q_S(t)-q_M(t))+\frac{1}{2}\Delta q_S(t)^2 > 0 \tag{7.15}$$

$$\Delta q_M(t)(q_M(t)-q_S(t))+\frac{1}{2}\Delta q_M(t)^2 > 0, \tag{7.16}$$

which indicates that additional damping is needed when one or both devices are moving towards and approaching the position of the other device. The proximity that the devices need to obtain with respect to each other in order to generate positive "virtual" energy depends on the velocity of the devices and the time delay.

Dissipating the amount of "virtual" energy that would be leaking into the physical world by an additional dissipative element, ensures passive behavior of the spring-coupling between the master and slave under all possible circumstances. From (7.12) it follows that the dissipative force to achieve this is the force that compensates the additive term due to the time delay. Furthermore, based on the reasoning above, this dissipative term should only be added when "virtual" energy is injected into the physical world by the spring, so

$$\begin{aligned} F_{Rm}(t) &= \begin{cases} -K_C\Delta q_S(t) & \text{if (7.15) and } -F_{Cm}(t)\dot{q}_M(t)<0 \\ 0 & \text{otherwise} \end{cases} \\ F_{Rs}(t) &= \begin{cases} -K_C\Delta q_M(t) & \text{if (7.16) and } -F_{Cs}(t)\dot{q}_S(t)<0 \\ 0 & \text{otherwise.} \end{cases} \end{aligned} \tag{7.17}$$

The corresponding damping coefficients, B_{Rm} and B_{Rs}, of the corresponding modulated dampers are

$$B_{Rm} \leq \frac{K_C\Delta q_S(t)}{\dot{q}_M(t)} \text{ and } B_{Rs} \leq \frac{K_C\Delta q_M(t)}{\dot{q}_S(t)}, \tag{7.18}$$

where $\leq$ indicates that the required additional damping can be zero (7.17).

Adding the additional damping force of (7.17) to (7.10) enforces passivity of the spring-elements in the controller. Pure spring-elements are passive, but marginally stable and will therefore exhibit an oscillatory response. Asymptotic stability of the system is obtained due to additional viscous damping present in the system (non-zero B_M, B_{Cm}, B_S, and B_{Cs}) as the system will be strictly passive. If desired, part of that additional viscous damping could be used as partial fulfillment of (7.18).

Naturally this is a purely theoretical result as it is impossible to obtain $\Delta q_M(t)$ and $\Delta q_S(t)$ in a realistic time-delayed telemanipulation application. It does however show that the minimal required damping is not only dependent on the stiffness and the time delays,

but also on the relative motions of the devices. In the fixed damping injection approaches arbitrary motions of each device are assumed. However, in reality the motions of the devices are influenced by the user, the environment and the device characteristics. As this influence is neglected in the analysis the resulting tuning rules of Section 7.3.1 must hold for all possible combinations of impedances and are therefore restrictive by nature as they have to consider the worst case situation of the relative motion of the devices.

The impedances of the user and the environment are non-linear, time-varying, and difficult to model at the least. For that reason they are often assumed to be unknown. However, their influence is present in the interaction with the devices, which can be measured. In the next section we will treat a TDP algorithm that uses this measured interaction data in order to determine a required amount of damping.

7.4 Time Domain Passivity

A different approach to stabilizing the system of Section 7.2 is presented by monitoring the energy balance of the system and applying damping only when required by the energy balance. The first of such approaches was the Time-Domain Passivity Control (TDPC) algorithm by Ryu et al. (2004*b*).

The energy balance of the system, H, is composed of the physical energy exchange at the master and slave side, H_{Im} and H_{Is}, respectively[1]:

$$H(\overline{k}) = H_{Im}(\overline{k}) + H_{Is}(\overline{k}). \tag{7.19}$$

The physical energy exchange during a sample period can be computed exactly *a posteriori* of the sample period for impedance-type displays as (Stramigioli et al., 2005):

$$\begin{aligned} \Delta H_I(k) &= \int_{(k-1)\Delta T}^{k\Delta T} -F_A(\overline{k})\dot{q}(t)dt \\ &= -F_A(\overline{k})\Delta q(k), \end{aligned} \tag{7.20}$$

where F_A and $\dot{q}$ are the force and velocity associated with the interaction point between the physical world and the controller in discrete time, e.g. the forces exerted by the control algorithm. (7.20) represent the energy which is supplied by the actuators at that side. so that

$$H(\overline{k}) = \sum_{i=1}^{k-1} \Delta H_{Im}(i) + \Delta H_{Is}(i), \tag{7.21}$$

where $\Delta H_{Im}(i)$ and $\Delta H_{Is}(i)$ are the energy exchange at the master and slave side during sample period $\overline{i}$, respectively. Both $\Delta H_{Im}(i)$ and $\Delta H_{Is}(i)$ are computed as (7.20).

If (7.21) becomes negative "virtual" energy is generated according to the TDPC algorithm. A modulated damper is activated to dissipate the generated "virtual" energy and

[1]Notation used in this paper: The index k is used to indicate instantaneous values at the sampling instant k and the index $\overline{k}$ is used to indicate variables related to an interval between sampling instants $k-1$ and k.

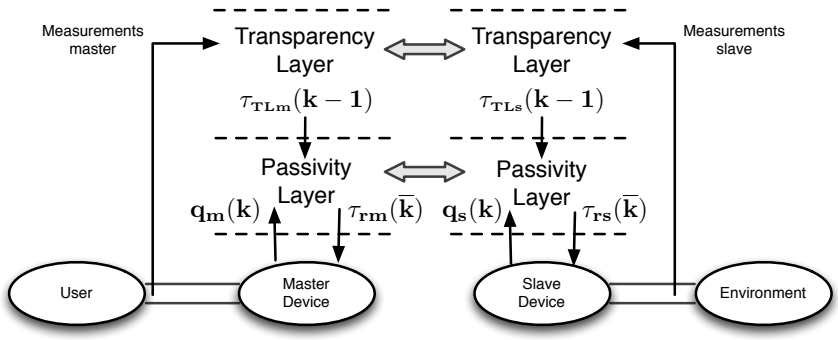

Figure 7.3: **Two-layer algorithm for bilateral telemanipulation.** The double connections indicate physical energy exchange.

restore passivity of the system. This implementation requires instantaneous knowledge of $\Delta H_{Im}(k)$ and $\Delta H_{Is}(k)$. As such it cannot be applied in time-delayed telemanipulation systems. A time-delayed formulation of the TDPC algorithm has been proposed by Ryu et al. (2010) and applied by Artigas et al. (2010*b*) to the P-P controller in the presence of time delay.

In this paper we will implement the two-layer framework as proposed by Franken et al. (2009), which is a different TDP algorithm. The framework consists of two control layers in a hierarchical structure, the *Transparency Layer* and the *Passivity Layer*, see Fig. 7.3. First the working of the *Passivity Layer* will be discussed. In (Franken et al., 2009) it was stated that any bilateral controller could be implemented in the *Transparency Layer* given their implementation of the *Passivity Layer*. However, with a P-P controller implemented in the *Transparency Layer* a modification in the *Passivity Layer* is required. This modification will be discussed in Section 7.4.2.

7.4.1 Passivity Layer

This layer enforces passivity of the bilateral telemanipulation system. When necessary the commands originating from the *Transparency Layer* are adjusted to maintain passivity. In the two-layer framework the energy balance of the system (7.21) is split into three components

$$H(\overline{k}) = H_M(\overline{k}) + H_C(\overline{k}) + H_S(\overline{k}), \tag{7.22}$$

where H_M, H_C, and H_S represent the energy present at the master side, the energy in the communication channel, and the energy at the slave side, respectively.

The energy at the master and slave side is stored in energy tanks and these tanks can exchange energy through the communication channel. There are three energy flows connected to each tank:

- Energy exchanged with the physical world, ΔH_{Im} and ΔH_{Is},
- Energy received from the communication channel, $\Delta H_{SM+}(k)$ and $\Delta H_{MS+}(k)$,

- Energy send into the communication channel, $\Delta H_{MS-}(k)$ and $\Delta H_{SM-}(k)$.

The energy flow received from the communication channel at the master side, ΔH_{SM+}, is the time-delayed energy flow sent into the communication channel at the slave side, ΔH_{SM-}, and vice versa. The level of the energy tank at each side is corrected each sampling instant with respect to these three energy flows. The change of the energy level in the master and slave tank, ΔH_M and ΔH_S, respectively, is given as

$$\begin{aligned} \Delta H_M(k) &= \Delta H_{Im}(k) + \Delta H_{SM+}(k) - \Delta H_{MS-}(k) \\ \Delta H_S(k) &= \Delta H_{Is}(k) + \Delta H_{MS+}(k) - \Delta H_{SM-}(k), \end{aligned} \tag{7.23}$$

and thus

$$\begin{aligned} H_M(\overline{k+1}) &= H_M(\overline{k}) + \Delta H_M(k) \\ H_S(\overline{k+1}) &= H_S(\overline{k}) + \Delta H_S(k). \end{aligned} \tag{7.24}$$

The energy exchange between the two tanks is determined by the implemented Energy Transfer Protocol. In this paper we will use the Simple Energy Transfer Protocol (SETP) in which each side transmits each iteration a fraction, β, of its available energy to the other side:

$$\Delta H_{MS-}(k) = \begin{cases} \beta H_M(\overline{k-1}) & \text{if } H_M(\overline{k-1}) > 0 \\ 0 & \text{otherwise,} \end{cases} \tag{7.25}$$

and (7.25) is likewise defined at the slave side to compute $\Delta H_{SM-}(k)$. This means that $\Delta H_{MS-}(k) \geq 0$ and $\Delta H_{SM-}(k) \geq 0$. The stability properties of the SETP have been analyzed in Franken et al. (2012). The SETP ensures passivity of the communication channel as (assuming zero initial energy in the communication channel):

$$\begin{aligned} H_C(\overline{k}) = \sum_{i=0}^{k-1} &\Delta H_{MS-}(i) + \Delta H_{SM-}(i) \\ &-\Delta H_{SM+}(i) - \Delta H_{MS+}(i) \geq 0. \end{aligned} \tag{7.26}$$

A Tank Level Controller (TLC) is defined at the master side to regulate the energy level in the system. The TLC is located at the master side as the user has to inject energy into the system for the slave device to be able to execute the commanded task. The TLC is implemented as a modulated viscous damper, that is activated when the energy level in the tank available during sample period $\overline{k+1}$, $H_M(\overline{k+1})$, drops below the desired level of the tank, H_D. The additional force, F_{TLC}, exerted by this modulated damper will extract additional energy from the user during sample period $\overline{k+1}$ to replenish the energy tank, and is given by

$$\begin{aligned} F_{TLC}(k) &= -B_{TLC}(k)\dot{q}_M(k) \\ B_{TLC}(k) &= \begin{cases} \alpha(H_D - H_M(\overline{k+1})) & \text{if } H_M(\overline{k+1}) < H_D \\ 0 & \text{otherwise,} \end{cases} \end{aligned} \tag{7.27}$$

where $d(k)$ is the modulated viscous damping coefficient, $\dot{q}_m(k)$ is the velocity of the master device at sample instant k and α is a tuning parameter for the rate at which the additional required energy is extracted from the user.

The energy tanks in this scheme can be regarded as energy budgets from which controlled motions of the devices can be powered. When the available energy is low, the forces that can be exerted by the devices are restricted. The manner in which the forces are restricted when the available energy is low can be designed to suit a specific device, environment, and/or task, (Franken et al., 2009).

At each side passivity is enforced with respect to the energy tank at that side, which means

$$\begin{aligned} H_{M}(\overline{k}) &\geq 0 \quad \forall \overline{k} \\ H_{S}(\overline{k}) &\geq 0 \quad \forall \overline{k}. \end{aligned} \tag{7.28}$$

This means that passivity of the entire telemanipulation system, (7.19), is guaranteed, independent of the time delay, as the amount of energy in the communication channel, H_C, due to the SETP can only be positive (7.26).

7.4.2 Modification

The *Passivity Layer*, as described in the previous section, enforces passivity of the bilateral system. However, with a P-P controller implemented in the *Transparency Layer* this implementation of the *Passivity Layer* is susceptible to a build-up effect. When the user executes a motion the energy that is injected into the system far exceeds the energy required at the slave side to execute the same motion. This is due to the inherent phase lag in the position response of the slave which influences the feedback force to the user. This mismatch in energy produces a build-up in the energy balance, which hinders the *Passivity Layer* from effectively stabilizing the system.

The user injects more energy into the system than is required at the slave side. This excess energy can be removed by an additional dissipation action is included in the *Passivity Layer* at the master side. If the tank level exceeds the desired tank level, the excess energy is dissipated:

$$H_{M}(\overline{k+1}) > H_{D} \Rightarrow H_{M}(\overline{k+1}) = H_{D}. \tag{7.29}$$

7.5 Experiments

In this section experimental results will be presented for the approaches discussed in Section 7.3.2 and Section 7.4. The experiments are carried out with the setup in Fig. 7.4. The setup consists of two identical one DOF lightweight devices with low internal friction powered by a DC motor without gearbox. The continuous torque that these motors can exert is $1.38\,\mathrm{Nm}$. A high-precision encoder with $65\,\mathrm{k}$ pulses per rotation is used to record the position of each device.

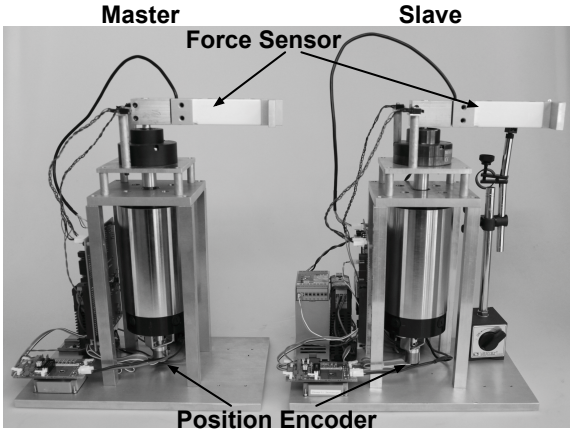

Figure 7.4: **Experimental setup:** The setup consists of two identical 1 d.o.f. lightweight devices.

Both devices are controlled from the same embedded controller running a real-time Linux distribution. The controllers are implemented in the program 20-sim (Controllab Products B.V., 2010) and real-time executable code specific for this setup is generated directly from 20-sim and uploaded to the embedded controller by means of the program 4C (Controllab Products B.V., 2010). The sampling frequency of the control loop is $1\,\mathrm{kHz}$.

The P-P controller is implemented as (7.10). A symmetric constant time delay is implemented in the communication channel, chosen as 20ms round-trip time delay (RTT) and 400ms RTT. All parameters used in the control algorithm are listed in Table 7.1. Experimental results will be demonstrated with the P-P controller extended with either the MDI approach or the TDP algorithm of Section 7.3.2 and Section 7.4, respectively.

The implemented TDP algorithm adds additional damping only at the master side. For comparison purposes we compute the required damping according to the least conservative approach of Section 7.3.1. The required damping at the master side according to (7.4) for a delay of 400ms RTT is:

$$B_{Cm} > 4.69\,{}^{\mathrm{Nms}}/_{\mathrm{rad}}. \tag{7.30}$$

It should be noted that this results from the condition $B_{Cm}B_{Cs} > 0.28$ and that therefore the damping could be distributed over the master and slave system. In reverse, the param-

Table 7.1: Parameter values in control algorithm

Parameter	Value	Parameter	Value
K_C	$3.75\,{}^{\mathrm{Nm}}/_{\mathrm{rad}}$	B_C	$0.06\,{}^{\mathrm{Nm\cdot s}}/_{\mathrm{rad}}$
H_D	$0.2\,\mathrm{J}$	α	$50\,{}^{\mathrm{Nm\cdot s}}/_{\mathrm{rad\cdot J}}$
β	0.01		

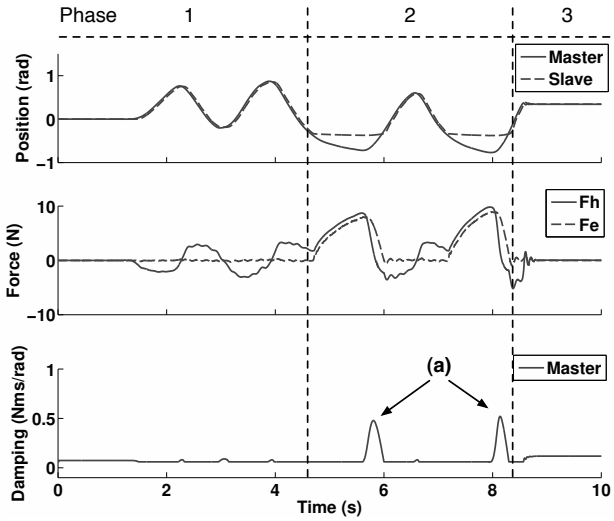

Figure 7.5: **Two-layer implementation with 20ms RTT :** A small amount of damping is added at the end of a contact phase, (a).

eters listed in Table 7.1 according to (7.4) guarantee asymptotic stability of the system for $T < 22.6\,\mathrm{ms}$.

Each experimental plot shows the position of both the master and slave device, the environment force and the force experienced by the user, and the additional damping applied by either the MDI or TDP algorithm, respectively. Phase 1 indicates free space motion, in phase 2 contact with a spring of $1500\,{}^{\mathrm{N}}/_{\mathrm{m}}$ is made twice, and in phase 3 the master device is released by the user during a motion.

In the first experiment, Fig. 7.5, the TDP algorithm is used in the presence of a communication delay of 20ms RTT. Fig. 7.5 shows that the influence of the TDP algorithm is minimal during phase 1. In phase 2 damping is added at the end of each contact phase. Therefore, the implemented modification presented in Section 7.4.2 is slightly conservative as this damping is not required. The P-P controller itself is ensured to be passive according to (7.4), $T = 10\,\mathrm{ms} < 22.6\,\mathrm{ms}$. Finally, during phase 3 the positions of both devices converge.

For the remainder of the experiments the communication delay is increased to 400ms RTT. For this delay the regular bilateral controller becomes unstable when the user does not apply a firm grasp on the device (added damping). It should be noted that for this amount of time delay the transparency of the system is very low and only during phases where both devices are stationary accurate force reflection occurs.

Fig. 7.6 shows the system response when the regular controller is extended with the MDI algorithm of Section 7.3.2. The MDI ensures that the system is strictly passive and thus that the position of both devices synchronize when the user releases the master device. Fig. 7.6 shows that the gains of the modulated dampers, resulting from the MDI algorithm, can be extremely large. However, the magnitude of the applied force by the

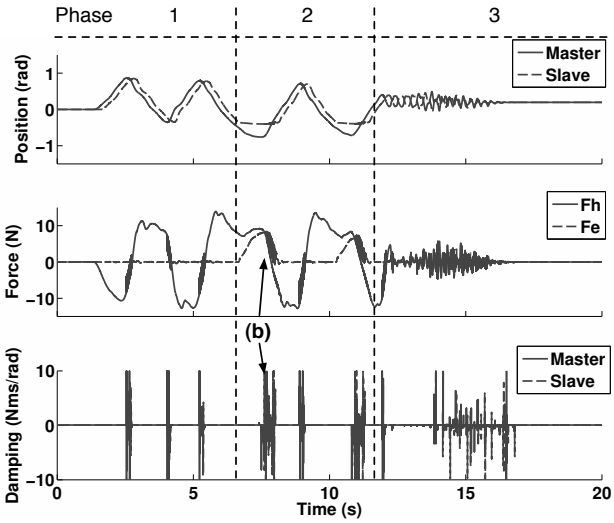

Figure 7.6: **MDI implementation with 400ms RTT:** The MDI stabilizes the system, but is susceptible to switching effects, (b).

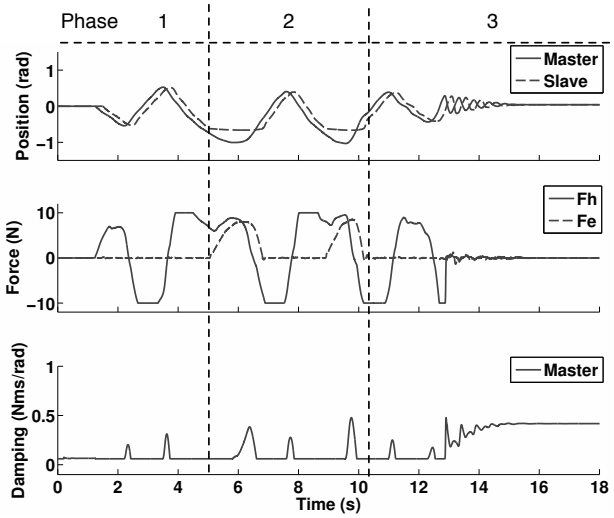

Figure 7.7: **Two-layer implementation with 400ms RTT:** Small amounts of additional damping are added when the user reverses motion.

MDI algorithm is always limited, but such a force is also applied when the velocity of the devices is very low and thus the resulting gain becomes very high. Fig. 7.6 also shows that the MDI algorithm is subject to switching effects which severely decrease the transparency of the system. Therefore, the performance of the MDI with respect to

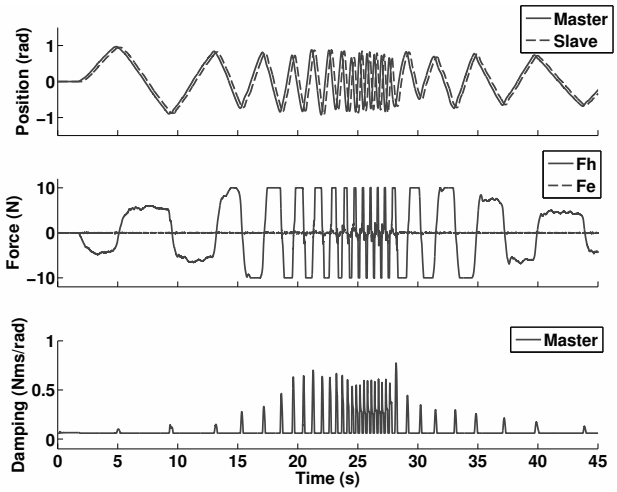

Figure 7.8: **Influence of relative motion in the two-layer implementation at 400ms RTT:** The additional damping is dependent on the relative motion.

transparency is limited, but it does stabilize the system during phase 3.

The TDP algorithm of Section 7.4 also computes a varying damping gain and is successful in guaranteeing stability of the system during all phases. Fig. 7.7 shows that the magnitude of the damping gain is very limited compared to (7.30). Furthermore, Fig. 7.7 shows that the additional damping is only applied when the user reverses the motion of the master device so that both devices are moving towards each other. This is in accordance with the analysis of when damping has to be applied of Section 7.3.2.

In the last experiment the influence of the motion initiated by the user relative to the time delay on the TDP algorithm is investigated. Fig. 7.8 shows that the damping computed by the TDP algorithm is dependent on the relative motion of the devices and the time delay. When the user moves very slowly almost no additional damping is applied. For faster movements of the master system the additional damping by the TDP algorithm increases. This is also in accordance with the analysis of Section 7.3.2.

7.6 Discussion

In the previous section it was shown that both the MDI scheme and the TDP algorithm were capable of stabilizing the system in the presence of time delays with minimum amounts of additional damping. As the amount of apparent damping for the user should be minimized to provide the best possible transparency it can be postulated that a TDP algorithm is better suited, compared to the fixed damping approach, to stabilize a telemanipulation system in the presence of time delays.

However, the conditions listed in Section 7.3.1 can be used to compute an upper bound for the time delay based on the device damping and control parameters. If it can be

guaranteed that the time delay will be below the computed bound, the system is already guaranteed to be stable by the damping present and no additional measures are needed. If the time delay exceeds the computed upper bound a TDP algorithm could be implemented to guarantee stability of the system while minimizing the added damping. The conditions of Section 7.3.1 serve the purpose of design checks on when the added complexity of a TDP algorithm is justified.

A critical note on the above reasoning is that P-P controllers are ill-suited to deal with time delays from a transparency point of view. Therefore, the implication of the above reasoning on the design of practical telemanipulation systems can be debated as this type of controller is unlikely to be applied in an application with severe time delays.

7.7 Conclusions

In this paper three methods to stabilize a position-based bilateral controller in the presence of arbitrary time delays were analyzed. It was found that the fixed damping approaches neglect the influence of important factors on the amount of damping required to stabilize the system. Therefore, the resulting conditions can be regarded as conservative. The application of a TDP algorithm results in the addition of smaller amounts of damping which benefits the obtainable transparency. The derived parameter relations can be used as a design check on when the time delay justifies the added complexity of a TDP algorithm. Future work will focus on deriving a modification of the *Passivity Layer* that is less conservative than (7.29).

Acknowledgment

The authors would like to thank J. Artigas of the German Aerospace Center Institute of Robotics and Mechatronics for his suggestions with respect to the structure of the paper.

CHAPTER 8

Conclusions and Recommendations

In this section we will summarize the conclusions of the various contributions described in this thesis and provide directions for future research.

8.1 Conclusions

The research question for this thesis was formulated in Chapter 1 as:
How should control algorithms for haptic feedback in telemanipulation and the haptic interaction with virtual environments be implemented such that the highest possible transparency is obtained while guaranteeing stability of the interaction?

8.1.1 Haptic interaction with virtual environments

In Chapter 2 the framework for PSPH systems has been revised. In the original implementation of the framework the dissipated energy was computed *a priori*, which could lead to contact instabilities with the virtual environment. A reformulation was proposed that computes the dissipated energy *a posteriori*. It was also shown the causality of the dissipative element determines the energy function that needs to be included in the energy balance. For multi-dimensional systems, this reformulation of the PSPH framework causes the entire port-Hamiltonian system to be broken down into several energy balances that need to be computed in a hierarchical order. As long as the model only contains elements with storage functions up to order 2 there will always exist a unique update for the state of the system. The applicability of the approach, taking the proposed revisions into account, have been verified with various experiments.

With respect to the stated control issues in Section 2.2 it can be concluded that the framework for PSPH systems offers a good compromise between the various desired goals. The realism of the interaction is determined by the implemented model and the PSPH framework is capable of handling models of arbitrary size and complexity. The realism of the interaction with the implemented model is only decreased up to minimum level to guarantee passivity and thus stability of the interaction for all possible operating conditions. Finally, the framework is an explicit integration method so it is possible to derive an upper bound for the implementable sample frequency given the cost of computation of the model and the available computing resources.

8.1.2 Bilateral telemanipulation

A new framework to guarantee stability of (time-delayed) bilateral telemanipulation systems was presented in Chapter 3. The two-layered approach allows the combination of passivity and transparency in a very intuitive manner. Using this framework any control architecture with an impedance causality can be implemented in a passive manner. A bilateral control algorithm to obtain a desired level of transparency is implemented in the *Transparency Layer*. The energy exchange between the control system and the physical world is monitored online in the *Passivity Layer*. If necessary the commands of the *Transparency Layer* are adapted to maintain passivity of the interaction with the system. Furthermore the framework allows many of its features to be tuned for specific devices and/or tasks. Especially the energy transfer protocol and saturation functions can be designed and optimized for a specific device, environment, and/or task. The presented experimental results show the benefits of the two-layered implementation. A single implementation of the *Passivity Layer* was shown to maintain stability of two different implementations of the *Transparency Layer* even in the presence of large time delays and hard contacts. The transparency properties of the bilateral controllers, implemented in the *Transparency Layer*, were maintained and their commands were only adjusted by the minimum to maintain passivity of the system.

In Chapter 4 the influence of mechanical friction in the devices on the obtainable transparency with the two-layered approach proposed in Chapter 3 is analyzed. Especially friction in the slave device was shown to have a negative effect in the *Passivity Layer* as it forms a continuous drain of energy that needs to be compensated by the user. As compensation method for this effect a model-based compensation method was proposed. This model is used to estimate the amount of dissipated energy each sample period, which is added to the energy tank in the *Passivity Layer*. This effectively extends the energy balance monitored by the *Passivity Layer* to include the device friction at the slave side. Passivity of the new energy balance, composed of the bilateral controller and the modeled device friction in the slave device, is enforced. The desired stability properties of the *Passivity Layer* are maintained as long as the implemented friction model underestimates the physically dissipated energy. The inclusion of any such friction model will increase the obtainable transparency with the telemanipulation system. The application of this extension is not limited to the two-layered approach, but will increase the obtainable transparency of any TDP algorithm when applied to devices with non-negligible mechanical friction, e.g. the TDPC approach by Ryu et al. (2004*b*, 2010).

The two-layered approach enforces passivity in the time domain based on the monitored energy exchange. The concept of passivity is also often used in the design of bilateral controllers in the frequency domain. In Chapter 5 it was shown that it is possible to improve the complimentary effect between passivity-based approaches for the design of bilateral controllers in the frequency domain and the enforcing of passive behavior in the time domain by means of a TDP algorithm. Several required extensions to the TDP algorithm were the model-based addition of the device dynamics to the monitored energy balance, methods for the prevention of an energy build up, and the inclusion of energy scaling. Using these extensions the influence of the TDP algorithm can be minimized

for the set of operating conditions that were considered in the frequency domain design phase. For operating conditions outside this set, and which can potentially destabilize the system, passivity and thus stability is enforced by the TDP algorithm. In Chapter 5 an implementation of the standard TDPC algorithm by Ryu et al. (2004*b*) was used, but the same results could also be obtained using the two-layered approach.

In Chapter 6 experimental results obtained with the two-layer framework for time-delayed bilateral telemanipulation were presented. The efficacy of the framework applied to bilateral telemanipulation over the internet was demonstrated. Two of the extensions proposed in Chapter 4 and Chapter 5, friction compensation and energy scaling, were discussed and experimentally validated. These extensions significantly improve the transparency of the system while maintaining the guaranteed stability properties of the two-layered approach.

The two-layered approach employs a modulated damper to maintain a desired energy level in the system. A different approach that has been proposed in literature is to analyze the amount of viscous damping needed using Lyapunov theory to guarantee asymptotic stability under all operating conditions. Chapter 7 analyzes the minimum amount of damping needed to ensure stability of a Position-Position controller in the presence of time-delays. It was found that the fixed damping approaches neglect the influence of important factors on the amount of damping required to stabilize the system. Therefore, the resulting parameter relations can be regarded as conservative. For the Position-Position controller the two-layered approach was found to be susceptible to the build-up effect and a simple additional dissipative action was included in the *Passivity Layer*. Due to this dissipative action the two-layered approach adds slightly more damping to the system compared to the considered Lyapunov-based approach when small time delays are present. For increased time delays the application of the two-layered approach results in the addition of far smaller amounts of damping. The Lyapunov-based approaches can be used as a design check on when the time delay justifies the added complexity of a TDP-algorithm like the two-layered approach.

8.2 Recommendations

The work described in this thesis provides several directions for further research. In this section we will treat remaining and newly established research questions organized by topic.

Framework for Passive Sampled Port-Hamiltonian Systems

- *Noise-sensitivity analysis* - A noise sensitivity analysis should be performed to indicate model structures where measurement noise can be problematic. Based on preliminary experience, viscous damping elements connected directly to the user's interaction point appear to be susceptible to measurement noise.

- *Scalability of models* - The models analyzed in Chapter 2 are still relatively simple models. If this framework is to be used in realistic applications the scalability of

the models needs to be analyzed. The applicability of the approach to large-scale finite element models of for instance deformable objects need to be investigated. This is required to make the approach suitable to be applied in surgical simulators, e.g. (Cotin et al., 2000), where the interaction with soft viscoelastic organs in combination with stiffer materials such as bone need to be reflected.

- *Automatic code generation* - Models of arbitrary size and complexity are usually composed of a discrete set of simple elements, e.g. masses, dampers, and springs. Manual coding of larger models is time-consuming and prone to small implementation errors. The framework does not differentiate between large and smaller models, only the number of energy balances that need to be evaluated will increase. Larger models will contain more submodels and each submodel has its own energy balance. As such it is suitable for automatic code generation where the designer only has to define the structure and components of the model and possible boundary conditions. The input method for the designer can then even be graphically as e.g. a bond graph or ideal physical model.

- *Benchmarking* - It is recognized that the computational burden of the framework is higher compared to other approaches. Therefore it is required to compare the performance of the framework with other existing methods taking the stability, realism, and the computational efficiency into account in the performance metric during benchmark tests representative of realistic applications.

Two-layer framework for bilateral telemanipulation

- *Systematic tuning* - The *Passivity*-layer has several parameters that influence the performance of the two-layer framework. Each parameter is related to a specific function and as such independent of other parameters. Although this simplifies tuning it is recommended to derive a systematic tuning scheme for the parameters of the TLC and the energy transfer protocol, and the desired level of the energy tank.

- *Saturation functions* - In Chapter 3 the concept of saturation functions is introduced to prevent a loss of passivity and to shape the interaction with the remote environment. So far only simple saturation functions have been sketched and implemented and no general design criteria have been provided. Specific saturation functions to handle problematic situations in realistic applications should be designed, implemented, and evaluated to investigate the added benefit of such saturation functions.

- *Build-up effect in Passivity-Layer* - In Chapter 7 it was shown that for a Position-Position control architecture a build-up effect occurs in the *Passivity Layer* as defined in Chapter 3. This build-up effect might occur for other control architectures also, e.g. the class of *Coupled Impedance Controllers*. It was shown in Chapter 7 that this problem can be adequately resolved by including additional dissipation in the *Passivity Layer*. However, it was also shown that this can increase the conservatism of the approach as the TLC can be unnecessarily activated. Other

formulations of the additional dissipation procedure might be possible that are less conservative.

- *Multiple degrees of freedom* - In this thesis only single degree of freedom devices have been used. With a transition to multiple degree of freedom devices several implementation options have to be analyzed. All degrees of freedom could be treated independently so that an n-degree of freedom device is treated as n 1-degree of freedom systems. However, from an energy point of view this does not make sense as energy is a single quantity and not coupled to a specific direction. Implementing the *Passivity*-layer using a single energy tank will also facilitate the implementation of the friction compensation technique of Chapter 4. For robotic systems composed of serial linkages, a friction model is easier to derive in joint space. With a single energy tank there is no longer a difference between joint- and cartesian-space. The possible coupling of degrees of freedom where the energy to sustain an undesired oscillation in one direction is extracted from another direction should be investigated on a physical system.

- *Friction compensation* - The proposed friction compensation technique in Chapter 4 should be further validated. Experiments with multiple degrees of freedom devices and friction effects other than mere coulomb friction have to be conducted. The use of online friction identification methods, e.g. observer-based and delineated feature identification methods, needs to be explored.

- *Complimentarity of frequency- and time-domain passivity approaches* - Experiments need to be conducted to demonstrate this complimentarity on a physical setup. A restriction here is that in the frequency-domain only viscous friction can be considered, whereas the experimental setup used in this thesis contains mostly coulomb friction. In Chapter 5 it was proposed to extend the balance monitored by the TDPC algorithm with energy functions for all components of the setup. Based on the simulation results presented in Chapter 5 it can be argued that the inclusion of kinetic (co-)energy of the devices appears not be strictly necessary. Further investigation should look into this effect and the applicability of the proposed extensions in the TDP algorithm to devices with structural compliance.

Haptic feedback systems in medical applications

- *Force-sensing* - For haptic feedback to be applied in surgical robotic systems an estimate of the interaction forces between the surgical tools and the tissue is needed. Many control algorithms perform the best when a direct force sensing at/near the interaction point is available. For surgical systems this poses a challenge as it means that at least part of the sensor system has to pass through the trocar. The diameter of a trocar is limited (usually 12mm or smaller) which imposes a very restrictive form factor for the sensor system. Furthermore the sensors need to be either disposable with a low cost-price, or sterilizable. So far several interesting prototypes have been developed by e.g. Seibold et al. (2008) and Peirs et al. (2004), but a truly

applicable force sensor (taking into account the desired low-cost price) has not yet been developed to the author's knowledge.

- *Task-enhancing transparency* - Haptic feedback can be added to a system for various reasons. When the intended goal of the haptic feedback is to improve the manipulation capabilities of the user in the remote environment, the standard definition of transparency does not cover the desired goal. In such applications we should only be interested in the haptic feedback that actually improves the performance of the user. This requires a deep understanding of how haptic information is incorporated in the human manipulation process. Such psychophysical studies are complicated due to the subjective nature of the comparison. The standard definition of transparency is conceptually more simple as objective comparison metrics can be applied on the basis of measured quantities (force and position/velocity). When the haptic feedback system is capable of perfectly reflecting the physical interaction the human cognition process will have to perceive it as a real and the manipulation performance should approximate the performance when the user is directly executing the task. This assumes sufficient dexterity of the telemanipulation system, so the system itself does not restrict the motions of the user.

  However, in order to obtain transparency stringent requirements will have to be placed on the various components of the system (e.g. sensors, mechanical structure of the system, actuators, and/or control algorithm). These stringent requirements might be unnecessary for a given application. A task-specific bound usually exists above which improved performance of the device, with respect to the obtained transparency, no longer results in improved performance of the task by the user (Christiansson, 2007). This is recognized by several researchers and interesting studies have already been performed towards task-enhancing transparency. Examples include the work of De Gersem et al. (2005) and Malysz and Sirouspour (2009) where mappings are investigated to improve the user's perception of e.g. stiffness differences in organic material and transparency itself is no longer the desired goal. Also interesting studies are performed with Shared Control Systems (SCS) as analyzed by e.g. Abbink (2006) for car following tasks. Reilink et al. (2011) applied SCS to enhance the performance during endoscopic navigation tasks by means of haptic cues. In this last category the haptic feedback does not reflect the physical interaction, but conveys information of a different type, e.g. proximity or navigation cues. Virtual fixtures as described by Abbott, Marayong and Okamura (2007) and Marayong et al. (2002) are also a type of SCS.

  The author believes that the manner in which haptic information is incorporated in the human manipulation process is highly dependent on the task to be executed and the background/training of the person executing the task. This means that a good understanding of the user and the task itself is required to determine if and how the feedback of haptic information can in fact increase the task performance. Therefore, it is recommended to involve more students from studies such as Technical Medicine in the research towards haptic feedback systems in medical applications. Technical Medicine is an interdisciplinary programme at the University

of Twente, linking science and technology with the clinical practice of medicine. The extended knowledge/understanding of these students of the application domain combined with basic technological skills can result in interesting, valuable, and as of yet unexplored applications.

Bibliography

Abbink, D. (2006), Neuromuscular Analysis of Haptic Gas Pedal Feedback during Car Following, PhD thesis, Delft University of Technology.

Abbott, A. (2006), 'Neuroprosthetics: In search of the sixth sense', *Nature* **442**, pp. 125–127.

Abbott, D., Becke, C., Rothstein, R. and Peine, W. (2007), 'Design of an endoluminal notes robotic system', *Proceedings of the IEEE/RSJ International Conference on Intelligent Robots and Systems* pp. 410 –416.

Abbott, J., Marayong, P. and Okamura, A. M. (2007), 'Haptic virtual fixtures for robot-assisted manipulation', *Proceedings of the 12th International Symposium on Robotic Research* **28**, pp. 49–64.

Abbott, J. and Okamura, A. M. (2005), 'Effects of position quantization and sampling rate on virtual-wall passivity', *IEEE Transactions on Robotics* **21**(5), pp. 952–964.

Adams, R. and Hannaford, B. (1999), 'Stable haptic interaction with virtual environments', *IEEE Transactions on Robotics and Automation* **15**(3), pp. 465–474.

Aliaga, I., Rubio, A. and Sanchez, E. (2004), 'Experimental quantitative comparison of different control architectures for master-slave teleoperation', *IEEE Transactions on Control Systems Technology* **12**(1), pp. 2–11.

Anderson, R. and Spong, M. (1989), 'Bilateral control of teleoperators with time delay', *IEEE Transactions on Automatic Control* **34**(5), pp. 494–501.

Ando, N., Szemes, P., Korondi, P. and Hashimoto, H. (2002), 'Friction compensation for 6dof cartesian coordinate haptic interface', *Proceedings of the IEEE/RSJ International Conference on Intelligent Robots and Systems* pp. 2893 – 2898.

Anvari, M., Broderick, T. and et al. (2005), 'The impact of latency on surgical precision and task completion during robotic-assisted remote telepresence surgery', *Computer Aided Surgery* **10**(2), pp. 93–99.

Arata, J., Takahashi, H. and et al. (2006), 'A remote surgery experiment between japan-korea using the minimally invasive surgical system', *Proceedings of the IEEE International Conference on Robotics and Automation* pp. 257–262.

Arcara, P. and Melchiorri, C. (2002), 'Control schemes for teleoperation with time delay: a comparative study', *Robotics and Autonomous Systems* **38**(1), pp. 49–64.

Arioui, H., Kheddar, A. and Mammar, S. (2002), 'A predictive wave-based approach for time-delayed virtual environments haptics systems', *Proceedings of the IEEE International Workshop on Robot and Human Interactive Communication* pp. 134–139.

Armstrong-Helouvry, B., Dupont, P. and Canudas de Wit, C. (1994), 'A survey of models, analysis tools, and compensation methods for the control of machines with friction', *Automatica (Oxf)* **30**(7), pp. 1083–1138.

Artigas, J., Preusche, C. and Hirzinger, G. (2007), 'Time domain passivity for delayed haptic telepresence with energy reference', *Proceedings of the IEEE/RSJ International Conference on Intelligent Robots and Systems* pp. 1612–1617.

Artigas, J., Preusche, C., Hirzinger, G., Borghesan, G. and Melchiorri, C. (2008), 'Bilateral energy transfer in delayed teleoperation on the time domain', *Proceedings of the IEEE International Conference on Robotics and Automation* pp. 671–676.

Artigas, J., Preusche, C., Hirzinger, G., Borghesan, G. and Melchiorri, C. (2009), 'Bilateral energy transfer for high fidelity haptic telemanipulation', *Proceedings of the Third Joint Eurohaptics Conference and Symposium on Haptic Interfaces for Virtual Environments and Teleoperator Systems* pp. 488–493.

Artigas, J., Ryu, J.-H. and Preusche, C. (2010*a*), 'Position drift compensation in time domain passivity based teleoperation', *Proceedings of the IEEE/RSJ International Conference on Intelligent Robots and Systems* pp. 4250–4256.

Artigas, J., Ryu, J.-H. and Preusche, C. (2010*b*), 'Time domain passivity control for position-position teleoperation architectures', *Presence* **19**(5), pp. 482–497.

Artigas, J., Vilanova, J., Preusche, C. and Hirzinger, G. (2006), 'Time domain passivity control-based telepresence with time delay', *Proceedings of the IEEE/RSJ International Conference on Intelligent Robots and Systems* pp. 4205–4210.

Aziminejad, A., Tavakoli, M., Patel, R. V. and Moallem, M. (2008), 'Stability and performance in delayed bilateral teleoperation: theory and experiments', *Control Engineering Practice* **16**(11), pp. 1329–1343.

Babakhani, B. (2008), Implementation of a 2d master-slave system, Msc thesis, Control Engineering Laboratory, University of Twente.

Basdogan, C., Ho, C.-H. and Srinivasan, M. (2001), 'Virtual environments for medical training: Graphical and haptic simulation of laparoscopic common bile duct exploration', *IEEE/ASME Transactions on Mechatronics* **6**(3), pp. 269–285.

Bejczy, A. (1994), *Teleoperation and Robotics in Space*, Vol. 161 of *Progress in Astronautics and Aeronautics*, American Institute of Astronautics and Aeronautics, chapter Towards advanced teleoperation in space, pp. 107–138.

Berestesky, P., Chopra, N. and Spong, M. (2004), 'Discrete time passivity in bilateral teleoperation over the internet', *Proceedings of the IEEE International Conference on Robotics and Automation* pp. 4557–4564.

Bernstein, L., Lawrence, D. and Pao, L. (2005), 'Friction modeling and compensation for haptic interfaces', *Proceedings of the World Haptics Conference* pp. 290–295.

Bethea, B. T., Okamura, A. M., Kitagawa, M., Fitton, T. P., Cattaneo, S. M., Gott, V. L., Baumgartner, W. A. and Yuh, D. D. (2004), 'Application of haptic feedback to robotic surgery', *Journal of Laparoendoscopic & Advanced Surgical Techniques* **14**(3), pp. 191–195.

Bi, D., Li, Y., Tso, S. and Wang, G. (2004), 'Friction modeling and compensation for haptic display based on support vector machine', *IEEE Transactions Industrial Electronics* **51**(2), pp. 491 – 500.

Bona, B. and Indri, M. (2005), 'Friction compensation in robotics: an overview', *Proceedings of the IEEE Conference on Decision and Control* pp. 4360–4367.

Borghesan, G., Macchelli, A. and Melchiorri, C. (2010), 'Interconnection and simulation issues in haptics', *IEEE Transactions on Haptics* **3**(4), pp. 266–279.

Botden, S., Buzink, S., Schijven, M. and Jakimowicz, J. (2007), 'Augmented versus Virtual Reality laparoscopic simulation: What is the difference?', *World Journal of Surgery* **31**, pp. 764–772.

Buisson, J., Cormerais, H. and Richard, P.-Y. (2000), 'Using trees to build non-singular bond graphs from electric circuit graphs', *Journal of the Franklin Institute* **337**(5), pp. 543 – 554.

Butner, S. and Ghodoussi, M. (2003), 'Transforming a surgical robot for human telesurgery', *IEEE Transactions on Robotics and Automation* **19**(5), pp. 818–824.

Canes, D., Desai, M., Aron, M., Haber, G.-P., Goel, R., Stein, R., Kaouk, J. and Gill, I. (2008), 'Transumbilical single-port surgery: Evolution and current status', *European Urology* **54**(5), pp. 1020 – 1030.

Canes, D., Lehman, A., Farritor, S., Oleynikov, D. and Desai, M. (2009), 'The future of NOTES instrumentation: flexible robotics and *in vivo* minirobots', *Journal of Endourology* **23**(5), pp. 787–792.

Ching, H. and Book, W. J. (2006), 'Internet-based bilateral teleoperation based on wave variable with adaptive predictor and direct drift control', *Journal of Dynamic Systems, Measurement, and Control* **128**(1), pp. 86–93.

Cho, H. and Park, J. (2005), 'Impedance control with variable damping for bilateral teleoperation under time delay', *JSME International Journal Series C* **48**(4), pp. 695–703.

Chopra, N., Spong, M., Hirche, S. and Buss, M. (2003), 'Bilateral teleoperation over the internet: the time varying delay problem', *Proceedings of the American Control Conference* pp. 155–160.

Christiansson, G. (2007), Hard Master Soft Slave Haptic Teleoperation, PhD thesis, Delft University of Technology.

Christiansson, G. (2008), Wave variables and the 4 channel architecture for haptic teleoperation, *in* 'Haptics: Perception, Devices and Scenarios', Springer Berlin / Heidelberg, pp. 169–174.

Colgate, J. (1993), 'Robust impedance shaping telemanipulation', *IEEE Transactions on Robotics and Automation* **9**(4), pp. 374–384.

Colgate, J., Grafting, P., Stanley, M. and Schenkel, G. (1993), 'Implementation of stiff virtual walls in force reflecting interfaces', *Proceedings of the IEEE Virtual Reality Annual International Symposium* pp. 202–208.

Colgate, J. and Schenkel, G. (1994), 'Passivity of a class of sampled-data systems: application to haptic interfaces', *Proceedings of the American Control Conference* pp. 3236–3240.

Colgate, J., Stanley, M. C. and Brown, J. M. (1995), 'Issues in the haptic display of tool use', *Proceedings of the IEEE/RSJ International Conference on Intelligent Robots and Systems* p. 140145.

Controllab Products B.V. (2010), '20-sim version 4.1', http://www.20sim.com/.

Cortesao, R., Park, J. and Khatib, O. (2006), 'Real-time adaptive control for haptic telemanipulation with kalman active observers', *IEEE Transactions on Robotics* **22**(5), pp. 987–999.

Cotin, S., Delingette, H. and Ayache, N. (2000), 'A hybrid elastic model for real-time cutting, deformations, and force feedback for surgery training and simulation', *The Visual Computer* **16**(8), pp. 437–452.

Csikesz, N., Singla, A., Murphy, M., Tseng, J. and Shah, S. (2010), 'Surgeon volume metrics in laparoscopic cholecystectomy', *Digestive Diseases and Sciences* **55**(8), pp. 2398–2405.

David, O., Loving, A., Palmer, J., Ciattaglia, S. and Friconneau, J. (2005), 'Operational experience feedback in JET Remote Handling', *Fusion Engineering and Design* **75-79**, pp. 519 – 523.

De Gersem, G. and Van Brussel, H. (2004), 'Influence of force disturbances on transparency in bilateral telemanipulation of soft environments', *Proceedings of the IEEE International Conference on Robotics and Automation* pp. 1227–1232.

De Gersem, G., Van Brussel, H. and Vander Sloten, J. (2005), 'Enhanced haptic sensitivity for soft tissues using teleoperation with shaped impedance reflection', *Proceedings of the World Haptics Conference* .

De, S., Rosen, J., Dagan, A., Hannaford, B., Swanson, P. and Sinanan, M. (2007), 'Assessment of tissue damage due to mechanical stresses', *International Journal of Robotics Research* **26**(11-12), pp. 1159–1171.

Diolaiti, N., Melchiorri, C. and Stramigioli, S. (2005), 'Contact impedance estimation for robotic systems', *IEEE Transactions on Robotics* **21**(5), pp. 925–935.

Diolaiti, N., Niemeyer, G., Barbagli, F. and Salisbury, Jr., J. K. (2006), 'Stability of haptic rendering: discretization, quantization, time delay and coulomb friction', *IEEE Transactions on Robotics* **22**(2), pp. 256–268.

Drake, J., Joy, M., Goldenberg, A. and Kreindler, D. (1991), 'Computer and robotic assisted resection of brain tumours', *Proceedings of the International Conference on Advanced Robotics* pp. 888 –892.

Fabrizio, M. D., Lee, B. R., Chan, D. Y., Stoianovici, D., Jarrett, T. W., Yang, C. and Kavoussi, L. R. (2000), 'Effect of time delay on surgical performance during telesurgical manipulation', *Journal of Endourology* **14**(2), pp. 133–138.

Famaey, N., Verbeken, E., Vinckier, S., Willaert, B., Herijgers, P. and Vander Sloten, J. (2010), 'In vivo soft tissue damage assessment for applications in surgery', *Medical Engineering & Physics* **32**(5), pp. 437–443.

Feemster, M., Vedagarbha, P., Dawson, D. M. and Haste, D. (1999), 'Adaptive control techniques for friction compensation', *Mechatronics* **9**(2), pp. 125 – 145.

Ferrell, W. (1966), 'Delayed force feedback', *IEEE Transactions on Human Factors in Electronics* **8**, pp. 449–455.

Ferrell, W. R. (1965), 'Remote manipulation with transmission delay', *IEEE Transactions on Human Factors in Electronics* **6**, pp. 24–32.

Ferrell, W. and Sheridan, T. (1967), 'Supervisory control of remote manipulation', *IEEE Spectrum* pp. 81–88.

Fite, K., Shao, L. and Goldfarb, M. (2004), 'Loop shaping for transparency and stability robustness in bilateral telemanipulation', *IEEE Transactions on Robotics and Automation* **20**(3), pp. 620 – 624.

Fite, K., Speich, J. E. and Goldfarb, M. (2001), 'Transparency and stability robustness in two-channel bilateral telemanipulation', *ASME Journal of Dynamic Systems, Measurement, Control* **123**, pp. 400–407.

Franken, M., Misra, S. and Stramigioli, S. (2010*a*), 'Friction compensation in energy-based bilateral telemanipulation', *Proceedings of the IEEE/RSJ International Conference on Intelligent Robots and Systems* pp. 5264–5269.

Franken, M., Misra, S. and Stramigioli, S. (2010*b*), 'Multi-dimensional passive sampled port-hamiltonian systems', *Proceedings of the IEEE International Conference on Robotics and Automation* pp. 1320–1326.

Franken, M., Misra, S. and Stramigioli, S. (2012), 'Internet-based two-layered bilateral telemanipulation: An experimental study', *IEEE International Conference on Robotics and Automation* . In Preparation.

Franken, M. and Stramigioli, S. (2009), 'Internal dissipation in passive sampled haptic feedback systems', *Proceedings of the IEEE/RSJ International Conference on Intelligent Robots and Systems* pp. 1755–1760.

Franken, M., Stramigioli, S., Misra, S., Secchi, C. and Macchelli, A. (2011b), 'Bilateral telemanipulation with time delays: A two-layer approach combining passivity and transparency', *IEEE Transactions on Robotics* . In press.

Franken, M., Stramigioli, S., Reilink, R., Secchi, C. and Macchelli, A. (2009), 'Bridging the gap between passivity and transparency', *Proceedings of Robotics: Science and Systems* pp. 281–288.

Franken, M., Willaert, B., Misra, S. and Stramigioli, S. (2011), 'Bilateral telemanipulation: Improving the complimentarity of the frequency- and time-domain passivity approaches', *Proceedins of the IEEE International Conference on Robotics and Automation* . In Press.

Friedland, B. and Park, Y.-J. (1992), 'On adaptive friction compensation', *IEEE Transactions on Automatic Control* **37**(10), pp. 1609 –1612.

Galambos, P., Baranyi, P. and Korondi, P. (2010), 'Extended TP model transformation for polytopic representation of impedance model with feedback delay', *WSEAS Transactions on Systems and Control* **5**(9), pp. 701–710.

Ganjefar, S., Momeni, H. and Sharifi, F. J. (2002), 'Teleoperation systems design using augmented wave-variables and smith predictor method for reducing time-delay effects', *Proceedings of the IEEE International Symposium on Intelligent Control* pp. 333–338.

Gil, J., Avello, A., Rubio, A. and Florez, J. (2004), 'Stability analysis of a 1 d.o.f. haptic interface using the routh-hurwitz criterion', *IEEE Transactions on Control Systems Technology* **12**(4), pp. 583–588.

Gillespie, B. and Cutkosky, M. (1996), 'Stable user-specific rendering of the virtual wall', *Proceedings of the ASME International Mechanical Engineering Conference and Exposition* pp. 397–406.

Goertz, R. (1952), 'Fundamentals of general-purpose remote manipulators', *Nucleonics* **10**(11), pp. 36–42.

Goertz, R. (1954*a*), 'Electronically controlled manipulator', *Nucleonics* **12**(11), pp. 46–47.

Goertz, R. (1954*b*), 'Mechanical master-slave manipulator', *Nucleonics* **12**(11), pp. 45–46.

Goethals, P., De Gersem, G., Sette, M. and Reynaerts, D. (2007), 'Accurate haptic teleoperation on soft tissues through slave friction compensation by impedance reflection', *Proceedings of World Haptics* pp. 458 –463.

Gourin, C. and Terris, D. (2007), 'History of robotic surgery', *Robotics in Surgery: History, Current and Future Applications* pp. 3–12.

Guenard, N., Hamel, T. and Eck, L. (2006), 'Control laws for the tele operation of an Unmanned Aerial Vehicle known as an X4-flyer', *Proceedings of the IEEE/RSJ International Conference on Intelligent Robots and Systems* pp. 3249–3254.

Haddadi, A. and Hashtrudi-Zaad, K. (2010), 'Bounded-impedance absolute stability of bilateral teleoperation control systems', *IEEE Transactions on Haptics* **3**(1), pp. 15 –27.

Hanna, G. B. and Cuschieri, A. (1999), 'Influence of the optical axis-to-target view angle on endoscopic task performance', *Surgical Endoscopy* **13**, pp. 371–375.

Hannaford, B. (1989), 'A design framework for teleoperators with kinesthetic feedback', *IEEE Transactions on Robotics and Automation* **5**(4), pp. 426–434.

Hannaford, B. and Anderson, R. (1988), 'Experimental and simulation studies of hard contact in force reflecting teleoperation', *Proceedings of the IEEE International Conference on Robotics and Automation* pp. 584–589.

Hannaford, B. and Ryu, J.-H. (2002), 'Time domain passivity control of haptic interfaces', *IEEE Transactions on Robotics and Automation* **18**(1), pp. 1–10.

Hannaford, B., Ryu, J.-H., Kwon, D.-S., Kim, Y. S. and Song, J.-B. (2002), 'Testing time domain passivity control of haptic enabled systems', *8th International Symposium on Experimental Robotics* .

Hansen Medical (2011), 'Sensei X Robotic Catheter System', http://www.hansenmedical.com/.

Hashizume, M., Shimada, M. and et al. (2002), 'Early experiences of endoscopic procedures in general surgery assisted by a computer-enhanced surgical system', *Surgical Endoscopy* **16**(8), pp. 1187–1191.

Hashtrudi-Zaad, K. and Salcudean, S. E. (1996), 'Adaptive transparent impedance reflecting teleoperation', *Proceedings of the IEEE International Conference on Robotics and Automation* pp. 1369–1374.

Hashtrudi-Zaad, K. and Salcudean, S. E. (1999), 'On the use of local force feedback for transparent teleoperation', *Proceedings of the IEEE International Conference on Robotics and Automation* pp. 1863 –1869.

Hashtrudi-Zaad, K. and Salcudean, S. E. (2001), 'Analysis of control architectures for teleoperation systems with impedance/admittance master and slave manipulators', *International Journal of Robotics Research* **20**(6), pp. 419–445.

Hasser, C. J. and Cutkosky, M. (2002), 'System identification of the human hand grasping a haptic knob', *Proc. 10th Symp. on Haptic Interfaces for Virtual Environments and Teleoperator Systems* pp. 171–180.

Haykin, S. (1970), *Active Network Theory*, Addison-Wesley Pub. Co.

Hertkorn, K., Hulin, T., Kremer, P., Preusche, C. and Hirzinger, G. (2010), 'Time Domain Passivity Control for multi-degree of freedom haptic devices with time delay', *Proceedings of the IEEE International Conference on Robotics and Automation* pp. 1313–1319.

Hirche, S. and Buss, M. (2004), 'Packet loss effects in passive telepresence systems', *Proceedings of the IEEE Conference on Decision and Control* pp. 4010–4015.

Hirzinger, G., Heindl, J. and Landzettel, K. (1989), 'Predictive and knowledge-based telerobotic control concepts', *Proceedings of the IEEE International Conference on Robotics and Automation* pp. 1768–1777.

Hogan, N. (1989), 'Controlling impedance at the man/machine interface', *Proceedings of the IEEE International Conference on Robotics and Automation* pp. 1626–1631.

Hokayem, P. and Spong, M. (2006), 'Bilateral teleoperation: an historical survey', *Automatica* **42**, pp. 2035–2057.

Hou, Y. and Luecke, G. (2005), 'Time delayed teleoperation system control, a passivity-based method', *Proceedings of the International Conference on Advanced Robotics* pp. 796–802.

Hua, C. C. and Liu, X. P. (2010), 'Delay-dependent stability criteria of teleoperation systems with asymmetric time-varying delays', *IEEE Transactions on Robotics* **26**(5), pp. 925–932.

Hulin, T., Preusche, C. and Hirzinger, G. (2008), 'Stability boundary for haptic rendering: Influence of human operator', *Proceedings of the IEEE/RSJ International Conference on Intelligent Robots and Systems* pp. 3483–3488.

Ibeas, A. and de la Sen, M. (2006), 'Robustly stable adaptive control of a tandem of master-slave robotic manipulators with force reflection using a multi-estimation scheme', *IEEE Transactions on Systems, Man, and Cybernetics - Part B: Cybernetics* **36**(5), pp. 1162–1179.

Intuitive Surgical, Inc. (2011), 'da Vinci Surgical System', http://www.intuitivesurgical.com/.

Iqbal, A. and Roth, H. (2006*a*), 'Predictive Time Domain Passivity Control for delayed teleoperation using energy derivatives', *Proceedings of the IEEE International Conference on Control, Automation, Robotics and Vision* pp. 1–6.

Iqbal, A. and Roth, H. (2006*b*), 'Stabilization of teleoperated systems with stochastic time delays using Time Domain Passivity Control', *Proceedings of the SICE-ICASE International Joint Conference* pp. 393–398.

Jonckheere, E. and Ma, C. (1989), 'A further simplification to Jury's Stability Test', *IEEE Transactions on Circuits and Systems* **36**(3), pp. 463–464.

Jun, B., Shim, H., Lee, P., Baek, H., Cho, S. and Kim, D. (2009), 'Workspace control system of underwater tele-operated manipulators on ROVs', *Proceedings of OCEANS 2009 - Europe* pp. 1 –6.

Karl Storz (2011), 'Anubis', http://www.karlstorz.com/.

Kawashima, K., Tadano, K., Sankaranarayanan, G. and Hannaford, B. (2008*a*), 'Bilateral teleoperation with time delay using modified wave variables', *Proceedings of the IEEE/RSJ International Conference on Intelligent Robots and Systems* pp. 424–429.

Kawashima, K., Tadano, K., Sankaranarayanan, G. and Hannaford, B. (2008*b*), 'Model-based passivity control for bilateral teleoperation of a surgical robot with time delay', *Proceedings of the IEEE/RSJ International Conference on Intelligent Robots and Systems* pp. 1427–1432.

Kawashima, K., Tadano, K., Wang, C., Sankaranarayanan, G. and Hannaford, B. (2009), 'Bilateral teleoperation with time delay using modified wave variable based controller', *Proceedings of the IEEE International Conference on Robotics and Automation* pp. 4326–4331.

Kazerooni, H., Tsay, T.-I. and Hollerbach, K. (1993), 'A controller design framework for telerobotic systems', *IEEE Transactions on Control Systems Technology* **1**(1), pp. 50–62.

Khayati, K., Bigras, P. and Dessaint, L.-A. (2009), 'LuGre model-based friction compensation and positioning control for a pneumatic actuator using multi-objective output-feedback control via LMI optimization', *Mechatronics* **19**(4), pp. 535 – 547.

Kim, D., Oh, K. W., Hong, D., Park, J.-H. and Hong, S.-H. (2008), 'Remote control of excavator with designed haptic device', *Proceedings of the International Conference on Control, Automation and Systems* pp. 1830 –1834.

Kim, J., Chang, P. H. and Park, H. S. (2005), 'Transparent teleoperation using two-channel control architectures', *Proceedings of the IEEE/RSJ International Conference on Intelligent Robots and Systems* pp. 1953–1960.

Kim, J.-P. and Ryu, J. (2010), 'Robustly stable haptic interaction control using an energy-bounding algorithm', *International Journal of Robotics Research* **29**(6), pp. 666–679.

Kim, K. and Kim, H. (2010), 'Remote robotic systems for nuclear environment application', *Proceedings of the International Conference on Control Automation and Systems* pp. 1843 –1846.

Kim, W., Hannaford, B. and Fejczy, A. (1992), 'Force-reflection and shared compliant control in operating telemanipulators with time delay', *IEEE Transactions on Robotics and Automation* **8**(2), pp. 176 –185.

Kim, Y. S. and Hannaford, B. (2001), 'Some practical issues in Time Domain Passivity Control of haptic interfaces', *Proceedings of the IEEE/RSJ International Conference on Intelligent Robots and Systems* pp. 1744 –1750.

King, C. H., Culjat, M. O., Franco, M. L., Lewis, C. E., Dutson, E. P., Grundfest, W. S. and Bisley, J. W. (2009), 'Tactile feedback induces reduced grasping force in robot-assisted surgery', *IEEE Transactions on Haptics* **2**(2), pp. 103–110.

King, H. H., Hannaford, B. and et al. (2010), 'Plugfest 2009: Global interoperability in telerobotics and telemedicine', *Proceedings of the IEEE International Conference on Robotics and Automation* .

Kuchenbecker, K., Fiene, J. and Niemeyer, G. (2006), 'Improving contact realism through event-based haptic feedback', *IEEE Transactions on Visualization and Computer Graphics* **12**(2), pp. 219–230.

Kuchenbecker, K. and Niemeyer, G. (2006), 'Induced master motion in force-reflecting teleoperation', *ASME Journal of Dynamic Systems, Measurement, and Control* **128**(4), pp. 800–810.

Kurose, J. and Ross, K. (2006), *Computer networking: a top-down approach*, Pearson Addison Wesley.

Kwoh, Y., Hou, J., Jonckheere, E. and Hayati, S. (1988), 'A robot with improved absolute positioning accuracy for CT guided stereotactic brain surgery', *IEEE Transactions on Biomedical Engineering* **35**(2), pp. 153 –160.

Kwon, D.-S. and Woo, K. (2000), 'Control of the haptic interface with friction compensation and its performance evaluation', *Proceedings of the IEEE/RSJ International Conference on Intelligent Robots and Systems* pp. 955–960.

Lawn, C. and Hannaford, B. (1993), 'Performance testing of passive communication and control in teleoperation with time delay', *Proceedings of the IEEE International Conference on Robotics and Automation* pp. 776–783.

Lawrence, D. (1993), 'Stability and transparency in bilateral teleoperation', *IEEE Transactions on Robotics and Automation* **9**(5), pp. 624–637.

Lee, D. (2009), 'Extension of Colgate's passivity condition for variable-rate haptics', *Proceedings of the IEEE/RSJ International Conference on Intelligent Robots and Systems* pp. 1761–1766.

Lee, D. and Huang, K. (2008*a*), 'On passive non-iterative varying-step numerical integration of mechanical systems for haptic rendering', *Proceedings of the ASME Dynamic Systems and Control Conference* pp. 1147–1154.

Lee, D. and Huang, K. (2009), 'Passive Set-Position Modulation approach for haptics with slow variable, and asynchronous update', *Proceedings of the World Haptics Conference* pp. 541–546.

Lee, D. and Huang, K. (2010), 'Passive-Set-Position-Modulation framework for interactive robotic systems', *IEEE Transactions on Robotics* **26**(2), pp. 354–369.

Lee, D. J. and Huang, K. (2008*b*), 'Passive position feedback over packet-switching communication network with varying-delay and packet-loss', *Proceedings of the Symposium of Haptic Interfaces for Virtual Environments and Teleoperator Systems* pp. 335–342.

Lee, D. and Li, P. Y. (2002), 'Passive coordination control of nonlinear bilateral teleoperated manipulators', *Proceedings of the IEEE International Conference on Robotics and Automation* pp. 3278–3283.

Lee, D. and Li, P. Y. (2003), 'Passive bilateral feedforward control linear dynamically similar teleoperated manipulators', *IEEE Transactions on Robotics and Automation* **19**(3), pp. 443–456.

Lee, D. and Li, P. Y. (2005), 'Passive bilateral control and tool dynamics rendering for nonlinear mechanical teleoperators', *IEEE Transactions on Robotics* **21**(5), pp. 936–951.

Lee, D. and Spong, M. (2006), 'Passive bilateral teleoperation with constant time delay', *IEEE Transactions on Robotics* **22**(2), pp. 269–281.

Leung, G., Francis, B. and Apkarian, J. (1995), 'Bilateral controller for teleoperators with time delay via mu-synthesis', *IEEE Transactions on Robotics and Automation* **11**(1), pp. 105–116.

Lim, J.-N., Ko, J.-P. and Lee, J.-M. (2003), 'Internet-based teleoperation of a mobile robot with force-reflection', *Proceedings of the IEEE Conference on Control Applications* pp. 680–685.

Liu, G., Goldenberg, A. A. and Zhang, Y. (2004), 'Precise slow motion control of a direct-drive robot arm with velocity estimation and friction compensation', *Mechatronics* **14**(7), pp. 821 – 834.

Llewellyn, F. B. (1952), 'Some fundamental properties of transmission systems', *Proceedings of the Institute of Radio Engineers* **40**(3), pp. 271–283.

Love, L. J. (1995), Adaptive Impedance Control, PhD thesis, Georgia Institute of Technology.

Love, L. J. and Book, W. (2004), 'Force reflecting teleoperation with adaptive adaptive impedance control', *IEEE Transactions on System, Man, and Cybernetics - Part B: Cybernetics* **34**(1), pp. 159–165.

Lum, M. J. H., Friedman, D., King, H. H. I., Donlin, R., Sankaranarayanan, G., Broderick, T., Sinanan, M. N., Rosen, J. and Hannaford, B. (2008), *Field and Service Robotics*, Vol. 42 of *STAR*, chapter Teleoperation of a Surgical Robot Via Airborne Wireless Radio and Transatlantic Internet Links, pp. 305–314.

Lum, M. J. H., Rosen, J., Lendvay, T. S., Sinanan, M. N. and Hannaford, B. (2009b), 'Effect of time delay on telesurgical performance', *Proceedings of the IEEE International Conference on Robotics and Automation* pp. 4246 –4252.

Lum, M. J. H., Trimble, D., Rosen, J., Fodero, K., King, H. H., Sanarayanaranan, G., Dosher, J., Leushke, R., Martin-Anderson, B., Sinanan, M. N. and Hannaford, B. (2006), 'Multidisciplinary approach for developing a new minimally invasive surgical robotic system', *Proceedings of the IEEE International Conference on Biomedical Robotics and Biomechatronics* pp. 841–846.

Lum, M., Rosen, J., King, H., Friedman, D., Lendvay, T., Wright, A., Sinanan, M. and Hannaford, B. (2009a), 'Teleoperation in surgical robotics; network latency effects on surgical performance', *Proceedings of the Annual International Conference of the IEEE Engineering in Medicine and Biology Society* pp. 6860 –6863.

Luursema, J. (2010), See Me, Touch Me, Heal Me, PhD thesis, University of Twente.

Macefield, V. G., Hager-Ross, C. and Johansson, R. S. (1996), 'Control of grip force during restraint of an object held between finger and thumb: responses of cutaneous afferents from the digits', *Experimental Brain Research* **108**(1), pp. 155–171.

Madhani, A. (1998), Design of Teleoperated Surgical Instruments for Minimally Invasive Surgery, PhD thesis, Massachusetts Institute of Technology.

Mahvash, M. and Okamura, A. M. (2007), 'Friction compensation for enhancing transparency of a teleoperator with compliant transmission', *IEEE Transactions on Robotics* **23**(6), pp. 1240–1246.

Malysz, P. and Sirouspour, S. (2009), 'Nonlinear and filtered force/position mappings in bilateral teleoperation with application to enhanced stiffness discrimination', *IEEE Transactions on Robotics* **25**(5), pp. 1134–1149.

Marayong, P., Bettini, A. and Okamura, A. (2002), 'Effect of virtual fixture compliance on human-machine cooperative manipulation', *Proceedings of the IEEE/RSJ International Conference on Intelligent Robots and Systems* pp. 1089–1095.

Marescaux, J., Dallemagne, B., Perretta, S., Wattiez, A., Mutter, D. and Coumaros, D. (2007), 'Surgery without scars: report of transluminal cholecystectomy in a human being', *Archives of Surgery* **142**(9), pp. 823–826.

Marescaux, J., Leroy, J., Gagner, M., Rubino, F., Mutter, D., Vix, M., Butner, S. and Smith, M. K. (2001), 'Transatlantic robot-assisted telesurgery', *Nature* **413**, pp. 379–380.

Melfi, F., Menconi, G., Mariani, A. and Angeletti, C. (2002), 'Early experience with robotic technology for thoracoscopic surgery', *European Journal of Cardio-Thoracic Surgery* **21**, pp. 864–868.

Misra, S. and Okamura, A. M. (2006), 'Environment parameter estimation during bilateral telemanipulation', *Proceedings of the Symposium on Haptic Interfaces for Virtual Environments and Teleoperator Systems* pp. 301–307.

Mitra, P. and Niemeyer, G. (2008), 'Model-mediated telemanipulation', *International Journal of Robotics Research* **27**(2), pp. 253–262.

Miyazaki, F., Matsubayashi, S., Yoshimi, T. and Arimoto, S. (1986), 'A new control methodology toward advanced teleoperation of master-slave robot systems', *Proceedings of the IEEE International Conference on Robotics and Automation* pp. 997–1002.

Monfaredi, R., Razi, K., Ghydari, S. S. and Rezaei, S. M. (2006), 'Achieving high transparency in bilateral teleoperation using stiffness observer for passivity control', *Proceedings of the IEEE/RSJ International Conference on Intelligent Robots and Systems* pp. 1686–1691.

MOOG FCS (2009), 'Simodont Dental Trainer', http://www.moog.com/.

Morris, D., Sewell, C., Barbagli, F., Salisbury, K., Blevins, N. and Girod, S. (2006), 'Visuohaptic simulation of bone surgery for training and evaluation', *IEEE Computer Graphics and Applications* **26**(6), pp. 48–57.

Munir, S. and Book, W. (2002), 'Internet-based teleoperation using wave variables with prediction', *IEEE/ASME Transactions on Mechatronics* **7**(2), pp. 124–133.

Naerum, E. and Hannaford, B. (2009), 'Global transparency analysis of the lawrence teleoperator architecture', *Proceedings of the IEEE International Conference on Robotics and Automation* pp. 4344–4349.

Niemeyer, G. (1996), Using Wave Variables in Time Delayed Force Reflecting Teleoperation, PhD thesis, Massachusetts Institute of Technolgy.

Niemeyer, G., Preusche, C. and Hirzinger, G. (2008), *Springer Handbook of Robotics*, Springer Berlin-Heidelberg, chapter Telerobotics, pp. 741–757.

Niemeyer, G. and Slotine, J.-J. (1998), 'Towards force reflecting teleoperation over the internet', *Proceedings of the IEEE International Conference on Robotics and Automation* pp. 1909–1915.

Niemeyer, G. and Slotine, J.-J. E. (2004), 'Telemanipulation with time delays', *International Journal of Robotics Research* **23**(9), pp. 873–890.

Nuno, E., Basanez, L., Ortega, R. and Spong, M. (2009), 'Position tracking for non-linear teleoperators with variable time delay', *Int. J. Robotics Research* **28**(7), pp. 895–910.

Nuno, E., Ortega, R., Barabanov, N. and Basanez, L. (2008), 'A globally stable PD controller for bilateral teleoperators', *IEEE Transactions on Robotics* **24**(3), pp. 753–758.

Okamura, A. M. (2004), 'Methods for haptic feedback in teleoperated robot-assisted surgery', *Industrial Robot: An International Journal* **31**(6), pp. 499–508.

Olympus (2011), 'Endosamurai', http://www.olympus.com/.

Onda, K., Osa, T., Sugita, N., Hashizume, M. and Mitsuishi, M. (2010), 'Asynchronous force and visual feedback in teleoperative laparoscopic surgical system', *Proceedings of the IEEE/RSJ International Conference on Intelligent Robots and Systems* pp. 844–849.

Pan, Y.-J., Canudas de Wit, C. and Sename, O. (2006), 'A new predictive approach for bilateral teleoperation with applications to drive-by-wire systems', *IEEE Transactions on Robotics* **22**(6), pp. 1146–1162.

Park, S., Seo, C., Kim, J.-P. and Ryu, J. (2010), 'An Energy-Bounding Approach to rate-mode bilateral teleoperation of remote vehicles in constant time-delayed environments', *Proceedings of the IEEE/RSJ International Conference on Intelligent Robots and Systems* pp. 5806 –5811.

Patil, P. V., Hanna, G. B. and Cuschieri, A. (2004), 'Effect of the angle between the optical axis of the endoscope and the instruments plane on monitor image and surgical performance', *Surgical Endoscopy* **18**(1), pp. 111–114.

Paul, H., Bargar, W., Mittlestadt, B., Kazanzides, P., Musits, B., Zuhars, J., Cain, P., Williamson, B. and Smith, F. (1992), 'Robotic execution of a surgical plan', *Proceedings of the IEEE International Conference on Systems, Man and Cybernetics* pp. 1621 –1623 vol.2.

Paynter, H. (1961), *Analysis and Design of Engineering Systems*, MIT Press, Cambridge, MA.

Peirs, J., Clijnen, J., Reynaerts, D., Van Brussel, H., Herijgers, P., Corteville, B. and Boone, S. (2004), 'A micro optical force sensor for force feedback during minimally invasive robotic surgery', *Sensors and Actuators A* **115**(2-3), pp. 447–455.

Polushin, I. G., Liu, P. X. and Horng, C. H. (2008), 'Projection-based force reflection algorithm for stable bilateral teleoperation over networks', *IEEE Transactions on Instrumentation and Measurement* **57**(9), pp. 1854–1865.

Polushin, I. G., Liu, P. X. and Lung, C. H. (2007), 'A force-reflection algorithm for improved transparency in bilateral teleopration with communication delay', *IEEE/ASME Transactions on Mechatronics* **12**(3), pp. 361–374.

Polychronidis, A., Laftsidis, P., Bounovas, A. and Simopoulos, C. (2008), 'Twenty years of laparoscopic cholecystectomy: Phillipe mouret - march 17, 1987', *Journal of the Society of laparoendoscopic Surgeons* **12**(1), pp. 109–111.

Preusche, C., Hirzinger, G., Ryu, J.-H. and Hannaford, B. (2003), 'Time domain passivity control for 6 degrees of freedom haptic displays', *Proceedings of the IEEE/RSJ International Conference on Intelligent Robots and Systems* pp. 2944–2949.

Preusche, C., Reintsema, D., Landzettel, K. and Hirzinger, G. (2006), 'Robotics component verification on ISS ROKVISS - preliminary results for telepresence', *Proceedings of the IEEE/RSJ International Conference on Intelligent Robots and Systems* pp. 4595–4601.

Prokopiou, P. A., Tzafestas, S. G. and Harwin, W. S. (1999), 'A novel scheme for human-friendly and time-delays robust neuropredictive teleoperation', *Journal of Intelligent and Robotic Systems* **25**, pp. 311–340.

Radi, M., Reiter, A., Zaidan, S., Reinhart, G., Nitsch, V. and Farber, B. (2010), 'Telepresence in industrial applications: Implementation issues for assembly tasks', *Presence* **19**(5), pp. 415–429.

Reilink, R., Stramigioli, S., Kappers, A. and Misra, S. (2011), 'Evaluation of flexible endoscope steering using haptic guidance', *International Journal of Medical Robotics and Computer Assisted Surgery* p. In press.

Ren, Z., Zhang, H. and Shao, H. (2003), 'Robust stability analysis of discrete-time linear systems with time delay', *Proceedings of the American Control Conference* pp. 4840–4844.

Rentschler, M., Platt, S., Berg, K., Dumpert, J., Oleynikov, D. and Farritor, S. (2008), 'Miniature in vivo robots for remote and harsh environments', *IEEE Transactions on Information Technology in Biomedicine* **12**(1), pp. 66 –75.

Rodriguez-Seda, E. J., Lee, D. and Spong, M. (2009), 'Experimental comparison study of control architectures for bilateral teleoperators', *IEEE Transactions on Robotics* **25**(6), pp. 1304–1318.

Rosen, J., Hannaford, B., Richards, C. and Sinanan, M. (2001a), 'Markov modeling of minimally invasive surgery based on tool/tissue interaction and force/torque signatures for evaluating surgical skills', *IEEE Transactions on Biomedical Engineering* **48**(5), pp. 579–591.

Rosen, J., Solazzo, M., Hannaford, B. and Sinanan, M. (2001b), 'Objective laparoscopic skills assessments of surgical residents using hidden markov models based on haptic information and tool/tissue interactions', *Studies in Health Technology and Informatics* **81**, pp. 417–423.

Ruurda, J., Draaisma, W. and et al. (2005), 'Robot-assisted endoscopic surgery: a four-year single-center experience', *Digestive Surgery* **22**, pp. 313–320.

Ryu, J.-H. (2007), 'Bilateral control with Time Domain Passivity Approach under time-varying communication delay', *Proceedings of the 13th International Conference on Advanced Robotics* pp. 502–507.

Ryu, J.-H., Artigas, J. and Preusche, C. (2010), 'A passive bilateral control scheme for a teleoperator with time-varying communication delay', *Mechatronics* **20**, pp. 812–823.

Ryu, J.-H., Hannaford, B., Kwon, D. S. and Kim, J.-H. (2005a), 'A simulation/experimental study of the noisy behavior of the Time-Domain Passivity Controller', *IEEE Transactions on Robotics* **21**(4), pp. 733–741.

Ryu, J.-H., Kwon, D.-S. and Hannaford, B. (2002), 'Stable teleoperation with Time Domain Passivity Control', *Proceedings of the IEEE International Conference on Robotics and Automation* pp. 3260–3265.

Ryu, J.-H., Kwon, D. S. and Hannaford, B. (2004*a*), 'Stability guaranteed control: Time Domain Passivity Approach', *IEEE Transactions on Control Systems Technology* **12**(6), pp. 860–868.

Ryu, J.-H., Kwon, D.-S. and Hannaford, B. (2004*b*), 'Stable teleoperation with Time-Domain Passivity Control', *IEEE Transactions on Robotics and Automation* **20**(2), pp. 365–373.

Ryu, J.-H. and Preusche, C. (2007), 'Stable bilateral control of teleoperators under time-varying communication delay: Time Domain Passivity Approach', *Proceedings of the IEEE International Conference on Robotics and Automation* pp. 3508–3513.

Ryu, J.-H., Preusche, C., Hannaford, B. and Hirzinger, G. (2005b), 'Time Domain Passivity Control with reference energy following', *IEEE Transactions on Control Systems Technology* **13**(5), pp. 737–742.

Sackier, J. M. and Wang, Y. (1994), 'Robotically assisted laparoscopic surgery: From concept to development', *Surgical Endoscopy* **8**, pp. 63–66.

Salcudean, S. E., Hashtrudi-Zaad, K., Tafazoli, S., DiMaio, S. P. and Reboulet, C. (1999), 'Bilateral matched-impedance teleoperation with application to excavator control', *IEEE Control Systems Magazine* **19**(6), pp. 29–37.

Salcudean, S. E., Zhu, M., Zhu, W.-H. and Hashtrudi-Zaad, K. (2000), 'Transparent bilateral teleoperation under position and rate control', *International Journal of Robotic Research* **19**(12), pp. 1185–1202.

Sayers, C. and Paul, R. (1994), 'Coping with delays: controlling robot manipulators under water', *Industrial Robot* **21**(5), pp. 124–133.

Secchi, C., Stramigioli, S. and Fantuzzi, C. (2005), 'Power scaling in port-Hamiltonian based telemanipulation', *Proceedings of the IEEE/RSJ International Conference on Intelligent Robots and Systems* pp. 1850 – 1855.

Secchi, C., Stramigioli, S. and Fantuzzi, C. (2006*a*), *Control of Interactive Robotic Interfaces*, Springer Tracts in Advanced Robotics vol. 29, Springer-Verlag, New York.

Secchi, C., Stramigioli, S. and Fantuzzi, C. (2006*b*), 'Position drift compensation in port-Hamiltonian based telemanipulation', *Proceedings of the IEEE/RSJ International Conference on Intelligent Robots and Systems* pp. 4211–4216.

Secchi, C., Stramigioli, S. and Fantuzzi, C. (2008*a*), 'Compensation of position errors in passivity based teleoperation over packet switched communication networks', *Proceedings of the IFAC World Congress* pp. 15648–15653.

Secchi, C., Stramigioli, S. and Fantuzzi, C. (2008*b*), 'Transparency in port-Hamiltonian based telemanipulation', *IEEE Transactions on Robotics* **24**(4), pp. 903–910.

Seibold, U., Kuebler, B. and Hirzinger, G. (2008), 'Prototypic foce feedback instrument for minimally invasive robotic surgery', *Medical Robotics: I-Tech Education and Publishing* pp. 377–400.

Seo, C., Kim, J., Kim, J.-P., Yoon, J. H. and Ryu, J. (2008), 'Stable bilateral teleoperation using the Energy-Bounding Algorithm: basic idea and feasibility tests', *Proceedings of the IEEE/ASME International Conference on Advanced Intelligent Mechatronics* pp. 335–340.

Shahdi, A. and Sirouspour, S. (2009*a*), 'An adaptive controller for bilateral teleoperation under time delay', *Proceedings of the Third Joint Eurohaptics Conference and Symposium on Haptic Interfaces for Virtual Environment and Teleoperator Systems* pp. 308–313.

Shahdi, A. and Sirouspour, S. (2009*b*), 'Adaptive/robust control time-delay teleoperation', *IEEE Transactions on Robotics* **25**(1), pp. 196–205.

Shahdi, A. and Sirouspour, S. (2009*c*), 'Improved transparency in bilateral teleoperation with variable time delay', *Proceedings of the IEEE/RSJ International Conference on Intelligent Robots and Systems* pp. 4616–4621.

Sheridan, T. B. (1989), 'Telerobotics', *Automatica* **25**(4), pp. 487–507.

Sheridan, T. B. (1993), 'Space teleoperation through time delay: review and prognosis', *IEEE Transactions on Robotics and Automation* **9**(5), pp. 592–606.

Sheridan, T. B. and Ferrell, W. R. (1963), 'Remote manipulative control with transmission delay', *IEEE Transactions on Human Factors in Electronics* **4**, pp. 25–29.

Sirouspour, S. (2005), 'Modeling and control of cooperative teleoperation systems', *IEEE Transactions on Robotics* **21**(6), pp. 1220–1225.

Speich, J. E., Fite, K. and Goldfarb, M. (2000), 'A method for simultaneously increasing transparency and stability robustness in bilateral telemanipulation', *Proceedings of the IEEE International Conference on Robotics and Automation* pp. 2671–2676.

Speich, J. and Goldfarb, M. (2005), 'An implementation of loop-shaping compensation for multidegree-of-freedom macro-microscaled telemanipulation', *IEEE Transactions on Control Systems Technology* **13**(3), pp. 459 – 464.

Stanford Research Institute (2011), 'M7 Robot', http://www.sri.com/robotics/telemedicine.

Stereotaxis (2011), 'Niobe Magnetic Navigation System', http://www.stereotaxis.com/niobe.

Stramigioli, S., Fasse, E. and Willems, J. (2002), 'A rigorous framework for interactive robot control', *International Journal of Control* **75**(18), pp. 1486–1503.

Stramigioli, S., Mahony, R. and Corke, P. (2010), 'A novel approach to haptic teleoperation of aerial robot vehicles', *Proceedings of the IEEE International Conference on Robotics and Automation* pp. 5302–5308.

Stramigioli, S., Secchi, C., van der Schaft, A. and Fantuzzi, C. (2002), 'A novel theory for sampled data system passivity', *Proceedings of the IEEE/RSJ International Conference on Intelligent Robots and Systems* pp. 1936–1941.

Stramigioli, S., Secchi, C., van der Schaft, A. and Fantuzzi, C. (2005), 'Sampled data systems passivity and discrete port-Hamiltonian systems', *IEEE Transactions on Robotics and Automation* **21**(4), pp. 574–587.

Stramigioli, S., van der Schaft, A., Maschke, B., Andreotti, S. and Melchiorri, C. (2000), 'Geometric scattering in tele-manipulation of port controlled Hamiltonian systems', *Proceedings of the IEEE Conference on Decision and Control* .

Suraneni, S., Kar, I., Murthy, O. R. and Bhatt, R. (2005), 'Adaptive stick-slip friction and backlash compensation using dynamic fuzzy logic system', *Applied Soft Computing* **6**(1), pp. 26 – 37.

Szemes, P. T., Korondi, P., Ando, N. and Hashimoto, H. (2001), 'Friction compensation for micro tele-operation systems', *Automatika* **42**(1-2), pp. 23–27.

Tanikawa, T. and Arai, T. (1999), 'Development of a micro-manipulation system having a two-fingered micro-hand', *IEEE Transactions on Robotics and Automation* **15**(1), pp. 152 –162.

Tanner, N. and Niemeyer, G. (2004), 'Practical limitations of wave variable controllers in teleoperation', *Proceedings of the IEEE Conference on Robotics, Automation and Mechatronics* pp. 25–30.

Tanner, N. and Niemeyer, G. (2005), 'Improving perception in time-delayed telerobotics', *International Journal of Robotics Research* **24**(8), pp. 631–644.

Tanner, N. and Niemeyer, G. (2006), 'High-frequency acceleration feedback in wave variable telerobotics', *IEEE/ASME Transactions on Mechatronics* **11**(2), pp. 119–127.

Tavakoli, M., Aziminejad, A., Patel, R. V. and Moallem, M. (2007), 'Stability of discrete-time bilateral teleoperation control', *Proceedings of the IEEE/RSJ International Conference on Intelligent Robots and Systems* pp. 1624–1630.

Tholey, G., Desai, J. and Castellanos, A. (2005), 'Force feedback plays a significant role in minimally invasive surgery', *Annals of Surgery* **241**(1), pp. 102–109.

Thompson, J. M., Ottensmeyer, M. P. and Sheridan, T. B. (1999), 'Human factors in telesurgery: Effects of time delay and asynchrony in video and control feedback with local manipulative assistance', *Telemedicine Journal* **5**(2), pp. 129–137.

Titan Medical Inc. (2011), 'Amadeus System', http://www.titanmedicalinc.com/.

Tomei, P. (2000), 'Robust adaptive friction compensation for tracking control of robot manipulators', *IEEE Transactions on Automatic Control* **45**(11), pp. 2164 – 2169.

Tsai, M. and Hsieh, M. (2010), 'Accurate visual and haptic burring surgery simulation based on a volumetric model', *Journal of X-ray Science and Technology* **18**(1), pp. 69–85.

Tzafestas, C., Velanas, S. and Fakiridis, G. (2008), 'Adaptive impedance control in haptic teleoperation to improve transparency under time-delay', *Proceedings of the IEEE International Conference on Robotics and Automation* pp. 212–219.

Uhrich, M., Underwood, R., Standeven, J., Soper, N. and Engsberg, J. (2002), 'Assessment of fatigue, monitor placement, and surgical experience during simulated laparoscopic surgery', *Surgical Endoscopy* **16**(4), pp. 635–639.

USGI Medical (2011), 'Transport Multi-lumen Operating Platform', http://www.usgimedical.com/.

van den Bedem, L. (2010), Realization of a Demonstrator Slave for Robotic Minimally Invasive Surgery, PhD thesis, Eindhoven University of Technology.

van den Bedem, L., Rosielle, P. and Steinbuch, M. (2008), 'Design of a slave robot for laparoscopic thoracoscopic surgery', *Minimally Invasive Therapy & Allied Technologies* **17**(4), p. 211.

van der Schaft, A. (1999), *L2-Gain and Passivity in Nonlinear Control*, Springer-Verlag, New York.

van Det, M., Meijerink, W., Hoff, C., Tott, E. and Pierie, J. (2009), 'Optimal ergonomics for laparoscopic surgery in minimally invasive surgery suites: a review and guidelines', *Surgical Endoscopy* **23**(6), pp. 1279–1285.

Vedagarbha, P., Dawson, D. and Feemster, M. (1999), 'Tracking control of mechanical systems in the presence of nonlinear dynamic friction effects', *IEEE Transactions Control Systems Technology* **7**(4), pp. 446 –456.

Villegas, L., Schneider, B., Callery, M. and Jones, D. (2003), 'Laparoscopic skills training', *Surgical Endoscopy* **17**, pp. 1879–1888.

Wagner, C. R. and Howe, R. D. (2007), 'Force feedback benefit depends on experience in multiple degree of freedom robotic surgery task', *IEEE Transactions on Robotics* **23**(6), pp. 1235–1240.

Wagner, C. R., Stylopoulos, N. and Howe, R. D. (2002), 'The role of force feedback in surgery: Analysis of blunt dissection', *Proceedings of the Symposium on Haptic Interfaces for Virtual Environments and Teleoperator Systems* pp. 68–74.

Webster, R., Zimmerman, D., Mohler, B., Melkonian, M. and Haluck, R. (2001), 'A prototype haptic suturing simulator', *Studies in Health Technology and Informatics* **81**, pp. 567–569.

Willaert, B., Corteville, B., Reynaerts, D., H. Van Brussel and E. B. Vander Poorten (2010a), 'A mechatronic analysis of the classical position-force controller based on bounded environment passivity', *International Journal of Robotics Research* pp. 1–18.

Willaert, B., Goethals, P., Reynaerts, D., Brussel, H. V. and Poorten, E. B. V. (2010b), *Advances in Haptics*, chapter Transparent and shaped stiffness reflection for telesurgery, pp. 259–282.

Willems, J. C. (1972), 'Dissipative dynamical systems part I: General theory', *Archive for Rational Mechanics and Analysis* **45**, pp. 321–351.

Wright, J., Trebi-Ollennu, A., Hartman, F., Cooper, B., Maxwell, S., Yen, J. and Morrison, J. (2005), 'Driving a rover on mars using the rover sequencing and visualization program', *International Conference on Instrumentation, Control and Information Tech.* .

Yamamoto, T., Vagvolgyi, B., Balaji, K., Whitcomb, L. L. and Okamura, A. (2009), 'Tissue property estimation and graphical display for teleoperated robot-assisted surgery', *Proceedings of the IEEE International Conference on Robotics and Automation* pp. 4239–4245.

Yan, J. and Salcudean, S. E. (1996), 'Teleoperation controller design using hinfinity-optimization with application to motion-scaling', *IEEE Transactions on Control Systems Technology* **4**(3), pp. 244–258.

Ye, Y., Pan, Y.-J. and Gupta, Y. (2008), 'A simplified Time Domain Passivity Control of haptic interfaces', *Proceedings of the IASTED International Conference on Intelligent Systems and Control* pp. 215–219.

Ye, Y., Pan, Y.-J. and Gupta, Y. (2009), 'Time Domain Passivity Control of teleoperation systems with random asymmetric time delays', *Proceedings of the Joint 48th IEEE Conference on Decision and Control and the 28th Chinese Control Conference* pp. 7533–7538.

Ye, Y., Pan, Y.-J., Gupta, Y. and Ware, J. (2010), 'A power-based Time Domain Passivity Control for haptic interfaces', *IEEE Transactions on Control Systems Technology* **18**(6), pp. 1–10.

Yokokohji, Y., Imaida, T. and Yoshikawa, T. (1999), 'Bilateral teleoperation under time-varying communication delay', *Proceedings of the IEEE/RSJ International Conference on Intelligent Robots and Systems* pp. 1854–1859.

Yokokohji, Y., Imaida, T. and Yoshikawa, T. (2000), 'Bilateral control with energy balance monitoring under time-varying communication delay', *Proceedings of the IEEE International Conference on Robotics and Automation* pp. 2684–2689.

Yokokohji, Y. and Yoshikawa, T. (1994), 'Bilateral control of master-slave manipulators for ideal kinesthetic coupling - formulation and experiment', *IEEE Transactions on Robotics and Automation* **10**(5), pp. 605–620.

Dankwoord

Ook al is het doel van een promotie onderzoek *Het tentoonstellen van het vermogen om zelfstandig wetenschappelijk onderzoek te verrichten* kom je gedurende de periode die dat onderzoek in beslag neemt in aanraking met veel mensen die direct of indirect een belangrijke bijdrage leveren.

De eerste persoon die ik daarom voor zijn bijdrage wil bedanken is Professor Stefano Stramigioli, a.ka. Capo. Sinds je colleges gedurende de master fase heb je mijn beeld op je geliefde vakgebied robotica vormgegeven. Ik was niet altijd even snel met het oppikken van wat je me wilde leren, want het heeft je ongeveer een jaar gekost om het 'Goedemorgen Professor Stramigioli' in 'Hoi Stefano' om te zetten. Ik heb het altijd als zeer plezierig ervaren om voor en met je te werken en stel alle mogelijkheden en het vertrouwen dat je me geboden hebt zeer op prijs. De afgelopen vier jaar waarin ik je 'Portaborse' heb mogen spelen is een mooie tijd geweest en ik hoop dat onze paden elkaar ook in de toekomst zullen blijven kruisen.

De tweede persoon die ik wil bedanken is mijn andere beleider. Sarthak, even though you became involved when I was already halfway down my PhD project you made a large impact. You have really helped me to improve my writing skills and it was a great relief when I started to get my papers back from you with less and less markings. Thank you for all your time, help and advice!

Bert Willaert van de Katholieke Universiteit Leuven wil ik bedanken voor de plezierige samenwerking. Bert bedankt voor het initiëren van onze gesprekken die op een gegeven moment wekelijks plaats vonden en soms wel 4 tot 5 uur in beslag konden nemen. Dit is wat betreft het doen van onderzoek voor mij de meest plezierige periode geweest uit de afgelopen vier jaar! Veel succes met de laatste loodjes van je eigen promotie!

Ook al is een promotie niet een standaard baan, de motivatie om eraan te werken zou hard achteruit gaan als er niet een maandelijkse vergoeding tegenover zou staan. Ik wil daarom MIRA bedanken voor de financiële ondersteuning die mij in staat gesteld heeft om vier jaar onderzoek te doen en de mogelijkheden om het enthousiasme voor techniek op hun studenten over te brengen. Professor Vooijs en Remke Burie wil ik bedanken voor hun constructieve opmerkingen tijdens ons jaarlijkse *vinger-aan-de-pols*-gesprek.

Iemand waarmee ik het wel en wee van het promoveren gedurende 3.5 jaar gedeeld heb is mijn 'roomy' Martin. Het delen van een kamer met jou heb ik geweldig gevonden. En ook al werkte je het liefste in stilte, hebben we denk ik alles besproken wat tussen onderzoek, politiek, en vrouwen ligt. Je was ook altijd bereid even mee te denken en ik ben je dankbaar voor de rol die je gehad hebt in het opstarten van het onderzoek dat uiteindelijk een groot deel van dit proefschrift is gaan vormen. Ik ben erg blij dat je nu een baan hebt waar je al je gedrevenheid in kwijt kunt!

Mijn meer recentelijke kamergenoten, Ramazan, Gijs, en Ludo, wil ik bedanken voor het verdragen van mijn constante aandrang om te praten en de hulp bij taalkundige vragen. Ik hoop dat het niet te irritant is geweest, maar voor alle afleiding een welgemeend 'Sorry,

maar bedankt!'. *Tour-operator* Ludo wil ik graag bedanken voor de onvergetelijke trip die we door Alaska gemaakt hebben na afloop van de ICRA. Ik ben nog steeds onder de indruk van het natuurschoon dat we tijdens die reis gezien hebben en vond het erg gezellig om samen met jou, Stefano, en Tamas op pad te zijn!

Met evenveel plezier kijk ik terug op de roadtrip die ik met Rob *Rally* gemaakt heb door Taiwan na afloop van de IROS. Ook tijdens deze reis was het erg gezellig en hebben we ontzettend veel mooie dingen/landschappen gezien zowel boven als onderwater. Van iedereen die uit Nederland naar die conferentie geweest is zijn wij de enige denk ik die Taiwan bij zonlicht gezien hebben. Ik krijg echter nog steeds zweethanden als ik terugdenk aan het autorijden 's avonds door Taichung en de rit door de bergen die we moesten maken om op tijd bij het vliegveld te zijn. Ook wil ik je graag bedanken voor al je nuttige opmerkingen en tips die ik in de loop van de tijd van je heb mogen ontvangen!

Om theorie met experimenten te kunnen onderbouwen heb je natuurlijk een testopstelling nodig. Gezien mijn twee linkerhanden heb ik veel baat gehad bij de hulp die ik gekregen heb tijdens de realisatie van die opstelling. Roel bedankt voor je inzet bij het ontwerpen en fabriceren van de mechanische onderdelen! 'Grote' Marcel bedankt voor het ontwerpen van de elektronica en het herstellen van mijn soldeer gepruts. 'Kleine' Marcel bedankt voor je hulp bij allerlei Linux, VHDL en overige software problemen. Hubert en Rob bedankt voor de implementatie van de netwerk communicatie. Zonder al jullie hulp en bijdragen zou ik waarschijnlijk nog steeds aan het prutsen zijn...

Eenzelfde dankbetuiging gaat uit naar de mensen van Controllab Products (met name Frank, Paul en Peter) bedankt voor jullie onschatbare bijdrage door mij in staat te stellen mijn simulaties en experimenten te doen met zo min mogelijk code te kloppen!

De lange lijst gaat verder met de moederfiguren van de vakgroep: Carla en Jolanda! Jullie zijn de verpersoonlijking van de gewijzigde uitdrukking *Achter elke succesvolle onderzoeksgroep staat een goed secretariaat*. Bedankt voor alle hulp en ondersteuning die ik van jullie gekregen heb! Dit geldt natuurlijk ook, en niet in mindere mate, voor de technici van onze groep. Gerben, Marcel, en Alfred bedankt voor alle tips en hulp die ik van jullie gekregen. Zonder jullie 'suggesties' zou ik waarschijnlijk veel meer componenten opgeblazen hebben.

De laatste jaren is de vakgroep flink gegroeid en kan ik dus niet iedereen bij naam noemen. Ik ben iedereen, staf en studenten, dankbaar voor de prettige sfeer waarin ik de afgelopen vier jaar heb mogen werken!

Een gezonde geest huist in een gezond lichaam en om van de overtollige energie af te komen na een dag alleen maar gezeten te hebben heb ik altijd graag aan sport gedaan. De laatste jaren zijn dat vooral triathlon bij Aloha en meer recentelijk klimmen bij Arqué geweest. Iedereen bedankt voor de gezellige trainingen, wedstrijden, uitstapjes en andere activiteiten!

Sinds 2007 kijk ik ook regelmatig op een andere manier naar het leven en dan met name vanonder het wateroppervlakte. In 2008 heb ik mijn eerste duik bij Piranha gemaakt samen met Rob en Erik en ik kan me vooral een gebrek aan zicht, snijdende kou en een resulterende voorhoofdsholte ontsteking herinneren. Desondanks ben ik toch blijven hangen en heb ik kennis gemaakt met de immer groeiende Piranha familie waar naast het duiken vooral gezelligheid hoog in het vaandel staat. Tot bubbels iedereen!

Ook op andere plaatsen heb ik het geluk gehad om veel mensen te leren kennen die ik tot mijn vriendengroep mocht rekenen. Veel van jullie heb ik de afgelopen tijd te weinig gezien door afstand en/of drukte, maar hopelijk komt daar weer snel verandering in! Mijn vrienden en vriendinnen uit Noord-Holland wil ik bedanken voor alle gezelligheid gedurende menig kroegavond en bij alle activiteiten daarbuiten. Al mijn vrienden die ik in Enschede heb leren kennen wil ik bedanken voor alles wat we samen meegemaakt hebben. Zonder jullie zou het studentenleven niet zo mooi geweest zijn! Een speciaal bedankje gaat uit naar Jeroen (Ah toe Michel, nog eentje) en Maaike. Bedankt dat jullie al die jaren je best gedaan hebben om me bij mijn verstand te houden als ik weer eens *da Stresskip* uithing.

Willeke, Hans en Wouter bedankt voor de vele gezellige weekendjes die ik bij/met jullie heb mogen beleven. Wil bedankt dat je er altijd was als ik weer eens in de put zat en voor de hechte relatie die we nu hebben. Het oom zijn is tot nog toe een van de leukste dingen waar ik me mee bezig hou!

De laatste plaats in dit dankwoord is voor de mensen waar ik het meeste aan te danken heb. Pa en Ma bedankt voor jullie onvoorwaardelijke interesse, steun en liefde! Het klinkt waarschijnlijk afgezaagd maar zonder jullie zou ik dit alles nooit bereikt kunnen hebben. Bedankt voor alles!

Michel Franken
April 2011, Enschede

About the author

Michel Franken was born on the 6th of April 1982 in Anna Paulowna, the Netherlands. He completed his secondary education at the Gemeentelijke Scholen Gemeenschap in Schagen. In 2001 he started his study in Electrical Engineering at the University of Twente. He received his Propaedeutic certificate cum laude in 2002 and his Bachelor of Science in 2004. During his master in Measurement and Control Engineering he was a participant of the study project Shouraizou, which included a three week study tour to Japan. For his internship he spend six months in 2006 in Detroit, USA, at JADI Inc. He worked with Edzko Smid, Ph.D., and Ka C. Cheok, Ph.D., on the autonomous navigation of robots using a UWB local positioning system. His Master of Science project dealt with ankle actuation in energy efficient planar bipedal robots under the supervision of Prof. Stefano Stramigioli. He finished his Master of Science cum laude in April 2007 and was awarded the Mechatronic Valley Twente award for best Mechatronics graduation project in 2008.

Right after completing his Master he started his Ph.D. position at the University of Twente, again under the supervision of Prof. Stefano Stramigioli. During his PhD he investigated new control algorithms for haptic interaction with virtual environments and telemanipulation systems,

His interests include beside robotics, mathmatics, control engineering, and modelling. His hobbies include music, movies, cooking, martial arts, mountainbiking, triathlon, diving, and sport climbing.

UNIVERSITY OF TWENTE.

Haptic feedback systems are systems that exert a desired force, to be experienced by the user, to recreate a physical interaction. This type of systems can increase the realism of the interaction with objects that are not in the direct area of influence of the user. The same applies to the interaction with virtual objects. The fundamental problem in the control of these systems is how to maximize the transparency of the system, and related to that the realism of the interaction as perceived by the user, while guaranteeing stability of the interaction under all possible operating conditions.

The analysis of the stability is made more difficult by the presence of a closed loop containing either one or two unknown, non-linear, and time-varying elements, the user and/or physical environment. Furthermore, the control algorithm is executed on a discrete medium which, depending on the algorithm, parameter settings, and remaining elements, can have a significant influence on the stability of the interaction.

In this thesis a solution is sought to all these factors by means of energy- and port-based reasoning. For both applications an algorithm is derived that is based on the energy exchange between the physical world and the system. By enforcing energy neutrality, in other words passivity, of this exchange stability of the interaction is guaranteed.